THEORETICAL AND EXPERIMENTAL STUDY OF A MULTI-PASS TWO-GLASS COVER SOLAR AIR HEATER UNDER TRANSIENT CONDITIONS.

BY

REUBEN MWANZA KIVINDU

F/56/7342/2002

A thesis submitted in partial fulfillment of the requirements for the award of the Degree of Master of Science in Mechanical Engineering of the University of Nairobi.

DECLARATION

This Thesis is my original work and has not been submitted for a degree in any other University.

R. M. Kivindu 8/9/2010

This Thesis has been submitted for examination with my approval as a University supervisor.

1st Supervisor: Prof. F. M. Luti 10/09/10

2nd Supervisor: Dr. A. A. Aganda — 9/9/2010

TABLE OF CONTENTS.

ACKNOWLEDGEMENT

First I do appreciate a lot for the advice, guidance and encouragement I received from my supervisors Prof. F. M. Luti and Dr. A. A. Aganda.

To Prof. F. M. Luti, I can only say "Thank you" for you went out of your normal duties to see that I have what is contained in this thesis.

Secondly, I would like to thank the lecturing and workshop staff of the Department of Mechanical Engineering for their help and advices during the fabrication and testing of the solar collector to validate the developed model.

Thirdly, I am grateful to my fellow postgraduate students who contributed extra ideas which made the project come a complete thesis as it is.

Finally, I would also like to greatly thank all members of my family for their patience, kindness and understanding during the course of the project and writing of this thesis.

Thanks to all.

ABSTRACT.

The major problems experienced with solar air heaters are their non-reliability as their operation largely depends on weather conditions which keep on changing. This study was aimed at providing and experimentally validating a transient based model for predicting the performance of multi-pass solar air heaters operating on changing weather conditions.

A transient prediction model was developed by considering the thermal capacities of the collector components and the flowing air. Differential equations were developed by considering the energy interactions and balances for the various components of the collector, and then solved numerically.

The developed model was tested with input data of insolation, ambient temperature, wind velocity and solar time and then validated experimentally by use of a single collector which was designed to accommodate all the four flow arrangements investigated (SPM, DMPM, DTPM and TPM).

The time constant of the collector constructed was determined experimentally to be 27 minutes. The theoretical collector performance results indicated a transient behavior for changing weather conditions. This was also confirmed by the experiment carried out whose data were recorded and plotted at intervals of two minutes.

Based on air temperature rise and collector efficiency both the developed theoretical model and experimental set up indicated that the triple pass mode is superior to the other modes, with the single pass mode ranked the lowest in performance. The developed

computational prediction model had a standard deviational error of 1.8 to 2.1% as compared to the experimental values which had an error of 2.7 to 9.6%. The TPM had the lowest error (1.8%) while the SPM had the highest (2.1%). When compared to other models and experiments, the results were in good agreement.

The developed model confirmed that air temperature rise in the collector is a function of available solar insolation and prevailing weather conditions such as; cloud cover, ambient temperature and wind.

It was found that, in actual sense thermal solar collectors do experience transient conditions and the developed transient model was necessary, and is expected to reduce the day long experiments that need to be carried out to acquire the performance characteristics of solar air heaters under changing weather conditions.

NOMENCLATURE.

a	A constant for determination of Nusselt number for lamina flow between two parallel flat plates.
a_l	Couette coefficient.
A	Constant term that combines the density, thickness and specific heat of glass, $m^2.K/J$
A	Area for radiation heat exchange, m^2
A	Area for conduction heat flow, m^2
A_d	Duct cross-sectional area, m^2
A_k	Collector box surface area, m^2
b	Collector width, m
b	A constant for determination of Nusselt number for lamina flow between two parallel flat plates.
b_l	Hagenbach coefficient.
b_r	Beam radiation component, W/m^2
B	A constant for simplification of glass properties, s^{-1}
Bi	Biot number.
c_l	Loss coefficient for filter.
c_p	Specific heat capacity, J/kg.K
c_{pa}	Specific heat capacity of air, J/kg.K
c_{pab}	Specific heat capacity of absorber plate material, J/kg.K
c_{pbp}	Specific heat capacity of back plate material, J/kg.K
c_{pg}	Specific heat capacity of glass, J/kg.K
c_{pins}	Specific heat capacity of insulation material, J/kg.K
c_s	Screen discharge coefficient
C	Discharge coefficient
C_1	A term grouping the heat transfer coefficients between the top glass cover and the ambient, and the first glass cover and the top glass cover in the single pass mode, $W/m^2.K$
C_2	A term grouping the heat transfer coefficients between the top glass cover and the Ambient, the flowing air and the first glass cover, and the radiation heat transfer coefficient between the first glass cover and the top glass cover for DTPM, $W/m^2.K$
C_3	A term grouping the heat transfer coefficients between the top glass cover and ambient , and the top glass and first glass covers for DMPM, $W/m^2.K$
C_4	A term grouping the heat transfer coefficients between the top glass cover and ambient, the flowing air and the top glass cover, and the radiation heat transfer coefficient between the first and top glass covers for triple pass mode, $W/m^2.K$
d	Duct diameter, m.
d_h	Hydraulic mean diameter, m.

d_r Diffuse radiation component, W/m^2

D A grouping term of heat transfer coefficients between the first glass cover and the top glass cover, and the absorber plate and the first glass cover for single pass mode, $W/m^2.K$

D_1 A grouping term of heat transfer coefficients between the flowing air and the first glass cover, the absorber plate and the first glass cover, and the radiation heat transfer coefficient between the first and top glass covers for DTPM, $W/m^2.K$

D_2 A grouping term for heat transfer coefficients between the flowing air and the first glass cover, the top and the first glass covers, and the radiation heat transfer coefficient between the first glass cover and the absorber plate for DMPM, $W/m^2.K$

D_3 A grouping term of heat transfer coefficients between the flowing air in the first flow channel and the top glass cover, the flowing air in the second flow channel and the top glass cover, and the radiation heat transfer coefficient between the absorber plate and the first glass cover for triple pass mode, $W/m^2.K$

DMPM Double (middle first) pass mode.
DTPM Double (top first) pass mode

E A constant term that combines the density, thickness and specific heat of the absorber plate, $m^2.K/J$
E Equation of time in minutes
E_e Emissive power, W/m^2

f Frictional loss coefficient
f_1 Fraction of incident insolation absorbed by the first glass cover
f_{ab} Fraction of incident insolation absorbed by the absorber plate
f_t Fraction of incident insolation absorbed by the top glass cover
F A constant term that represents combined properties of the absorber plate, s^{-1}
F_{12} Radiation view factor for surfaces 1 and 2
F_R Collector heat-removal factor.

G Ratio of the mass flow rate of air per unit cross-sectional area of duct, $Kg/s.m^2$
G Irradiance, W/m^2

G_1 A grouping for heat transfer coefficients between the absorber plate and the first glass cover, the absorber plate and the back plate, and the flowing air and the absorber plate for single pass mode, $W/m^2.K$

G_2 A grouping term for heat transfer coefficients between the absorber and the first glass cover, the absorber plate and the back plate, and between the flowing air and the absorber plate for DTPM, $W/m^2.K$

G_3 A grouping term for heat transfer coefficients between the flowing air and absorber plate, the absorber plate and the first glass cover, and the absorber plate and the back plate for DMPM, $W/m^2.K$

G_4 A grouping term for heat transfer coefficients between the flowing air and the absorber plate, the absorber plate and the first glass cover, and the absorber plate and the back plate for triple pass mode, $W/m^2.K$

G_{on} Extraterrestrial radiation, W/m^2

Gr Grashof number

G_s Recorded solar irradiance, W/m^2

G_{sc} Solar constant, W/m^2

h Heat transfer coefficient, $W/m^2.K$

h_1 A term representing the convective and radiation heat transfer coefficients between the absorber plate and the first glass cover, $W/m^2.K$

h_{1t} Natural convection heat transfer coefficient between the top and first glass covers, $W/m^2.K$

h_a A term combining the convection and radiation heat transfer coefficients between the top glass cover and the ambient, $W/m^2.K$

h_{ab} A term representing the radiation heat transfer coefficient between the absorber and the back plates, $W/m^2.K$

h_{ab1} Natural convection heat transfer coefficient between the absorber plate and the first glass cover, $W/m^2.K$

$h_{ab\text{-}fm}$ Convection heat transfer coefficient between the absorber plate and the flowing air $W/m^2.K$

$h_{bp\text{-}fm}$ Convection heat transfer coefficient between the back plate and the flowing air, $W/m^2.K$

h_c Conduction heat transfer coefficient, $W/m^2.K$

h_{fl} A term representing the heat transfer coefficient between the flowing air and the top glass cover, $W/m^2.K$

$h_{fl\text{-}1}$ Convection heat transfer coefficient between the flowing air and the first glass cover, $W/m^2.K$

$h_{fl\text{-}ab}$ Convection heat transfer coefficient between the flowing air and the absorber plate, $W/m^2.K$

h_{f1-t} Convection heat transfer coefficient between the flowing air and the top glass cover, $W/m^2.K$

h_{f2} A term representing the heat transfer coefficient between the flowing air in the second flow channel and the absorber plate, $W/m^2.K$

h_{f2-ab} Convection heat transfer coefficient between the flowing air in the second flow channel and the absorber plate, $W/m^2.K$

h_{f2-bp} Convection heat transfer coefficient between the flowing air in the second flow channel and the back plate, $W/m^2.K$

h_{f3-ab} Convection heat transfer coefficient between the flowing air in the third flow channel and the absorber plate, $W/m^2.K$

h_{f3-bp} Convection heat transfer coefficient between the flowing air in the third flow channel and the back plate, $W/m^2.K$

h_{fb} A term representing the heat transfer coefficient between the flowing air and the back plate, $W/m^2.K$

h_{ins} A term combining the convection and radiation heat transfer coefficients from the bottom of the collector, $W/m^2.K$

$h_{ins-a\ l}$ Convection heat transfer coefficient between the insulation and the ambient, $W/m^2.K$

h_r Radiation heat transfer coefficient, $W/m^2.K$

h_{rlt} Radiation heat transfer coefficient between the top and the first covers, $W/m^2.K$

h_{rabl} Radiation heat transfer coefficient between the absorber plate and the first glass cover, $W/m^2.K$

h_{rab-bp} Radiation heat transfer coefficient between the absorber plate and the back plate, $W/m^2.K$

h_{rga} Radiation heat transfer coefficient between the top glass cover and the ambient, $W/m^2.K$

h_{rins-a} Radiation heat transfer coefficient between the insulation and the ambient, $W/m^2.K$

h_{t2} A term representing the radiation heat transfer coefficient between first and the top glass covers, $W/m^2.K$

h_{ta} Convection heat transfer coefficient between the top glass cover and the ambient, $W/m^2.K$

h_w Wind heat transfer coefficient, $W/m^2.K$

H A term representing the flowing air properties for single pass mode, $m^2.K/J$

H_1 A term representing the flowing air properties in the first flow channel for DTPM, $m^2.K/J$

H_2 A term representing the flowing air properties in the second flow channel for DTPM, $m^2.K/J$

H_3 A term representing the flowing air properties in the first flow channel for DMPM, $m^2.K/J$

H_4 A term representing the flowing air properties in the second flow channel for DMPM, $m^2.K/J$

H_5 A term representing the flowing air properties in the first flow channel for Triple pass mode, $m^2.K/J$

H_6 A term representing the flowing air properties in the second flow channel for Triple pass mode, $m^2.K/J$

H_7 A term representing the flowing air properties in the third flow channel for Triple pass mode, $m^2.K/J$

H_i Hourly irradiation, J/m^2

H_x Enthalpy entering with the air into the control volume, W

$H_{x+\Delta x}$ Enthalpy leaving with the air from the control volume, W

I Irradiation for one day, J/m^2

I Radiation intensity

I_T Incident total insolation, J/m^2

J A term representing the air properties together with the mass flow rate and the collector dimensions for single pass mode, s^{-1}

J_1 A term representing the air properties together with the mass flow rate and the collector dimensions in the first flow channel for DTPM, s^{-1}

J_2 A term representing the air properties together with the mass flow rate and the collector dimensions in the second flow channel for DTPM, s^{-1}

J_3 A term representing the air properties together with the mass flow rate and the collector dimensions in the first flow channel for DMPM, s^{-1}

J_4 A term representing the air properties together with the mass flow rate and the collector dimensions in the second flow channel for DMPM, s^{-1}

J_5 A term representing the air properties together with the mass flow rate and the collector dimensions in the first flow channel for triple pass mode, s^{-1}

J_6 A term representing the air properties together with the mass flow rate and the collector dimensions in the second flow channel for triple pass mode, s^{-1}

J_7 A term representing the air properties together with the mass flow rate and the collector dimensions in the third flow channel for triple pass mode, s^{-1}

J_r Radiosity, W/m^2

k Thermal conductivity, W/m.K

k Extinction coefficient

k_a Air thermal conductivity, W/m.K

k_{ab} Absorber plate thermal conductivity, W/m.K

k_{bp} Back plate thermal conductivity, W/m.K

k_c Number of velocity head losses

k_g Glass thermal conductivity, W/m.K

k_{ins} Insulation material thermal conductivity, W/m.K

K	A grouping term for heat transfer coefficient between the flowing air and the absorber plate, and the flowing air and the back plate for single pass mode, $W/m^2.K$
K_1	A grouping term for the heat transfer coefficients between the flowing air and the toglass cover, and the flowing air and the first glass cover for DTPM, $W/m^2.K$
K_2	A grouping term for the heat transfer coefficients between the flowing air and the absorber plate, and the flowing air and the back plate for DTPM, $W/m^2.K$
K_3	A grouping term for the heat transfer coefficients between the flowing air and the first glass cover, and the flowing air and the absorber plate for DMPM, $W/m^2.K$
K_4	A grouping term for the heat transfer coefficients between the flowing air and the absorber plate, and the flowing air and the back plate for DMPM, $W/m^2.K$
K_5	A grouping term for the heat transfer coefficients between the flowing air and the top glass cover, and the flowing air and the first glass cover for TPM, $W/m^2.K$
K_6	A grouping term for the heat transfer coefficients between the flowing air and the first glass cover, and the flowing air and the absorber plate for TPM, $W/m^2.K$
K_7	A grouping term for the heat transfer coefficients between the flowing air and the absorber plate, and the flowing air and the back plate for TPM, $W/m^2.K$
L	A constant term that combines the back plate density, thickness and specific heat capacity, $m^2.K/J$
L	Plate spacing, m
L_d	Duct length, m
L_e	Equivalent length, m
L_g	Glass thickness, m
L_{loc}	Longitude of the location in question, degrees
L_{st}	Standard meridian for the local time zone, degrees
m	A constant for determination of Nusselt number for Lamina flow between two parallel flat plates
m	Air mass
$\dot{m}$	Air mass flwo rate, kg/s
m_{ab}	Mass of absorber plate, kg
m_{bp}	Mass of back plate, kg
m_g	Mass of glass, kg
m_{ins}	Mass of insulation, kg
m_n	Mass of a given component, kg
M	A constant representing grouped back plate material properties, s^{-1}
M_f	Mass of the air in the control volume for the single pass mode, kg
M_{f1}	Mass of the air in the control volume of the first flow channel for DTPM, DMPM, and TPM, kg
M_{f2}	Mass of the air in the control volume of the second flow channel for DTPM, DMPM, and TPM, kg
M_{f3}	Mass of the air in the control volume of the third flow channel for TPM, kg
n	A constant for determination of Nusselt number for lamina flow between two parallel flat plates
n	Day of the year
n_o	Refractive index of any medium

n_1 Refractive index of medium 1

n_2 Refractive index of medium 2

n_s Number of screens in series

N Daylight hours

N A grouping term for the heat transfer coefficients between the flowing air and the back plate, and absorber plate and back plate for single pass mode, $W/m^2.K$

N1 A grouping term for the heat transfer coefficients between the flowing air and the back plate, and absorber plate and back plate for DTPM, $W/m^2.K$

N_2 A grouping term for the heat transfer coefficients between the flowing air and the back plate, and absorber plate and back plate for DMPM, $W/m^2.K$

N_3 A grouping term for the heat transfer coefficients between the flowing air and the back plate, and absorber plate and back plate for TPM, $W/m^2.K$

Nu Nusselt number

P A constant term combining the insulation material density, thickness and specific heat capacity, $m^2.K/J$

P Pressure, N/m^2

Pr Prandtl number

P_t Total pressure against which air is moved, Kpa.

q Heat conducted per unit area, W/m^2

q_u Useful energy collected, W/m^2

Q A constant term representing a combination of insulation material properties, s^{-1}

Q Heat flow, W

Q_L Air flow rate, L/s

Q_u Total useful energy collected, W

r Reflection of unpolarized radiation

$r_{(o)}$ Reflection of unpolarized radiation at normal incidence

R Hydraulic radius, m

R Insulation thermal resistance, $m^2.K/W$

Ra Raleigh number

Re Reynolds number

s Flow duct height, m

S Solar radiation absorbed by the collector, W/m^2

S_1, S_2 Time constants

t Time in seconds

t_{ab} Absorber plate thickness, m

t_{bp} Back plate thickness, m

$t_{f,e,t}$ Fluid exit temperature at end of time t, K

t_g Glass thickness, m

t_{ins} Insulation thickness, m

$t_{f,e,initial}$ Initial fluid exit temperature, K

$t_{f,i}$ Fluid inlet temperature, K

T Absolute temperature, K

T_1 Temperature of the first glass cover, K

T_a	Ambient temperature, K
T_{ab}	Temperature of the absorber plate, K
T_{bp}	Temperature of the back plate, K
T_{fi}	Air inlet temperature, K
$T_{fin,1}$	First flow channel inlet temperature, K
$T_{fin,2}$	Second flow channel inlet temperature, K
$T_{fin,3}$	Third flow channel inlet temperature, K
T_{fm}	Air mean temperature, K
T_{fm1}	Mean temperature for air flowing in the first flow channel, K
T_{fm2}	Mean temperature for air flowing in the second flow channel, K
T_{fm3}	Mean temperature for air flowing in the third flow channel, K
T_{fo}	Air exit temperature, K
T_{fout1}	Air exit temperature from the first flow channel, K
T_{fout2}	Air exit temperature from the second flow channel, K
T_{fout3}	Air exit temperature from the third flow channel, K
T_{ins}	Insulation surface temperature, K
T_n	Initial component temperature, K
T_n^1	Final component temperature after the time step, K
T_{sky}	Equivalent sky temperature, K
T_x	Spatial component temperature at distance x, K
$T_{x+\Delta x}$	Spatial component temperature at distance x+Δx, K
TPM	Triple pass mode
U_L	Overall heat transfer coefficient, $W/m^2.K$
v	Mean velocity in the duct, m/s
v_s	Superficial velocity ahead of a screen, m/s
V	Air velocity in the collector, m/s
V_s	Wind velocity, m/s
w	Duct width, m
W_t	Theoretical power required to move a given mass of air, W
α	Thermal diffusivity, m^2/s
α_a	Absorbed radiation
α_{ab}	Absorber plate absorptivity
α_d	Duct divergence angle, degrees
α_f	Fractional free projected area of screen
β	Slope, degrees
β^1	Volumetric coefficient of expansion
γ	Surface azimuth angle, degrees
γ_b	Transmission coefficient for beam solar radiation
γ_d	Transmission coefficient for diffuse solar radiation
γ_t	Transmission coefficient for total radiation
δ	Declination of the sun, degrees
Δh	Head loss, m
Δh_f	Head loss due to friction in the duct, m
Δt	Time step, s

ΔT	Temperature difference, K
ε	Emissivity
ε_g	Glass emissivity
η	Solar collector efficiency
θ	Angle of incidence of falling beam radiation, degrees
θ_1	Angle of incidence, degrees
θ_2	Angle of refraction, degrees
θ_z	Zenith angle, degrees
μ	Absolute viscosity of air, kg/m.s
ρ	Reflected radiation
ρ_a	Density of air, kg/m^3
ρ_{ab}	Density of absorber plate material, kg/m^3
ρ_{ar}	Absorber plate reflectivity
ρ_{bp}	Density of back plate material, kg/m^3
ρ_g	Density of glass, kg/m^3
ρ_{gr}	Ground reflectivity
ρ_{ins}	Density of insulation material, kg/m^3
σ	Stefan-Boltzmann constant, $W/m^2.K^4$
τ	Fraction of transmitted radiation
τ_a	Transmittance with only absorption losses
τ_g	Transmittance glass
τ_r	Transmittance of unpolarized radiation through one non-absorbing cover with only reflection losses
τ_{rN}	Transmittance of unpolarized radiation through N non-absorbing covers with only reflection losses
υ	Kinematical viscosity, m^2/s
ϕ	Latitude, degrees
ϕ	Plate angle with the vertical, degrees
ω	Hour angle, degrees

ACRONYMS

ABP9	Absorber plate experimental temperature, degree Celsius.
AINTf	Air inlet temperature, degree Celsius.
AMBT	Ambient temperature, degree Celsius.
BBP10	Back plate experimental temperature, degree Celsius.
CEF	Collector efficiency.
DMPM	Double (Middle first) pass mode.
DTPM	Double (Top first) pass mode.
FGC8	Experimental first glass covers temperature, degree Celsius.
INS11	Insulation material temperature.
INS TEMP	Insulation temperature for time constant determination.
SPM	Single pass mode.
Tab1	Theoretical absorber plate temperature.
Tbp1	Theoretical back plate temperature.
TEMP 1	Experimental air temperature at the left end of top flow channel.
TEMP 2	Experimental air temperature at the left end of middle flow channel.
TEMP 3	Experimental air temperature at the left end of bottom flow channel.
TEMP 4	Experimental air temperature at the right end of top flow channel.
TEMP 5	Experimental air temperature at the right end of middle flow channel.
Tf1	Air exit temperature for SPM.
Tf11	Air exit temperature from first flow channel for DMPM, DTPM and TPM.
Tf21	Air exit temperature from second flow channel for DMPM, DTPM and TPM.
Tf31	Air exit temperature from third flow channel for TPM.
TGC7	Experimental Top glass covers temperature, degree Celsius.
TPM	Triple pass mode.
Tt1	Theoretical top cover temperature.
T11	Theoretical first cover temperature.

LIST OF TABLES.

LIST OF FIGURES.

CHAPTER1: INTRODUCTION

1.0: INTRODUCTION

Due to the development of technology and the high population growth rate, the demands for energy are tending to exceed the supply, hence resulting to what is commonly termed as 'Energy Crisis'. Governments and institutions are working hard to encourage the use of alternative energy sources. The main alternative energy sources are; - solar, geothermal, biomass, wind, and other small scale renewable energies such as; tidal and wave power.

As part of the change in energy policies that followed the 'oil crisis', many industrialized countries have expanded their development efforts in renewable energy, and a substantial technical progress has been made.

Many energy issues have been brought forward to control the depletion of fossil fuels, these calls for increased oil prices. One of the energy issues is fuel wood provision, which are largely unaffected by oil price fluctuations and are affordable to the rural poor. Another issue is the use of renewable energies which do not affect the environment and are relatively affordable.

It has been assumed that, the third world can rapidly bypass the era of fossil fuel and go straight into a solar future. The optimists argued that solar energy is an abundant free resource, especially in the third world, and that lack of an existing infrastructure, including administration, is an advantage because there is little technological inertia. But this is not true because lack of infrastructure is an obstacle to change.

The weak economies of the third world, which are characterized by lack of foreign exchange and limited household purchasing power, slow down the rate of technical change. Any large-scale implementation of new and renewable energy technologies, like most features of industrial development, will therefore first occur in the advanced economies. This is clearly shown by today's development trends. In the present world the role of such technologies in the third world is limited, especially in the rural areas. Therefore, until economic development has brought the majority of farmers above the subsistence level, wood and agriculture wastes will continue to be the dominating source of energy for the foreseeable future.

The energy problem of the third world is not one single, simple problem. It is a complex and multi-faceted problem experienced in modern industry and the traditional households. Effective energy demand, which is not to be confused with energy need, covers a wide range of end-uses. Thus attention should be paid to questions of both supply and demand. Fuel and technologies will have to be matched to the task, which also means that renewable energies and conventional energy must be seen as complementary to each other. Current energy plans in for example, China and India explicitly state that, 'neither conventional nor renewable energy can solve the problems of rural energy development on their own'. For the foreseeable future, it will not be possible to supply rural areas with oil or grid power in large enough quantities to support the desired economic growth. This means an increased reliance on local and therefore renewable energy sources [1].

Judging from the situation in the industrialized countries, general electrification is one of the main keys to industrialization and development, this is also true in the rural areas of the

developing world. In this context, new and renewable energy technologies may also have an important role to play, sometimes as a crucial first step.

Energy is not simply a commodity – it has become a critical factor of production in addition to land, labour, and capital. There is a need to promote the renewable energy technologies, for, in the energy futures of developing countries, every contribution is critical. Local, small-scale, decentralized initiatives are indispensable in this respect as the ongoing depletion of wood fuel threatens even the subsistence base of the third world population.

Since 1981, there have been improved technologies that are viable to assess the future prospects of renewable energy. For instance, on solar energy, there are solar cookers and solar thermal pumps. More emphasize has been on photovoltaic cells and solar crop-driers which continue to develop, and seem to be spreading gradually into larger and lager market niches. Also, the use of solar water-heaters for urban and institutional water heating applications is gaining popularity [1].

It is clear that the so called 'new and renewable' sources of energy will have a very useful role to play in developing and powering the third world, as an integral part of the energy systems.

Solar energy is one form of renewable energies that has found many areas of applications both domestically and in industry. It is mainly used for water heating, air heating, and supply of electrical power, and crop drying- since the temperatures achieved are those required for drying.

The available solar energy depends on: -

1. Position of the sun in the sky.
2. The weather conditions, especially clouds.
3. The location.

On the other hand, the solar energy that will be made use of will depend on: -

1. The available solar energy.
2. The technology used to harness it.
3. The prevailing weather conditions.

The main advantages of solar energy are: -

- ❖ The energy is virtually free – after the initial cost.
- ❖ The payback period is very short.
- ❖ It is a stand-alone system (no grids and pipe networks).
- ❖ It comes in unlimited supply.
- ❖ It has no pollution effects.
- ❖ It is extremely clean.

Some of the major limitations to use of solar energy include;

- In most cases it can only be utilized during the day.
- It depends on weather conditions.
- Some solar components such as glass and battery are expensive.
- It requires technical skills.
- Condensing vapours will affect the transmittance of glass.
- Most solar energy utilizing equipments have very low efficiencies.

1.1: CROP DRYING

Drying is a preservation method for grain crops and also a necessary stage in the processing of crops like tea, pyrethrum and coffee.

Drying of crops after harvesting is an important process in the preservation of agricultural produce, yet it is at this stage where much of the crop deterioration may take place due to poor handling and incomplete drying.

Generally the main reasons for crop drying are: -

- ❖ Reduction of moisture content thereby reducing weight.
- ❖ Prolonging of crop shelf life.
- ❖ Preservation of nutritional value.
- ❖ Reduces chances of attack by insects (weevils).
- ❖ Reduction of the risk of contamination by toxic moulds.
- ❖ It allows early harvest and preparation of the land for the next season.

The drying of organic produce such as vegetables, fruits, coffee, grains, fish, cocoa, tobacco, and timber has been a regular and important feature of village life in the rural areas of developing countries. Most of the drying process is carried out using open-air techniques and, this is one of the oldest uses of solar energy. This often involves spreading the produce out on the ground and exposing it to the sun during the day and covering it at night to protect it from rain, dust, and other dangers.

The major shortcomings with this traditional open-air sun drying method are: -

- ❖ Product quality cannot be controlled since there is no control of the drying temperatures.
- ❖ There are high chances of infestation by insects.
- ❖ High losses due to scavenging animals, birds, and rodents- about 10-15% of the crop.
- ❖ Contamination by dirt, and birds and rodents droppings.
- ❖ High chances of rewetting due to rain.
- ❖ The drying process is slow, tedious, and incomplete.
- ❖ Requires constant supervision.
- ❖ Continued rewetting and drying in variable weather conditions may cause cracking in kernels and reduced chances of germination.

In order to adequately dry a material, it is first necessary to know the initial moisture content of the material to be dried and the desired moisture content of the final product. For instant cereal grains and grain legumes need to be dried from an initial moisture content of about 30% at harvest to a level of 12%, while leafy green vegetables, tomatoes, fruits, fish, and meat have an initial moisture content of about 60-80%, which must be reduced to the range of 10-25% [2].

Drying rates are controlled by the rate at which: -

- ❖ Heat is applied to the product.
- ❖ The product's internal moisture is reduced from its surface.
- ❖ Moist air is removed from the area surrounding the product.

Varying the air temperature and humidity controls the drying rate; and since, insolation levels can vary widely, solar driers must be carefully designed. Since warm dry air can only absorb so much moisture at one time, unless the air is frequently replaced, it becomes saturated and the drying process slows or stops altogether.

In general, solar air driers dry crops more slowly than conventional oil-fired hot air systems since the drying process is carried out using low temperatures and high air flow rates, whereas conventional systems use relatively high temperatures and low air flow rates. Rapid drying rates are often inappropriate for crops such as rice, which are dried to best effect when subjected to slower drying rates which are usually obtained with solar driers.

Controlled drying in specially designed driers produces much better quality products with greatly reduced losses. In controlled solar driers, air is heated in a solar collector and then ducted through to the drying chamber, where the material to be dried is situated. This preserves the quality of the material from deterioration.

Some of the crops that can be dried by using a solar collector incorporated into a drier include: - Cereals (maize, beans and groundnuts), Leafy green vegetables, Tobacco, Coffee, Tea and Cacao. Most of these crops require dry warm air at moderate temperatures in the range 50-70°C which are attainable in flat-plate collectors. For instance, a maximum grain temperature of 40°C is usually recommended for drying grain for seed (more than this will kill the germ in most grains), while grains for milling require temperatures below 60°C to avoid decrease in separation (mill ability). Therefore since these temperatures are attainable in flat-plate solar collectors, there is a need to emphasize their use and improvement in efficiency [3].

1.2: FLAT-PLATE SOLAR AIR HEATERS [COLLECTORS].

Solar energy is converted into thermal energy by use of solar collectors, which make use of the greenhouse effect. The thermal solar collection systems fall into two broad categories: -

1. Concentrating collectors and,
2. Flat-plate collectors.

Concentrating collectors collect the sun's rays from a relatively large area and focus them on a point. The collector makes use of parabolic (bowl-shaped) mirrors that can create extremely high temperatures (over 1000°C) which can be used to generate steam. The concentrating collectors require precisely constructed surfaces and a tracking device to follow the sun across the sky during the day. Due to this, they are relatively expensive and need much maintenance. In drying, there are rare cases of the need for very high temperatures, hence the concentrating collector do not have much applications.

The flat-plate collector requires no tracking device to capture the sun's energy and, absorbs energy directly from the sun as well as indirect or diffuse radiation. They are capable of providing air temperatures up to 65-93°C and are relatively simple to build [4]. There are many different designs for flat-plate collectors, but they all have two common characteristics;

1. A flat plate to absorb energy from the sun.
2. A circulating medium to pick heat up from the plate and transport it to storage or the point of use. The two media most commonly used for absorbing and transferring the heat are air and water.

Air for drying grains can be heated by passing it through a solar air collector. The use of a solar air heater is appropriate since, most parts of Kenya have plenty of sunshine during harvesting seasons.

The flat-plate solar collector for heating air is simply a box insulated at the bottom and sides, with one or more transparent covers made of glass or plastic in order to minimize heat loss to the surroundings. However, more than two covers are discouraged to eliminate shading effects. An absorber plate is positioned below the covers which in most cases is painted black and under it is a back plate. Between the glass covers, the absorber plate and the back plate are insulation air gaps or flow channels depending on the nature of the collector design and the purposed application of the heated air.For a two cover flat-plate collector, when solar irradiation strikes the outer cover, it may be transmitted, reflected or absorbed. For a transparent cover, most of irradiation will be transmitted. The transmitted energy is incident on the second cover where, it is mostly transmitted to the absorber plate. The absorber plate heats up; thereby transferring heat to the air flowing over it.

Figures 1.1, 1.2, 1.3, and 1.4 (page 12) show the various modes in which air can be made to pass through a two cover solar collector- as explained below;

- Figure 1.1 shows the single pass mode in which air passes between the absorber plate and the back plate.
- Figure 1.2 shows the double (top first) pass mode in which the air passes between the two covers in the first pass and then between the absorber plate and back plate in the second pass.

- Figure 1.3 shows the double (middle first) pass mode in which air passes between the lower cover and the absorber plate in the first pass and then between the absorber plate and the back plate in the second pass.
- Figure 1.4 shows the triple pass mode in which air passes between the two covers in the first pass, between the lower cover and absorber plate in the second pass and then between the absorber plate and the back plate in the third pass.

Most of the research previously done has been based on steady state conditions and has concentrated on determining collector efficiency, effects of parameters such as: mass flow rate, solar insolation, collector dimensions and components on the collector performance. The relation equations were based on steady state conditions, which is not normally the case in varying weather conditions [4, 5, 6].

For instance, the criterion generally used to compare the performance of solar collectors is efficiency which is the fraction of the incoming solar radiation that is transferred to the flowing air, and assumes the existence of steady weather conditions. Also most of the relations and equations describing the performance of solar air heaters have been arrived at by assuming the existence of steady state conditions which are not experienced in reality because of changing weather conditions [7].

The major problem experienced with solar dryers is their unreliable performance since their operation depends largely on local weather conditions that in turn mostly affect the quality of the dried product.

This thesis has attempted to provide a method of predicting the thermal performance of solar air heaters operating under transient varying conditions. This will assist in determining the most optimal system both technically and economically. The prediction method took into account the time varying and weather changing processes of the system. It involves the use of theoretical approaches in analyzing the collectors operating in the four modes, together with the use of simple and easily measurable system and environmental data such as insolation, ambient temperature, and wind velocity. The validity of this prediction method was checked using the results of a series of experiments done on the collector operating on the four modes of pass.

1.3: OBJECTIVES.

The objectives of this study were to:

1. Develop a theoretical model based on the steady state works of Korir[4] and Luti[6] and, the transient work of Kabeel[17} to predict the performance of solar air heaters operating under transient conditions for the four modes of flow;
2. Use the results of a series of experiments to check the validity of the theoretical model

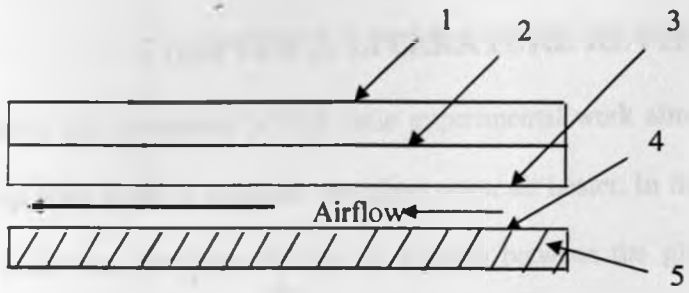

Figure. 1.1. Single pass mode.

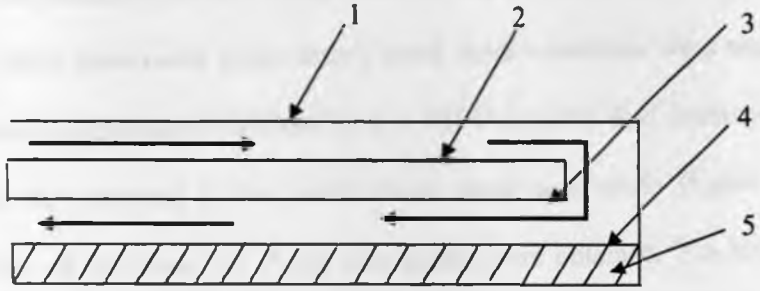

Figure. 1.2. Double (Top first) pass mode

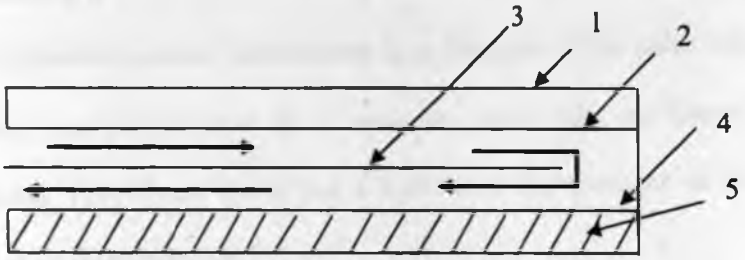

Figure. 1.3. Double (middle first) pass mode.

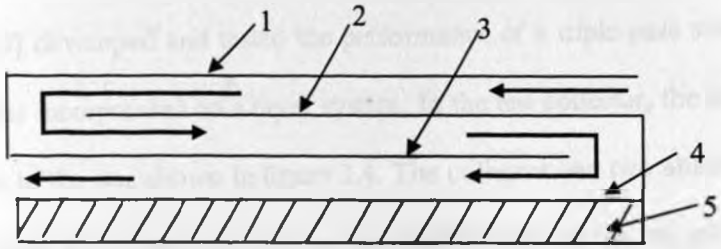

Figure. 1.4. Triple pass mode.

1. Top glass cover.
2. First glass cover.
3. Absorber plate.
4. Back plate.
5. Insulation.

Satcunanathan and Deonarine [8] did some experimental work aimed at reducing the losses from the top glass cover of a simple two-glass cover air heater. In this, a unit was constructed in which there was provision for the air to pass between the glass panes before passing through the blackened metal collector, double (top first) pass mode (figure 1.2). It was found that, the outer glass cover temperatures under these conditions were significantly much near atmospheric temperatures (differed by 4 to 10^0 C over the day) compared to those when the collector was operated in the conventional single-pass mode (figure 1.1). Consequently, efficiencies of the order 10- 15 per cent higher were obtained. The behaviour of the heater efficiency, heat collected and rise in air temperature were studied as functions of time, with the time starting at solar noon and steady state conditions assumed. The results indicated that the solar collector thermal performance is a function of the solar time of day. This work concentrated on performance of a two-pass mode solar air heater, which was purely experimental. They found that it had a significant improvement on the performance of the collector at no increased cost.

Ezeike [9] developed and tested the performance of a triple-pass solar collector (figure 1.4) which was incorporated on a dryer system. In the test collector, the air flowed in the opposite direction to the one shown in figure 1.4. The collector had two absorber plates and one glass cover. Solar insolations and temperature distributions inside the collector were measured at 30-min intervals. Outlet air temperatures in the range of 90-100°C on clear days and at air velocities of up to 3.5 m/s were achieved with efficiencies of 73-81%. These were attributed to the minimized heat losses to the environment, as a result of the air flow pattern in the collector. From the performance curves obtained, it was clear that the thermal performance of

the collector depended on the time of the day, but there was neither mention of such nor theoretical analysis to explain the relations.

Wijeysundera [10] developed heat transfer models based on steady state conditions for two-pass flow arrangements (figures 1.2 and 1.3) and compared them with the performance of the conventional single-pass design (figure1.1). The computer models were validated with experimental data from a series of collector testing experiments. Design curves for the two-pass systems over a range of variables were presented, which were aimed at providing optimum design conditions for such collectors. Also the model was used to predict the collector efficiency and the fluid temperature rise. The experimental data were obtained by averaging over 15 minute intervals with some intervals having intermittent cloudy periods. Also the experiment was set for a constant value inlet air temperature that was difficult to maintain. Hence the models can not be used for collector performance prediction under transient conditions, because it concentrated mostly on the collector parameters without giving attention to the changing weather condition.

Persad and Satcunanathan [11] developed steady state analytical models for the performance prediction of a two-glass cover solar air heater operated in both the single-pass (figure 1.1) and double-pass modes (figures 1.2 and 1.3). Their work concentrated on the comparison of the performance of the collector for different operating and design parameters such as; air inlet temperature, length of the collector and, plate spacing. The model yielded closed-form solutions for the temperature profiles of the glass covers, plates and air streams. The resulting equations could be solved by numerical methods, which required boundary conditions or by use of analytical methods. In the analysis, the effects of the thermal capacitance of the collector components were not considered since steady state conditions were assumed. Again

the analysis was based on a typical clear day, which is not normally the case in use of solar air heaters. Although it was found that the two-pass modes were superior to the single-pass mode of operation, the modes were not compared based on transient conditions.

Ramjattan [16] designed, tested and described the performance of single (figure 1.1), double (figures 1.2 and 1.3) and triple (figure 1.4) pass modes air heaters. The testing was done for several operating parameters and the performances compared. Theoretical analysis for the heat balances on the components was done based on steady state conditions. The component temperatures were expressed as functions of the heat transfer coefficients, and then the heat gain solution obtained. The solutions were obtained based on the assumption that the heat transfer coefficients are independent of the component temperatures which is not the case, since they vary with temperature.

Elsewhere, Satcunanathan and Persad [12] had simultaneous testing of three identical collectors operating in the single-pass (figure 1.1), two-pass (top first) (figure 1.2), and three-pass (figure 1.4) modes in ambient conditions. They concentrated on the nature of performance for a range of mass flow rates. The collectors used consisted of two glass covers, an absorber plate, a rear plate, rear and side insulation, and an outer casing. The component temperatures were measured at appropriate points by copper-constantan thermocouples connected to a 24-point Honeywell strip chart recorder. The experiment generated plots of heat collected, collector efficiency, and air temperature rise against time of the day. Satcunanathan and Persad [12] noted that further experimental or analytical studies were needed to draw conclusive evidence in order to know the best mode of pass to operate flat-plate collectors. There was no computational or analytical model that could help predict the performance of the collectors.

Luti [6] used a model to extensively predict the performance of the two glass cover solar air heater operating in the single (figure 1.1) and double pass (figures 1.2 and 1.3) modes. It was revealed that some conclusions arrived at previously were not of a general nature as the parameter ranges were not wide enough. More extensive 'design curves' were presented and it was deduced from the curves that, it was possible to delineate which parameters and their ranges are critical and should be paid special attention in laboratory modeling. The method used for the model was same as that of Satcunanathan and Persad [12], yielding closed form solutions. The net solar radiation method was used to calculate the solar radiation absorbed by the glass covers and the absorber plate. The ambient air velocity was assumed to be zero while the ambient air and inlet air temperatures were taken as fixed parameters. Although a wider range of parameters were used, the analysis was for quasi-steady state conditions.

Maclennan [14] determined the effects of changing the input parameters on the efficiency for various solar air heaters. This involved a computer simulation model that used various mass flow rates and input temperatures. There was consideration of laminar flow for all the passages of the heater. An iterative procedure was used to solve the computer simulation model with the heat transfer coefficients set as the convergence criterion. This analysis assumed that, the system was in steady state conditions, and constant wind velocity prevailed.

Duffie and Beckman [15] describe the work of Hotel and Woertz as the first attempt to analyze a solar collector on single pass mode. They analyzed a water solar heater, which had a blackened-metal as the absorbing surface. Above and parallel to the absorbing surface were three sheets of high quality glass. Their model was based on an overall energy balance on the absorbing surface. The energy influx was the solar energy incident on the collector's surface that was transmitted through the glass plates and absorbed by the absorbing surface. The

thermal losses were categorized as top losses, back losses and heat capacity losses. The prediction of the top losses was simplified by the introduction of the concept of the top loss coefficient, which was based on the mean top plate temperature. Calculation of this coefficient was done using an empirical formula. The effects of dust and dirt on the collector, and the shading of the absorbing surface by the collector sidewalls and cover supports were included in the empirical model. The effect of the side losses and the solar energy absorbed by the glass covers on the performance of the collector were not considered, this could have significant effects on the predicted values.

Duffie and Beckman [15] noted that the model of Hotel and Woertz was improved by Whillier, who introduced the concept of the effective transmittance-absorptance product to account for the energy absorbed by the glass covers. Whillier derivation of the collector efficiency factor for overlapped-glass plate collector had numerous assumptions and hence, over-simplified to accurately predict the performance of the collector.

Bliss presented the derivation of the collector efficiency factors for several collector designs not considered by Whillier from fundamental heat transfer concepts. He noted that his results were in agreement with those of Whillier, Hottel and Woertz, but that his analysis was more refined in that he included the effects of atmospheric radiation. As Duffie and Beckman [15] describes.

Buchberg and Roulet presented a model for a solar water heater. Their model was based on the assumptions that the temperature of the glass cover and the absorbing plate were uniform and that the temperature rise of the water in any channel was linear and steady state. The equations of this model included the solar energy absorbed by the glass cover, and were

solved for the thermal efficiency of the collector in terms of the non-linear thermal resistances of the collector's thermal network and the solar energy absorbed by the glass cover and absorber plates, which yielded a closed form solution for the efficiency of the collector. As Duffie and Beckman [15] describes.

Selcuk analyzed the overlapped-glass plate solar air heater for the purposes of optimizing the design features of the collector under steady state conditions. His solution was a numerical one, the procedure being to divide each section of the collector into ten subdivisions. Comparisons of the experimental and theoretical results showed good agreement at high flow rates and poor agreements at low flow rates. He concluded that for low flow rates, free convection effects are important and thus the flow regime is one of mixed flow. However, he noted that no heat transfer coefficients for this flow regime existed and hence the use of the forced convection heat transfer coefficient led to the observed discrepancy between the theoretical and experimental results. As described by Duffie and Beckman [15].

Klein investigated the heat capacity effects of a sheet and tube type solar water heater using three different models. The first, a quasi-steady-state model, where he simulated the performance of a collector of zero capacitance. The second model accounted for capacitance effects by assuming that a single value of thermal capacitance can be determined for the collector as a unit. The third model, a quasi-steady-state divided the collector into many isothermal segments or nodes. He noted that the time constant of all the nodes of a multi-node model were of the order of a few minutes. He then concluded that since, in general, the best meteorological data available are in hours, using this data, no collector model, regardless of its complexity, would be capable of predicting the transient response of the collector. He further concluded that a one-node model is as complex a model as is needed to predict the

performance of a flat-plate solar collector based on hourly meteorological data and that the zero capacitance model provided almost as good prediction as the one-node model with less computational effort. He further concluded that, the use of more complex models cannot be justified when adequate meteorological data are not available. This calls for a model that can work with minimum meteorological data. As Duffie and Beckman [15] describes.

Ramsay and Schmidt presented a numerical model for a solar water heater. Their model, which accounted for non-uniform temperature distributions and transient conditions, was developed by dividing the collector into a number of physical elements or nodes. They noted that, for steady-state conditions, the performance of the collector predicted by their model was in good agreement with that predicted by the Hottel-Whillier and Bliss (HWB) model, no model was provided for solar air heaters under transient conditions. As described by Duffie and Beckman [15}.

Wijeysundera presented a model for predicting the transient behaviour of a single cover solar air heater operating on the single pass mode (figure 1.1). His model was based on lumped formulation and the resulting non-linear coupled partial differential equations were linearized. He found that the response time of the collector increased with the thickness of the cover material and the absorber plate, and decreased with decreasing plate emissivity. Also, higher absorber operating temperatures and lower collector efficiencies resulted in larger response times while, within operating limits, the extinction coefficient of the cover material and the insulation heat losses did not affect the response time significantly. As Duffie and Beckman [15] describes.

Caouris et al presented the first analysis of a multi-pass collector. In this work the collector consisted of a series of parallel plates, which were transparent in the visible and near infrared part of the spectrum and had small thermal conductivities. The last plate, which was painted black, absorbed the solar radiation. The working fluid that was a liquid had a high transmittance in the visible and near infrared part of the spectrum and nearly zero transmittance at longer wavelengths. They presented a theoretical analysis for a collector of multi-glass covers. The model was a simplified one, for it was assumed that the fluid temperature in every pass varied in a linear manner with the spatial coordinate in the direction of flow. The equations resulting from this analysis were solved numerically. As described by Duffie and Beckman [15].

Persad [2], developed a generalized analysis for the prediction of the performance of flat-plate solar collectors, this was done by postulating a generalized multi-pass solar air heater under steady state conditions and deriving a mathematical model for it. The model was shown to be capable of representing any multi-pass solar air heater design. This model yielded closed form solutions for the temperature distributions of the plates and air streams. The model was also capable of predicting the performance of multi-pass solar air heaters *when both the hydrodynamic and thermal boundary layers merge within the flow channels* and also when neither the hydrodynamic nor thermal boundary layers merge within the flow channels. A generalized method based on the model developed was presented for the determination of the effective transmittance-absorptance product, the overall loss coefficient and the collector efficiency factor for single pass solar air heaters. It was shown that the generalized performance equation developed for multi-pass solar air heaters is the generalized performance equation for flat-plate solar collectors and can predict the performance of other collector types and the effect of various parameters on the performance

of flat-plate solar collectors. The developed model was tested by predicting the performance of a two-glass cover solar air heater when operated in both the single-pass (figure 1.1) and two-pass (top first) modes of operation. This indicated that the two-pass mode of operation led to improved collector performance. Although the developed equation gave comparable results to the HWB model, it was developed based on steady-state mode of operation and conditions.

Korir [4], presented expressions for predicting steady state performance of solar air heaters operating in four modes as shown in figures 1.1, 1.2, 1.3, and 1.4. The expressions were derived and solved using a computer program and, validated by use of results from a series of experiments. It was found that the four modes differed in their performance over the range of parameters considered. The triple pass mode gave the best performance followed by the double pass modes. The single pass mode was found to give the most inferior performance as compared to other modes. The superior performance of the triple pass mode as compared to other modes was attributed to a lower top cover temperature, which meant a lower heat loss to the surroundings. In this work, steady state conditions were taken at intervals of 15 minutes, effects of change in weather conditions within the 15 minutes were neglected.

Luti [6] analyzed Korir's experimental data of the comparative performance of double glazed solar air heaters operating in the single pass, double passes, and triple pass modes, as in figures 1.1,1.2,1.3,and 1.4. The four heaters used were tested side by side and were of identical construction. The collectors were of fixed effective width and length of 0.9m and 1.5m respectively with the stationary air gaps fixed at 40mm. Air was blown into the heaters rather than being sucked, since air emerging from the collectors exceeded the maximum permissible temperature of the fans. The experiment was conducted for three mass flow rates

of 0.004Kgs^{-1}, 0.0081Kgs^{-1}, and 0.0121Kgs^{-1} and three flow channel heights of 10mm, 20mm, and 30mm. The experimental results of interest were air temperature rise, solar insolation and collector efficiency, as functions of solar time for a given mass flow rate. The data was averaged over 30 minute intervals. For high temperature production, the triple pass mode was found to be far superior to the other modes when operating at a flow channel height of 10mm. For normal insolation, temperature rises of over 100°C were achieved at reasonable efficiencies. The magnitude of the temperature rise could be controlled by regulating the mass flow rate. In discussing the results, when the insolation was compared to the air temperature rises, it was apparent that there was a time lag between the two. This obviously suggested that the use of steady state models to predict solar collector performance cannot yield good agreement with observation, except in the rare (and hence unimportant) cases when prolonged nearly constant insolation periods prevail.

Simonson [3] gives a transient analysis of flat-plate collectors. He takes into consideration that, solar irradiance may be subjected to very rapid transients as well as diurnal and seasonal variations. A solar collector has a very small time constant, and consequently a rapid response to changes in solar irradiance. Two approaches have been considered in handling the transient problem, one is an analytical method and the other is a simple finite-difference scheme based on a transient heat-exchanger.

In the analytical approach, a single-glass-cover collector was considered, and divided into two main thermal components. The first being the absorber plate, back-insulation, and the fluid contained in the channels, which formed a combined thermal capacity. The second was the transparent cover with its own thermal capacity. Energy balances were done on the two thermal capacities with an assumption of uniform absorber plate and cover plate temperatures

during the considered transient period. A simplification in the solution of the two equations obtained was made by assuming that at any given time the loss between the absorber plate and the surroundings is proportional to the loss between the cover and the surroundings. This led to the assumption that, steady-state conditions are existing for the temperatures attained at any particular instant, but this is least likely to be so at the beginning and end of any given transient. The edges and back losses were neglected and the ambient temperature assumed to be constant. The derived equation could be solved for given input values for solar insolation and ambient temperature to give a value for the future absorber plate temperature. This was a purely theoretical analysis of single-glass-cover collector and there was no experimental data to validate the expression.

The finite-difference approach method is easily applicable to collectors with one or more covers, and is suitable for a simple computer program. Also it can be used to study the performance over periods of a few hours or a day under varying input conditions. Here the absorber plate and the insulation are considered as a single element at a common initial temperature and in thermal contact with the fluid flowing through the collector. Then the covers are considered such that each is a separate element. Finally separate energy balance equations are written for each element and the future component temperatures solved using a forward time step. The set of equations considered gave a maximum time step of around 80-100 seconds with a permissible smaller time step of 60 seconds considered to be convenient. The prediction expression has no experimental validation and, depended on data obtained under steady-state conditions recorded on hourly basis. It was found that the transient program calculated a smaller total solar gain for the day than does the hourly steady-state procedure. This indicated that, if the transient effects are neglected, the steady-state procedures could result in overestimates of the solar gain. As Simson [3] describes.

Kabeel and Mecarik [17] constructed two solar air heaters, one with longitudinal fins absorber and the other with a triangular absorber plate. The area of the first collector was equal to 1.66 that of the second. This work involved studying the numerical model and computer program for the two types of solar air heaters. The temperatures at different points on the solar air collector, useful heat gain, collector efficiency, and all collector parameters were calculated. A comparison between the theoretical and experimental analysis was made. The theoretical model depended on the energy balance equation for each part of the solar air heater. It was assumed that the flow is one dimensional, unsteady state conditions prevail, flow is incompressible, properties of air are constant, viscous dissipation is negligible, and back and side losses are negligible. The two air heaters had the same main shape, dimensions and construction. For the longitudinal fin collector, the distance between the fins was 0.05m with a height of 0.05m. While the triangular cross section shaped absorber plate had an angle of 60^{o} with a triangular height of 0.05m. The theoretical model indicated that the collector component temperatures increased with the length at different times from morning till solar noon for a mass flow rate of $0.005kgs^{-1}$. For the triangular absorber solar air heater, the absorber plate temperature reached a maximum of $158^{o}C$ with a mass flow rate of $0.005kgs^{-1}$, while it reached a maximum of $112^{o}C$ for the longitudinal fin absorber with a mass flow rate of $0.02kgs^{-1}$. A comparison of both the theoretical and experimental results indicated that the triangular absorber plate collector was superior to the longitudinal fins absorber collector. This analysis considered two parallel flow channels, which are located above and below the absorbing surface, through which air was simultaneously passed, the direction of air in each channel being the same. There was no consideration of multi-pass collectors with the air flowing in one channel at a time; hence there is a need to examine the collector behaviour for this case under transient conditions.

Solar flat-plate collectors are normally tested under steady state or quasi-steady conditions. It takes long time to test a collector in view of the stringent requirements of steady state methods. Due to this, transient test methods have been developed to circumvent the difficulties associated with steady state tests. Based on these methods experimental tests could be conducted round the year and under highly variable weather conditions. Amer's et al [18] reviewed the existing transient methods and classified them into six groups according to their approach methods. Further the methods were assessed and their limitations pointed out. The groupings are identified as: indoors methods, multi-node methods, response function methods, multi-test methods, and unvalidated methods.

Munroe [19] conducted an indoor test using a simulation model. The test was performed in front of an artificial sun. A single lumped capacitance for the collector was assumed, and it was referenced to the mean temperature of the fluid. During the test, the collector was connected to a storage tank and temperature, mass flow rate, and solar insolation measurements taken every minute. An expression for the instantaneous efficiency was obtained, and a linear graph plotted from which the values of the overall heat transfer coefficient and the collector transmittance-absorptance product could be obtained. This test was not based on the natural weather conditions and also it considered a single lumped capacitance, which might be not good enough to compare with practical situations.

Souproun [20] proposed an indoor method based mainly on the analysis of a single experimental heating and cooling curve. The method required long heating hours, for instance about 90 minutes for the heat transfer fluid to exceed a temperature of 60°C, if the test is performed outdoors; hence the method is suitable for indoor tests where a solar simulator is used. Analyzing the curves, helped to calculate the heat losses and the thermal efficiency of

the collector as functions of the ratio between heating and cooling times elapsed to cause a temperature change between certain levels. This being an indoor test method is costly and requires long hours for outdoor test under steady state conditions. Also it is difficult to have a realistic simulation of the actual sky temperature in the indoor environment.

Arronovitch [21] proposed a simple test method that simply adds the thermal capacity of the collector to the steady state energy balance. In his approach, he defined efficiency as the ratio of the sum of the stored and carried away energies to the incident energy. It was suggested that, during the test, the inlet temperature need not be measured. A limitation to this method was that, it can only be applied to slowly varying insolation.

Perers [22] described a simple method for collector array testing. The model characterizes the thermal power output of a collector using one-node capacitance to include the dynamic effects and separate incidence angle modifiers for direct and diffuse radiation. A continuous flow was applied in the collector loop during the test and data for the whole day recorded with a sampling interval of 6 seconds. Applying multiple regression routines to the experimental measurements identified the collector performance parameters.

Hawlader and Wijeysundera [23] extended the single flow technique of testing of heat exchangers to test solar collectors. A two region mathematical model was developed in which the cover capacitance was lumped with the absorber plate as region while the fluid was treated as a separate region. The model was solved analytically using Laplace transforms technique for plate and fluid temperatures. The test was conducted in a place where the collector was not exposed to the sun. Temperatures measured were, fluid inlet and outlet, and absorber plate mid-point. The experiment was repeated at different flow rates and inlet

temperatures. The model required a guess of the collector parameters in order to find a best fit for the experimental measurements with theoretical calculations. This method did not provide any information about collector optical efficiency and, required measurements of absorber plate temperature that is not always practicable. Further, the fluid outlet temperature estimated from the model differed substantially from the experimental measurements.

Kamminga [24] developed a 3-node mathematical model (cover, plate, and fluid) to describe the transient behaviour of collectors. Relations for the collector characteristics were obtained using Fourier transformations. The collector parameters were found using least square analysis to experimental measurements. The model has a limitation due to the instability of data processing; hence only a limited range of time interval and Fourier variables lead to appropriate regression coefficients. Also the results from different time intervals indicated a large scatter.

Amer's et al [18] reviewed the work of Spirkl [59] which involved developing a dynamic parameter identification method for testing flat-plate solar collectors under non-stationary conditions. The method involved;

1. Estimation of the residual difference between the measured and the predicted collector output.
2. Low pass filtering of this difference to minimize the impact of transient modeling and measurement errors that cancel within a short time while retaining a maximum amount of information.
3. A least squares technique to minimize the resultant residual.

According to the model, the dynamic behaviour of the collector was characterized by a thermal capacity which lumped together the fluid content and the collector thermal mass. The collector was divided into two segments in the flow direction, each segment being treated as a separate node. Measurements were made for several days at constant mass flow rate and variable fluid inlet temperature and solar radiation. To predict the collector output, an initial guess for the collector parameters had to be made. Muschaweek and Spirkl validated this model for a flat plate collector. They found that the theoretical prediction of the fluid outlet temperature was close to experimental measurements within 0.2K. A limitation to this model is its inconsistence thermal capacitance of the collector. As Amer's et al [18] describes.

Saunier and Chungpaibulpatana [25] developed a model which considers one-node capacitance and assumes a quadratic function (in temperature difference, ΔT) for collector heat losses. On the basis of this model, a transient method was proposed to test flat-plate collectors under zero efficiency conditions. The method required two tests;

1. A night test when the collector is subjected to several heating and cooling cycles each about 1.5 hours.
2. A day test when the collector is exposed to prevailing environmental conditions.

Measurements of solar radiation, fluid and ambient temperatures, and power consumption were taken every minute. The collector performance parameters were determined using multiple regression analysis to experimental measurements. This was a good method since there were no measurements of mass flow rate and temperature rise across the collector, but it requires a long inconvenient night time test.

Rogers [26] outlined a response function method employing a test approach and a set-up similar to those of steady methods. The British Standard Institution has adopted the method as a standard for collector testing under transient conditions (BS6757; 1986). The model assumed that the thermal output of a collector during any time is the sum of the fractions of energy gained during that time interval and a few preceding intervals. These fractions are the coefficients of the impulse response function of the collector which characterizes its dynamic response to weather variations. Experiments were held at 4 different fluid inlet temperatures evenly spread over the operating range of the collector. The experimental data were averaged over one minute. For every inlet temperature, 60 records of average values for the measured parameters have to be made. Collector parameters as well as the response function coefficients were determined using Linear Least Square regression method. The results of this method are lower than steady state results. Limitations for this method are:

1. The method leads to handling of large sets of data and enormous off-line computations are needed.
2. The response function is obtained indirectly.
3. Stringent control of fluid flow rate and inlet temperature is required.

Wang et al [27] suggested that a modified one-node model in the form of equation (2.1) could describe the performance of solar collectors under transient conditions.

$$S_1 S_2 \frac{d^2 q_u}{dt^2} + (S_1 + S_2)\frac{dq_u}{dt} + q_u = F_R(\tau\alpha) I_T - F_R U_L (T_i - T_a) \quad \text{----------2.1}$$

Where,

$S_2 = 0$ refers to First Order model.

The time constants S_1 and S_2 are obtained from a separate shielding test and are used to construct the response function.

F_R = the heat removal factor (as defined by Duffie and Beckman [15]).

Linear Least Square analysis was used to identify collector parameters. The method yields results similar to those obtained when using Rogers's method.

Frid [28] developed two-node and three-node collector models. The exact solutions of the models were also obtained. The solutions gave the collector useful heat as functions of its parameters and other response functions. Regression analysis was suggested to find collector parameters and response function elements. So far, an experimental study has not been carried out to justify the cumbersome analytic solution.

Up to this point, it is clear that there is a need for models of collectors performances based on transient conditions since the flat-plate solar air heaters will nearly always operate under transient conditions. This model will help in giving accurate predictions concerning the collectors and through this the installation of solar collectors will be cost effective since there will be no overestimates or underestimates. Also given the fact that, the insolation fluctuates with time; the transient models will be able to predict the air outlet temperatures for specified insolation levels.

From the foregoing literature, it can be observed that:

1. No comprehensive analysis has been done on the performance of the two glass cover multi-pass solar air heaters operating under transient conditions.
2. Not enough experimental data has been given to validate or back the theoretical models for transient conditions.
3. There are no prediction models for flat plate solar air heaters for transient conditions.

CHAPTER 3: RELATED THEORY

3.1: SOLAR RADIATION.

The sun is one of a vast number of stars within the Milky Way Galaxy and it contains over 99 per cent of the matter within the solar system. It is a sphere of intensely hot gaseous matter with a diameter of 1.39 X 10^9m and is, on the average, 1.5 X10^{11}m from the earth. The sun has an effective surface temperature of approximately 5760K and emits radiant energy at the rate of 380 X10^{15}GW.

The earth travels round the sun in $365\frac{1}{4}$ days with the axis of rotation of the earth at an angle of 23.45° to the plane of rotation around the sun, which results in seasonal changes in the illumination of the earth. In addition the path of the earth around the sun is slightly elliptical, so that the intensity of solar radiation outside the earth's atmosphere, the solar constant, varies slightly throughout the year. The value of the solar constant, G_{sc}, is estimated to be 1353W/m^2 [15].

3.1.1: Extraterrestrial radiation on horizontal surface.

Most radiation calculations are conveniently done using normalized radiation levels, that is, the ratio of radiation level to the maximum possible radiation that would be available if there were no atmosphere.

At any point in time, the solar radiation outside the atmosphere, G_o, incident on a horizontal plane is,

$$G_o = G_{sc}\left[1+0.033\cos\left(\frac{360n}{365}\right)\right]\cos\theta_z \qquad (3.1)$$

3.2: CALCULATION OF INCIDENT RADIATION.

To predict solar performance, past measurements of solar radiation at the location in question or from a nearby similar location are used. The following terms are involved;

1. Solar or short-wave radiation: These is radiation originating from the sun in the wavelength range of 0.3 to 3.0μm, includes both beam and diffuse components.
2. Long-wave radiation. This is radiation originating from sources at temperatures near ordinary ambient temperatures and thus substantially all of wavelengths greater than 3.0μm. Can be emitted by the atmosphere, by a collector, or by any other body at ordinary temperatures.

Calculation of incident solar radiation depends on the available solar radiation data which can be obtained by use of either a Pyrheliometer (measures only beam radiation) or a Pyranometer (Solarimeter) - measures total radiation.

The data recorded must include total and diffuse irradiation on a horizontal surface, with their difference being equal to the beam radiation.

The angle θ is continually changing, but since δ is taken to be constant for any particular day and ω is assumed to be constant at the mid of every hour, the value of θ may be considered constant for a given hour and then used with irradiation values of I, rather than irradiance values of G.

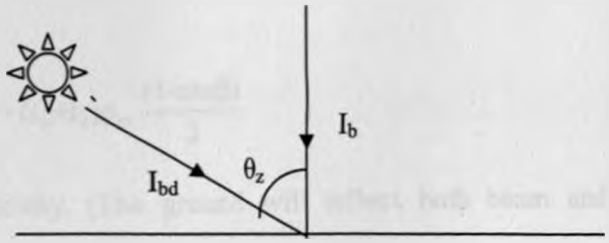

$$I_b = I_{bd}\cos\theta_z$$

Figure 3.1: Beam radiation

Where, I_b= component normal to the surface

The magnitude of the sun's direct beam component I_{bd} is related to the beam component normal on a horizontal surface by [15],

$$I_b = I_{bd} \cos \theta_Z \tag{3.2}$$

Where θ_Z is the zenith angle.

For an inclined surface at angle β to the horizontal, the beam component normal to the collector surface I_{bn} is given as,

$$I_{bn} = I_{bd}\cos \theta \tag{3.3}$$

Where, θ is the sun's zenith angle, for an inclined surface at angle β.

An inclined surface will receive diffuse radiation from the sky plus reflected radiation from the ground. A simple approach that was used by Liu and Jordan [29] is to assume isotropic diffuse sky radiation, and use a view factor of $\frac{(1+\cos\beta)}{2}$, so that the diffuse sky radiation reaching a flat inclined surface, I_{di}, may be obtained by,

$$I_{di} = \frac{(1+\mathrm{Cos}\beta)}{2} \tag{3.4}$$

For an inclined flat surface of infinite extent the view factor for reflection from the ground is $\frac{(1-\cos\beta)}{2}$, so that ground reflected contribution on the inclined surface, $I_{gr_{ref}}$, is;

$$I_{gr} = (I_b + I_d)\rho_{gr}\frac{(1-\cos\beta)}{2} \quad (3.5)$$

Where ρ_{gr} is the ground reflectivity. (The ground will reflect both beam and diffuse radiations). Total incident irradiation on the inclined surface in the hour is therefore,

$$I_n = R_b I_b + I_d \frac{(1+\cos\beta)}{2} + (I_b + I_d)\rho_{gr}\frac{(1-\cos\beta)}{2} \quad (3.6a)$$

Where,

$$R_b = \frac{I_{bn}}{I_b} = \frac{\cos\theta}{\cos\theta_z} \quad (3.6b)$$

ρ_{gr} is usually taken as 0.2 for ground not covered by snow, and 0.7 for a ground covered with fresh snow.

For a horizontal surface $\beta=0$, hence $R_b=1$ (since $\theta = \theta_z$) and there will be no ground reflection, thus total irradiation on a horizontal surface in the hour is,

$$I_n = I_b + I_d. \quad (3.7)$$

As solar radiation penetrates the atmosphere, it is depleted by absorption and scattering. Not all of the scattered radiation is lost since part of it eventually arrives at the surface of the earth in the form of diffuse radiation. Liu and Jordan [29] gave the assumption that, the diffuse radiation received on a horizontal surface is half of the solar radiation scattered by the atmospheric constituents.

Liu and Jordan [29] developed an empirical relationship between the transmission coefficients for beam and diffuse radiation for clear day:

$$\tau_d = 0.2710 - 0.2939\tau_b \quad (3.8)$$

Where, $\tau_b = \frac{G_b}{G_o}\left(\text{or}\frac{I_b}{I_o}\right)$ is the transmission coefficient for direct solar radiation and

$\tau_d = \frac{G_d}{G_o}\left(\text{or}\frac{I_d}{I_o}\right)$ the transmission coefficient for diffuse radiation on a horizontal surface (ratio of diffuse radiation to extraterrestrial radiation on a horizontal plane).

Further, a relation between the transmission coefficients for total radiation and diffuse radiation on a horizontal plane was derived [30] as;

$$\tau_d = 0.3840 - 0.4160\tau_T \tag{3.9}$$

where τ_T is the ratio of the intensity of total radiation on a horizontal surface to the intensity of radiation incident upon a horizontal surface on top of the atmosphere

and τ_T is given by , $\tau_T = \frac{G_T}{G_o}$ (3.10)

At any time the beam radiation on a surface is given by,

$$G_b = G_{on}\tau_b\cos\theta \tag{3.11}$$

3.3: HEAT TRANSFER RELATIONS.

Thermal radiation is electromagnetic energy that is propagated through space at the speed of light. Solar radiation outside the earths' atmosphere has most of its energy in the range of wavelength 0.3 to 3.0μm, whereas solar energy received at the ground is substantially in the range of 0.29 to 2.5μm.

3.3.1: Some Fundamentals of Radiation.

Thermal radiation comprises the ultra violet, visible, and infrared radiation in the wavelength range of about 0.1 to 100μm. Solar radiation occurs in the range 0.1 to 3.0μm.

All mater at a temperature above absolute zero emits thermal radiation. Energy incident on the surface of a body may be partly absorbed, partly reflected and partly transmitted.

If the fractions of the incident energy that are absorbed, reflected and transmitted are denoted as α,ρ and τ respectively, then it must follow that;

$$\alpha + \rho + \tau = 1 \qquad (3.12)$$

For opaque materials $\tau = 0$ and consequently $\alpha + \rho = 1$.

Absorption takes place at the surface, which results in an increase in temperature. This gains in internal energy of the cooler regions, or convected away. But some of it is radiated at a wavelength in amount corresponding to the temperature and the nature of the surface.

For transparent materials, for which $o < \tau < 1$, absorption will take place throughout the passage of radiation through the body, and hence the absorptivity will depend on the thickness.

If, I_o, is the incident radiation, the intensity, I, at a depth, t, is given by;

$$I = I_o \exp(-\alpha_a t) \qquad (3.13)$$

Where, α_a represents the coefficient of absorption.

The reflection of radiation at a surface may be either specular or diffuse. Specular reflection occurs when the angle of reflection is equal to the angle of incidence, such as at the surface of glass. Diffuse reflection occurs when the reflected radiation is distributed uniformly throughout the hemispherical enclosure. Highly polished surfaces approach the specular while rough surfaces approach the diffuse. In the flat-plate solar collector, the transparent covers are regarded as specular and the absorber plate as diffuse.

A black body is an ideal body for which $\rho = 0$ at the surface and $\alpha = 1$.

3.3.1.1: Sky Radiation.

To predict the performance of solar collectors, it will be necessary to evaluate the radiation exchange between a surface and the sky. The sky is considered as a blackbody at some equivalent sky temperature, T_{sky}. Thus, the net radiation to the top cover surface is given by,

$$Q = \varepsilon_g A\sigma\left(T_{sky}^4 - T_t^4\right) \tag{3.14}$$

There are several relations [15] to relate T_{sky} for clear skies to other measured meteorological variables. One of the relations relates sky temperature to the local air temperature, T_a, in a simple relationship, this gives better results compared to the other relations,

$$T_{sky} = 0.0552T_a^{1.5} \tag{3.15}$$

Where T_{sky} and T_a are in kelvin.

3.3.1.2: Radiation heat transfer coefficient.

To retain the simplicity of linear equations it is convenient to define a radiation heat transfer coefficient such that the heat radiated is given by,

$$Q = Ah_r[T_2 - T_1] \tag{3.16}$$

where the heat transfer coefficient h_r is be defined by,

$$h_r = \frac{\sigma[T_2^2+T_1^2]\,[T_2+T_1]}{\frac{1}{\varepsilon_1}+\frac{1}{\varepsilon_2}-1} \qquad (3.17)$$

3.3.2: Natural Convection between Parallel Flat Plates at different Temperatures

Free convection heat transfer are usually correlated in terms of three dimensionless parameters; the Nusselt number, Nu, the Rayleigh number, Ra, and the Prandtl number, Pr. The ratio of the Rayleigh number to the Prandtl number is known as the Grashof number, Gr, and is sometimes used.

These numbers are defined as;

- Nusselt number, $Nu = \frac{hl}{k}$ (3.18-a)
- Rayleigh number, $Ra = \frac{g\beta^1 \Delta T L^3}{\nu\alpha}$ (3.18-b)
- Prandtl number, $Pr = \frac{\nu}{\alpha} = \frac{\mu c_p}{k}$ (3.18-c)
- Grashof number, $Gr = \frac{\beta^1 g \Delta T L^3}{\nu^2}$ (3.18-d)

Where,

- h = heat transfer coefficient.
- L = plate spacing
- k = thermal conductivity.
- g = gravitational constant
- β^1 = volumetric coefficient of expansion (for an ideal gas $\beta^1 = 1/T$)
- c_p = specific heat at constant pressure.

- ΔT = temperature difference between plates

- ν = kinematic viscosity

- α = thermal diffusivity.

A relationship between the Nusselt number and Rayleigh number for flow over a flat surface tilted between 0 to 75° is given as, [4, 15]

$$Nu = 1+1.44\left[1-\frac{1708}{Ra\cos\beta}\right]^{+}\left[1-\frac{(\sin 1.8\beta)^{1.6}\,1708}{Ra\cos\beta}\right]+\left[\left(\frac{Ra\cos\beta}{5830}\right)^{\frac{1}{3}}-1\right]^{+} \qquad (3.19)$$

Where the meaning of the + exponent is that only positive values of the terms in the square brackets are to be used (i.e., use zero if the term is negative). β is the tilt angle for the flat surface [15].

3.3.3: Forced convection heat transfer coefficient.

This is the mode of heat transfer between a surface and the flowing fluid, and makes use of the Reynolds number, Re.

$$Re = \frac{uL}{\nu} \qquad (3.20)$$

Where, u = velocity of flow, m/s

L = characteristic dimension, m

The heat transfer coefficient to air that is flowing between parallel plates where one plate only is heated (the absorber plate) may be obtained from a relationship that was recommended by Duffie and Beckman [15];

$$Nu = \frac{h_d d_h}{k} = 0.0158Re^{0.8} \qquad (3.21)$$

for, $Re > 2300$ and, $0.1 \leq Pr \geq 0.7$.

This is for a fully developed turbulent flow.

The local Nusselt number for laminar flow between two flat plates with one side insulated and the other subjected to a constant heat flux has been obtained by Heaton et al, as noted by Maclennan [14]. The correlation takes the form,

$$Nu = Nu_{\infty} + \frac{a\left(Re.Pr\frac{d_h}{L}\right)^m}{1+b\left(Re.Pr\frac{d_h}{L}\right)^n} \qquad (3.22)$$

Where, $d_h = \frac{4 \times A_d}{\text{wetted perimeter}}$

L= length of the plate.

a, b, m, and n are constants as given in table 3.1.

Table. 3.1. Constants for infinite Flat Plate Local Nusselt number.

Prandtl number	a	b	m	n
0.7	0.00190	0.00563	1.71	1.17
10	0.00041	0.00156	2.12	1.59
∞	0.00021	0.00060	2.24	1.77
$Nu_{\infty} = 5.4$				

3.3.4: Heat transfer due to wind.

Convection will occur from the upper exposed surface of a collector. The underneath surface of the backing insulation will not be significantly above ambient temperature if this surface is exposed.

In conditions of wind the convection coefficient is given by a dimensional empirical correlation developed by Jurges, quoted in [15, 31]:

$$h = 5.7 + 3.8V \quad W/m^2K \tag{3.23}$$

where V is the wind velocity in m/s.

The above expression takes into consideration the effects of free convection.

In conditions of no wind, natural convection over the exposed surface occurs, Wong [28] gives for such conditions;

$$\bar{Nu} = 0.8(Gr\,Cos\varphi\,Pr)^{1/4}\left[\frac{Cos\varphi}{1+(1+\frac{1}{Pr^{0.5}})^2}\right]^{1/4} \tag{3.24}$$

where φ is the angle with the vertical.

When the wind speed is very low, free convection conditions may dominate.

3.4: Absorption of Radiation.

The absorption of radiation in a partially transparent medium is described by Bouguer's law [15], which is based on the assumption that the absorbed radiation, dI, is proportional to the local intensity, I, in the medium and the distance the radiation travels in the medium, x;

$$dI = I\kappa\,dx. \tag{3.25}$$

Where κ is the proportionality constant, called the extinction coefficient, and is assumed to be constant in the solar spectrum, for a particular medium.

Integrating along the actual path length in the medium (i.e., from 0 to $L/Cos\theta_2$) yields,

$$\tau_a = \frac{I_\tau}{I_o} = e^{-kL/\cos\theta_2} \tag{3.26}$$

where subscript, a, is a reminder that only absorption losses have been considered.

For glass, the value of, K,varies from approximately $4m^{-1}$ for "water white" glass to approximately $32m^{-1}$ for poor (greenish cast of edge) glass.

3.5: Optical Properties of Cover Systems.

The transmittance, reflectance and absorbance of a single cover, allowing for both reflection and absorption losses, can be determined by ray-tracing techniques.

The transmittance of a single cover is estimated to be,

$$\tau \simeq \tau_a \tau_r \qquad (3.27\text{-a})$$

The absorbance of solar collector cover can be approximated as,

$$\alpha = 1 - \tau_a \qquad (3.27\text{-b})$$

The reflectance of a single cover is then found from, $\rho = 1 - \alpha - \tau$ so that,

$$\rho \simeq \tau_a (1 - \tau_r) = \tau_a - \tau \qquad (3.27\text{-c})$$

For identical multiple covers, the above equations, (3.27-a to 3.27-c) apply equally with τ_a, evaluated from equations 3.26, while L is the total cover system thickness.

3.6: THEORY OF FLAT-PLATE COLLECTORS.

A solar collector is a special kind of heat exchanger that transforms solar radiant energy into heat. For a solar collector, energy transfer is from a distant source of radiant energy to a fluid.

Flat-plate collectors are designed for applications requiring energy delivery at moderate temperatures, up to perhaps 100°C above ambient temperature. They use both beam and diffuse solar radiation, and do not track the sun.

The thermal energy obtained in the conversion process is manifested as an enthalpy increase of the fluid that is flowing through the collector.

3.6.1: Brief Description of Flat-plate Collector.

The important parts of a two-cover flat-plate solar air heater are shown in figure 3.2.

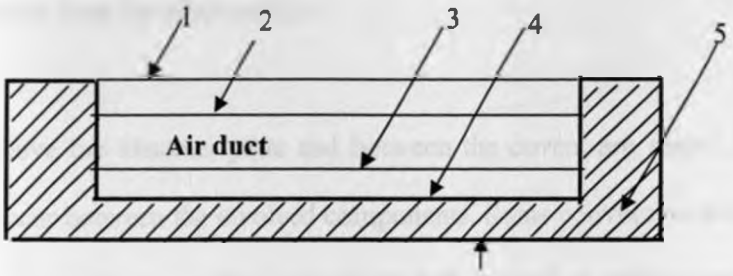

Fig. 3.2. A two-cover Solar Collector Collector box.

1. Top glass cover.
2. First glass cover.
3. Absorber plate.
4. Back plate.
5. Insulation.

The absorber plate is a black solar-energy absorbing surface and should have a means of transferring the absorbed energy to the flowing fluid. While the covers are envelopes; transparent to solar radiation and, reduce convective and radiative heat losses to the atmosphere.

3.6.2: Heat-transfer Mechanism in a Flat-plate Collector.

Irradiance is incident on the outer cover, which is mostly transmitted but it is also partially absorbed and partially reflected. The energy transmitted is incident on the second cover and again transmitted to the absorber plate depending on angle of incidence. The energy reflected from the second is partially transmitted back through the first cover. Of the energy transmitted through both covers some 90 per cent is absorbed by the absorber plate, the remainder being reflected [16]. The temperature of the absorber plate therefore increases, and heat transfer from the absorber plate to its immediate surroundings will commence. At the same time there will be radiation and convection from the upper surface of the plate and

conduction through the insulation on the reverse side of the plate. The air and plate temperatures will also increase above the plate in the direction of the airflow. The air is heated by convection from the plate surface.

The air spaces above the absorber plate and between the covers are sealed. Hence natural convection will occur between the involved components. Some convection and radiation will also occur from the outer cover. The convection will depend on wind-velocity, while the effective sky temperature determines the radiation.

The extent to which high temperatures can be achieved in a flat-plate collector depends on successful reduction of heat loss. This will depend on adequate back-insulation of the absorber plate, reflection of long-wave radiation on the inside surfaces of the covers, and suppression of natural convection between the absorber plate and the first cover.

Energy is removed from the absorber plate by the circulating fluid, where the heat-transfer process due to forced convection to the flowing air.

3.6.2.1: The Basic Flat-plate Energy Balance Equation.

In steady state, an energy balance that indicates the distribution of incident solar energy into useful energy gain, thermal losses, and optical losses describes the performance of a solar collector. The solar radiation absorbed by a collector, S, is equal to the difference between the incident solar radiation and the optical losses as defined by [55],

$$S = R_b I_b (\tau\alpha)_b + I_d (\tau\alpha)_d \left(\frac{1+\cos\beta}{2}\right) + \rho_g (I_b + I_d)(\tau\alpha)_g \left(\frac{1-\cos\beta}{2}\right) \text{ Per unit area} \qquad (3.28)$$

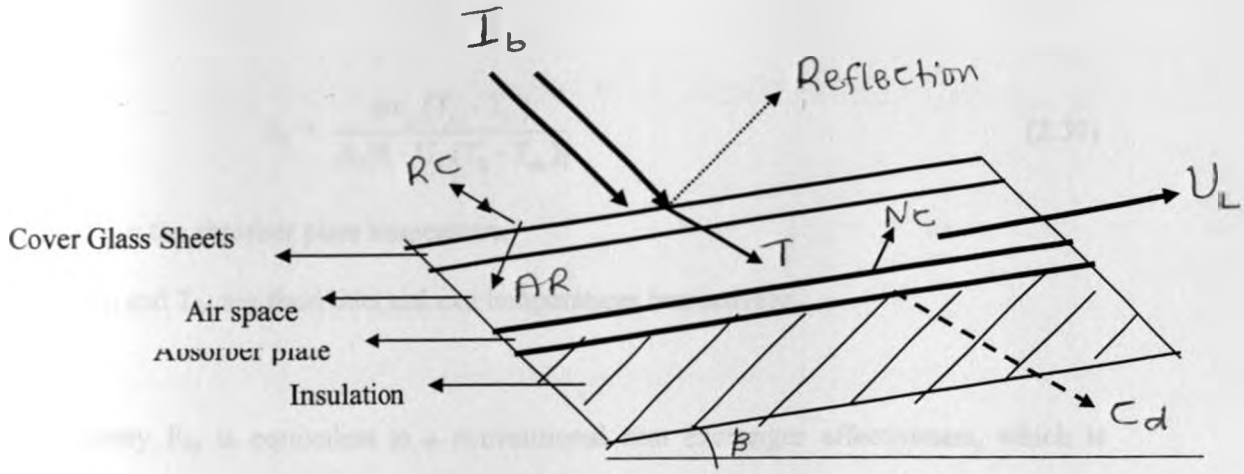

I_b... Beam incoming solar radiation
U_L--- Collected usefull heat
C_d--- Conducted heat
RC--- Radiation and concvection from absorber plate
AR--- Absorption and reradiation from cover
T---- Transmission through covers
Nc--- Natural convection
β--- Tilt angle

Figure 3.3: Diagrammatic section of a flat-plate collector showing an energy balance.

The thermal energy lost from the collector to the surroundings by conduction, convection, and infrared radiation can be represented by a heat transfer coefficient, U_L, times the difference between the mean absorber plate temperature, T_{ab}, and the ambient temperature, T_a. In steady state the useful energy output of the collector is then the difference between the absorbed solar radiation and the thermal loss:

$$Q_u = A_k[S - U_L(T_{ab} - T_a)] \qquad (3.29)$$

where A_k is the collector area.

The efficiency of collection is the fraction of incident energy on the outer surface of the top cover that is actually removed by the circulating fluid.

3.6.2.2: Collector heat-removal factor, F_R.

The heat-removal factor, F_R, is a quantity that relates the actual useful energy gain of a collector to the useful gain if the whole collector were at the fluid inlet temperature. Mathematically, this quantity is given by [55],

$$F_R = \frac{mc_p(T_{f,o} - T_{f,i})}{A_c[S - U_L(T_{f,i} - T_{ab})]} \tag{3.30}$$

where, T_{ab} = the absorber plate temperature,

$T_{f,i}$ and $T_{f,o}$ are fluid inlet and exit temperatures respectively.

The quantity F_R, is equivalent to a conventional heat exchanger effectiveness, which is defined as the ratio of the actual heat transfer to the maximum possible heat transfer. The maximum possible useful energy gain (heat transfer) in a solar collector occurs when the whole collector is at the inlet fluid temperature; heat losses to the surroundings are negligible.

The collector heat removal factor times this maximum possible useful energy gain is equal to the actual useful energy gain Q_u,

$$Q_u = A_k F_R [S - U_L(T_{f,i} - T_{ab})]. \tag{3.31}$$

This is an extremely useful equation and applies to most flat-plate collectors and, is generally known as the Hottel- Whillier- Bliss equation.

3.6.2.3: Collector Efficiency.

The collector efficiency, η, is defined as the ratio between the useful energy gained by the flowing air to the solar radiation incident on the surface of the solar collector;

$$\eta_i = \frac{mc_p[T_{f,o} - T_{f,i}]}{A_k Q_i} \tag{3.32}$$

where, Q_i is total solar radiation intensity, W/m^2.

CHAPTER 4: THEORETICAL MODELING.

4.1: INTRODUCTION.

The theoretical models were obtained by considering an energy balance for the heat flow processes through the collector. The several processes of heat flow considered in the analysis are convection, radiation and conduction.

To effect the analysis, some working assumptions were made during the modeling process. Some of the major assumptions that were made are [3, 13, 28]:

1. Unsteady state conditions prevail during the operations of the flat plate solar collector, meaning that the heat capacity effects cannot be neglected.
2. Heat flow through the covers and the back insulation will be one-dimensional.
3. The temperature of the covers and the absorber plate is spatially uniform. This means that the absorber and cover plate can be represented each as a single node in the flow direction in the heat transfer models.
4. The bulk-mean temperature of the cooling fluid changes with time only in the flow direction.
5. The area of the collector is large compared with the thickness so that end losses and shading can be neglected.
6. Effects due to air leakages and temperature drop in the plenums are negligible.
7. The absorber plate and the covers are diffuse-grey for long wave radiation. But for incoming solar radiation the covers behave like specular reflectors.
8. Irradiation on the collector plates will be uniformly distributed.
9. Effects of dust and dirt on the collector will be negligible.

10. The sky will be considered to be a black body source of infra-red radiation of an equivalent sky temperature.
11. To avoid the difficult of handling the diffuse radiation component of solar radiation, an equivalent beam radiation component will be used.
12. Air will be transparent to both solar and long wavelength thermal radiation.
13. For the absorber plate and the glass covers, absorptivity will be equal to emmisivity. This is true for near normal incidence of radiation. But it should be noted that the absorptivity and emmisivity are not the same for short (solar) and long wave (infrared) radiation. The surface should have high solar absorbance and low long-wave emittance.
14. For flow in the heater channels, suitably averaged heat transfer coefficients will be used (though they will vary with time).
15. The temperature of the air flowing in the flow channel varies linearly with distance so that the effective temperature of the air will be the mean of the inlet and outlet values at a given instant of time. Thus the flowing air properties will be taken at the mean temperature.
16. Due to the thin sizes of the plates and the low thermal conductivity of the air, the heat transfer in the plates and in the flowing air in the flow direction will be very small, so that the effects of axial conduction can be neglected.
17. The flow channels will be considered to be parallel plate channels of finite width and finite length (in the flow direction) in the calculation of convective heat transfer coefficients.
18. The flow channels and the stagnant air gaps will be treated as bounded by parallel plates of infinite width and length in the calculation of radiative heat transfer

coefficients, since the space between the plates is very small compared to the dimensions of the plates.

19. Convective heat losses from the top and bottom of the collector will be to the same ambient temperature. This assumes the collector will be suspended and not resting on the ground.
20. Radiative heat loss from the bottom and sides of the collector will be neglected.
21. Material properties such as; transmissivity, reflectance, absorptance and extinction coefficient are independent of temperature.
22. The working fluid (air) enters each flow channel with uniform temperature and velocity profiles.
23. There are no fluid leakages between the passes and no air leaks into or out of the collector.
24. It is also assumed that incompressible flow exists and effects of viscous dissipation are negligible.
25. Entry effects are also negligible and the flow will be fully developed.

To have a complete model that can predict the thermal performance of a solar collector, three main steps were undertaken: -

i). Theoretical analysis which lead to differential equations.

ii). Numerical analysis that attempts to solve the differential equations.

iii). Solution methods for the unknown parameters in the differential equations.

4.2: SINGLE PASS MODE.

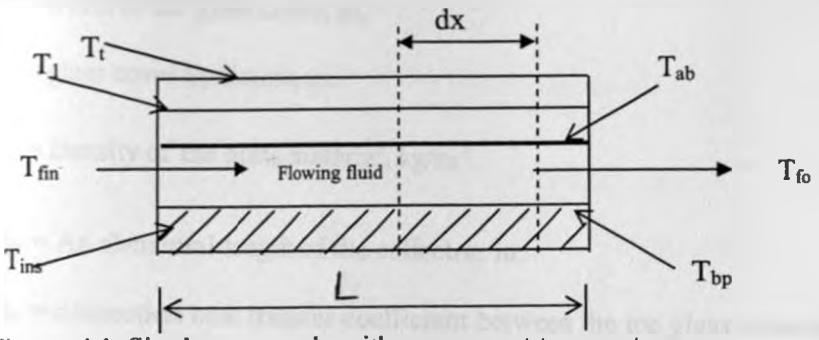

Figure. 4.1. Single pass mode with component temperatures.

Taking an energy balance for an element of the collector, differential equations are obtained for the collector components.

1. TOP GLASS COVER.

$$dm_t c_{p_g} \frac{dT_t}{dt} = G_s f_t dA_k - k_g bt_g dx \frac{d^2T_t}{dx^2} - h_{ta} dA_k (T_t - T_a) - h_{r_{ta}} dA_k (T_t - T_a) + h_{lt} dA_k (T_l - T_t) + h_{r_{lt}} dA_k (T_l - T_t) \quad (4.2.1\text{-a})$$

Dividing through by dA_k:

$$\frac{dm_t}{dA_k} c_{p_g} \frac{dT_t}{dt} = G_s f_t - k_g bt_g \frac{dx}{dA_k} \frac{d^2T_t}{dx^2} - h_{ta}(T_t - T_a) - h_{r_{ta}}(T_t - T_a) + h_{lt}(T_l - T_t) + h_{r_{lt}}(T_l - T_t) \quad (4.2.1\text{-b})$$

where;

$dm_t = \rho_g bt_g dx$ (is elemental mass of glass in the control volume, kg).

c_{p_g} = Specific heat of glass, J/kg. K.

G_s = Solar irradiance, rate at which radiant energy is incident on a unit area of the surface, W/m^2. (Both beam and diffuse).

f_t = Fraction of incident radiation absorbed by the top glass cover.

$dA_k = bdx$ (elemental surface area, m^2).

k_g = Thermal conductivity of glass, W/m. K.

b = width of the glass cover, m.

t_g = glass cover thickness, m.

ρ_g = Density of the glass material, kg/m^3.

dx = An elemental length of the collector, m.

h_{ta} = convection heat transfer coefficient between the top glass cover and the ambient, W/m^2. K.

$h_{r_{ta}} = \sigma \varepsilon_g \frac{(T_t^4 - T_{sky}^4)}{T_t - T_a}$ (Radiation heat transfer coefficient between the glass cover and the ambient, W/m^2. K).

h_{1t} = Convection heat transfer coefficient between the top glass cover and the first glass cover, W/m^2. K.

$h_{r_{1t}} = \frac{\sigma(T_1^4 - T_t^4)}{(\frac{1}{\varepsilon_{g1}} + \frac{1}{\varepsilon_{gt}} - 1)(T_1 - T_t)} = \frac{\sigma(T_1^2 + T_t^2)(T_1 + T_t)}{\frac{2}{\varepsilon_g} - 1}$ Radiation heat transfer coefficient between the top glass cover and the first glass cover, W/m^2. K (assuming the two glass covers have the same emissivity).

σ = Stefan- Boltzmann constant.

ε_g = Glass emissivity.

T_t = Top glass cover temperature, K.

T_1 = First glass cover temperature, K.

T_a = Ambient temperature, K.

2. FIRST GLASS COVER.

There will be multiple reflections that will affect the radiation;

i). Absorbed by the top glass cover.

ii). Absorbed and reflected by first glass cover.

iii). Absorbed by the absorber plate.

Taking an energy balance for an elemental mass gives;

$$\frac{dm_1}{dA_k} c_{p_g} \frac{dT_1}{dt} = G_s f_1 - k_g bt_g \frac{dx}{dA_k} \frac{d^2T_1}{dx^2} - h_{1t}(T_1 - T_t) - h_{r_{1t}}(T_1 - T_t) + h_{ab1}(T_{ab} - T_1) + h_{r_{ab1}}(T_{ab} - T_1) \quad (4.2.2)$$

Where;

f_1 = fraction of original incident radiation absorbed by the cover, when the effect of multiple reflections is taken into account.

h_{ab1} = convection heat transfer coefficient between the first glass cover and the absorber plate.

h_{rab1} = radiation heat transfer coefficient between the first glass cover and the absorber plate.

Assumptions made here were;

a). The glass covers have similar optical properties.

b). The glass covers have the same thickness.

c). There will be multiple reflections.

3. ABSORBER PLATE.

$$\frac{dm_{ab}}{dA_k} c_{p_{ab}} \frac{dT_{ab}}{dt} = G_s f_{ab} - k_{ab} bt_{ab} \frac{dx}{dA_k} \frac{d^2T_{ab}}{dx^2} - h_{ab1}(T_{ab} - T_1) - h_{r_{ab1}}(T_{ab} - T_1) - h_{r_{ab\text{-}bp}}(T_{ab} - T_{bp}) - h_{ab\text{-}fm}(T_{ab} - T_{fm}) \quad (4.2.3)$$

where;

dm_{ab} -- elemental mass of the absorber plate.

$c_{p_{ab}}$ -- specific heat of the absorber plate.

k_{ab} -- thermal conductivity of the absorber plate.

T_{ab} -- temperature of the absorber plate.

T_{fm} -- mean fluid temperature.

f_{ab} -- fraction of original incident radiation absorbed by the absorber plate.

The assumption made here was that; there is no transmissivity on the absorber plate and there are multiple reflections between the glass cover and the absorber plate. With this, the absorber plate behaves as a black body, but in reality this is not the case hence the absorptivity of the material were used.

4. THE FLOWING FLUID (AIR).

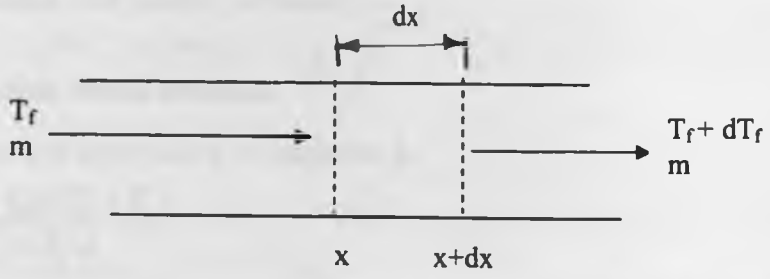

Figure. 4.2. Air in the flow channel

Enthalpy in, $H_x = mc_{p_f} T_f$

Enthalpy out, $H_{x+dx} = \frac{\partial (H_x)}{\partial x} dx$

$$= mc_{p_f} T_f + mc_{p_f} \frac{\partial T_f}{\partial x} dx$$

Thus energy balance for the flowing fluid is,

$$Mc_{p_f} \frac{dT_f}{dt} = h_{ab-fm} dA_k (T_{ab} - T_{fm}) + h_{bp-fm} dA_k (T_{bp} - T_{fm}) - \dot{m} c_{p_f} \frac{\partial T_f}{\partial x} dx . \quad (4.2.4)$$

where;

M = mass of the fluid in the flow channel control volume considered, kg.

c_{p_f} = specific heat capacity of the flowing fluid.

h_{ab-fm} = convection heat transfer coefficient between the back plate and the flowing fluid.

m = mass flow rate of flowing fluid, kg/s

$T_{fm} = \frac{T_{f_{in,0}} + T_{f_{out,0}}}{2}$ = mean fluid temperature, K

$T_{f_{in,0}}$ = fluid inlet temperature at the initial time, K

$T_{f_{out,0}}$ = fluid exit temperature at the initial time, K

5. BACK PLATE.

$$\frac{dm_{bp}}{dA_k} c_{p_{bp}} \frac{dT_{bp}}{dt} = -k_{bp} bt_{bp} \frac{dx}{dA_k} \frac{d^2T_{bp}}{dx^2} - h_{bp\text{-}fm}(T_{bp} - T_{fm}) + h_{r_{ab\text{-}bp}}(T_{ab} - T_{bp}) - U_L(T_{bp} - T_{ins}) \quad (4.2.5)$$

where;

$U_L = \frac{1}{R}$ (insulation heat transfer coefficient), $\frac{W}{m^2.K}$

$R = \frac{t}{k}$ (insulation thermal resistance), $\frac{m^2.K}{W}$

T_{ins} = temperature at outer surface of insulation, K.

$h_{r_{ab\text{-}bp}} = \frac{\sigma(T_{ab} + T_{bp})(T_{ab}^2 + T_{bp}^2)}{\frac{1}{\varepsilon_{ab}} + \frac{1}{\varepsilon_{bp}} - 1}$

(radiation heat transfer coefficient between the absorber plate and the back plate), $W/m^2.K$

6. INSULATION.

The heat conducted through the insulation will be transferred to the atmosphere at the collector surface by convection and radiation.

A heat balance equation will take the form;

Heat capacity = (Heat conducted from back plate

- Heat conducted along insulation

- Heat convected away at insulation surface

- Heat radiated away at the insulation surface).

$$\frac{dm_{ins}}{dA_k} c_{p_{ins}} \frac{dT_{ins}}{dt} = U_L(T_{bp} - T_{ins}) - k_{ins} bt_{ins} \frac{dx}{dA_k} \frac{d^2T_{ins}}{dx^2} - h_{r_{ins-a}}(T_{ins} - T_a) - h_{ins-a}(T_{ins} - T_a) \quad (4.2.6)$$

where, T_a is the ambient temperature in Kelvins.

4.2.1: FINITE DIFFERENCE EXPRESSIONS.

Equations (4.2.1-b to 4.2. 6) were solved using finite difference numerical method. The finite-difference formulation used was based on a simple explicit scheme that was presented by Laasonen. The Laasonen scheme uses an explicit time marching formulation and a central difference formulation approximating the spatial derivatives.

For first order differential equations the forward-difference formulation was used, while for second order derivatives, the central-finite difference formulation was used.

The following simplifying finite-difference expressions were used;

$$\frac{dT_n}{dt} = \frac{T_n^1 - T_n}{\Delta t} \quad (4.2.7\text{-a})$$

$$\frac{dT}{dx} = \frac{T_{x+\Delta x} - T_x}{\Delta x} \quad (4.2.7\text{-b})$$

$$\frac{d^2T}{dx^2} = \frac{T_{x+\Delta x} - 2T_x + T_{x-\Delta x}}{(\Delta x)^2} \quad (4.2.7\text{-c})$$

where;

Δt —— time step

n —— -subscript denoting the component considered

T_n^1 —— temperature after time step

T_n —— temperature initially.

And where equation,

2.4.7.a –– is the explicit time marching.

2.4.7.b –– spatial forward-difference formulation.

2.4.7.c –– spatial central-difference formulation.

Also the following relations were be employed,

$$dm_n = \rho_n bt_n dx \qquad (4.2.7\text{-d})$$
$$dA_k = bdx$$

Simplifying equations (4.2.1-a to 4.2.6 by use of the above finite difference relations, we get;

1. TOP GLASS COVER.

$$\frac{dm_t}{dA_k} c_{p_g} \frac{dT_t}{dt} = G_s f_t - k_g bt_g \frac{dx}{dA_k}\frac{d^2T_t}{dx^2} - h_{ta}(T_t - T_a) - h_{r_{ta}}(T_t - T_a) + h_{lt}(T_l - T_t) + h_{r_{lt}}(T_l - T_t)$$

On using equation 7,

$$\frac{\rho_g bt_g dx}{bdx} c_{p_g} \frac{T_t^1 - T_t}{\Delta t} = G_s f_t - k_g bt_g \frac{dx}{bdx}\left(\frac{T_{t_{x+\Delta x}} - 2T_{t_x} + T_{t_{x-\Delta x}}}{(\Delta x)^2}\right) - h_{ta}(T_t - T_a) - h_{r_{ta}}(T_t - T_a) + h_{lt}(T_l - T_t) + h_{r_{ta}}(T_l - T_t)$$

Or,

$$T_t^1 = T_t + \frac{G_s f_t \Delta t}{\rho_g t_g c_{p_g}} - \frac{k_g \Delta t}{\rho_g c_{p_g}}\left(\frac{T_{t_{x+\Delta x}} - 2T_{t_x} + T_{t_{x-\Delta x}}}{(\Delta x)^2}\right) - \frac{h_{ta}\Delta t}{\rho_g t_g c_{p_g}}(T_t - T_a) - \frac{h_{r_{ta}}\Delta t}{\rho_g t_g c_{p_g}}(T_t - T_a) + \frac{h_{lt}\Delta t}{\rho_g t_g c_{p_g}}(T_l - T_t) + \frac{h_{r_{lt}}\Delta t}{\rho_g t_g c_{p_g}}(T_l - T_t)$$

On using,

$$h_{ta} + h_{r_{ta}} = h_a$$
$$h_{lt} + h_{r_{lt}} = h_l$$

and letting;

$$\frac{1}{\rho_g t_g c_{p_g}} = A \quad \text{(a constant)}$$

$$\frac{k_g}{\rho_g c_{p_g} (\Delta x)^2} = B \quad \text{(a constant)}$$

(It has been assumed that Δx will be fixed and uniform).

$$T_t^1 = T_t + AG_s f_t \Delta t - B\Delta t(T_{t_{x+\Delta x}} - 2T_{t_x} + T_{t_{x-\Delta x}}) - A\Delta t\, h_a (T_t - T_a) + A\Delta t\, h_t (T_1 - T_t)$$

Expanding;

$$T_t^1 = T_t + AG_s f_t \Delta t + A\Delta t(h_t T_1 - h_t T_t - h_a T_t + h_a T_a) - B\Delta t(T_{t_{x+\Delta x}} - 2T_{t_x} + T_{t_{x-\Delta x}})$$

Or,

$$T_t^1 = T_t + A\Delta t(G_s f_t + h_t T_1 + h_a T_a - CT_t) - B\Delta t(T_{t_{x+\Delta x}} - 2T_{t_x} + T_{t_{x-\Delta x}}) \qquad (4.2.8)$$

Where,

$C = h_t + h_a$ (will change with changes in h_t and h_a).

2. FIRST GLASS COVER.

$$\frac{dm_1}{dA_k} c_{p_g} \frac{dT_1}{dt} = G_s f_1 - k_g bt_g \frac{dx}{dA_k} \frac{d^2T_1}{dx^2} - h_{1t}(T_1 - T_t) - h_{t_1}(T_1 - T_t) + h_{ab1}(T_{ab} - T_1) + h_{r_{ab1}}(T_{ab} - T_1)$$

Which can be written as,

$$\rho_g bt_g \frac{dx}{bdx} c_{p_g} \frac{T_1^1 - T_1}{\Delta t} = G_s f_1 - k_g bt_g \frac{dx}{bdx}\left[\frac{T_{1_{x+dx}} - 2T_{1_x}\, T_{1_{x-dx}}}{(\Delta x)^2}\right] - h_t(T_1 - T_t) + h_1(T_{ab} - T_1)$$

where, $h_{ab1} + h_{r_{ab1}} = h_1$

on rearranging;

$$T_g^1 = T_g + \frac{G_s f_g \Delta t}{\rho_g t_g c_{p_g}} - \frac{k_g \Delta t}{\rho_g c_{p_g} (\Delta x)^2}(T_{g_{x+\Delta x}} - 2T_{g_x} T_{g_{x-\Delta x}})$$
$$- \frac{h_t \Delta t}{\rho_g t_g c_{p_g}}(T_g - T_t) + \frac{h_l \Delta t}{\rho_g t_g c_{p_g}}(T_{ab} - T_g)$$

On using the constants A and B (as defined earlier) and then expanding, we arrive at,

$$T_l^1 = T_l + A\Delta t(G_s f_l - h_t T_l + h_t T_t + h_l T_{ab} - h_l T_l)$$
$$- B\Delta t(T_{l_{x+\Delta x}} - 2T_{l_x} T_{l_{x-\Delta x}})$$

Or,

$$T_l^1 = T_l + A\Delta t(G_s f_l + h_t T_t + h_l T_{ab} - DT_l)$$
$$- B\Delta t(T_{l_{x+\Delta x}} - 2T_{l_x} T_{l_{x-\Delta x}}) \qquad (4.2.9)$$

Where, $D = h_l + h_t$, and changes with h_l and h_t.

3. ABSORBER PLATE.

$$\rho_{ab} bt_{ab} \frac{dx}{bdx} c_{p_{ab}} \frac{dT_{ab}}{dt} = G_s f_{ab} - k_{ab} bt_{ab} \frac{dx}{bdx} \frac{d^2 T_{ab}}{dx^2} - h_{abl}(T_{ab} - T_l)$$
$$- h_{r_{ab-l}}(T_{ab} - T_l) - h_{r_{ab-bp}}(T_{ab} - T_{bp}) - h_{ab\text{-}fm}(T_{ab} - T_{fm})$$

Or,

$$\frac{T_{ab}^1 - T_{ab}}{\Delta t} = \frac{G_s f_{ab}}{\rho_{ab} t_{ab} c_{p_{ab}}} - \frac{k_{ab}}{\rho_{ab} c_{p_{ab}} (\Delta x)^2}(T_{ab_{x+\Delta x}} - 2T_{ab_x} + T_{ab_{x-\Delta x}})$$
$$- \frac{h_l}{\rho_{ab} t_{ab} c_{p_{ab}}}(T_{ab} - T_l) - \frac{h_{r_{ab-bp}}}{\rho_{ab} t_{ab} c_{p_{ab}}}(T_{ab} - T_{bp}) - \frac{h_{ab\text{-}fm}}{\rho_{ab} t_{ab} c_{p_{ab}}}(T_{ab} - T_{fm})$$

Simplifying,

$$T_{ab}^1 = T_{ab} + EG_s f_{ab}\Delta t - F\Delta t(T_{ab_{x+\Delta x}} - 2T_{ab_x} + T_{ab_{x-\Delta x}})$$
$$- Eh_l \Delta t(T_{ab} - T_l) - Eh_{r_{ab-bp}} \Delta t(T_{ab} - T_{bp}) - Eh_{ab\text{-}fm} \Delta t(T_{ab} - T_{fm})$$

Where,

$$E = \frac{1}{\rho_{ab} t_{ab} c_{p_{ab}}} \text{ (a constant).}$$

$$F = \frac{k_{ab}}{\rho_{ab} c_{p_{ab}} (\Delta x)^2} \text{ (a constant).}$$

On using,

$$h_{r_{ab-bp}} = h_{ab}$$
$$h_{ab-fm} = h_f$$

$$T_{ab}^{l} = T_{ab} + E\Delta t[G_s f_{ab} - h_l T_{ab} + h_l T_l - h_{ab} T_{ab} + h_{ab} T_{bp} - h_f T_{ab} + h_f T_{fm}] - F\Delta t(T_{ab_{x+\Delta x}} - 2T_{ab_x} + T_{ab_{x-\Delta x}})$$

Finally the equation to be solved becomes,

$$T_{ab}^{l} = T_{ab} + E\Delta t[G_s f_{ab} + h_l T_l + h_{ab} T_{bp} + h_f T_{fm} - GT_{ab}] - F\Delta t(T_{ab_{x+\Delta x}} - 2T_{ab_x} + T_{ab_{x-\Delta x}}) \quad (4.2.10)$$

Where, $G = h_l + h_{ab} + h_f$

4. THE FLOWING FLUID (AIR).

$$Mc_{p_f} \frac{dT_f}{dt} = h_{ab\text{-}fm} dA_k (T_{ab} - T_{fm}) + h_{bp\text{-}fm} dA_k (T_{bp} - T_{fm}) - \dot{m} c_{p_f} \frac{\partial T_f}{\partial x} dx$$

Where, $M = \rho_f b t_f dx$

Or,

$$\rho_f b t_f \frac{dx}{bdx} c_{p_f} \frac{dT_f}{dt} = h_{ab\text{-}fm} (T_{ab} - T_{fm}) + h_{bp\text{-}fm} (T_{bp} - T_{fm}) - \dot{m} c_{p_f} \frac{\partial T_f}{\partial x} dx$$

Rearranging, takes the form;

$$T_f^{l} = T_f + \frac{h_{ab\text{-}fm} \Delta t}{\rho_f t_f c_{p_f}} (T_{ab} - T_{fm}) + \frac{h_{bp\text{-}fm} \Delta t}{\rho_f t_f c_{p_f}} (T_{bp} - T_{fm}) - \frac{\dot{m}}{\rho_f t_f b} \Delta t \frac{T_{f_{x+\Delta x}} - T_{f_x}}{\Delta x}$$

Or,

$$T_f^{l} = T_f + Hh_f \Delta t (T_{ab} - T_{fm}) + Hh_p \Delta t (T_{bp} - T_{fm}) - J\Delta t (T_{f_{x+\Delta x}} - T_{f_x})$$

Where,

$$H = \frac{1}{\rho_f t_f c_{p_f}} \text{ (a constant).}$$

$$J = \frac{\dot{m}}{\rho_f t_f b \Delta x} \text{ (a constant).}$$

$$h_p = h_{bp\text{-}fm}$$

Changes in c_{pf} and ρ_f with temperature are negligible.

Expanding, results to;

$$T_f^1 = T_f + H\Delta t(h_f T_{ab} + h_p T_{bp} - KT_{fm}) - J\Delta t(T_{f_{x+\Delta x}} - T_{f_x}) \qquad (4.2.11)$$

Where, $K = h_f + h_p$

For the element considered,

$$T_{f_{x+\Delta x}} = T_{f_o} \text{ and } T_{f_x} = T_{f_m}$$

5. BACK PLATE.

$$\rho_{bp} bt_{bp} \frac{dx}{bdx} c_{p_{bp}} \left(\frac{T_{bp}^1 - T_{bp}}{\Delta t} \right) = -k_{bp} bt_{bp} \frac{dx}{bdx} \frac{d^2 T_{bp}}{dx^2} - h_{bp\text{-}fm}(T_{bp} - T_{fm}) + h_{t_{ab\text{-}bp}}(T_{ab} - T_{bp}) - U_L(T_{bp} - T_{ins})$$

Or,

$$T_{bp}^1 = T_{bp} - \frac{k_{bp}\Delta t}{\rho_{bp} c_{p_{bp}} (\Delta x)^2}(T_{bp_{x+\Delta x}} - 2T_{bp_x} + T_{bp_{x-\Delta x}}) - \frac{h_p \Delta t}{\rho_{bp} c_{p_{bp}} t_{bp}}(T_{bp} - T_{fm}) + \frac{h_b \Delta t}{\rho_{bp} c_{p_{bp}} t_{bp}}(T_{ab} - T_{bp}) - \frac{U_L \Delta t}{\rho_{bp} c_{p_{bp}} t_{bp}}(T_{bp} - T_{ins})$$

Where, $h_b = h_{t_{ab\text{-}bp}}$

Letting,

$$L = \frac{1}{\rho_{bp} t_{bp} c_{p_{bp}}} \text{ (a constant).}$$

$$M = \frac{k_{bp}}{\rho_{bp} c_{p_{bp}} (\Delta x)^2} \text{ (a constant).}$$

We get,

$$T_{bp}^{1} = T_{bp} - L\Delta t h_p (T_{bp} - T_{fm}) + L\Delta t h_b (T_{ab} - T_{bp}) - L\Delta t U_L (T_{bp} - T_{ins}) - M\Delta t (T_{bp_{x+\Delta x}} - 2T_{bp_x} + T_{bp_{x-\Delta x}})$$

Or,

$$T_{bp}^{1} = T_{bp} + L\Delta t (h_b T_{ab} + h_p T_{fm} - NT_{bp}) - L\Delta t U_L (T_{bp} - T_{ins}) - M\Delta t (T_{bp_{x+\Delta x}} - 2T_{bp_x} + T_{bp_{x-\Delta x}}) \quad (4.2.12)$$

Where, $N = h_b + h_p$

6. INSULATION.

$$\frac{dm_{ins}}{dA_k} c_{p_{ins}} \frac{dT_{ins}}{dt} = U_L (T_{bp} - T_{ins}) - k_{ins} bt_{ins} \frac{dx}{dA_k} \frac{d^2 T_{ins}}{dx^2} - h_{ins-a} (T_{ins} - T_a) - h_{r_{ins-a}} (T_{ins} - T_a)$$

Letting;

$$h_{ins-a} + h_{r_{ins-a}} = h_{ins}$$

and simplifying,

$$\frac{T_{ins}^{1} - T_{ins}}{\Delta t} = \frac{U_L}{\rho_{ins} t_{ins} c_{p_{ins}}} (T_{bp} - T_{ins}) - \frac{k_{ins}}{\rho_{ins} c_{p_{ins}} (\Delta x)^2} (T_{ins_{x+\Delta x}} - 2T_{ins_x} + T_{ins_{x-\Delta x}}) - \frac{h_{ins}}{\rho_{ins} t_{ins} c_{p_{ins}}} (T_{ins} - T_a)$$

Letting,

$$\frac{1}{\rho_{ins} t_{ins} c_{p_{ins}}} = P \text{ (a constant).}$$

and

$$\frac{k_{ins}}{\rho_{ins} c_{p_{ins}} (\Delta x)^2} = Q \text{ (a constant).}$$

We get,

$$T^1_{ins} = T_{ins} + PU_L \Delta t(T_{bp} - T_{ins}) - Ph_{ins} \Delta t(T_{ins} - T_a) - Q\Delta t(T_{ins_{x+\Delta x}} - 2T_{ins_x} + T_{ins_{x-\Delta x}}) \quad (4.2.13)$$

Equations (4.2.8 to 4.2.13) were used to predict the future temperatures $T^1_t, T^1_1, T^1_{ab}, T^1_{f_o}, T^1_{bp}$, and T^1_{ins}.

The expressions allowed determination of the present temperatures in terms of the temperatures and parameters evaluated in the previous time step. This kept the system of the equations linear.

The parameters h and h_r are determined based on the previous temperatures. While the value G_s was the previous measured incident solar radiation, thus the transient predictions were linked to the available data.

4.3: DOUBLE [TOP FIRST] PASS MODE (DTPM)

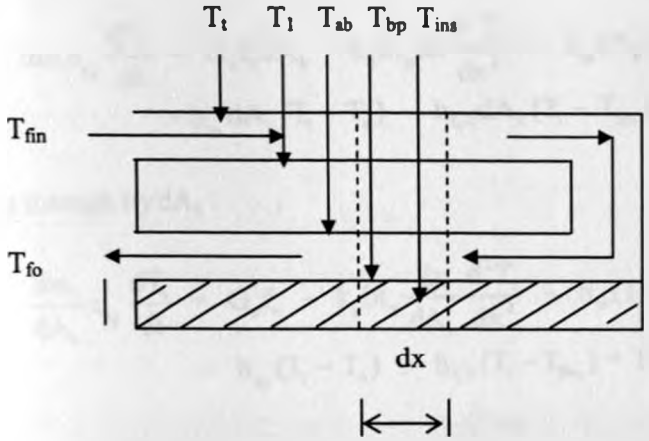

Figure 4.3. Double (Top first) pass mode

Working assumptions:

- The fluid temperature at any section in the flow channel is uniform.
- The inlet temperature to the second flow channel is equal to the outlet temperature from the first flow channel.
- For the elemental section considered, the exit temperature from the first flow channel is not equal to the inlet temperature into the second flow channel.
- In the analysis the notations used in the single pass mode will be used with the following extra notations;
    1. First flow channel fluid temperatures, $T_{fin\,1}$ and $T_{fout\,1}$.
    2. Second flow channel fluid temperatures, $T_{fin\,2}$ and $T_{fout\,2}$.
- The transmissivity of air is unity (does not absorb or reflect).

1. TOP GLASS COVER.

An energy balance leads to;

$$dm_t c_{p_g} \frac{dT_t}{dt} = G_s f_f dA_k - k_g bt_g dx \frac{d^2T_t}{dx^2} - h_{ta} dA_k (T_t - T_a)$$
$$- h_{r_{ta}} dA_k (T_t - T_a) - h_{f_{1-t}} dA_k (T_t - T_{fm_1}) + h_{r_{1t}} dA_k (T_1 - T_t)$$

Dividing through by dA_k :

$$\frac{dm_t}{dA_k} c_{p_g} \frac{dT_t}{dt} = G_s f_t - k_g bt_g \frac{dx}{dA_k} \frac{d^2T_t}{dx^2} - h_{ta} (T_t - T_a) \qquad (4.3.1)$$
$$- h_{r_{ta}} (T_t - T_a) - h_{f_{1-t}} (T_t - T_{fm_1}) + h_{r_{1t}} (T_1 - T_t)$$

where, $T_{fm_1} = \frac{T_{f_{1x}} + T_{f_{1x+dx}}}{2}$

2. FLOWING FLUID IN THE FIRST FLOW CHANNEL.

$$M_{f_1} c_{p_f} \frac{dT_{f_1}}{dt} = h_{f_{1-t}} dA_k (T_t - T_{fm_1}) + h_{f_{1-1}} dA_k (T_1 - T_{fm_1}) \qquad (4.3.2)$$
$$- m_1 c_{p_f} \frac{\partial T_{f_1}}{\partial x} dx$$

where, M_{f_1} = mass of the fluid in the first flow channel control volume considered, kg.

3. FIRST GLASS COVER.

$$dm_1 c_{p_g} \frac{dT_1}{dt} = G_s f_1 dA_k - k_g bt_g dx \frac{d^2T_1}{dx^2} - h_{f-1_1} dA_k (T_1 - T_{fm_1})$$
$$- h_{r_{1-t}} dA_k (T_1 - T_t) + h_{ab-1} dA_k (T_{ab} - T_1) + h_{r_{ab-1}} dA_k (T_{ab} - T_1)$$

dividing through by dA_k ,

$$\frac{dm_1}{dA_k} c_{p_g} \frac{dT_1}{dt} = G_s f_1 - k_g bt_g \frac{dx}{dA_k} \frac{d^2T_1}{dx^2} - h_{f_1-1} (T_1 - T_{fm_1}) \qquad (4.3.3)$$
$$- h_{r_{1-t}} (T_1 - T_t) + h_{ab-1} (T_{ab} - T_1) + h_{r_{ab-1}} (T_{ab} - T_1)$$

4. ABSORBER PLATE.

$$dm_{ab}c_{p_{ab}}\frac{dT_{ab}}{dt} = G_s f_{ab}dA_k - k_{ab}bt_{ab}dx\frac{d^2T_{ab}}{dx^2} - h_{ab\text{-}1}dA_k(T_{ab} - T_1)$$
$$- h_{r_{ab\text{-}1}}dA_k(T_{ab} - T_1) - h_{r_{ab\text{-}bp}}dA_k(T_{ab} - T_{bp}) - h_{f_2\text{-}ab}dA_k(T_{ab} - T_{fm_2})$$

dividing through by dA_k,

$$\frac{dm_{ab}}{dA_k}c_{p_{ab}}\frac{dT_{ab}}{dt} = G_s f_{ab} - k_{ab}bt_{ab}\frac{dx}{dA_k}\frac{d^2T_{ab}}{dx^2} - h_{ab\text{-}1}(T_{ab} - T_1)$$
$$- h_{r_{ab\text{-}1}}(T_{ab} - T_1) - h_{r_{ab\text{-}bp}}(T_{ab} - T_{bp}) - h_{f_2\text{-}ab}(T_{ab} - T_{fm_2}) \quad (4.3.4)$$

5. FLOWING FLUID IN THE SECOND FLOW CHANNEL.

$$M_{f_2}c_{p_f}\frac{dT_{f_2}}{dt} = h_{f_2\text{-}ab}dA_k(T_{ab} - T_{fm_2}) + h_{f_2\text{-}bp}dA_k(T_{bp} - T_{fm_2})$$
$$- \dot{m}_2 c_{p_f}\frac{\partial T_{f_2}}{\partial x}dx \quad (4.3.5)$$

where, M_{f_2} = mass of the fluid in the second flow channel control volume considered, kg.

It will be assumed that the mass flow rate in the second flow channel is equal to the mass flow rate in the first channel, that is: $\dot{m}_1 = \dot{m}_2 = \dot{m}$

6. THE BACK PLATE.

$$dm_{bp}c_{p_{bp}}\frac{dT_{bp}}{dt} = h_{r_{ab\text{-}bp}}dA_k(T_{ab} - T_{bp}) - k_{bp}bt_{bp}dx\frac{d^2T_{bp}}{dx^2} - h_{f_2\text{-}bp}dA_k(T_{bp} - T_{fm_2})$$
$$- U_L dA_k(T_{bp} - T_{ins})$$

Or,

$$\frac{dm_{bp}}{dA_k}c_{p_{bp}}\frac{dT_{bp}}{dt} = h_{r_{ab\text{-}bp}}(T_{ab} - T_{bp}) - k_{bp}bt_{bp}\frac{dx}{dA_k}\frac{d^2T_{bp}}{dx^2}$$
$$- h_{f_2\text{-}bp}(T_{bp} - T_{fm_2}) - U_L(T_{bp} - T_{ins}) \quad (4.3.6)$$

7. INSULATION.

$$dm_{ins}c_{p_{ins}}\frac{dT_{ins}}{dt} = -\,h_{r_{ins-a}}dA_k(T_{ins}-T_a) - k_{ins}bt_{ins}dx\frac{d^2T_{ins}}{dx^2} - h_{ins-a}dA_k(T_{ins}-T_a) + U_L dA_k(T_{bp}-T_{ins})$$

Or,

$$\frac{dm_{ins}}{dA_k}c_{p_{ins}}\frac{dT_{ins}}{dt} = -\,h_{r_{ins-a}}(T_{ins}-T_a) - k_{ins}bt_{ins}\frac{dx}{dA_k}\frac{d^2T_{ins}}{dx^2} - h_{ins-a}(T_{ins}-T_a) + U_L(T_{bp}-T_{ins}) \qquad (4.3.7)$$

SIMPLIFICATION BY FINITE-DIFFERENCE EXPRESSIONS.

Using equation (4.2.7) enabled simplification of the above equations.

1. TOP GLASS COVER.

$$\frac{\rho_g bt_g dx}{dx}c_{p_g}\frac{T_t^1-T_t}{\Delta t} = G_s f_t - k_g bt_g\frac{dx}{bdx}\frac{T_{t_{x+\Delta x}}-2T_{t_x}+T_{t_{x-\Delta x}}}{(\Delta x)^2} - h_{t-a}(T_t-T_a) - h_{r_{t-a}}(T_t-T_a) - h_{f_{1-t}}(T_t-T_{fm_1}) + h_{f_{1-t}}(T_1-T_t)$$

Or,

$$\rho_g t_g c_{p_g}\frac{T_t^1-T_t}{\Delta t} = G_s f_t - k_g t_g\frac{T_{t_{x+\Delta x}}-2T_{t_x}+T_{t_{x-\Delta x}}}{(\Delta x)^2} - h_{t-a}(T_t-T_a) - h_{r_{t-a}}(T_t-T_a) - h_{f_{1-t}}(T_t-T_{fm_1}) + h_{f_{1-t}}(T_1-T_t)$$

Simplifying;

$$T_t^1 = T_t + \frac{G_s f_t\Delta t}{\rho_g t_g c_{p_g}} - \frac{k_g\Delta t}{\rho_g c_{p_g}}\left(\frac{T_{t_{x+\Delta x}}-2T_{t_x}+T_{t_{x-\Delta x}}}{(\Delta x)^2}\right) - \frac{h_{t-a}\Delta t}{\rho_g t_g c_{p_g}}(T_t-T_a) - \frac{h_{r_{t-a}}\Delta t}{\rho_g t_g c_{p_g}}(T_t-T_a) - \frac{h_{f_{1-t}}\Delta t}{\rho_g t_g c_{p_g}}(T_t-T_{fm_1}) + \frac{h_{f_{1-t}}\Delta t}{\rho_g t_g c_{p_g}}(T_1-T_t)$$

On using, A and B as defined for single pass mode, and letting;

$$h_{t-a} + h_{r_{t-a}} = h_a$$
$$h_{f_{1-t}} = h_{t2}$$
$$h_{f_{1-t}} = h_{f1}$$

We arrive at;

$$T_t^1 = T_t + AG_s f_t \Delta t - B\Delta t(T_{t_{x+\Delta x}} - 2T_{t_x} + T_{t_{x-\Delta x}}) - A\Delta t h_a (T_t - T_a) - A\Delta t h_{f1}(T_t - T_{fm_1}) + A\Delta t h_{t2}(T_1 - T_t)$$

Or,

$$T_t^1 = T_t + A\Delta t[G_s f_t - h_a T_t + h_a T_a - h_{f1} T_t + h_{f1} T_{fm_1} + h_{t2} T_1 - h_{t2} T_t] - B\Delta t(T_{t_{x+\Delta x}} - 2T_{t_x} + T_{t_{x-\Delta x}})$$

Finally, we have;

$$T_t^1 = T_t + A\Delta t[G_s f_t + h_a T_a + h_{f1} T_{fm_1} + h_{t2} T_1 - C_2 T_t] - B\Delta t(T_{t_{x+\Delta x}} - 2T_{t_x} + T_{t_{x-\Delta x}}) \quad (4.3.8)$$

Where, $C_2 = h_a + h_{f1} + h_{t2}$.

2. FLOWING FLUID IN THE FIRST FLOW CHANNEL.

Here,

$$M_{f_1} = \rho_{f_1} b t_{f_1} dx$$

$$\frac{\rho_{f_1} b t_{f_1}}{bdx} c_{pf} \frac{T_{f_1}^1 - T_{f_1}}{\Delta t} = h_{f_{1-t}}(T_t - T_{fm_1}) + h_{f_{1-1}}(T_1 - T_{fm_1}) - \frac{\dot{m}}{bdx} c_{pf} \frac{\partial T_{f_1}}{\partial x} dx$$

Or,

$$\frac{T_{f_1}^1 - T_{f_1}}{\Delta t} = \frac{h_{f_{1-t}}}{\rho_{f_1} t_{f_1} c_{pf}}(T_t - T_{fm_1}) + \frac{h_{f_{1-1}}}{\rho_{f_1} t_{f_1} c_{pf}}(T_1 - T_{fm_1}) - \frac{\dot{m}}{\rho_{f_1} t_{f_1} b} \frac{T_{f_{x+\Delta x}} - T}{\Delta x}$$

On letting,

$$H_1 = \frac{1}{\rho_{f_1} t_{f_1} c_{pf}}$$

$$J_1 = \frac{\dot{m}}{\rho_{f_1} t_{f_1} b \Delta x}$$

$$T_{f_1}^1 = T_{f_1} + H_1 h_{f_1} \Delta t\left(T_t - T_{fm_1}\right) + H_1 h_{f_{1-1}} \Delta t\left(T_1 - T_{fm_1}\right) - J_1 \Delta t\left(T_{f_{1_{x+\Delta x}}} - T_{f_{1_x}}\right)$$

Giving;

$$T_{f_1}^1 = T_{f_1} + H_1 \Delta t[h_{f_1} T_t + h_{f_{1-1}} T_1 - K_1 T_{fm_1}] - J_1 \Delta t\left(T_{f_{1_{x+\Delta x}}} - T_{f_{1_x}}\right) \qquad (4.3.9)$$

Where, $K_1 = h_{f_1} + h_{f_{1-1}}$.

3. FIRST GLASS COVER.

$$\frac{\rho_g b t_g dx}{dx} c_{p_g} \frac{T_1^1 - T_1}{\Delta t} = G_s f_1 - k_g b t_g \frac{dx}{bdx} \frac{T_{1_{x+\Delta x}} - 2T_{1_x} + T_{1_{x-\Delta x}}}{(\Delta x)^2} - h_{f_{1-1}}(T_1 - T_{fm_1})$$
$$- h_{r_{1-4}}(T_1 - T_t) + h_{ab-1}(T_{ab} - T_1) + h_{r_{ab-1}}(T_{ab} - T_1)$$

Or,

$$\rho_g t_g c_{p_g} \frac{T_1^1 - T_1}{\Delta t} = G_s f_1 - k_g t_g \frac{T_{1_{x+\Delta x}} - 2T_{1_x} + T_{1_{x-\Delta x}}}{(\Delta x)^2} - h_{f_{1-1}}(T_1 - T_{fm_1})$$
$$- h_{r_{1-4}}(T_1 - T_t) + h_{ab-1}(T_{ab} - T_1) + h_{r_{ab-1}}(T_{ab} - T_1)$$

Reducing to;

$$T_1^1 = T_1 + A\Delta t G_s f_1 - B\Delta t\left(T_{1_{x+\Delta x}} - 2T_{1_x} + T_{1_{x-\Delta x}}\right) - A\Delta t h_{f_{1-1}}\left(T_1 - T_{fm_1}\right)$$
$$- A\Delta t h_{r_{1-4}}\left(T_1 - T_t\right) + A\Delta t h_{ab-1}\left(T_{ab} - T_1\right) + A\Delta t h_{r_{ab-1}}\left(T_{ab} - T_1\right)$$

On letting,

$$h_{ab-1} + h_{r_{ab-1}} = h_1$$

$$T_1^1 = T_1 + A\Delta t[G_s f_1 + h_{f_{1-1}} T_{fm_1} + h_{t2} T_t + h_1 T_{ab} - D_1 T_1] \qquad (4.3.10)$$
$$- B\Delta t\left(T_{1_{x+\Delta x}} - 2T_{1_x} + T_{1_{x-\Delta x}}\right)$$

where, $D_1 = h_{f_{1-1}} + h_{t2} + h_1$.

4. ABSORBER PLATE.

$$\rho_{ab} t_{ab} b \frac{dx}{bdx} c_{p_{ab}} \frac{T_{ab}^{1} - T_{ab}}{\Delta t} = G_s f_{ab} - k_{ab} b t_{ab} \frac{dx}{bdx} \frac{T_{ab_{x+\Delta x}} - 2T_{ab_x} - T_{ab_{x-\Delta x}}}{(\Delta x)^2} - h_1 (T_{ab} - T_1)$$
$$- h_{f_{ab-bp}} (T_{ab} - T_{bp}) - h_{f_{2-ab}} (T_{ab} - T_{fm_2})$$

Or,

$$T_{ab}^{1} = T_{ab} + \frac{G_s f_{ab} \Delta t}{\rho_{ab} t_{ab} c_{p_{ab}}} - \frac{k_{ab} \Delta t}{\rho_{ab} c_{p_{ab}} (\Delta x)^2} (T_{ab_{x+\Delta x}} - 2T_{ab_x} + T_{ab_{x-\Delta x}}) - \frac{h_1 \Delta t}{\rho_{ab} t_{ab} c_{p_{ab}}} (T_{ab} - T_1)$$
$$- \frac{h_{f_{ab-bp}} \Delta t}{\rho_{ab} t_{ab} c_{p_{ab}}} (T_{ab} - T_{bp}) - \frac{h_{f_{2-ab}} \Delta t}{\rho_{ab} t_{ab} c_{p_{ab}}} (T_{ab} - T_{fm_2})$$

On letting;

$$\frac{1}{\rho_{ab} t_{ab} c_{p_{ab}}} = E$$

$$\frac{k_{ab}}{\rho_{ab} c_{p_{ab}} (\Delta x)^2} = F$$

$$h_{f_{ab-bp}} = h_{ab}$$

$$h_{f_{2-ab}} = h_{f2}$$

$$T_{ab}^{1} = T_{ab} + E\Delta t G_s f_{ab} - E\Delta t h_1 (T_{ab} - T_1) - E\Delta t h_{ab} (T_{ab} - T_{bp})$$
$$- E\Delta t h_{f2} (T_{ab} - T_{fm_2}) - F\Delta t [T_{ab_{x+\Delta x}} - 2T_{ab_x} + T_{ab_{x-\Delta x}}]$$

Or,

$$T_{ab}^{1} = T_{ab} + E\Delta t [G_s f_{ab} + h_1 T_1 + h_{ab} T_{bp} + h_{f2} T_{fm_2} - G_1 T_{ab}]$$
$$- F\Delta t [T_{ab_{x+\Delta x}} - 2T_{ab_x} + T_{ab_{x-\Delta x}}] \qquad (4.3.11)$$

Where,

$$G_1 = h_1 + h_{ab} + h_{f2}.$$

5. FLOWING FLUID IN THE SECOND FLOW CHANNEL.

Here,

$$M_{f_2} = \rho_{f_2} b t_{f_2} dx$$

$$\frac{\rho_{f_2} b t_{f_2}}{bdx} c_{p_f} \frac{T_{f_2}^1 - T_{f_2}}{\Delta t} = h_{f_{2\text{-}ab}} (T_{ab} - T_{fm_2}) + h_{f_{2\text{-}bp}} (T_{bp} - T_{fm_2}) - \frac{\dot{m}}{bdx} c_{p_f} \frac{\partial T_{f_2}}{\partial x} dx$$

Or,

$$\frac{T_{f_2}^1 - T_{f_2}}{\Delta t} = \frac{h_{f_{2\text{-}ab}}}{\rho_{f_2} t_{f_2} c_{p_f}} \left(T_{ab} - T_{fm_2}\right) + \frac{h_{f_{2\text{-}bp}}}{\rho_{f_2} t_{f_2} c_{p_f}} \left(T_{bp} - T_{fm_2}\right) - \frac{\dot{m}}{\rho_{f_2} t_{f_2} b} \frac{T_{f_{2_{x+\Delta x}}} - T_{f_{2_x}}}{\Delta x}$$

On letting,

$$H_2 = \frac{1}{\rho_{f_2} t_{f_2} c_{p_{f_2}}}$$

$$J_2 = \frac{\dot{m}}{\rho_{f_2} t_{f_2} b \Delta x}$$

$$h_{fb} = h_{f_{2\text{-}bp}}$$

$$T_{f_2}^1 = T_{f_2} + H_2 h_{f_2} \Delta t \left(T_{ab} - T_{fm_2}\right) + H_2 h_{fb} \Delta t \left(T_{bp} - T_{fm_2}\right) - J_2 \Delta t \left(T_{f_{2_{x+\Delta x}}} - T_{f_{2_x}}\right)$$

Giving;

$$T_{f_2}^1 = T_{f_2} + H_2 \Delta t [h_{f_2} T_{ab} + h_{fb} T_{bp} - K_2 T_{fm_2}] - J_2 \Delta t \left(T_{f_{2_{x+\Delta x}}} - T_{f_{2_x}}\right) \qquad (4.3.12)$$

Where, $K_2 = h_{f_2} + h_{fb}$.

6. THE BACK PLATE.

$$\rho_{bp} b t_{bp} \frac{dx}{bdx} c_{p_{bp}} \frac{T_{bp}^1 - T_{bp}}{\Delta t} = h_{f_{b\text{-}bp}} (T_{ab} - T_{bp}) - h_{f_{2\text{-}bp}} (T_{bp} - T_{fm_2}) - U_L (T_{bp} - T_{ins}) - k_{bp} b t_{bp} \frac{dx}{bdx} \frac{d^2 T_{bp}}{dx^2}$$

Or,

$$T'_{bp} = T_{bp} + \frac{h_{r_{ab\text{-}bp}}\Delta t}{\rho_{bp} t_{bp} c_{p_{bp}}}(T_{ab} - T_{bp}) - \frac{h_{f_{2\text{-}bp}}\Delta t}{\rho_{bp} t_{bp} c_{p_{bp}}}(T_{bp} - T_{fm_2})$$
$$- \frac{U_L \Delta t}{\rho_{bp} t_{bp} c_{p_{bp}}}(T_{bp} - T_{ins}) - \frac{k_{bp}\Delta t}{\rho_{bp} c_{p_{bp}} (\Delta x)^2}(T_{bp_{x+\Delta x}} - 2T_{bp_x} + T_{bp_{x-\Delta x}})$$

On using,

$$h_{r_{ab\text{-}bp}} = h_{ab}$$
$$h_{f_{2\text{-}bp}} = h_{fb}$$
$$\frac{1}{\rho_{bp} t_{bp} c_{p_{bp}}} = L$$
$$\frac{k_{bp}}{\rho_{bp} c_{p_{bp}} (\Delta x)^2} = M$$

We get,

$$T'_{bp} = T_{bp} + L\Delta t h_{ab}(T_{ab} - T_{bp}) - L\Delta t h_{fb}(T_{bp} - T_{fm_2})$$
$$- LU_L\Delta t(T_{bp} - T_{ins}) - M\Delta t(T_{bp_{x+\Delta x}} - 2T_{bp_x} + T_{bp_{x-\Delta x}})$$

Or,

$$T'_{bp} = T_{bp} + L\Delta t(h_{ab}T_{ab} + h_{fb}T_{fm_2} - N_1 T_{bp})$$
$$- LU_L\Delta t(T_{bp} - T_{ins}) - M\Delta t(T_{bp_{x+\Delta x}} - 2T_{bp_x} + T_{bp_{x-\Delta x}}) \qquad (4.3.13)$$

where, $N_1 = h_{ab} + h_{fb}$

7. INSULATION.

$$\rho_{ins} b t_{ins} \frac{dx}{bdx} c_{p_{ins}} \frac{T'_{ins} - T_{ins}}{\Delta t} = U_L(T_{bp} - T_{ins}) - h_{ins\text{-}a}(T_{ins} - T_a) - h_{r_{ins\text{-}a}}(T_{ins} - T_a)$$
$$- k_{ins} b t_{ins} \frac{dx}{bdx(\Delta x)^2}\left(T_{ins_{x+\Delta x}} - T_{ins_x} + T_{ins_{x-\Delta x}}\right)$$

Or

$$T'_{ins} = T_{ins} + \frac{U_L \Delta t}{\rho_{ins} t_{ins} c_{p_{ins}}}\left(T_{bp} - T_{ins}\right) - \frac{h_{ins}\Delta t}{\rho_{ins} t_{ins} c_{p_{ins}}}(T_{ins} - T_a)$$
$$- \frac{k_{ins}\Delta t}{\rho_{ins} c_{p_{ins}} (\Delta x)^2}\left(T_{ins_{x+\Delta x}} - 2T_{ins_x} + T_{ins_{x-\Delta x}}\right)$$

On using,

$$\frac{1}{\rho_{ins} t_{ins} c_{p_{ins}}} = P$$

$$\frac{k_{ins}}{\rho_{ins} c_{p_{ins}} (\Delta x)^2} = Q$$

$$T_{ins}^{l} = T_{ins} + PU_L \Delta t(T_{bp} - T_{ins}) - Ph_{ins} \Delta t(T_{ins} - T_a) - Q\Delta t(T_{ins_{x+\Delta x}} - 2T_{ins_x} + T_{ins_{x-\Delta x}}) \quad (4.3.14)$$

The component temperatures were predicted using equations (4.3.8 to 4.3.14).

4.4: DOUBLE [MIDDLE FIRST] PASS MODE (DMPM).

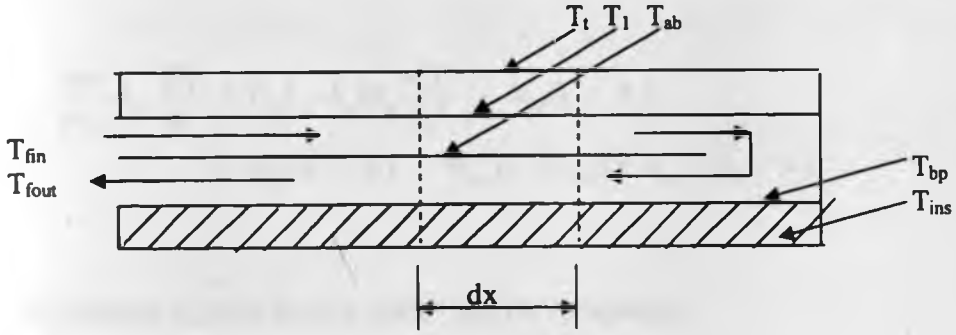

Figure.4.4.Double (middle First) pass mode

It was assumed that the assumptions made for the double (top first) pass mode do apply here equally. The energy balance analysis was done as follows;

1. TOP GLASS COVER.

$$dm_t c_{p_g} \frac{dT_t}{dt} = G_s f_t dA_k - k_g bt_g dx \frac{d^2T_t}{dx^2} - h_{ta} dA_k (T_t - T_a) - h_{r_{ta}} dA_k (T_t - T_a) + h_{1t} dA_k (T_1 - T_t) + h_{r_{1t}} dA_k (T_1 - T_t)$$

Dividing through by dA_k,

$$\frac{dm_t}{dA_k} c_{p_g} \frac{dT_t}{dt} = G_s f_t - k_g bt_g \frac{dx}{dA_k} \frac{d^2T_t}{dx^2} - h_{ta} (T_t - T_a) - h_{r_{ta}} (T_t - T_a) + h_{1t} (T_1 - T_t) + h_{r_{1t}} (T_1 - T_t) \quad (4.4.1)$$

2. FIRST GLASS COVER.

$$dm_1 c_{p_g} \frac{dT_1}{dt} = G_s f_1 dA_k - k_g bt_g dx \frac{d^2T_1}{dx^2} - h_{f_{1-1}} dA_k (T_1 - T_{fm_1}) + h_{r_{ab-1}} dA_k (T_{ab} - T_1) - h_{1t} dA_k (T_1 - T_t) - h_{r_{1t}} dA_k (T_1 - T_t)$$

Or,

$$\frac{dm_1}{dA_k} c_{p_g} \frac{dT_1}{dt} = G_s f_1 - k_g bt_g \frac{d^2T_1}{dx^2} - h_{1t} (T_1 - T_t) - h_{r_{1t}} (T_1 - T_t) - h_{f_{1-1}} (T_1 - T_{fm_1}) + h_{r_{ab-1}} (T_{ab} - T_1) \quad (4.4.2)$$

3. FLOWING FLUID IN THE FIRST FLOW CHANNEL.

$$M_{f_1} c_{p_{f_1}} \frac{dT_{f_1}}{dt} = h_{f_{1-1}} dA_k (T_1 - T_{fm_1}) + h_{f_{1-ab}} dA_k (T_{ab} - T_{fm_1}) - m c_{p_{f_1}} \frac{\partial T_{f_1}}{\partial x} dx \quad (4.4.3)$$

4. ABSORBER PLATE.

$$dm_{ab} c_{p_{ab}} \frac{dT_{ab}}{dt} = G_s f_{ab} dA_k - k_{ab} bt_{ab} dx \frac{d^2T_{ab}}{dx^2} - h_{f_{1-ab}} dA_k (T_{ab} - T_{fm_1}) - h_{f_{2-ab}} dA_k (T_{ab} - T_{fm_2}) - h_{r_{ab-1}} dA_k (T_{ab} - T_1) - h_{r_{ab-bp}} dA_k (T_{ab} - T_{bp})$$

Or,

$$\frac{dm_{ab}}{dA_k} c_{p_{ab}} \frac{dT_{ab}}{dt} = G_s f_{ab} - k_{ab} bt_{ab} \frac{dx}{dA_k} \frac{d^2T_{ab}}{dx^2} - h_{f_{1-ab}} \left(T_{ab} - T_{fm_1}\right) - h_{f_{2-ab}} \left(T_{ab} - T_{fm_2}\right) - h_{r_{ab-1}} \left(T_{ab} - T_1\right) - h_{r_{ab-bp}} \left(T_{ab} - T_{bp}\right) \quad (4.4.4)$$

5. FLOWING FLUID IN THE SECOND FLOW CHANNEL.

$$M_{f_2} c_{p_{f_2}} \frac{dT_{f_2}}{dt} = h_{f_{2-ab}} dA_k (T_{ab} - T_{fm_2}) + h_{f_{2-bp}} dA_k (T_{bp} - T_{fm_2}) - \dot{m} c_{p_{f_2}} \frac{\partial T_{f_2}}{\partial x} dx \quad (4.4.5)$$

6. BACK PLATE.

$$dm_{bp} c_{p_{bp}} \frac{dT_{bp}}{dt} = h_{r_{ab-bp}} dA_k (T_{ab} - T_{bp}) - h_{f_{2-bp}} dA_k (T_{bp} - T_{fm_2}) - U_L dA_k (T_{bp} - T_{ins}) - k_{bp} bt_{bp} dx \frac{d^2T_{bp}}{dx^2}$$

Or,

$$\frac{dm_{bp}}{dA_k} c_{p_{bp}} \frac{dT_{bp}}{dt} = h_{r_{ab-bp}} (T_{ab} - T_{bp}) - h_{f_{2-bp}} (T_{bp} - T_{fm_2}) - U_L (T_{bp} - T_{ins}) - k_{bp} bt_{bp} \frac{dx}{dA_k} \frac{d^2T_{bp}}{dx^2} \quad (4.4.6)$$

7.INSULATION.

$$dm_{ins} c_{p_{ins}} \frac{dT_{ins}}{dt} = U_L dA_k \left(T_{bp} - T_{ins}\right) - k_{ins} bt_{ins} dx \frac{d^2T_{ins}}{dx^2} - h_{ins-a} dA_k (T_{ins} - T_a) - h_{r_{ins-a}} dA_k (T_{ins} - T_a)$$

Or,

$$\frac{dm_{ins}}{dA_k} c_{p_{ins}} \frac{dT_{ins}}{dt} = U_L (T_{bp} - T_{ins}) - h_{ins-a} (T_{ins} - T_a) - h_{r_{ins-}} (T_{ins} - T_a) - k_{ins} bt_{ins} \frac{dx}{dA_k} \frac{d^2 T_{ins}}{dx^2} \quad (4.4.7)$$

The above equations were simplified by use of finite-difference expressions (appendix I).

4.5. TRIPLE PASS MODE.

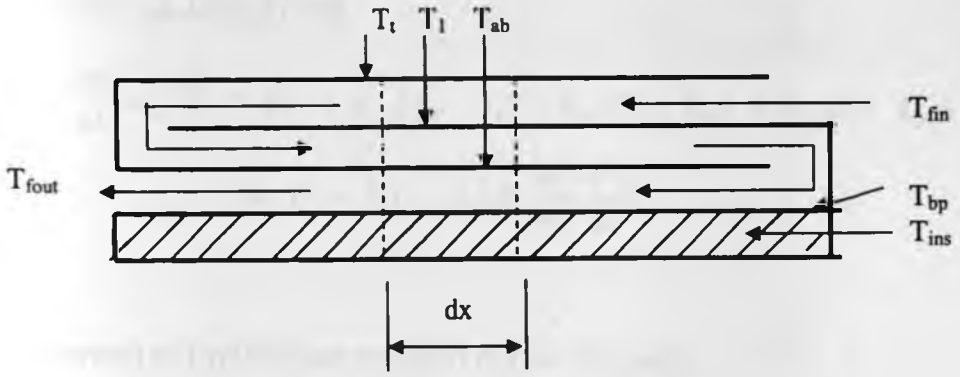

Figure. 4.5. Triple pass mode

Performing an energy balance;

1. TOP GLASS COVER.

$$dm_t c_{p_g} \frac{dT_t}{dt} = G_s f_t dA_k + h_{r_{t-1}} dA_k (T_1 - T_t) - h_{r_{t-a}} dA_k (T_t - T_a) - h_{t-a} dA_k (T_t - T_a) - h_{f_{t-1}} dA_k (T_1 - T_{fin_1}) - k_g t_g b dx \frac{d^2 T_t}{dx^2}$$

Or,

$$\frac{dm_t}{dA_k}c_{p_f}\frac{dT_f}{dt} = G_s f_t + h_{r_{t-1}}(T_1 - T_t) - h_{r_{t-a}}(T_t - T_a) - h_{t-a}(T_t - T_a) - h_{f_{1-t}}(T_1 - T_{fm_1}) - k_g t_g b\frac{dx}{dA_k}\frac{d^2T}{dx^2} \quad (4.5.1)$$

2. FLOWING FLUID IN THE FIRST FLOW CHANNEL.

$$M_{f_1}c_{p_f}\frac{dT_{f_1}}{dt} = h_{f_{1-t}}dA_k(T_t - T_{fm_1}) + h_{f_{1-1}}dA_k(T_1 - T_{fm_1}) - \dot{m}c_{p_f}\frac{\partial T_{f_1}}{\partial x}dx \quad (4.5.2)$$

3. FIRST GLASS COVER.

$$\frac{dm_1}{dA_k}c_{p_f}\frac{dT_1}{dt} = G_s f_1 + h_{r_{ab-1}}(T_{ab} - T_1) - h_{f_{1-1}}(T_1 - T_{fm_1}) - h_{f_{2-1}}(T_1 - T_{fm_2}) - h_{r_{1-t}}(T_1 - T_t) - k_g t_g b\frac{dx}{dA_k}\frac{d^2T_1}{dx^2} \quad (4.5.3)$$

4. FLOWING FLUID IN THE SECOND FLOW CHANNEL.

$$M_{f_2}c_{p_f}\frac{dT_{f_2}}{dt} = h_{f_{2-1}}dA_k(T_1 - T_{fm_2}) + h_{f_{2-ab}}dA_k(T_{ab} - T_{fm_2}) - \dot{m}c_{p_f}\frac{\partial T_{f_2}}{\partial x}dx \quad (4.5.4)$$

5. ABSORBER PLATE.

$$dm_{ab}c_{p_{ab}}\frac{dT_{ab}}{dx} = G_s f_{ab}dA_k - h_{f_{2-ab}}dA_k(T_{ab} - T_{fm_2}) - h_{f_{3-ab}}dA_k(T_{ab} - T_{fm_3}) - h_{r_{1-ab}}dA_k(T_{ab} - T_1) - h_{r_{bp-ab}}dA_k(T_{ab} - T_{bp}) - k_{ab}t_{ab}bdx\frac{d^2T_{ab}}{dx^2}$$

Or,

$$\frac{dm_{ab}}{dA_k}c_{p_{ab}}\frac{dT_{ab}}{dx} = G_s f_{ab} - h_{f_{2-ab}}(T_{ab} - T_{fm_2}) - h_{f_{3-ab}}(T_{ab} - T_{fm_3}) - h_{r_{1-ab}}(T_{ab} - T_1) - h_{r_{bp-ab}}(T_{ab} - T_{bp}) - k_{ab}t_{ab}b\frac{dx}{dA_k}\frac{d^2T}{dx^2} \quad (4.5.5)$$

6. FLOWING FLUID IN THE THIRD FLOW CHANNEL.

$$M_{f_3} c_{p_f} \frac{dT_{f_3}}{dt} = h_{f_{3-ab}} dA_k (T_{ab} - T_{fm_3}) + h_{f_{3-bp}} dA_k (T_{bp} - T_{fm_3}) - \dot{m} c_{p_f} \frac{\partial T_{f_3}}{\partial x} dx \qquad (4.5.6)$$

7. BACK PLATE.

$$dm_{bp} c_{p_{bp}} \frac{dT_{bp}}{dt} = h_{r_{bp-ab}} dA_k (T_{ab} - T_{bp}) - h_{f_{3-bp}} dA_k (T_{bp} - T_{fm_3}) - U_L dA_k (T_{bp} - T_{ins}) - k_{bp} t_{bp} b dx \frac{d^2 T_{bp}}{dx^2}$$

Or,

$$\frac{dm_{bp}}{dA_k} c_{p_{bp}} \frac{dT_{bp}}{dt} = h_{r_{bp-ab}} (T_{ab} - T_{bp}) - h_{f_{3-bp}} (T_{bp} - T_{fm_3}) - U_L (T_{bp} - T_{ins}) - k_{bp} t_{bp} b \frac{dx}{dA_k} \frac{d^2 T_{tp}}{dx^2} \qquad (4.5.7)$$

8. INSULATION.

$$dm_{ins} c_{p_{ins}} \frac{dT_{bp}}{dt} = U_L dA_k (T_{bp} - T_{ins}) - h_{ins-a} dA_k (T_{ins} - T_a) - h_{r_{ins-a}} dA_k (T_{ins} - T_a) - k_{ins} t_{ins} b dx \frac{d^2 T_{ins}}{dx^2}$$

Or,

$$\frac{dm_{ins}}{dA_k} c_{p_{ins}} \frac{dT_{ins}}{dt} = U_L (T_{bp} - T_{ins}) - h_{ins-a} (T_{ins} - T_a) - h_{r_{ins-a}} (T_{ins} - T_a) - k_{ins} t_{ins} b \frac{dx}{dA_k} \frac{d^2 T_{ins}}{dx^2} \qquad (4.5.8)$$

Equations (4.5.1 to 4.5.8) were simplified using the finite-difference expressions (appendix 2). Then the resulting expressions used to predict the future temperatures of the collector components and the flowing air.

To solve the temperature equations assumptions that, due to the thin sizes of the plates and the low thermal conductivity of air, the heat transfer in the plates and in the flowing air in the flow direction are very small, hence the axial conduction terms can be dropped since they are very small compared to the other terms were used.

All the sets of equations developed were solved as explained in the solution procedure section to determine the component temperatures after the defined time interval.

4.6: CORRELATIONS.

To be in a position to solve the developed equations, some correlations and constants had to be used in simplifying the terms involved. The correlations used are given in the following sub-sections.

4.6.1: Determination of the Incident Radiation absorbed by the Components.

According to Simonson[3], Duffie and Beckman[15], there will be multiple reflection between the collector components. This will have an effect on the fraction of incident radiation that will be absorbed by the collector components. Hence there is a need to trace the incident radiation rays and get expressions for the radiation that will be absorbed by the glass covers and the absorber plate.

The glass covers will reflect, transmit, and absorb the incident radiation, while the absorber plate will reflect and absorb.

Expressions for the reflectivity, transmissivity, and absorptivity of the glass covers are given in section 3.4, while the absorptivity of the absorber plate will be a known constant.

A part of the expected radiation ray diagram is given in figure 4.6.

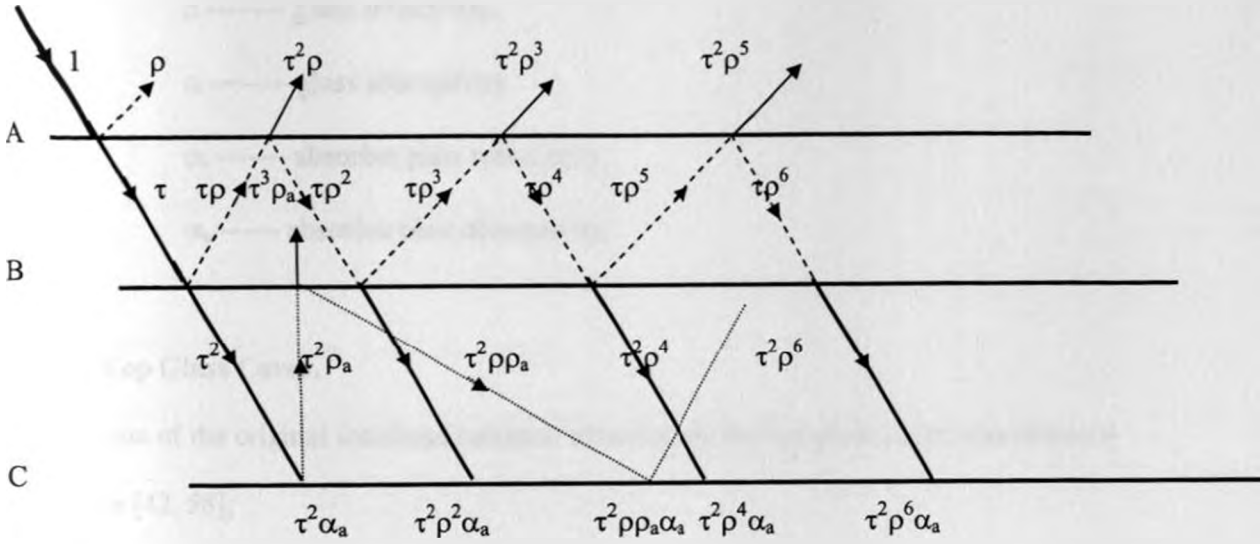

Figure.4.6. Radiation ray diagram.

Where;

A = Top glass cover.

B = First glass cover.

C = Absorber plate.

Incident radiation.

Transmitted radiation.

Reflected radiation.

Absorber plate reflections.

Assumptions made:

a) The material properties are constant (do not change with temperature).

b) The glass covers have the same optical properties.

c) The transmissivity of the glass is very high, hence the glass reflectivity and absoptivity can be considered to be very small.

d) The absober plate has high absorptivity, low reflectivity, and no transmissivity.

Symbols used;

τ ------- glass transmissivity.

ρ -------- glass reflectivity.

α -------- glass absorptivity.

ρ_a ------- absorber plate reflectivity.

α_a ------ absorber plate absorptivity.

4.6.1.1: Top Glass Cover.

The fraction of the original incidence radiation absorbed by the top glass cover, was obtained as follows [42, 58];

Total reflection by the top cover to the ambient,

$$\rho + \tau^2\rho + \tau^2\rho^3 + \tau^2\rho^5 + \tau^2\rho^7 + \text{------} \qquad (4.6.1)$$

Total absorbed radiation:

$$= (1 - \rho - \tau) + (\tau\rho - \tau^2\rho - \tau\rho^2) + (\tau\rho^3 - \tau^2\rho^3 - \tau\rho^4) + (\tau\rho^5 - \tau^2\rho^5 - \tau\rho^6) + \text{--------}$$

$$= (1 - \rho - \tau) + \tau\rho(1 - \rho - \tau) + \tau\rho^3(1 - \rho - \tau) + \tau\rho^5(1 - \tau - \rho) + \text{------}$$

$$= (1 - \rho - \tau)\ [1 + \tau\rho + \tau\rho^3 + \tau\rho^5 + \text{---------}]$$

Or,

$$(1 - \rho - \tau)\ [1 + \tau(\rho + \rho^3 + \rho^5 + \text{-------})]$$

$$= (1 - \rho - \tau)\ [1 + \tau\sum_{n=1}^{\infty}\rho^{2n-1}] \qquad (4.6.2)$$

Since, efficient operations of the collector requires that the reflectivity be very small, higher powers of ρ can be neglected, hence

$$\sum_{n=1}^{\infty}\rho^{2n-1} \simeq \rho \qquad (4.6.3)$$

Thus, absorption by the top glass cover can be given by:

$$(1 - \rho - \tau)\,(1 + \tau\rho) = f_t \qquad (4.6.4)$$

NOTE:

The term $\tau\rho$ accounts for multiple reflection.

4.6.1.2: First Glass Cover Total Absorption.

Total absorbed radiation by the first glass cover is obtained as [42, 58],

$$(\tau - \tau^2 - \tau\rho) + (\tau\rho^2 - \tau^2\rho^2 - \tau\rho^3) + (\tau\rho^4 - \tau^2\rho^4 - \tau\rho^5) + (\tau\rho^6 - \tau^2\rho^6 - \tau\rho^7) + \text{-----}$$

$$= \tau(1 - \rho - \tau) + \tau\rho^2(1 - \rho - \tau) + \tau\rho^4(1 - \rho - \tau) + \tau\rho^6(1 - \rho - \tau) + \text{-------}$$

Or,

$$(1 - \rho - \tau)\,[\tau + \tau\rho^2 + \tau\rho^4 + \tau\rho^6 + \text{--------}]$$

$$= (1 - \rho - \tau)\,\tau[1 + \rho^2 + \rho^4 + \rho^6 + \text{----------}]$$

Hence the first glass cover total absorption is ,

$$f_1 = (1 - \rho - \tau)\,\tau\sum_{n=0}^{\infty}\rho^{2n} \qquad (4.6.6)$$

Since ρ is supposed to be very smal, we can write,

$$\sum_{n=0}^{\infty}\rho^{2n} \simeq 1 + \rho^2 \qquad (4.6.7)$$

Hence, the first glass cover total absorption will be given by,

$$f_1 = (1 - \rho - \tau)\,(\tau + \tau\rho^2) \qquad (4.6.8)$$

Where the term $\tau\rho^2$ accounts for multiple reflections.

4.6.1.3: Absorber Plate Total Radiation Absorption.

The absorber plate will absorb radiations transmitted through the covers and also will absorb reflected radiation from the absorber and back to the absorber from the first glass cover.

Total radiation absorbed from the initial incident radiation is given as,

$$\tau^2\alpha_a + \tau^2\rho^2\alpha_a + \tau^2\rho^4\alpha_a + \tau^2\rho^6\alpha_a + \text{--------}$$

Or,

$$\tau^2\alpha_a\left(1 + \rho^2 + \rho^4 + \rho^6 + \text{----------}\right)$$

$$= \tau^2\alpha_a \sum_{n=0}^{\infty}\rho^{2n} \qquad (4.6.9)$$

The radiation absorbed by the absorber plate from plate reflections is obtained as;

$$\tau^2\rho_a\rho\alpha_a + \tau^2\rho_a^2\rho^2\alpha_a + \tau^2\rho_a^3\rho^3\alpha_a + \tau^2\rho_a^4\rho^4\alpha_a + \text{---------}$$

Or,

$$\tau^2\alpha_a\left(\rho_a\rho + \rho_a^2\rho^2 + \rho_a^3\rho^3 + \rho_a^4\rho^4 + \text{----------}\right)$$

$$= \tau^2\alpha_a \sum_{n=1}^{\infty}(\rho_a\rho)^n \qquad (4.6.10)$$

Hence, total absorbed radiation is ;

$$\tau^2\alpha_a \sum_{n=0}^{\infty}\rho^{2n} + \tau^2\alpha_a \sum_{n=1}^{\infty}(\rho_a\rho)^n \qquad (4.6.11)$$

Since, ρ_a and ρ are considered small, we can neglect terms of 3rd order and higher. Hence;

$$f_{ab} = \tau^2\alpha_a\left(1+\rho^2\right) + \tau^2\alpha_a\left(\rho_a\rho\right)$$

Or,

$$f_{ab} = \tau^2 \alpha_a [1 + \rho^2 + \rho_a \rho] \quad (4.6.12)$$

Where f_{ab} is the optical efficiency of the collector.

The term ρ^2 accounts for multiple reflection between the glass covers whereas the term $\rho_a \rho$ accouts for multiple reflection between the first glass cover and the absorber plate.

4.6.2 Heat Transfer Coefficients and Empirical Correlations.

The following empirical correlations were used to determine the heat transfer coefficients.

4.6.2.1: CONDUCTIVE HEAT TRANSFER.

The heat conducted per unit area, q, through the back plate and the insulation layer was determined usingFourier's equation (3.35) which was rewritten as,

$$\dot{q} = \frac{\dot{Q}}{A} = \frac{T_1 - T_2}{\left(\frac{x_1}{k_1} + \frac{x_2}{k_2}\right)} \quad (4.6.13)$$

Where,

$\dot{Q}$ = heat conducted through the given slab, W.
A = area for the heat flow, m^2.

T_1 = temperature of the back plate, K.

T_2 = temperature of the outer surface of the insulation, K.

x_1 = thickness of the back plate, m.
x_2 = thickness of the insulation material, m.
k_1 = thermal conductivity of the back plate material,m.
k_2 = thermal conductivity of the insulation material, m.

When electrical analogy was used, R , a term giving the thermal resistance, was defined as;

$$R = \left(\frac{x_1}{k_1} + \frac{x_2}{k_2}\right) \ m^2.K/W \quad (4.6.14)$$

Hence, $q = h_c(T_1 - T_2)$ (4.6.15)

Where,

$h_c = \frac{1}{R}$ — conduction heat transfer coefficient, $W/m^2.K$

4.6.2.2: Radiative Heat Transfer.

i) Sky radiation.

This is the radiative heat transfer between the top cover and the atmosphere.

The net radiation to the top glass cover surface was determined by considering its radiation exchange with the sky. The following relation was used [16, 28, 31];

$$Q = \varepsilon A\sigma(T_{sky}^4 - T^4) \quad \text{(Equation 3.14)}$$

Where,

Q = the net radiation heat exchage, W.
ε = emittance of the glass.
A = area of the heat exchange, m^2.
σ = Stefan-Boltzmann constant.
T = temperature of the glass cover, K.
T_{sky} = sky temperature, which is realated to the local air temperature by the relation,[16],
$= 0.0552T_a^{1.5}$
T_a = the ambient temperature, K.

Radiation heat transfer coefficient was obtained as;

$$h_{r_a} = \frac{\sigma\varepsilon[T^4 - T_{sky}^4]}{(T - T_a)} \quad (4.6.16)$$

ii) Radiation between two parallel flat plates.

Radiative heat transfer coefficient between two parallel flat plates with an enclosed air gap was obtained using,

$$h_{r_{12}} = \frac{\sigma[T_1^2 + T_2^2][T_1 + T_2]}{\frac{1}{\varepsilon_1} + \frac{1}{\varepsilon_2} - 1} \qquad \text{(Equation 3.17)}$$

Where,

ε_1 – emissivity of first plate.
ε_2 – emissivity of second plate.
T_1 – temperature of first plate, K.
T_2 – temperature of second plate, K.

4.6.2.3:Convective Heat Transfer Coefficients

i) Forced convection by wind.

Forced convection from the top glass surface to the ambient had its heat transfer coefficient determined using the correlation;

$$h_w = 5.7 + 3.8v \quad W/m^2.K \qquad \text{(Equation 3.23)}$$

Where,

h_w – is the heat transfer coefficient by wind.
v – is the wind velocity in m/s.

ii) Natural convection between parallel flat plates.

Equation (3.19) was used to compute the natural convection heat transfer coefficient between parallel flat plates and, for a horizontal flat plate collector, was reduced to;

$$Nu = 1 + 1.44\left[1 - \frac{1708}{Ra}\right]^{+} + \left[\left(\frac{Ra}{5830}\right)^{\frac{1}{3}} - 1\right]^{+} \qquad (4.6.17)$$

Where the, +, exponent means only positive values of the terms in the square brackets are to be used, otherwise use zero for a negative value.

Then the heat transfer coefficient was obtained from the relation;

$$Nu = \frac{h \times d}{k} \qquad (4.6.18)$$

Where,

Nu – the Nusselt number.

d – the plate spacing, m.

k – thermal conductivity of the air in the plate gapping, W/m.K.

iii) Forced convection between horizontal parallel plates.

The forced convection heat transfer coefficient between air and the glass covers, or the absorber plate was determined using;

$$Nu = \frac{h_d d_h}{k} = 0.0158Re^{0.8} \qquad \text{(Equation 3.21)}$$

which is for a fully developed turbulent flow.

Where,

d_h - is the hydraulic mean diameter of the rectangular duct.

$$= \frac{4 \times \text{cross-sectional area of duct}}{\text{perimeter of duct}}$$

k - thermal conductivity of the flowing fluid.

This relation was found to be in agreement with a Shewen and Hollands recommendation for solar air heaters operating in the range of Reynolds numbers from 2000 to 10,000 (which is the common turbulent region for commercial solar air heat collectors), which was based on data by Kays and London. As Jansen [55] quoted the relation.

$$Nu = 0.00269Re. \qquad (4.6.19)$$

and,

$$h = \frac{Nu.\, k}{2b} \qquad (4.6.20)$$

where, b, is the duct height which was considered to be very small compared to the duct width.

This relation was applied to all channels, since it had negligible differences when compared with other correlations.

4.6.3: Setting the Distance and Time Intervals.

i) **Distance interval.**

To set the distance interval to be used in the computational model, the Biot number criteria were used [16], where;

$$Bi = \frac{hl}{k} \tag{4.6.21}$$

where,

Bi = Biot number.
h = convection heat transfer coefficient
k = thermal conductivity of the plate material.

The Biot number criteria, that is $Bi \leq 0.1$, for lumped-heat capacity method to be used, was used to set the distance interval with an approximated heat transfer coefficient of 13.3 $W/m^2.K$ to the ambient. The thermal conductivity of glass, which is low, was used, $(k = 1.05\ W/m^2.K)$ [32].

Hence,

$$l = \frac{Bi \times k}{h}$$

$$l = \frac{0.1 \times 1.05}{13.3} = 7.895 \times 10^{-3} m.$$

ii) **Time interval.**

The time interval was set theoretically using a relation given by Simonson [3];

$$\Delta t = \frac{l^2}{\alpha} \text{ seconds.} \qquad (4.6.22)$$

Where,

Δt - is the time interval to be used in the computational model.

l - is the already determined distance interval.

α - thermal diffusivity for the material considered.

$$= \frac{k}{\rho c_p}$$

ρ - density of the material.

c_p - specific heat of the material.

4.6.4: Properties of Air.

Air properties do vary with temperature. Hence for accuracy and reliability of the computed results, these effects had to be taken into account.

The density (ρ_a), specific heat capacity at constant pressure (c_p), thermal conductivity (k_a), and viscosity (μ) of air at a temperature T such that $300K \leq T \leq 450K$ and a pressure (P), were determined from the following expressions [3]:

$$\rho(kg/m^3) = \frac{P}{RT} = \frac{P}{287T} = \frac{292.86}{T} \qquad (4.6.23\text{-a})$$

$$c_p(J/kg.K) = 970.174 + 6.788\times10^{-2}T + 1.657\times10^{-4}T^2 - 6.787\times10^{-8}T^9 \qquad (4.6.23\text{-b})$$

$$k_a(W/m.K) = 7.2\times10^{-5}T + 4.64\times10^{-3} \qquad (4.6.23\text{-c})$$

$$\mu(kg/m.s) = 4.4\times10^{-8}T + 4.64\times10^{-6} \qquad (4.6.23\text{-d})$$

Note: The atmospheric pressure, P, for Nairobi is approximately 84.052 kPa (630 mmHg).

The values obtained from these expressions are in agreement with the values given by Jansen [55] for the temperatures expected in the collector.

4.6.5: Other Constants

Stefan- Boltzman constant [15]

$$\sigma = 5.669 \times 10^{-8} \ W/m^2.K^4.$$

4.6.6: Geographical Data for Nairobi [4].

Local longitude = $36^{\circ}49^{1}E$

Standard longitude for local time zone = $45^{1}E$

Latitude = $1^{\circ}19^{1}S$

Sunshine duration = 7hours (on average)

Altitude = 1669 m

CHAPTER 5: EXPERIMENTAL SET UP AND ANALYSIS.

An experimental set up was necessary to validate the models obtained from the theoretical analysis. This called for construction of a collector that could be operated in a manner that accommodated the four modes of airflow described earlier on. The experiments were carried out according to testing methods described in ASHRAE Standards 93- 77 [30].

The collector box was designed by considering several design parameters that are outlined in section 5.2, while the measurements that were made are mentioned and described in part 5.26 of the same section.

The other accessories used together with the collector box for this experiment were as shown in figure 5.1.

Experimental results were obtained and analyzed for the dates given in the results sheets.

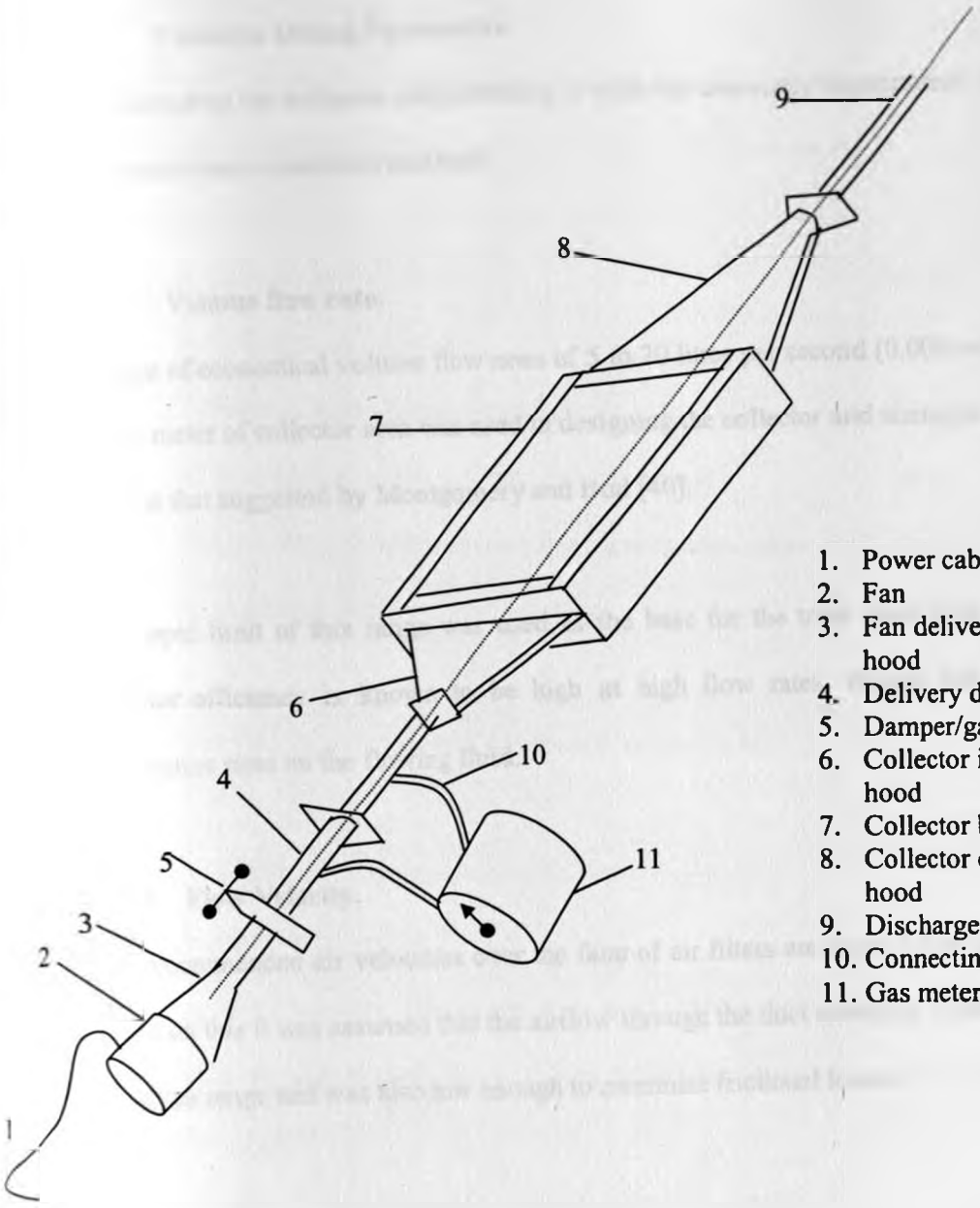

1. Power cable
2. Fan
3. Fan delivery adaptor hood
4. Delivery duct
5. Damper/gate valve
6. Collector intake adaptor hood
7. Collector box
8. Collector outlet adaptor hood
9. Discharge duct
10. Connecting hose pipe
11. Gas meter

Figure.5.1, Experimental set-up.

5.1. Collector Design Parameters.

In constructing the collector and matching it with the associated components, the following parameters were considered and used.

5.1.1. Volume flow rate.

A range of economical volume flow rates of 5 to 20 litres per second [0.005 to 0.02 m^3/s] per square meter of collector area was used in designing the collector and sizing its components – same as that suggested by Montgomery and Bud [40].

The upper limit of this range was used as the base for the total mass flow rate since the collector efficiency is known to be high at high flow rates, though this result to low temperature rises on the flowing fluid.

5.1.2. Flow Velocity.

The recommended air velocities over the face of air filters are from 1.524 to 2.54 m/s [41]. Based on this it was assumed that the airflow through the duct would be 2.5m/s which was in the given range and was also low enough to minimize frictional losses.

5.1.3. Air Density.

At sea level incompressibility can be assumed on the basis that air pressure and density may not vary substantially from the atmospheric conditions [42] and thus the air standard density may be taken as 1.2 kg/m^3 [39]. For Nairobi, where the experiment was carried out, the standard air density could not be applied hence the perfect gas equation (equation. 4.6.23-a) was considered suitable for determination of the air density.

5.1.4. Collector Dimensions.

The collector dimensions used were those used by Luti [13], which were chosen based on the available standard sizes of glass. The most crucial dimensions were:

i) Collector overall length = 1500mm.

ii) Collector overall width = 900mm.

iii) Main airflow channel height = 20mm.

iv) Insulation gap between first and top glasses = 25mm.

v) Insulation gap between absorber plate and first glass = 30mm.

vi) Insulation thickness = 13mm.

[All these were set in accordance to dimensions quoted in 4, 6].

The collector box was constructed using the following materials;

a. A wooden frame.
b. Two ordinary window glass covers 4mm thick, 1500 by 900 mm.
c. A 16mm thick mild steel sheet, painted with black matt paint (1500 by 900) used as absorber plate.
d. A back plate; 12mm thick mild steel sheet, 1500 by 900mm.
e. 10mm fiberglass insulation at the back, covered with 3mm thick plywood.
f. Timber strips for changing the mode of flow.

Note:

1. The air gap heights were minimized to reduce convection losses and shading effects.
2. Multi-layer glazing may result in serious shading for larger angles of incidence.
3. The main airflow channel is the gap between the absorber plate and the back plate.

These materials were arranged as show in figure 5.2. The flow channels and the stationary air gaps were sealed using steel putty and plasticine

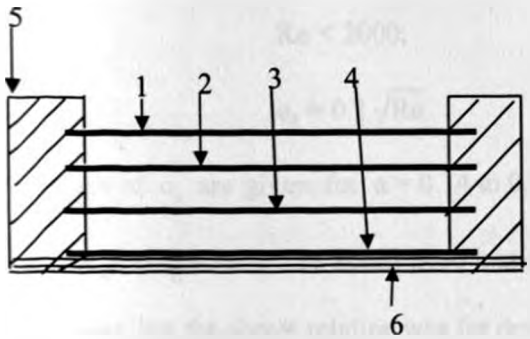

1. Top glass cover.
2. First glass cover.
3. Absorber plate.
4. Back plate.
5. Wooden frame.
6. Insulation

Figure.5.2. Material arrangement.

5.1.5: Pressure Drop in the collector.

This was done for all components through which the flowing air losses some pressure due to friction.

5.1.5.1: Screen (Air inlet guard).

The flow through the screen was considered as flow through a number of orifices or nozzles in parallel. The pressure drop or head loss across the screen was computed using an orifice type equation [44], and the screen head loss equation that resulted was;

$$\Delta h = \left(\frac{n}{c_s}\right)\left(\frac{1-\alpha^2}{\alpha^2}\right)\frac{v^2}{2g} \qquad (5.1)$$

Where,

Δh = head loss,m

n = number of screens in series.

c_s = screen discharge coefficient.

α = fractional free projected area of screen.

v = superficial velocity ahead of screen, m/s.

For laminar flow region,

$$Re < 2000;$$

$$c_s = 0.1\sqrt{Re} \qquad (5.2)$$

Also values of c_s are given for $\alpha = 0.14$ to 0.79 as a plot of C versus Re [36]. Where C is the discharge coefficient. The actual head loss across the screen could be measured by use of a manometer, but the above relation was for design purposes.

5.1.5.2:Filters/ Strainers.

An air filter was located at the fan inlet, with a recommended size of 50μm. The head loss due to the filter was calculated using the expression;

$$h = k\frac{v^2}{2g} \qquad (5.3)$$

Where k is a loss coefficient, which is taken to be equal to 2.0. The value is so assumed that it prevents under-design to avoid failure of the system to deliver the required capacity [45].

5.1.5.3: Adaptor Hoods.

Adaptor hoods were used to ensure uniform distribution of air in the collector. Dynamic losses occur as a result of turbulence caused by a change in direction or velocity at the hood entry.

The hood entry losses can be expressed as a number of velocity pressure heads using a hood pressure loss factor, k_h, [37].

The head loss due to a hood is given by;

$$\Delta h = k_h \frac{v^2}{2g} \tag{5.4}$$

Where the value of k_h needs to be determined experimentally by measuring the pressure drop across the hood. But the following approximate values were used, which were considered after referring to data given in [37].

Expanding hood, k_h = 1.0 (inlet to collector).
Reducing hood, k_h = 0.7 (exit from the collector).

5.1.5.4: Pressure Drop in the Duct Length.

The Darcy-Weisbach equation was used to determine the head loss due to flow through the pipes;

$$h_f = f\frac{L}{D}.\frac{v^2}{2g} \tag{5.5}$$

Where, f = frictional loss coefficient.

For laminar flow,

$$f = \frac{64}{Re} \tag{5.6}$$

For turbulent flow,

$$f = \frac{0.04}{Re^{0.16}} \quad Re > 3000 \ [38] \tag{5.7}$$

Also f can be determined from the Moody chart.

5.1.5.5: Gate valve/ Damper

The head loss was expressed in terms of an equivalent length of straight pipe, and was based on the equation;

$$h = f\frac{L_e}{d}.\frac{v^2}{2g} \tag{5.8}$$

Where the values of $\frac{L_e}{d}$ for the gate valve can be determined from the table 5.1. [38]

Table 5.1

Description	$\frac{L_e}{d}$
Fully open	13
$\frac{3}{4}$ open	35
$\frac{1}{2}$ open	160
$\frac{1}{4}$ open	900

5.1.5.6: Fittings (Joints)

Head loss due to fittings was calculated based on equivalent pipe length [38,34], using the relation;

$$h_l = f\frac{L_e}{d}.\frac{v^2}{2g} \tag{5.9}$$

Representative equivalent lengths in pipe diameters ($\frac{L_e}{d}$) for the fittings were taken to be as in table 5.2. [38];

Table 5.2.

Fitting Type	Equivalent length $\frac{L_e}{d}$
90° Standard elbow	30
45° Standard elbow	16
90° Elbow	20
90° Street elbow	50
45° Street elbow	26

5.1.5.7: Entrance Losses

For a sharp-edged entrance to a pipe or a sudden reduction in the cross-sectional area, the head loss is obtained as [36];

$$\Delta h = k_c\left(\frac{v_2^2}{2g}\right) \text{ - for turbulent flow} \tag{5.10}$$

Where,

v_2 = average velocity in the smaller pipe

k_c = number of velocity head losses.

For entrance, the value of k_c was taken to be, 0.5.

For laminar flow, the friction head loss is determined based on the equivalent length of straight pipe, whose value is given as [36];

$$\frac{L_e}{D} = a + b(Re) \qquad \text{for } \frac{A_2}{A_1} < 0.2 \tag{5.11}$$

Where,

Re-- Reynolds number in smaller pipe

a = 0.30 – Couette coefficient

b = 0.0391 – Hagenbach coefficient

A_1 = cross-sectional area of larger pipe, m^2

A_2 = cross-sectional area of smaller pipe,m^2

5.1.5.8: Enlargement and exit losses.

For ducts of any cross-section, the frictional loss for a sudden enlargement with turbulent flow is given by the simple Borda-Carnot equation [36];

$$\Delta h = \frac{(v_1 - v_2)^2}{2g} = \frac{v_1^2}{2g}\left(1 - \frac{A_1}{A_2}\right)^2 \tag{5.12}$$

Note:

This is applicable for incompressible flow of gases with velocities less than 60m/s, or where change in density is less than 10% [37].

For uniform diverging duct, figure 5.3, Gibson gave an expression that can be used to determine the head loss [36];

$$\Delta h = k\frac{(v_1 - v_2)^2}{2g} \tag{5.13}$$

Where,

k ; 0.13 for α = 5 to 7°

; $0.0110(\alpha^{1.22})$ for 7.5° < α < 35°, with α in degrees.

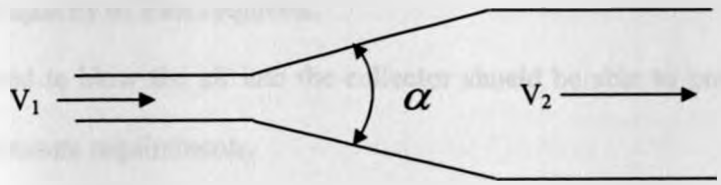

Figure.5.3. Uniform diverging duct.

5.1.5.9: Pressure Drop in the Solar Air Collector.

The pressure drop in the collector (which can be considered as a duct) was obtained from the Fanning equation [47], as;

$$\Delta P = \frac{fLG}{2\rho R} \tag{5.14}$$

Or could be measured directly by use of a manometer after constructing the collector.

Where,

f = Fanning friction factor

L = Length of the duct,m

G = Ratio of the mass flow rate of air per unit cross-sectional area duct (collector), $kg/m^2.s$

ρ = Density of air, kg/m^3

R = Hydraulic radius ,m, -which in a rectangular duct of width, 'w', and height,'s',is given as;

$$= \frac{ws}{2(w+s)}$$

The friction factor 'f' may be obtained from the Moody chart by using Reynolds number (Re) as;

$$Re = \frac{4\rho vR}{\mu} \tag{5.15}$$

Where, v, is the air velocity given by the ratio of the volume flow rate to the cross-sectional area; μ, is the absolute viscosity of the air.

Or the Fanning friction factor, f, for turbulent flow, Re >3000 could be obtained by use of equation (5.7).

5.1.5.10: Capacity of Fan required.

The fan used to blow the air into the collector should be able to provide enough power to meet the pressure requirements.

The work done by a fan can be measured by the quantity of air it delivers, and the pressure against which this is delivered. Assuming the fan is 100% efficient, the theoretical power (W_t) required for moving a given volume of air (Q) against a total pressure (P_t) could be calculated as follows;

$$W_t = \frac{Q \times P_t}{1000} \tag{5.16}$$

Where,

W_t = theoretical power required to move air at 100% efficiency, KW

Q = air flow, $(\%_s)$

P_t = total pressure against which air is moved, Kpa.

After computing all the associated head losses, the required fan capacity on using equation (5.16) was found to be 10W. Since this was a theoretical value, a fan with a capacity slightly higher was considered in order to overcome fan losses and avoid backpressure in the system. The available fan had a rating of 25W, which was suitable for this experiment, since it could be regulated so as to draw the required power from the power source.

5.1.6: Experimental Procedure.

The experimental set-up was as shown in figure 5.1.

Air was drawn from the ambient by a fan that passed it to the 6-inch internal diameter mild steel suction duct of the collector box.

There was a damper on the delivery duct to regulate the airflow to the required mass flow rate. After the damper the air passed through a wet gas meter for metering, although the gas meter was disconnected after setting the required mass flow rate to avoid pressure drop due to the small diameter of the hose pipe used for the connection.

The air entered the collector box through an adaptor hood that ensured uniform distribution of the airflow. The hood was constructed from a 12mm thick mild steel sheet and painted white on the outside to minimize heat absorption from the ambient. To maintain the performance and efficiency of the system, the construction, size and shape of the hood matters a lot, and also the hood should operate at the same level with the source of the airflow. The hood was connected to the 6inch main duct by a 38.1mm internal diameter mild steel pipe, which was chosen in accordance with ASHRAE Standard 93-77 [30].

After taking the required number of passes in the collector box, the air exited to the discharge duct through another adaptor hood, which was constructed and connected in a similar manner to the inlet adaptor hood.

Sealing all joints with steel putty and plasticine minimized air leakages in the collector box. The ambient wind speed was necessary for the determination of the convective heat transfer coefficient between the top cover and ambient air. This was done using a wind vane anemometer that was constructed of slightly curved radially disposed vanes. Since the anemometer counter recorded the distance of wind through it in meters, the mean wind velocity was obtained by dividing the counter reading by the timed time interval. With this anemometer care should be taken to ensure that it's a way from any obstruction that is not in the flowing stream. For accuracy, the bearing friction has to be minimized by oiling. The

other problem with this instrument is when the wind changes direction; it reverses its direction of rotation, so it required to be monitored continuously. The calibration of the wind vane anemometer was done by using a cup anemometer, which gave almost the same readings for same time intervals.

The incident total insolation was measured using a tube solarimeter (tube pyranometer), which had a Delta-T Devices millivolt integrator digital recorder. The solarimeter measures the rate at which solar energy is received by a unit area of a horizontal surface; it gives a spatial average of the irradiance in situations where the distribution of radiant energy is not uniform. It gives a millivolt output, which can be recorded directly or can be integrated electronically to give the solar energy received by the surface over a period of time.

The solarimeter detector consisted of alternate matt black and white sections that reach different equilibrium temperatures when exposed to short-wave radiation. The junctions of a thermopile embedded in the black and white sections respond to the temperature difference and generate a millivolt output which is directly proportional to the irradiance. The detector is enclosed in a tube of Pyrex glass, which is transparent to visible and infrared radiation ($< 2\mu m$) but not to long-wave radiation from the surroundings or the atmosphere.

Tube solarimeters are supplied calibrated from the factory, with their sensitivity adjusted to 15mV per kWm^{-2}. They lack perfect symmetry and their sensitivity varies somewhat with the angle of the incident radiation as a result of reflection from the surface of the glass tube; hence for absolute values of solar radiation they are not as accurate as when used for comparative measurements.

The tube pyranometer was mounted such that its sensor was coplanar with the plane of the collector aperture; this was to ensure that it does not cast shadow onto the collector aperture at any time during the test period. Also it was mounted at the same level to the collector. The cover plate and the solarimeter were wiped clean and dry prior to the tests, and then the test was given 15 minutes of running before collection of data was done.

The Delta-T Devices millivolt integrator responds only to positive inputs and displays a count proportional to the integral of that voltage with time. The millivolt integrator incurred a very low error (less than 1%), which made it suitable for this experiment. Since the solarimeter was calibrated to 15mV per kWm^{-2}, the total count was divided by 1.5 to give the total irradiance over a chosen time interval. For convenience and to justify the test to be transient, the period chosen for integration of insolation values was two minutes that was also the time interval used in the anemometer readings.

The fan power consumption was determined using a voltmeter to measure the voltage across the fan and an ammeter to measure the current to the fan.

To measure the mass flow rate, a wet gas meter, AW 1319 of Alex Wright & Co. Ltd, Westminster was used. For accuracy, it was kept level and the level of water in it maintained during the test period. The wet gas meter measures the volume of air through it, so readings in a known time interval divided by that time interval gave the volumetric flow rate of the air. Then the volumetric flow rate of the air was converted to mass flow rate after its density was determined (it was assumed that the air behaved as a perfect gas and the perfect gas equation used to find the density).

The atmospheric pressure was read from a barometer that is located in the thermodynamics laboratory while the ambient temperature was determined by use of a thermocouple. The atmospheric pressure was found to be almost constant during the test period.

All the collector component temperatures, and the ambient air, air inlet and outlet temperatures were measured directly by use of thermocouples connected to a Delta-T Logger. The thermocouples were attached to the components by use of supper glue while the air thermocouples were suspended at the relevant points. The ambient air thermocouple was shielded from direct sun by use of a soft board that was painted white.

Based on availability, three types of thermocouples were used, that is type J(iron/constantan), type K(chromel/alumel) and type T(copper/constantan), which had typical errors of 1.5°C, 1.5°C,and 0.5°C respectively.

The readings of the thermocouples were taken to be correct, since when placed in a water bath assumed to be at uniform temperature they all gave readings that compared reasonably well with readings from mercury-in-glass and digital thermometers that were placed in the same water bath.

In thermocouples, temperatures are derived from voltages, hence cable resistance does not adversely affect the measurements, and thus the length of cables used could not affect the measurements.

Thermocouple sensors are not themselves very accurate since their output for small temperature differences is low. Further to this, their accuracy is affected by contributions

form cold junction temperature errors, which is as a result of non-isothermality, and from logger input offset voltages.

The Delta-T Logger of Delta-T Devices (Burwell-Cambridge-U.K) used was a programmable data-logging device, capable of taking readings and storing data from a wide variety of sources. The Delta-T Logger was considered an excellent choice for logging data in this experiment.

Computer software was used to program the logger by specifying the type of sensors to be connected to the logger, and setting it to record data after every single minute. The data recorded from the sensors was transferred to a computer at the end of every test to create room in the logger's memory for more data- for this any type of IBM- compatible computer running MS-DOS can be used.

The logger had an internal clock that was set to record data at regular intervals of one minute.

The logger terminal is designed to be isothermal under typical operating conditions and is fitted with a cold junction thermistor for measuring its temperature and for providing a cold junction reference for the thermocouple measurements. The logger by its design is able to perform cold junction compensation by adding the cold junction temperature to the temperature difference derived from the thermocouple voltage.

5.1.7: The Collector Time Constant.

It was necessary to determine the time response of the solar collector in order to be able to evaluate the transient behaviour of the collector, and to select the proper time intervals for the

transient efficiency tests. A separate test was carried out to determine the time constant in accordance to procedures described by ASHRAE Standard 93-77 [35].

The inlet temperature of the air was noticed to be as close to the ambient temperature while passing the air through the collector, this observation was made at the collector design mass flow rate and an incident insolation of greater than $790W/m^2$ for all the pass modes considered.

The air was allowed to flow for some time, and then the incident insolation reduced abruptly to zero by shielding the solar collector with a ceiling board that was painted white on the outside. The board was suspended off the surface of the collector such that ambient air continued to pass over the collector as prior to the beginning of the test. Then the air temperatures at inlet and outlet of the collector were monitored continuously as a function of time. The actual time constant was the time it took the quantity,

$$\frac{t_{f_{out}} - t_{f_i}}{t_{f_{out,initial}} - t_{f_i}}$$ to change from 1.0 to 0.368.

The above relation together with a plot of the outlet temperature against time enabled the determination of the time constant.

A series of tests were conducted for the described (section 1.2) modes of air pass through the collector with the necessary data being recorded at time intervals of two minutes, after which the data were analyzed.

CHAPTER 6: RESULTS AND DISCUSSION.

One of the main reasons for a theoretical analysis is to be able to predict the performance of a solar collector as accurately as possible without having to do an experiment.

The following table and figures show the experimental and theoretical modeled results.

6.1: EXPERIMENTAL AND COMPUTED RESULTS.

Table 6.1: TPM Air Temperature Rise and Efficiency. (29/10/2004)

Insolation (W/m^2)	Experimental air temperature rise (deg. c)	Modeled air temperature rise (deg.c)	Experimental Efficiency	Model Efficiency
205.6	17.37	21.70	0.407	0.756
244.4	14.63	22.96	0.313	0.786
255.6	12.32	22.91	0.347	0.778
294.4	19.06	19.29	0.324	0.618
322.2	17.53	22.93	0.294	0.812
344.4	17.90	32.89	0.317	0.769
376.7	18.63	25.67	0.624	0.748
388.9	18.37	20.08	0.351	0.764
405.6	23.45	26.61	0.313	0.760
411.1	20.43	25.66	0.320	0.812
433.3	23.36	19.27	0.370	0.837

455.6	21.28	25.97	0.242	0.685
477.8	24.15	24.93	0.291	0.700
527.8	21.97	20.5	0.255	0.668
538.9	10.63	25.31	0.286	0.763
561.1	18.97	24.27	0.280	0.735
566.7	18.09	21.48	0.295	0.727
572.2	20.78	22.70	0.239	0.755
577.8	21.65	25.95	0.271	0.691
583.3	21.57	25.97	0.326	0.691
594.4	21.85	25.32	0.268	0.672
605.6	19.25	19.52	0.288	0.694
611.1	24.54	17.3	0.191	0.699
633.3	23.89	24.37	0.243	0.731
661.1	21.32	17.14	0.243	0.722
666.7	23.84	24.89	0.235	0.748
672.2	23.15	17.79	0.245	0.713
683.3	24.05	25.70	0.226	0.735
688.9	24.63	25.18	0.228	0.755
694.4	23.91	38.92	0.349	0.758
700.0	26.06	39.16	0.443	0.746
711.1	25.73	27.04	0.313	0.754
727.8	24.93	25.05	0.377	0.744
738.9	27.43	38.07	0.125	0.757
772.2	24.02	29.25	0.289	0.780

811.1	33.04	21.02	0.251	0.805
833.3	21.33	36.52	0389	0.776
850.0	23.41	32.54	0.538	0.797
888.9	30.84	24.37	0.235	0.800
894.4	20.71	29.89	0.372	0.764
911.1	25.00	28.64	0.500	0.769
916.7	27.06	39.16	0.443	0.763
922.2	27.8	38.4	0.328	0.763
933.3	32.4	40.88	0.244	0.758
938.9	28.54	40.29	0.266	0.776
944.4	31.31	41.21	0.279	0.760
950.0	26.24	25.09	0.265	0.738

Table 6.2: SPM Air Temperature Rise and Efficiency. (20/ 1/ 2005)

INSOLATION (W/m^2)	Experimental air Temp.rise(deg.c)	Modeled air Temp.rise (deg. c)	Experimental efficiency	Model efficiency
598.9	10.00	7.98	0.336	0.330
606.7	10.00	8.21	0.332	0.335
634.4	10.08	7.77	0.320	0.332
637.8	10.16	7.64	0.321	0.329
672.2	10.24	8.99	0.306	0.328
700.0	11.08	9.39	0.318	0.334
715.6	13.24	9.55	0.372	0.327

731.1	13.48	10.81	0.371	0.329
742.2	15.24	10.70	0.413	0.332
758.9	15.00	11.38	0.398	0.333
778.9	15.48	10.37	0.400	0.333
795.6	15.92	10.85	0.403	0.333
808.9	16.00	10.83	0.398	0.329
816.7	16.52	11.12	0.407	0.331
833.3	16.68	11.43	0.403	0.332
841.1	15.96	11.38	0.382	0.327
850.0	16.44	11.71	0.389	0.333
854.4	16.44	11.67	0.387	0.330
866.7	16.16	11.99	0.375	0.334
884.4	16.88	12.27	0.384	0.336
893.3	16.56	12.34	0.373	0.334
897.8	16.32	12.56	0.366	0.338
902.2	16.96	12.50	0.378	0.335
906.7	16.16	12.34	0.353	0.329
911.1	16.16	12.59	0.357	0.334
915.6	15.88	12.49	0.349	0.330

Table 6.3: DMPM Air Temperature Rise and Efficiency. (3/2/2005)

Insolation (W/m^2)	Experimental air temperature rise (deg. c)	Modeled air temperature rise (deg. c)	Experimental efficiency	Model efficiency
594.4	13.39	14.20	0.544	0.628
600.0	13.46	14.53	0.542	0.634
605.6	13.45	14.72	0.536	0.636
611.1	13.88	13.68	0.548	0.640
616.7	14.06	14.78	0.550	0.642
638.9	14.56	17.01	0.550	0.643
661.1	15.67	17.83	0.572	0.651
666.7	15.68	18.08	0.568	0.655
672.2	15.36	18.24	0.552	0.655
688.9	16.24	18.93	0.569	0.664
705.6	16.40	19.62	0.561	0.672
711.1	17.12	19.84	0.581	0.674
716.7	16.93	20.07	0.570	0.677
722.2	16.80	20.32	0.562	0.680
727.8	17.12	20.46	0.568	0.696
733.3	17.12	20.73	0.564	0.683
744.4	21.91	21.57	0.711	0.701
755.6	17.36	21.48	0.555	0.688
766.7	17.60	22.06	0.554	0.696
772.2	18.00	22.22	0.563	0.696

783.3	18.00	22.63	0.555	0.699
805.6	18.64	23.47	0.559	0.705
811.1	22.9	23.94	0.682	0.714
816.7	23.52	24.20	0.695	0.717
827.8	19.75	24.49	0.576	0.716
833.3	18.16	24.66	0.526	0.717
838.9	18.53	24.87	0.533	0.718
844.4	19.40	25.09	0.555	0.719
850.0	18.72	25.13	0.532	0.716
855.6	19.12	25.41	0.539	0.719
866.7	19.41	25.93	0.541	0.725
872.2	18.36	26.14	0.508	0.726
877.8	17.84	26.31	0.491	0.726
883.3	17.89	26.68	0.489	0.731
888.9	17.82	26.70	0.484	0.727
894.4	18.08	26.86	0.488	0.727

Table 6.4: DTPM Air Temperature Rise and Efficiency. (17/2/2005)

Insolation (W/m^2)	Experimental temp.rise (deg.c)	Modeled temperature rise (deg. c)	Experimental efficiency	Model efficiency
544.4	9.92	14.10	0.425	0.714
594.4	13.28	15.50	0.469	0.712
605.6	13.92	17.94	0.504	0.715

611.1	15.52	18.20	0.540	0.719
622.2	13.52	17.50	0.470	0.718
627.8	12.96	18.85	0.466	0.725
633.3	13.04	16.03	0.510	0.724
638.9	10.80	16.21	0.439	0.725
644.4	14.96	18.99	0.560	0.711
655.6	11.68	19.42	0.454	0.715
661.1	14.00	18.96	0.539	0.691
666.7	14.08	23.12	0.51	0.751
672.2	15.20	19.86	0.497	0.731
677.8	16.08	19.10	0.469	0.739
694.4	17.20	20.27	0.575	0.722
705.6	16.96	20.50	0.571	0.714
716.7	17.36	21.47	0.576	0.723
722.2	18.16	22.54	0.607	0.720
727.8	16.08	21.71	0.517	0.720
733.3	18.48	22.03	0.562	0.724
738.9	16.24	22.12	0.497	0.722
744.4	14.08	23.47	0.551	0.734
750.0	20.32	22.09	0.601	0.711
755.6	16.08	22.14	0.514	0.707
766.7	18.00	22.61	0.566	0.712
772.2	15.28	23.08	0.464	0.721
777.8	17.92	21.48	0.454	0.723

783.3	14.48	23.78	0.520	0.734
788.9	16.00	23.9	0.490	0.733
794.4	20.72	24.16	0.559	0.736
805.6	13.80	24.41	0.402	0.734
811.1	19.28	24.50	0.574	0.730
816.7	18.32	21.4	0.572	0.723
822.2	16.72	24.49	0.491	0.721
827.8	17.04	24.59	0.497	0.727
833.3	17.04	24.91	0.493	0.723
838.9	14.96	25.42	0.443	0.719
844.4	22.24	25.21	0.624	0.724
855.6	16.48	25.17	0.478	0.712
861.1	18.72	25.54	0.496	0.719
866.7	20.40	25.44	0.534	0.711
872.2	16.48	25.62	0.454	0.711
877.8	15.92	25.77	0.436	0.711
883.3	15.68	25.72	0.415	0.706
886.7	20.24	25.52	0.551	0.713
888.9	16.36	25.87	0.419	0.705
905.6	18.16	26.08	0.499	0.698
911.1	15.36	26.19	0.431	0.696
916.7	19.60	26.20	0.534	0.693
922.2	19.20	21.35	0.535	0.692
927.8	20.72	26.48	0.536	0.692

961.1	19.52	27.08	0.514	0.683

Table 6.5: Time constant data. (22nd February 2005)

SOLAR TIME	AIR EXIT TEMP (^{0}C)	INSULATION TEMP (^{0}C)	AMBIENT TEMP (^{0}C)
12:14:28	76.88	34.80	30.28
12:15:28	76.40	34.86	30.00
12:16:28	75.36	35.01	31.39
12:17:28	74.16	35.28	32.65
12:18:28	72.80	35.49	32.48
12:19:28	71.36	35.61	30.96
12:20:28	69.76	35.91	32.21
12:21:28	68.32	36.01	32.72
12:22:28	66.80	35.91	31.34
12:23:28	65.36	35.88	32.89
12:24:28	63.92	36.14	33.27
12:25:28	62.64	36.57	33.59
12:26:28	61.60	36.20	30.00
12:27:28	60.48	36.32	31.95
12:28:28	59.44	36.16	31.34
12:29:28	58.48	36.45	33.22
12:30:28	57.60	36.43	32.50
12:31:28	56.64	36.60	33.06
12:32:28	55.84	36.39	32.31
12:33:28	55.04	36.14	30.33
12:34:28	54.32	36.13	31.71
12:35:28	53.44	36.01	32.43
12:36:28	52.48	35.91	31.59
12:37:28	51.52	35.97	30.81

12:38:28	50.72	36.22	32.19
12:39:28	49.92	36.22	32.43
12:40:28	48.96	36.22	31.25
12:41:28	48.40	36.20	32.31
12:42:28	47.76	36.20	31.68
12:43:28	47.44	36.18	32.21
12:44:28	47.20	36.11	30.98
12:45:28	47.04	36.34	32.33
12:46:28	46.80	36.14	31.08
12:47:28	46.56	36.13	31.63
12:48:28	46.40	36.07	31.08
12:49:28	46.08	36.11	32.07
12:50:28	45.68	36.28	32.45
12:51:28	45.36	36.51	31.68
12:52:28	45.20	36.39	30.98
12:53:28	45.04	36.30	31.27
12:54:28	44.80	36.47	32.72
12:55:28	44.56	36.36	31.20
12:56:28	44.24	36.59	32.33
12:57:28	43.92	36.66	33.15
12:58:28	43.68	36.81	32.84
12:59:28	43.52	36.64	31.61
13:00:28	43.28	36.74	31.85
13:01:28	43.12	36.66	32.19
13:02:28	42.96	36.68	32.31
13:03:28	42.72	36.91	32.81
13:04:28	42.48	36.85	32.36
13:05:28	42.16	36.87	32.65
13:06:28	41.92	36.83	32.36

13:07:28	41.76	36.74	31.44
13:08:28	41.68	36.81	32.24
13:09:28	41.52	36.81	31.97
13:10:28	41.28	36.97	33.63
13:11:28	41.04	36.68	32.07
13:12:28	40.92	36.85	33.08
13:13:28	40.92	36.95	32.69
13:14:28	40.75	36.83	32.14
13:15:28	40.60	37.06	33.30
13:16:28	40.51	37.26	32.45
13:17:28	40.62	37.24	30.98
13:18:38	40.58	37.39	33.01
13:19:28	40.51	37.16	32.12
13:20:28	40.41	37.01	32.53
13:21:28	40.28	36.68	31.68
13:22:28	40.13	36.78	32.48
13:23:28	40.03	36.83	32.19
13:24:28	39.96	36.60	31.78
13:25:28	39.69	36.85	33.15

This study was aimed at providing a prediction method for the performance of multi-pass solar air heaters under transient conditions (since they operate on changing weather conditions). The study involved a theoretical analysis and an experimental set up to validate the computed values. The solar collector time constant is an important factor in transient analysis since it helps to know the time step to be used in predictions.

6.2: THE COLLECTOR TIME CONSTANT.

The collector time constant was determined according to the experimental procedure described in chapter 5. Two sets of experimental data were acquired and graphs of exit temperature against time plotted, (table 6.5 and figure 6.1). The collector time constant was determined as the time it took (after covering the collector) for the difference in air exit and inlet temperatures to reach 36.8% of the initial value.

During the test period, the insulation temperature remained almost constant ($\pm 2\ ^{0}$ c) which enabled to make the assumption that, the performance of a solar collector is function of insolation, whereas insolation varies with time.

An averaged value of 27 minutes was reached as the time constant for the collector constructed for this work. This meant that, if the steady state analysis were to be carried out for the collector, the weather data would have to be averaged at intervals of 27 minutes, which calls for long duration in collecting the experimental data. This value was in agreement to the time intervals that have been used on quasi-steady state analysis. For instant, Korir(4), Luti(6), Satcunanathan and Deonarine(8) used a time interval of 15 minutes in their steady state experimental analysis on multi-pass solar air heaters while Satcunanathan and Persad (12) used a time interval of 30 minutes.

The value of time constant obtained for the collector constructed for this study may have been affected slightly by experimental errors and difficulties that could not be eliminated completely, such as air leakages, instrumental errors and time delay. This means, if the constructed collector were to be tested under steady-state conditions, the weather data (temperature, irradiance and wind velocity) would have to be integrated over a period of 27 minutes in order to determine the thermal performance of the collector.

6.3: CORRELATIONS:

In this study, a flat-plate collector was considered and was positioned on horizontal plane hence the effects of the angle of incidence were negligible. This made it possible to work with no correlation for the computation of the collector incidence angle modifier.

Of all the parameters used in developing this model, the heat transfer coefficients were the most difficult to estimate accurately. This is because most sources of the heat transfer correlations do not clarify on what correlation to be used especially for solar air heaters which are additional equipments in the field of heat exchangers.

Hodge (56) gives correlations for forced convection heat transfer coefficients for laminar flows ($Re_{Dh} \angle 5\times10^5$ with $0.1 \le Pr \le \infty$) and turbulent flow ($Re_{Dh} > 5\times10^5$ with $Pr > 0.5$ for flows over flat plates. These correlations are applicable to low-speed flows (Mach number $\angle 0.5$) of gases and liquids, where all the physical properties are obtained at the mean film temperatures. These correlations could be used, but it was not possible since there is no mention of the operational characteristics encountered in solar air heaters such as flow between parallel flat plates when one is heated and variation of the incident heat energy.

The Colburn correlation (42) for fully developed turbulent flow could also have enabled the determination of the forced convection heat transfer coefficient but it was developed for internal flows in pipes and then adopted for flows in non-circular channels by defining a hydraulic mean diameter. These correlations are for turbulent $(Re_{Dh} > 10000)$ flows in smooth tubes with Prandtl numbers of $0.7 \leq Pr \leq 160$, and hydrodynamic entry length of $\frac{L}{D} \geq 60$. The range of Reynolds numbers encountered in flat-plate air heaters are below the given limit and the Prandtl numbers are $0.5 \leq Pr \leq 1$, and the issue of hydrodynamic entry length becomes difficult to define, hence the correlation was not suitable for use in this study.

Shewen and Hollands recommends the use of a correlation that was developed based on data by Kays and London. (As Jansen T. J describes (55)) This correlation is recommended for solar air heaters operating in the range of Reynolds numbers from 2000 to 10000.This range is considered suitable for commercial forced convection collectors where the flow is usually in the turbulent region $(2000 \angle Re \angle 10000)$ and has large mass flow rates. The absorber of a solar air heater used for space heating and drying crops (category of the collector used in this study) consists of a wide, shallow duct with laminar or low turbulent air flows, hence this made it difficult to consider the use of this correlation. Again, when values of this correlation where compared with experiments and other correlations, where slightly lower (22.14% lower.)

Kabeel and Mecarik (17) calculated the forced convection heat transfer coefficient between the air and the two plates of the solar air heater or between the air and the glass cover from a correlation that appeared simple to use. They did not give a range of the Reynolds and Prandtl numbers for which the correlation should be used. When the correlation was compared with experiments and other correlations, it gave much higher values (106% higher)

which seemed unreliable in this study. Also their work considered divided air streams in collector and streams made only a single pass in one direction.

Korir (4) used a correlation that gave almost similar values to those obtained when the correlation recommended by Beckmann and Duffie (15) was used. In actual sense these two correlations are same only that, the one used by Korir had a term of Prandtl number. The Beckmann and Duffie correlation has assumed a constant value for the Prandtl number (Pr $\simeq 0.722$). Both correlations are recommended for use in determination of the forced convection heat transfer coefficient between parallel plates only when one plate is heated. The Beckmann and Duffie correlation (equation 3.31) was adopted for use in this work since it gave reasonable values when related to the experiment, and the Prandtl numbers encountered were also in the recommended range (0.688 to 0.730) when using this correlation.

In solar collectors operating on windy conditions, the collector- to- ambient air heater transfer coefficient is very important. The forced convection heat transfer loss effects during the hours of collection are critical, because if these losses are large the collection efficiency can be lowered significantly whenever the sun heats the collector above the ambient temperature. The external heat transfer coefficients are static in that; any change in wind direction or speed will change them, so a correlation that is reliable should be chosen.

Jurges in his study on heat transfer loss coefficients used a 50 cm by 50 cm plate with sharp edges, positioned vertically and parallel to the wind, and heated with steam (Presumably at 100° C). (As described by Francis de Winter (57)).From this he recommended a correlation for use in determination of solar collectors' heat transfer coefficient on windy

conditions. The correlation is a dimensional equation that covers two different wind velocity ranges. It is appreciated that most collectors are much larger than 50 cm by 50 cm and that they do not start with a sharp edge, so because of this the heat transfer coefficients of Jurges are too high for the higher range of wind velocity. The Jurge equation is considered suitable for use in cases where the wind velocities are in the lower range. Due to its simplicity and the fact that the wind velocities encountered in this study were too low, the Jurges equation (equation 3.33) was adopted for use.

The rate of heat transfer between two parallel plates is of importance in the performance of flat-plate collectors. Free (natural) convection heat transfer data are usually correlated in terms of two or three dimensionless parameters (Nusselt number, Raleigh number and Prandtl number.)

Several correlations have been commended for use in the determination of free convection heat transfer coefficient. For instance, Kabeel and Macarik (17) used a simple correlation that did not consider the collector angle of inclination. Of all the correlations encountered, the one of Hollands etal (equation 3.29) was adopted for use because it covers a wide range of the angle of inclination of the solar collector and also is gave reasonable values compared to the others, as described by Duffie and Beckman (15).

6.4: THE SOLAR COLLECTOR CONSTRUCTED.

The performance of the collector depends mainly on the weather conditions, design and operating parameters (mass flow rate, collector area and material). To estimate the optimum values for the operating parameters in different weather (for this case transient) conditions using full experiments is costly and time consuming. Therefore the development of a

computational model offers a better alternative and is expected to prove to be a powerful tool in evaluation of the performance of solar collectors under changing weather conditions. In this study, transient analytical expressions are obtained for various temperatures of the collector components and the flowing air. The obtained model represents an extension of the steady state expressions represented by Korir (4) and Luti (6).

The solar collector is a main component in harnessing of thermal solar energy. Its characteristics represent an important factor to the performance and efficiency of any solar unit. The solar collector used had an absorber plate which had its upper surface painted matt black to increase the absorptivity of the system. The absorber plate was covered with two glass covers of high transmissivity to solar radiation, under the absorber plate was a back plate which together with the casing were well insulated to reduce heat losses to the ambient air. The air passed through the gaps between the glass covers, absorber plate and back plate according to the desired mode of flow.

6.5: THE DEVELOPED MODEL.

In this study, solar radiation (I), ambient temperature and wind velocity were considered perturbations that affect the solar collector due to their random behaviour.

The theoretical model developed depends on the energy equation for each part of the solar air heater. Some assumptions were made to be able to develop this model (section 4.1), the main ones being, the flow in the collector is one dimensional, and incompressible, unsteady state conditions prevail, and viscous dissipation of heat is negligible.

The model involved developing differential equation based on thermal energy balances and then solving them numerically by use of finite difference method to obtain expressions for the present temperatures. To obtain numerical value, the model requires an initial guess of the collector components and flowing air temperatures, with the input of the experimental measurements of insolation, ambient temperature and wind velocity. This required the use of a computer program which was written in Fortran 90 (Appendix 6). The obtained model allows the assessment of the collector performance for variable solar intensity levels and ambient temperature. The computer program was organized such that on inputting the data the program runs till convergence.

6.6: VALIDATION OF THE DEVELOPED MODEL.

To validate the proposed model, experimental measurements were made. During the experiments, the parameters affecting the performance of the system were constantly monitored; these were used to validate the developed model. The values of solar radiation, ambient temperature and wind velocity were used as input for the computational model.

To facilitate the understanding and acceptance of this approach, the recommended test sequence, mounting and other test requirements were closely connected to those widely accepted for steady- state or quasi-steady –state testing of solar thermal collectors as outlined in e.g., ASHRAE Standard 93-77(39), FSEC-GP-5-80 (40), ISO 9806-1 and ISO 9806-3. However, test data needed to contain more and the proper information to be able to identify the non-stationary behaviour of the developed model due to changing weather conditions. But depending on the actual weather conditions at the test site steady-state testing can require more test days due to its requirements for clear sky conditions around solar noon. The main difference however, is that the measurements in this study can be made during any time of

the day from early in the morning to late in the afternoon instead of a few hours around solar noon each day. By being able to perform the test any time, the total solar irradiance at the plane of the collector was allowed to vary between 150 to about 980 Wm^{-2}, and there were partially cloudy conditions during the test period, which made it possible to be in a position to identify the dependence of the performance of solar collectors on weather conditions. The following measurements were made;

- The global solar irradiance at the collector surface.
- The ambient wind velocity.
- The air flow rate. (Held constant for all the tests).
- The temperature of the flowing air at the collector inlet and outlet.
- The temperatures of the two glass covers, absorber plate, back plate and the back of the insulation.

6.7: EQUIPMENT AND DATA ACQUISITION.

Thermocouples were used to measure temperatures of the various components and the inlet and outlet temperature of the collector as functions of time. The surrounding air temperature and total solar radiation incident on the solar collector were also measured. All thermocouple sensors were connected to a Delta-T- logger data acquisition system. During the experimentation all the parameters were measured and recorded every two minutes for duration of about three hours for each experiment. It is worthy to mention the following points about the experimentation;

- Several experimental tests were made for each mode of air pass and they gave almost similar results.
- A single collector was used for all the modes studied; hence comparing them directly in this work possesses some limitations due to different weather conditions.

- All the experimental tests were carried out at the same location.
- Only flat-plate collectors on horizontal plane were considered.

6.8: Experimental and computed Graphs.

TEMPERATURE VERSUS SOLAR TIME

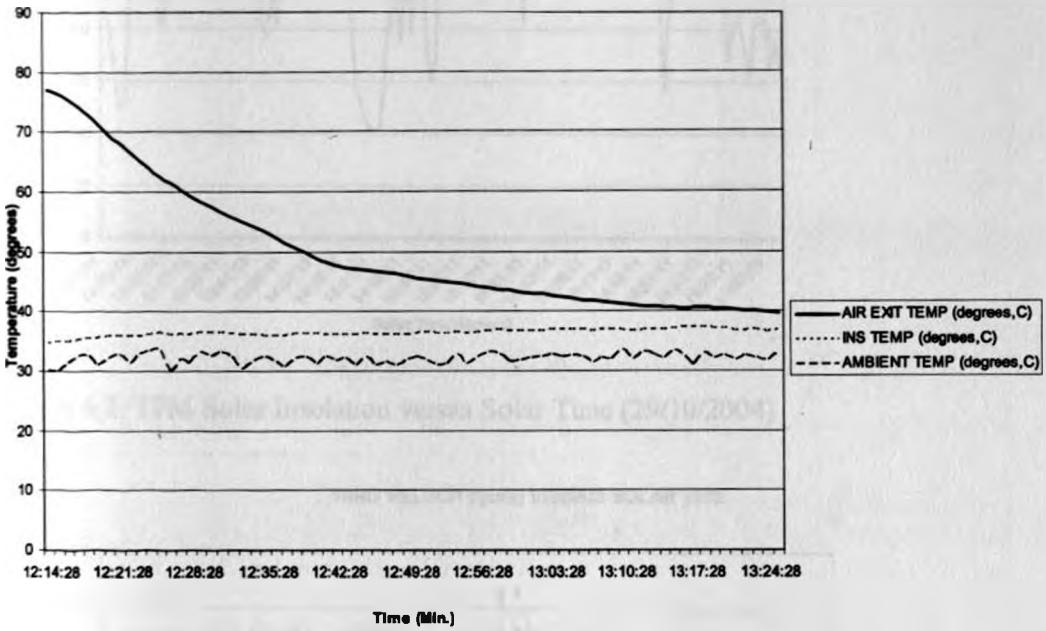

Figure 6 1: Time constant.

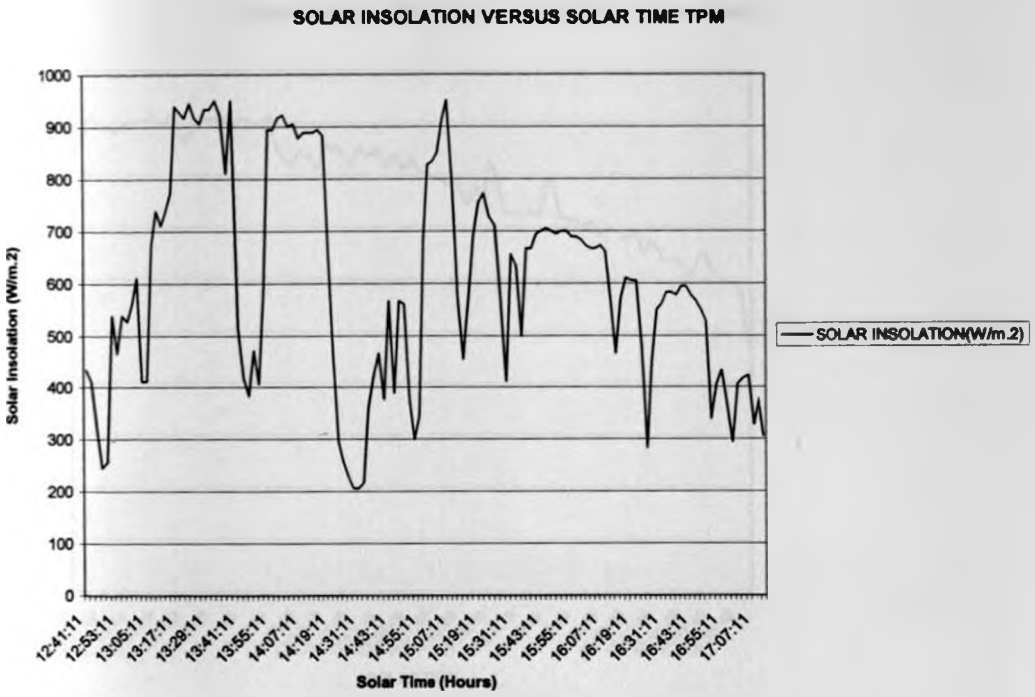

Figure 6.2: TPM Solar Insolation versus Solar Time (29/10/2004)

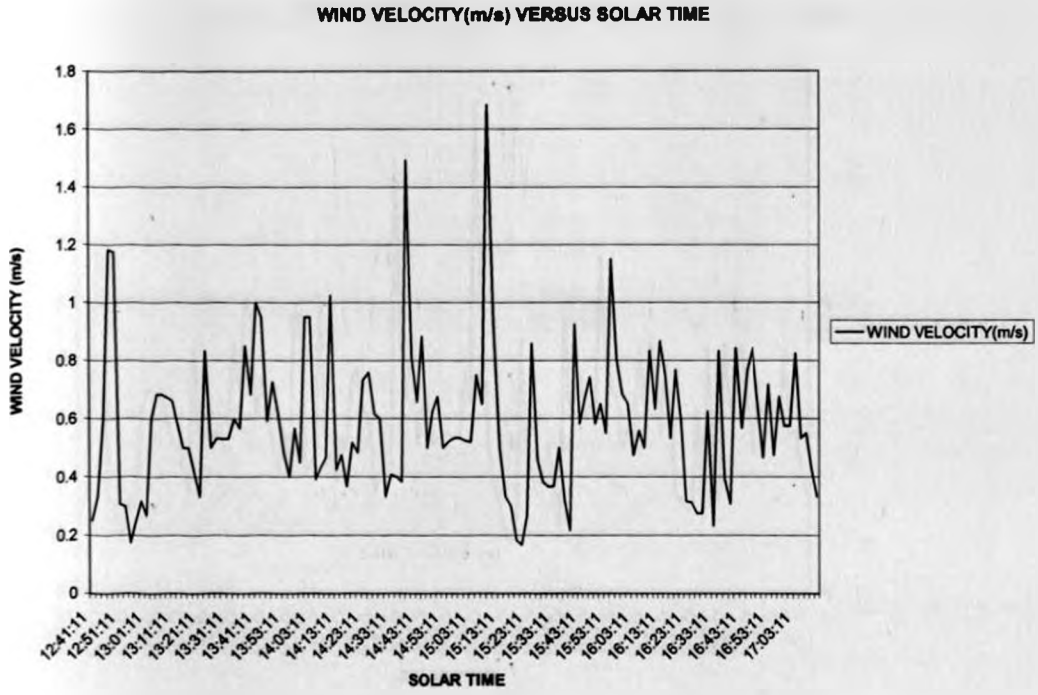

Figure 6.3: TPM Wind Velocity versus Solar Time (29/10/2004)

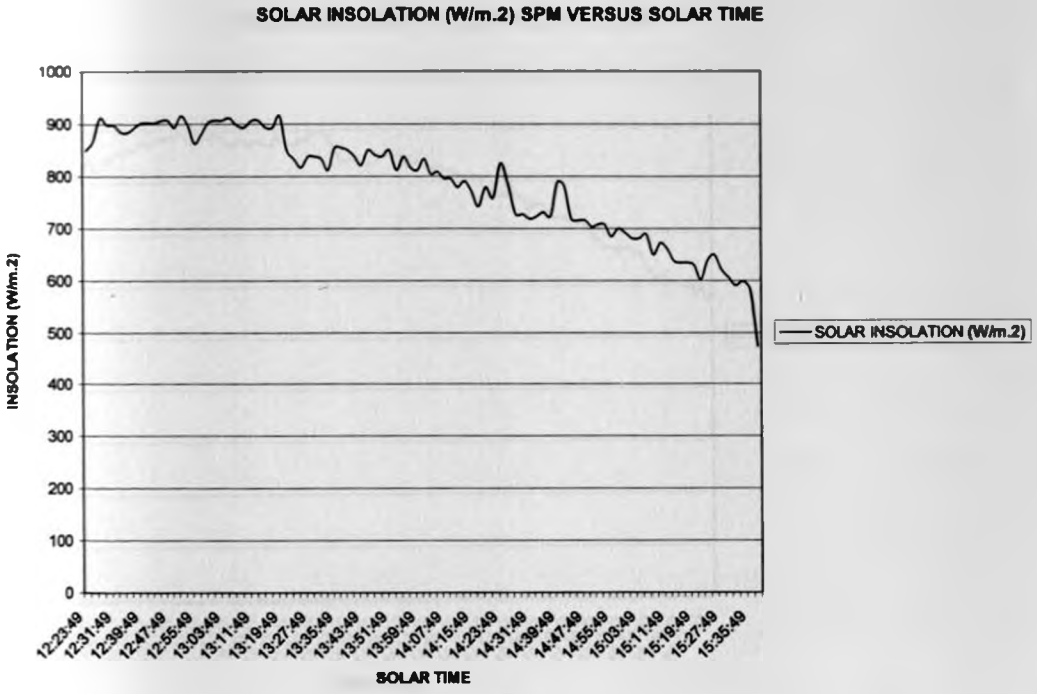

Fig. 6.4: SPM Insolation versus Solar Time (20/01/2005)

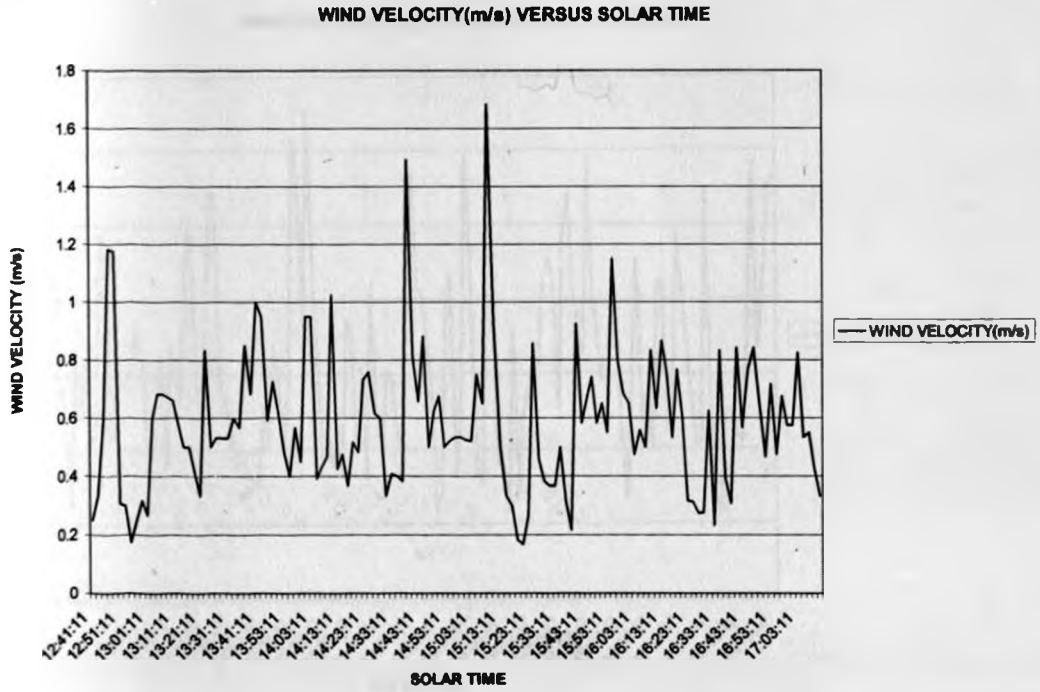

Fig. 6.5: SPM Wind velocity versus Solar Time (20/01/2005)

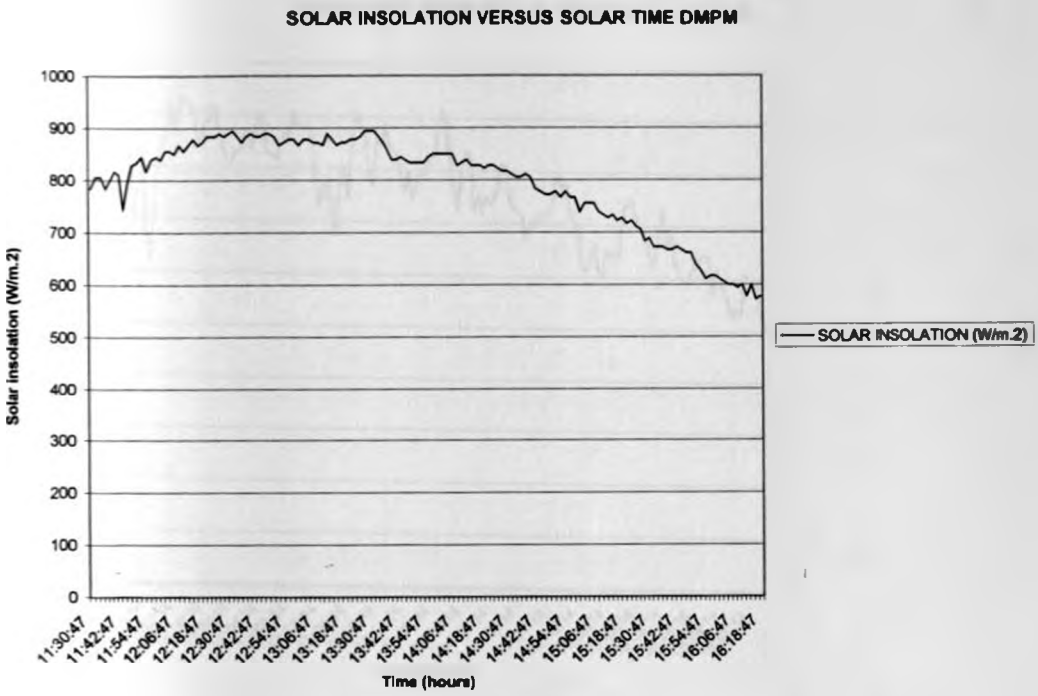

Figure 6.6: DMPM Insolation versus Solar Time (03/02/2005)

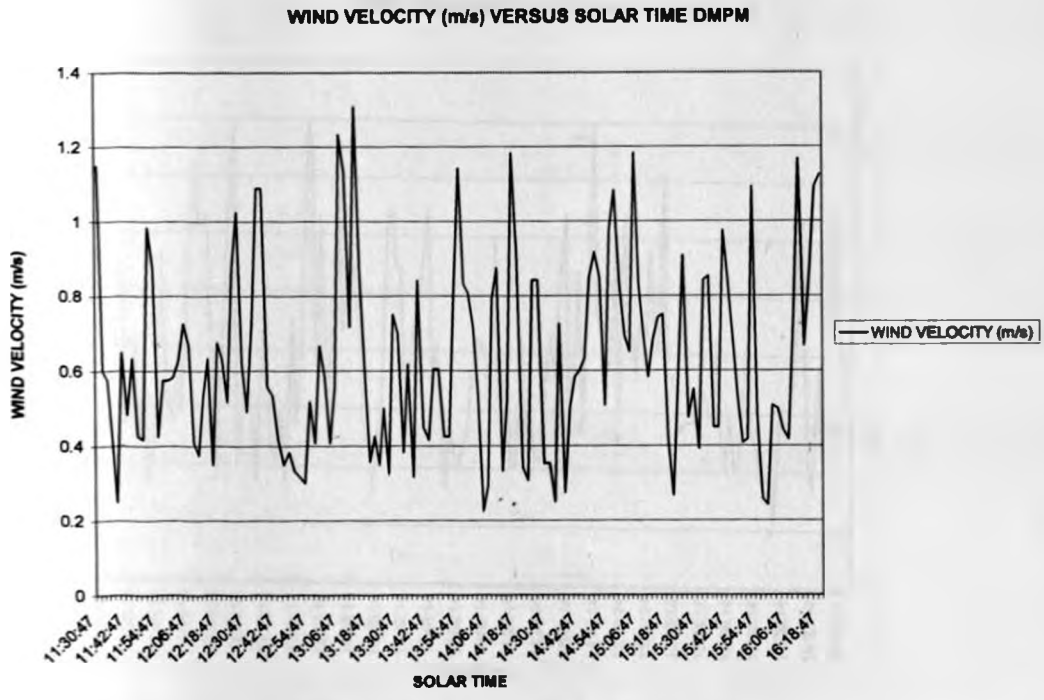

Figure 6.7: DMPM Wind Velocity versus Solar Time (03/02/2005)

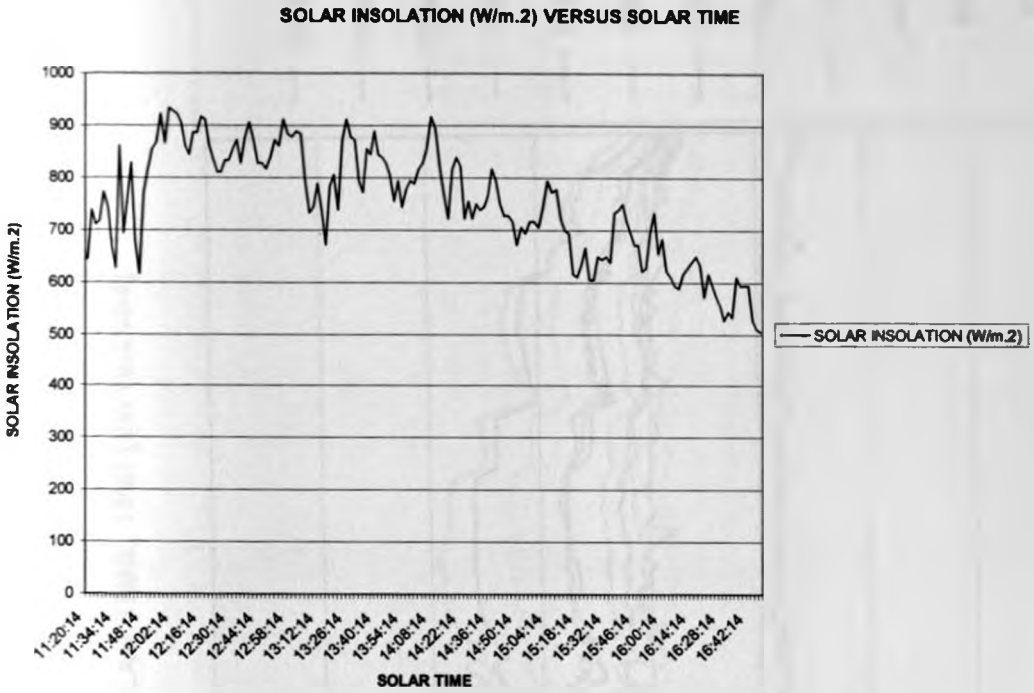

Figure 6.8: DTPM Insolation versus Solar Time (17/02/2005)

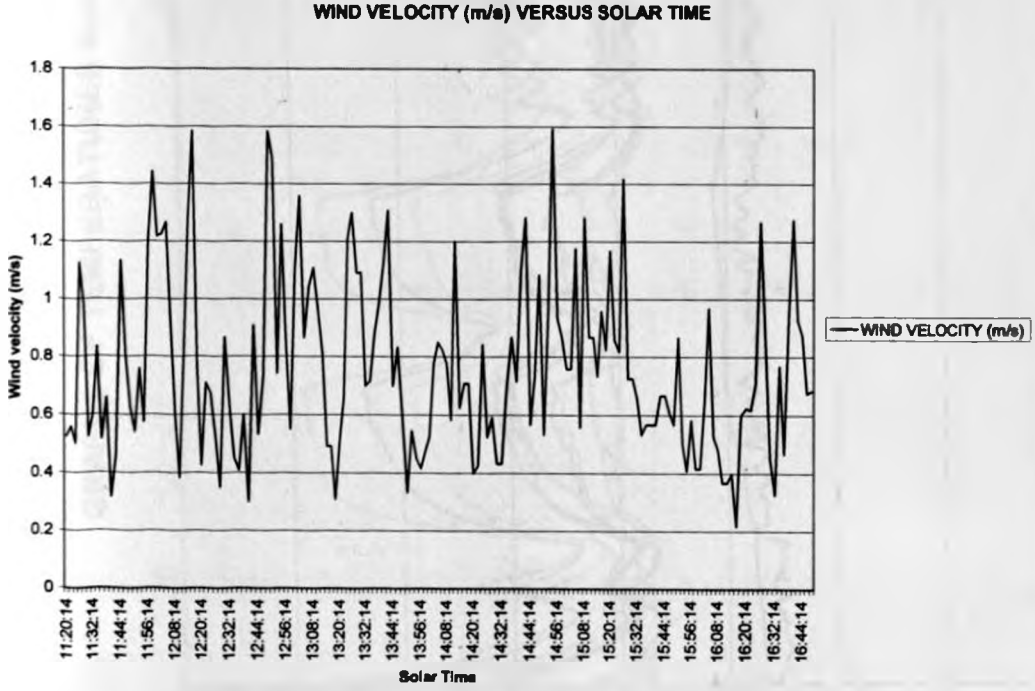

Figure 6.9: DTPM Wind Velocity versus Solar Time (17/02/2005)

Fig. 6.10

GRAPHS OF TEMPERATURES AGAINST SOLAR TIME, TPM (29/10/2004)

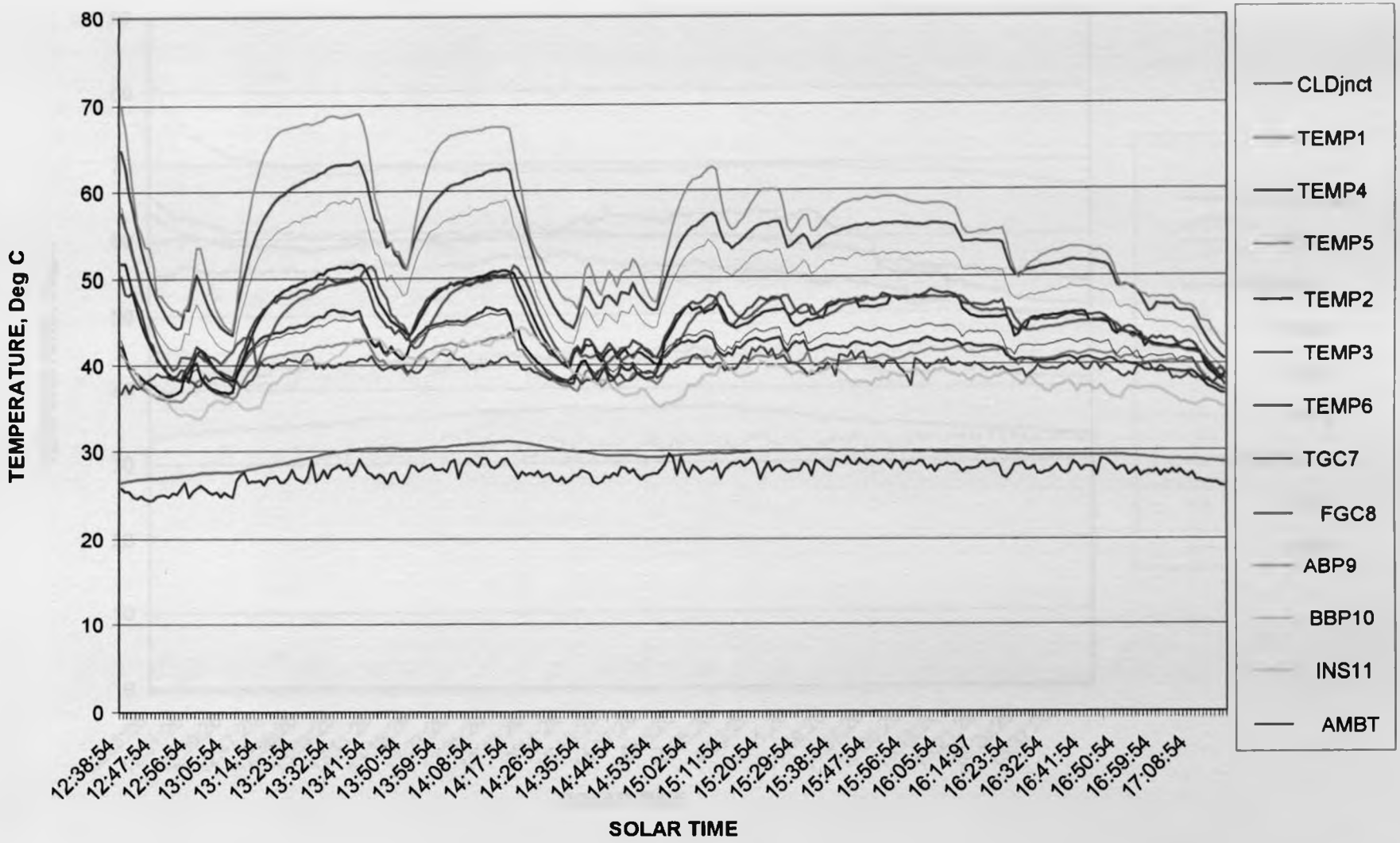

Fig. 6.11

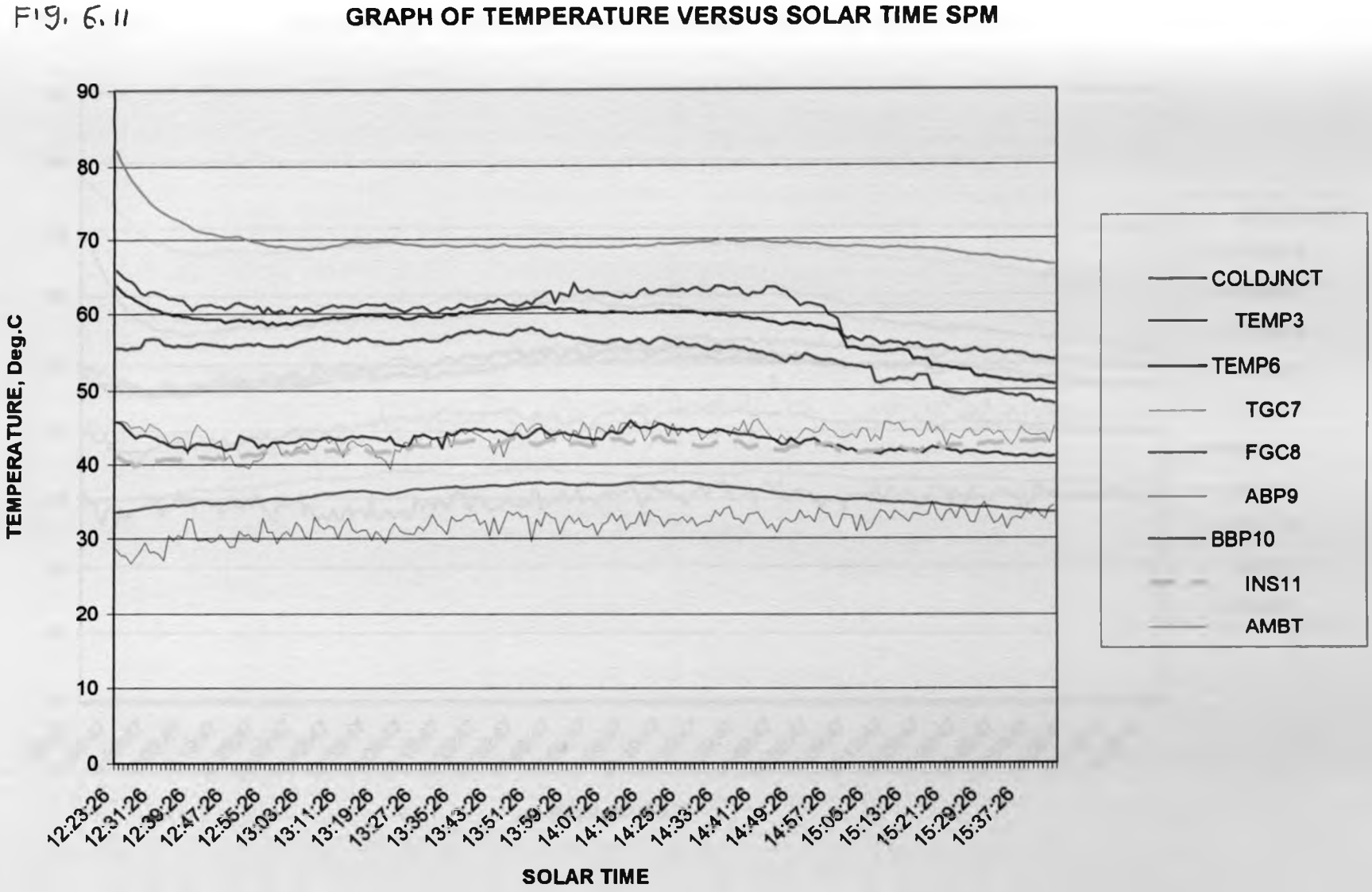
GRAPH OF TEMPERATURE VERSUS SOLAR TIME SPM
TEMPERATURE, Deg.C
90
80
70
60
50
40
30
20
10
0
12:23:26
12:31:26
12:39:26
12:47:26
12:55:26
13:03:26
13:11:26
13:19:26
13:27:26
13:35:26
13:43:26
13:51:26
13:59:26
14:07:26
14:15:26
14:25:26
14:33:26
14:41:26
14:49:26
14:57:26
15:05:26
15:13:26
15:21:26
15:29:26
15:37:26
SOLAR TIME
COLDJNCT
TEMP3
TEMP6
TGC7
FGC8
ABP9
BBP10
INS11
AMBT

Fig. 6.12

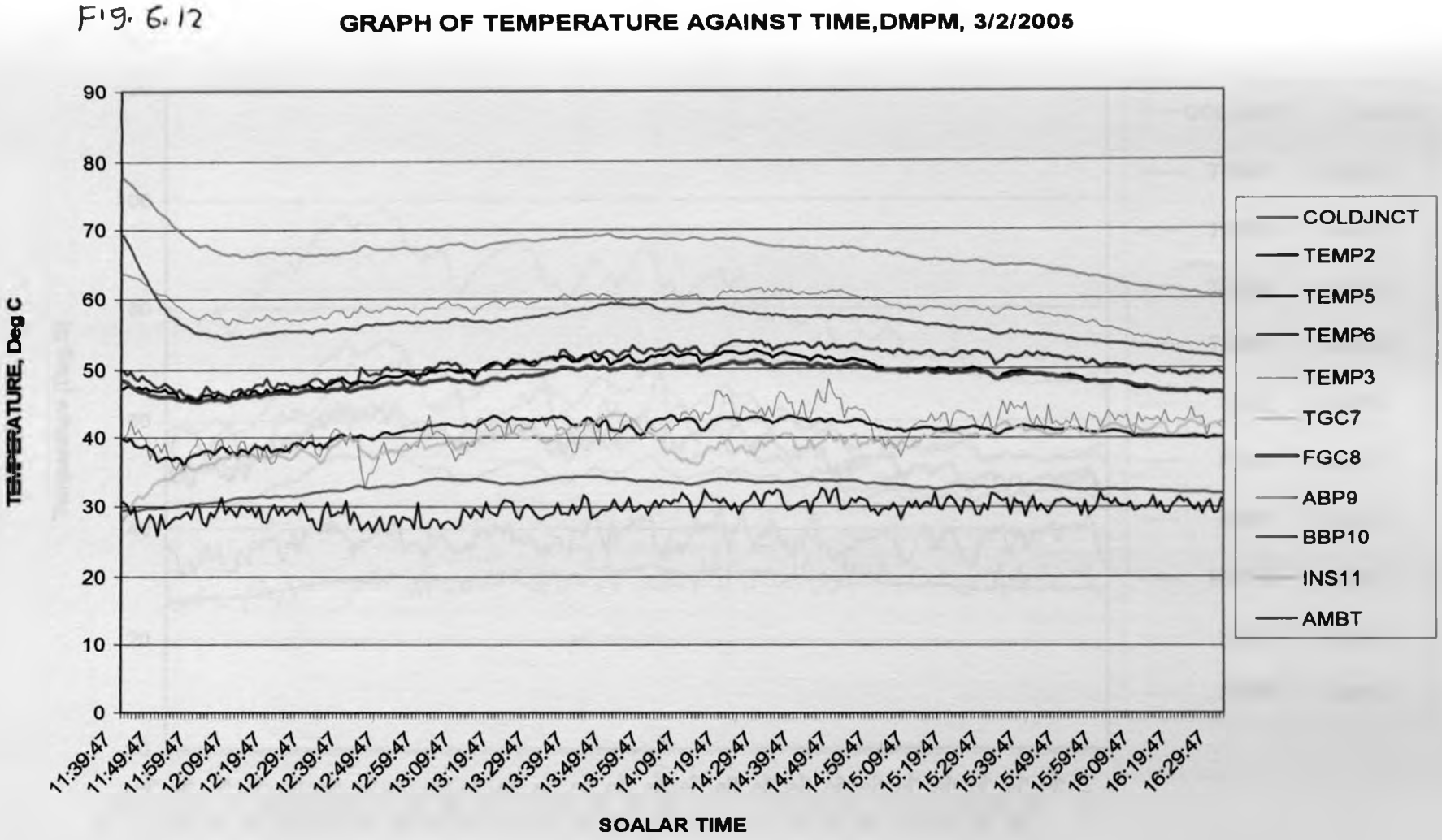
GRAPH OF TEMPERATURE AGAINST TIME,DMPM, 3/2/2005
TEMPERATURE, Deg C
90
80
70
60
50
40
30
20
10
0
11:39:47
11:49:47
11:59:47
12:09:47
12:19:47
12:29:47
12:39:47
12:49:47
12:59:47
13:09:47
13:19:47
13:29:47
13:39:47
13:49:47
13:59:47
14:09:47
14:19:47
14:29:47
14:39:47
14:49:47
14:59:47
15:09:47
15:19:47
15:29:47
15:39:47
15:49:47
15:59:47
16:09:47
16:19:47
16:29:47
SOALAR TIME
COLDJNCT
TEMP2
TEMP5
TEMP6
TEMP3
TGC7
FGC8
ABP9
BBP10
INS11
AMBT

Fig. 6.13 **GRAPHS OF TEMPERATURE VERSUS TIME** DTPM

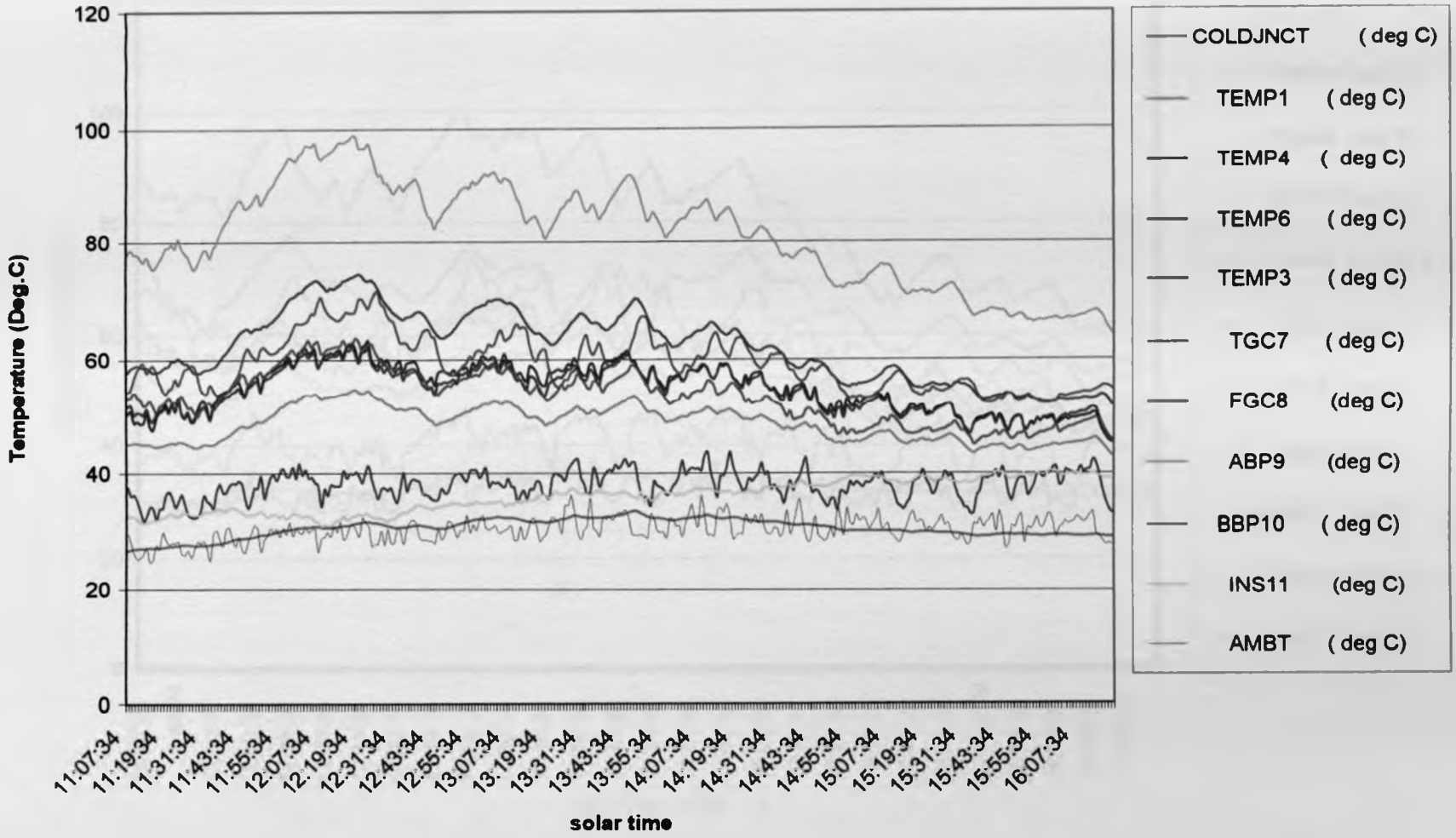

Fig. 6.14

GRAPHS OF TEMPERATURE AGAINST TIME, DTPM

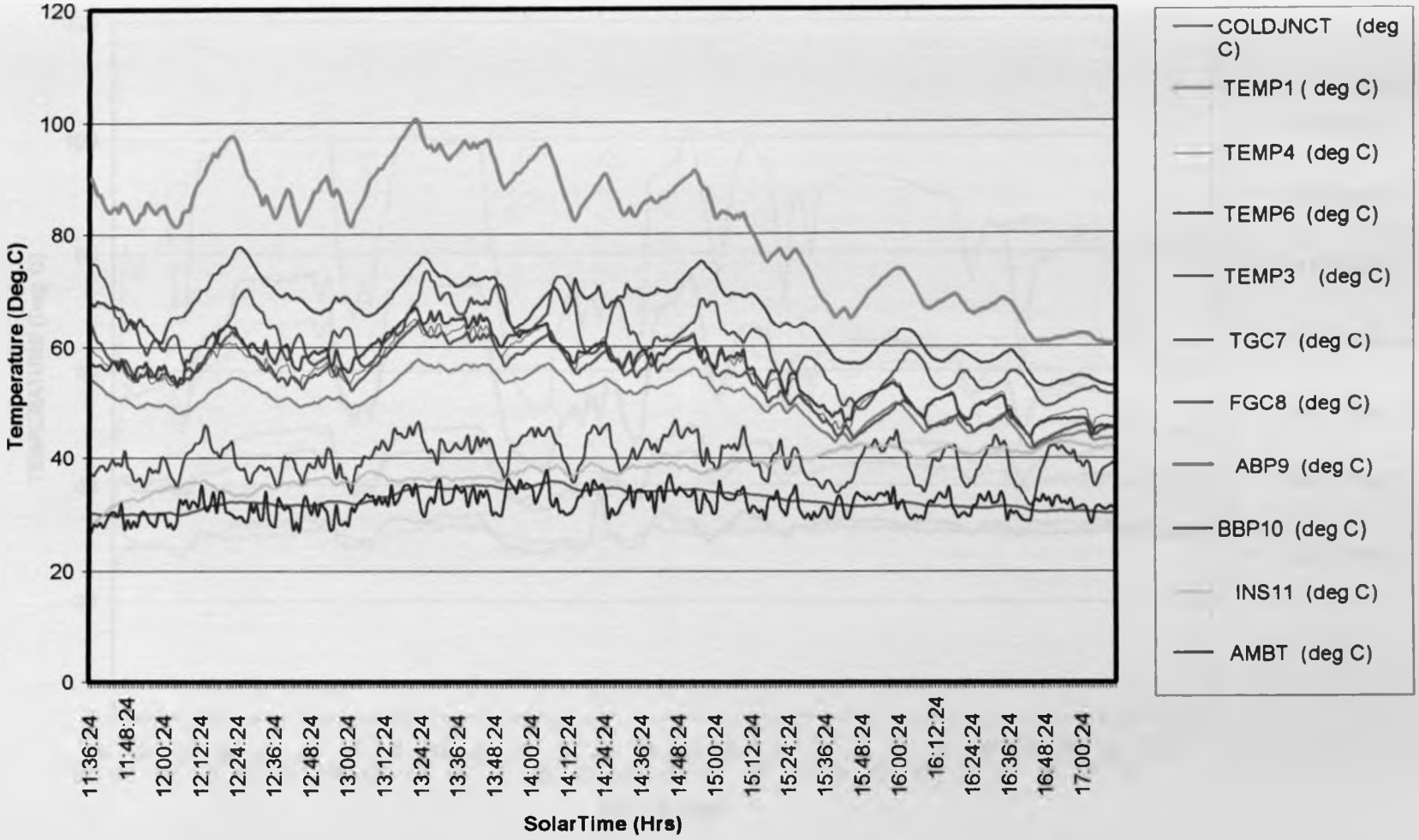

Fig. 6.15 TPM

COMPUTED TEMPERATURES VERSUS SOLAR TIME

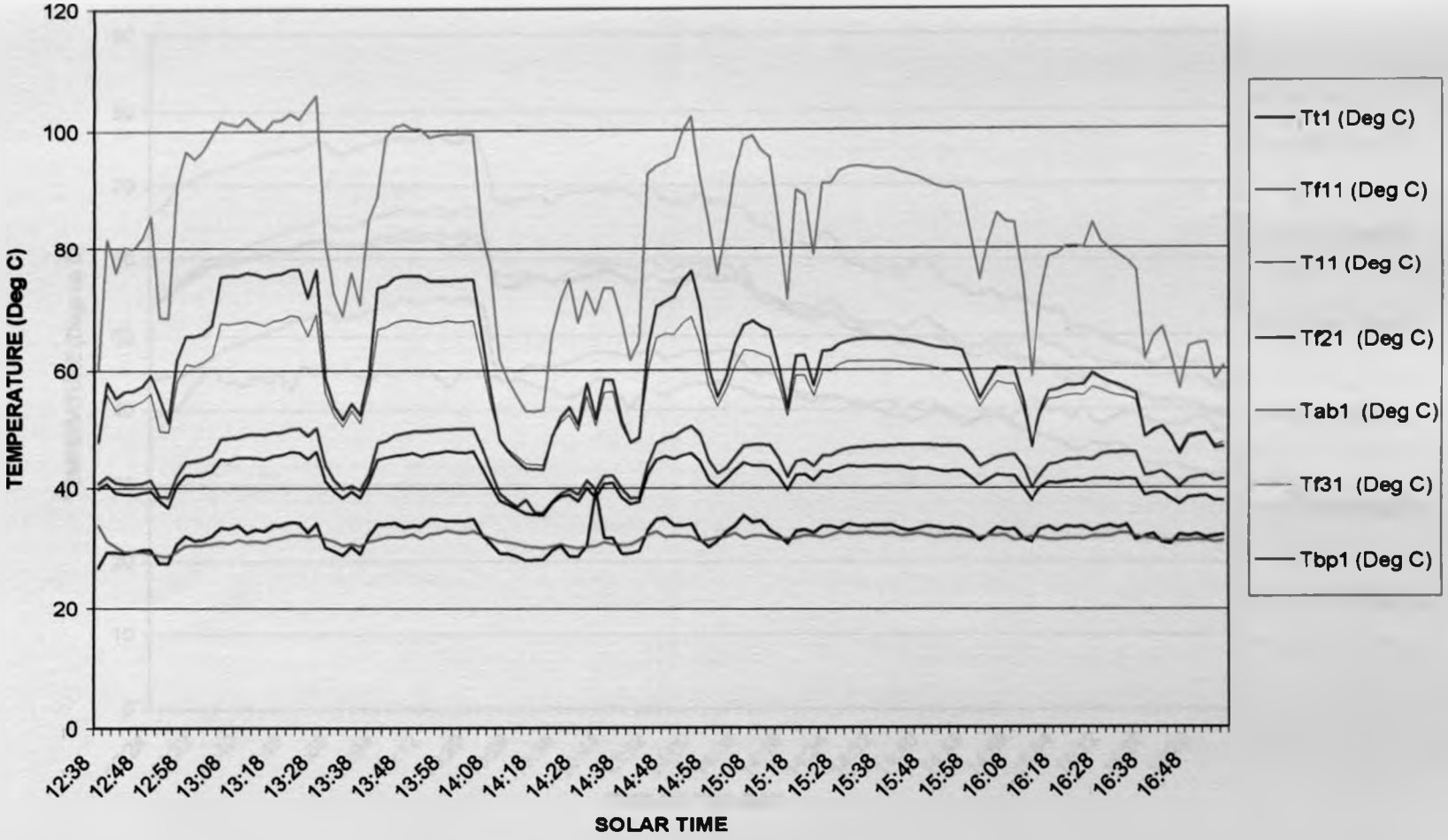

Fig. 6.16

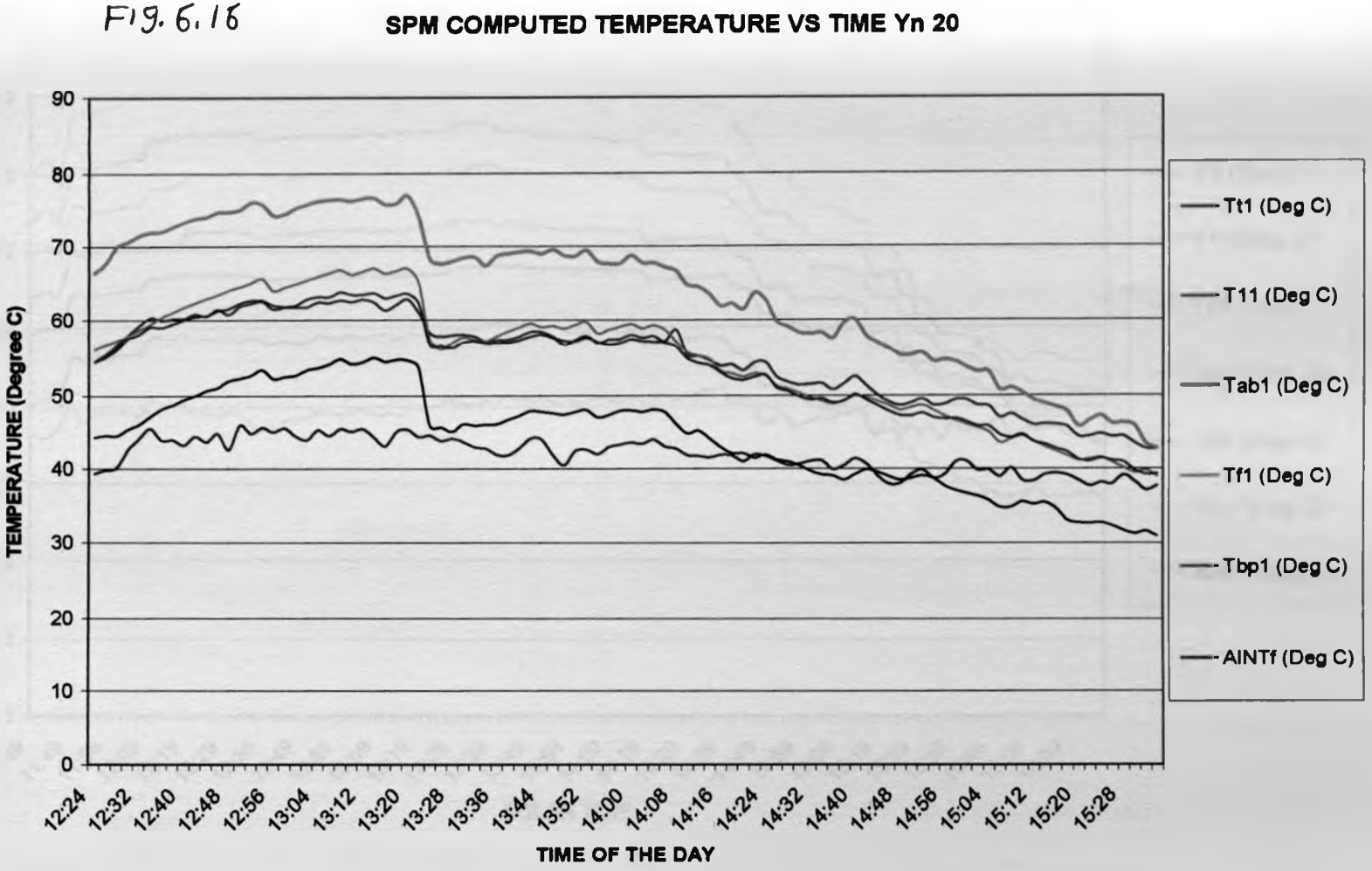
SPM COMPUTED TEMPERATURE VS TIME Yn 20
TEMPERATURE (Degree C)
90
80
70
60
50
40
30
20
10
0
12:24
12:32
12:40
12:48
12:56
13:04
13:12
13:20
13:28
13:36
13:44
13:52
14:00
14:08
14:16
14:24
14:32
14:40
14:48
14:56
15:04
15:12
15:20
15:28
TIME OF THE DAY
Tt1 (Deg C)
T11 (Deg C)
Tab1 (Deg C)
Tf1 (Deg C)
Tbp1 (Deg C)
AINTf (Deg C)

Fig. 6.17

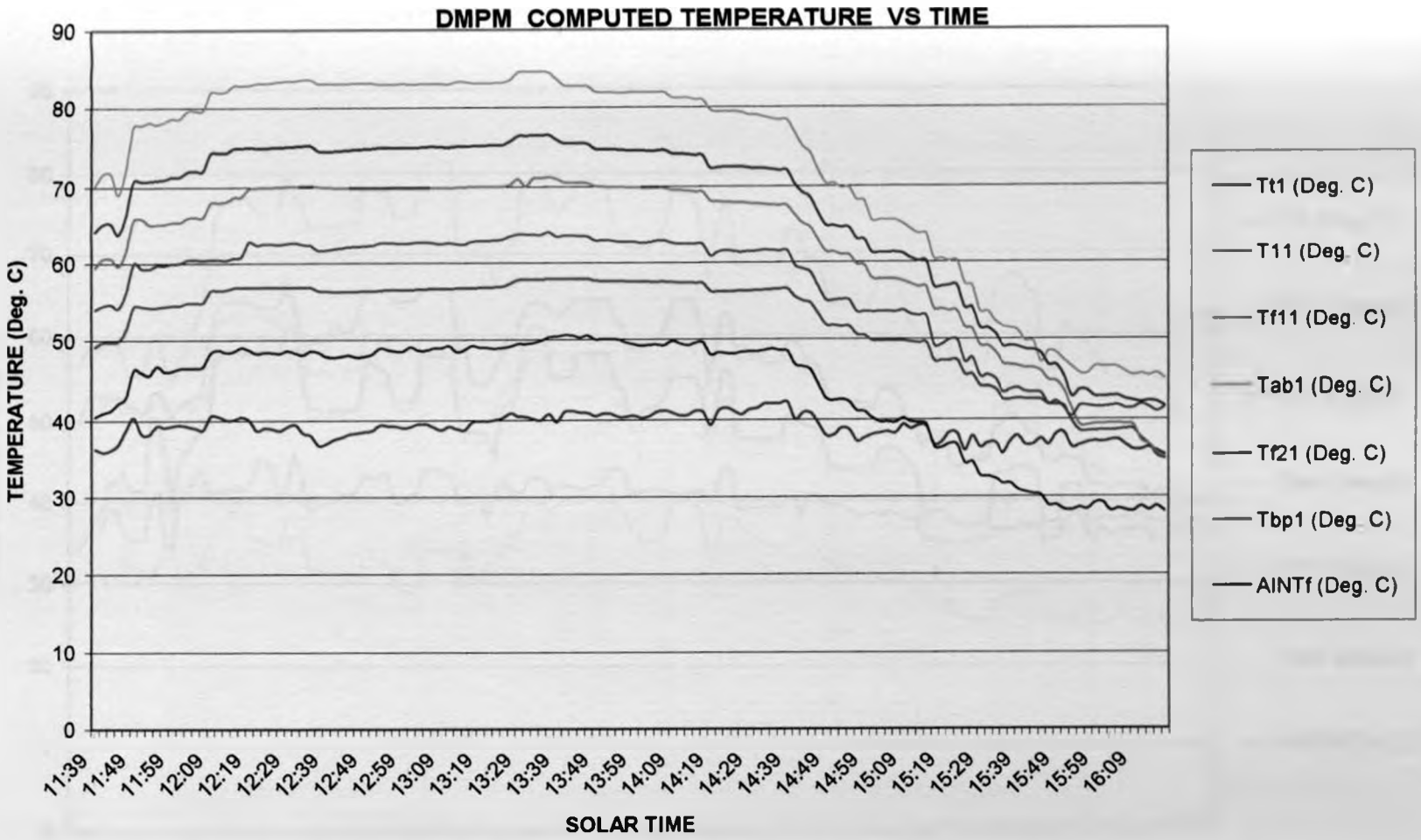
DMPM COMPUTED TEMPERATURE VS TIME
TEMPERATURE (Deg. C)
90
80
70
60
50
40
30
20
10
0
11:39
11:49
11:59
12:09
12:19
12:29
12:39
12:49
12:59
13:09
13:19
13:29
13:39
13:49
13:59
14:09
14:19
14:29
14:39
14:49
14:59
15:09
15:19
15:29
15:39
15:49
15:59
16:09
SOLAR TIME
Tt1 (Deg. C)
T11 (Deg. C)
Tf11 (Deg. C)
Tab1 (Deg. C)
Tf21 (Deg. C)
Tbp1 (Deg. C)
AINTf (Deg. C)

Fig. 6.18

DTPM Computed temperatures versus solar time

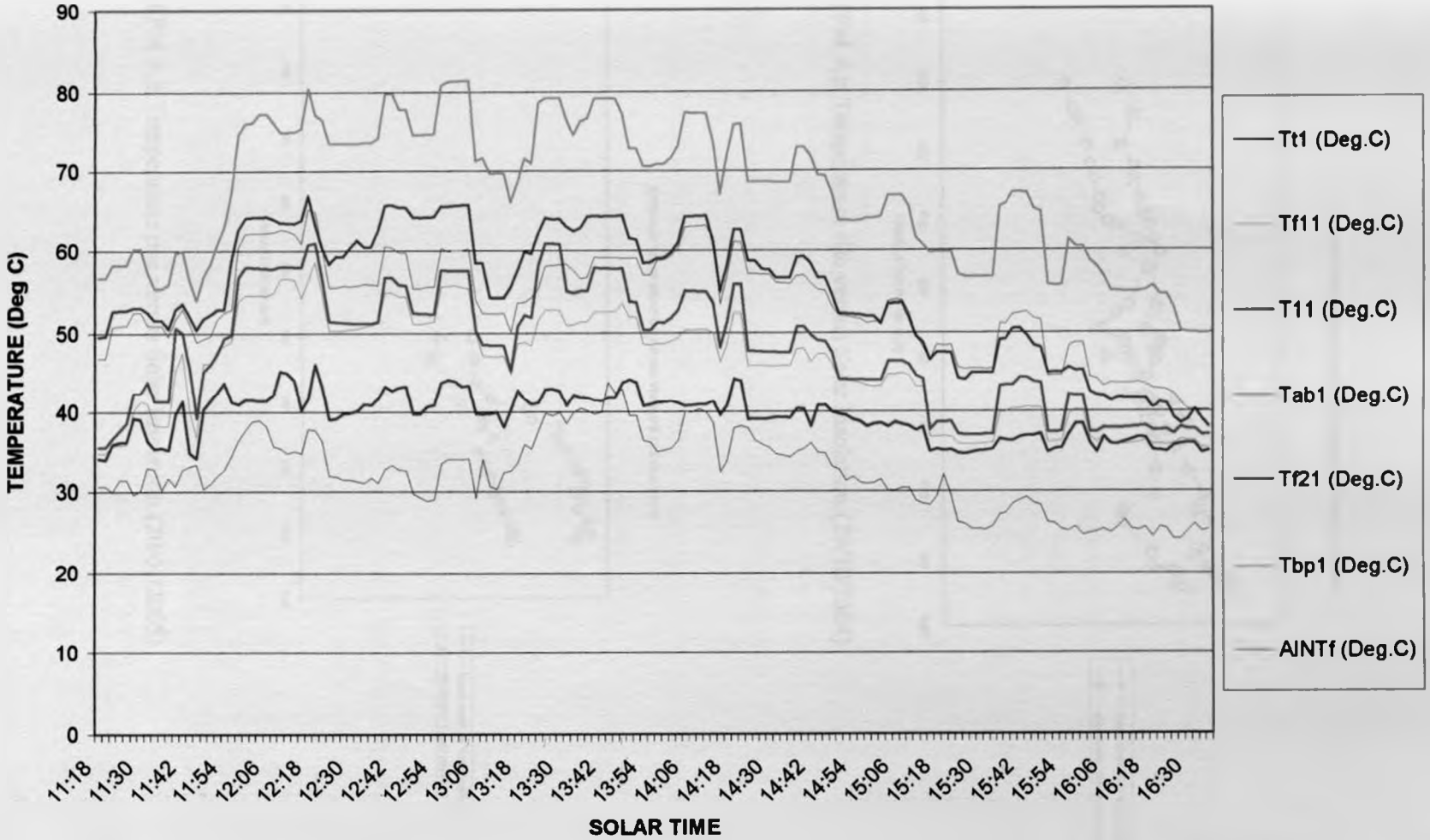

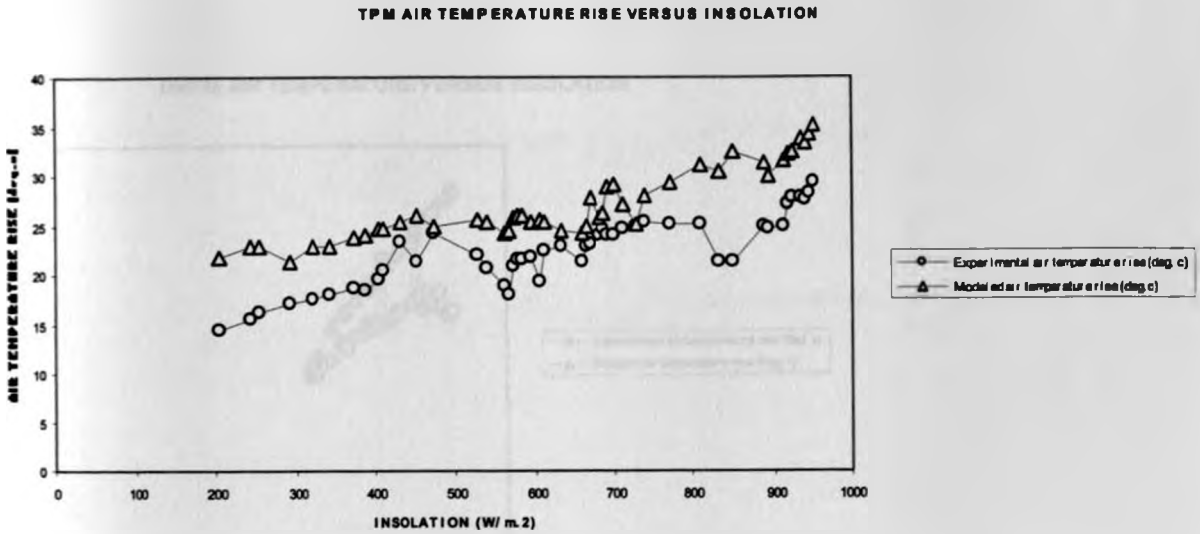

Figure 6.19: TPM Air Temperature rise versus Solar Insolation.(29/10/2004)

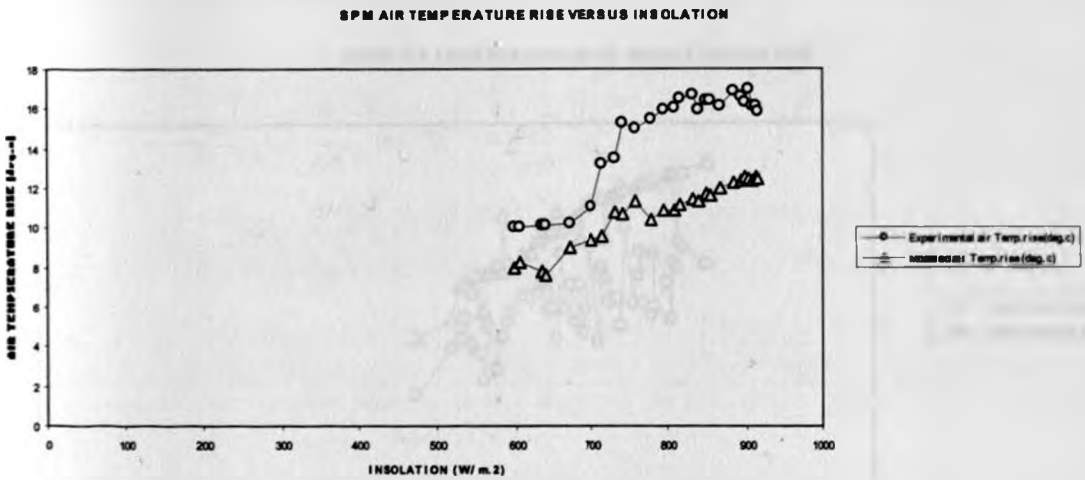

Figure 6.20: SPM Air Temperature rise versus Solar Insolation.(20/01/2005)

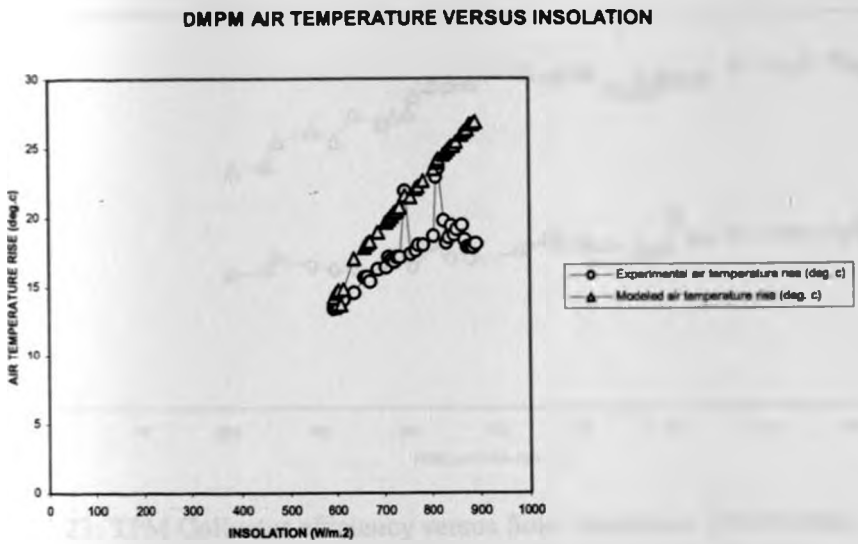

Figure 6.21: DMPM Air Temperature Rise versus Solar Insolation. (03/02/2005)

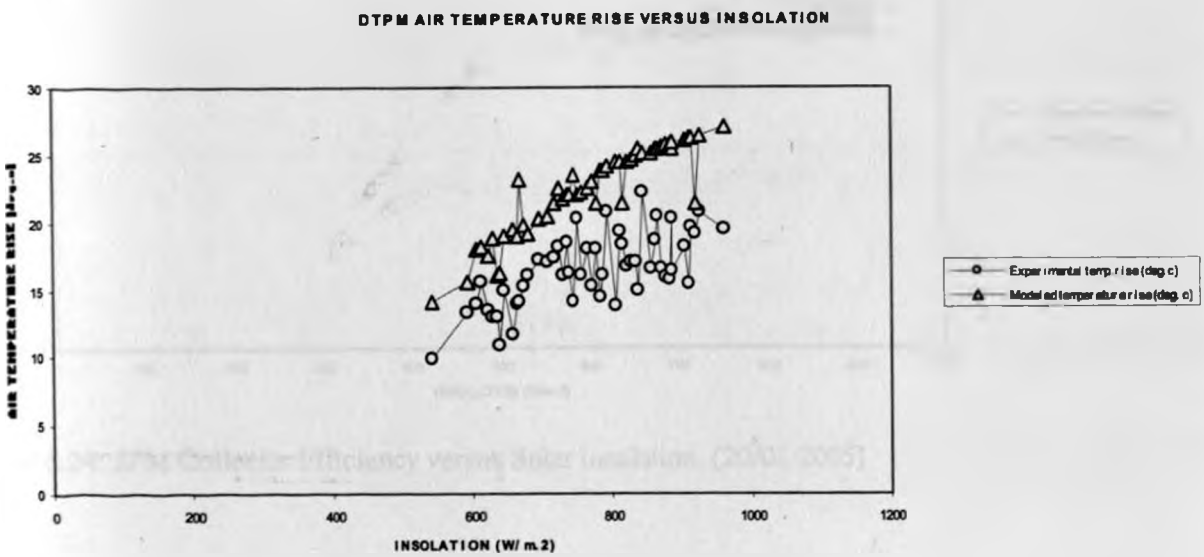

Figure 6.22: DTPM Air Temperature Rise versus Solar Insolation. (17/02/2005)

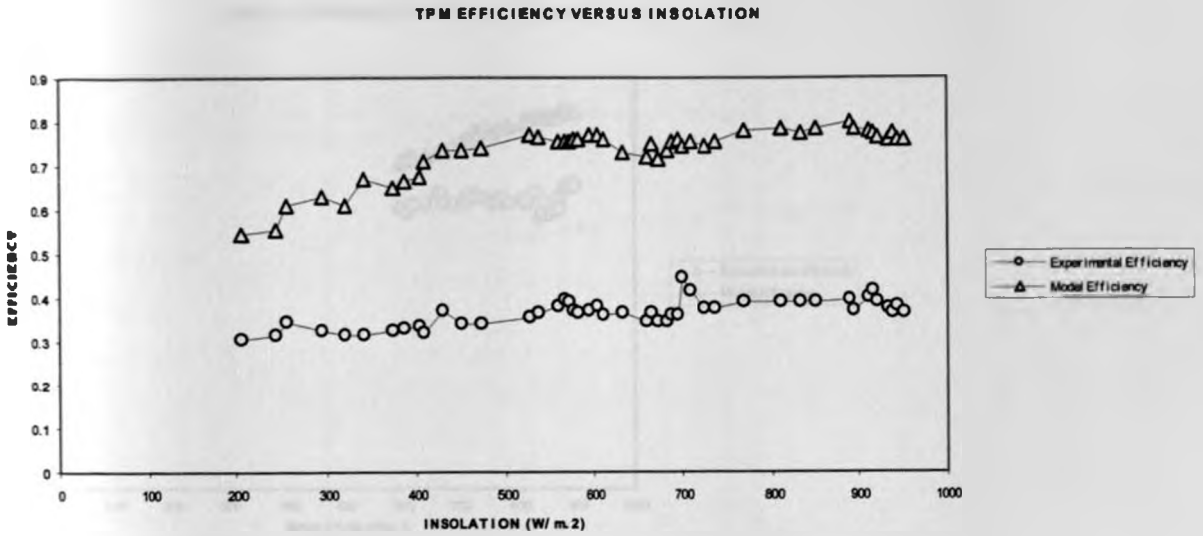

Figure 6.23: TPM Collector efficiency versus Solar Insolation. (29/10/2004)

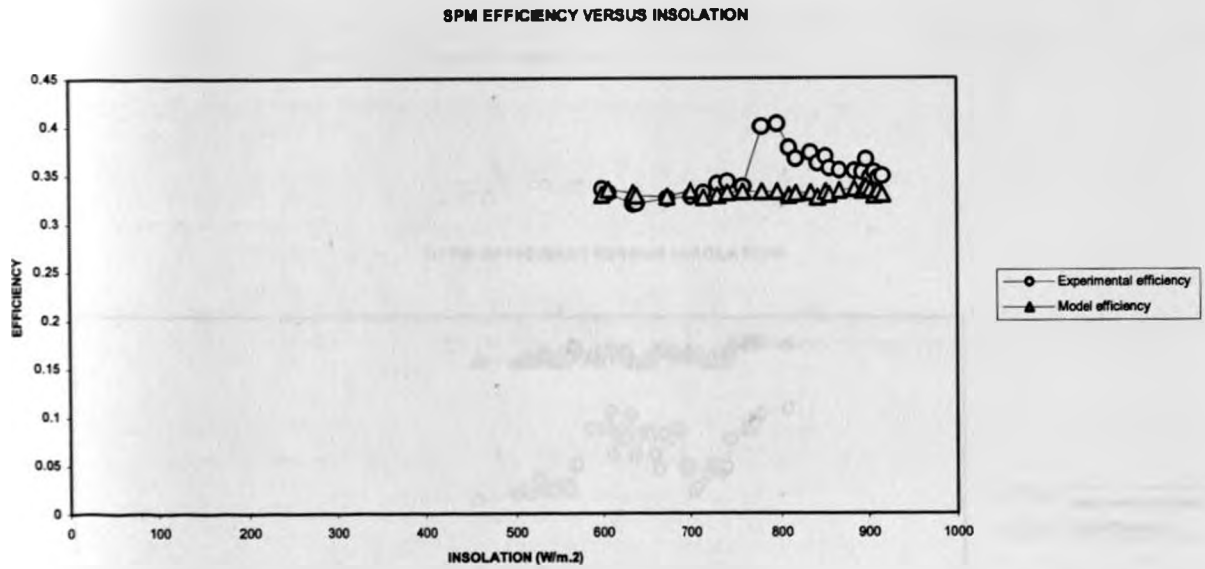

Figure 6.24: SPM Collector Efficiency versus Solar Insolation. (20/01/2005)

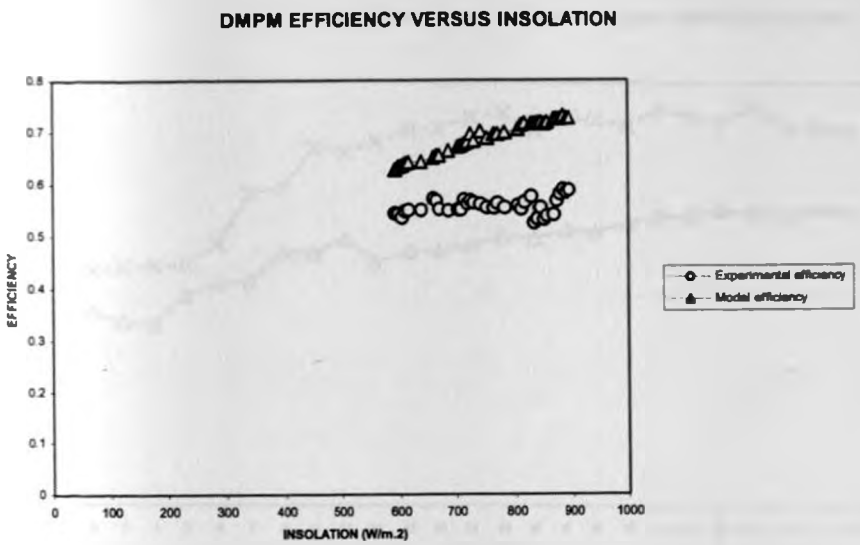

Figure 6.25: DMPM Collector Efficiency versus Solar Insolation. (03/02/2005)

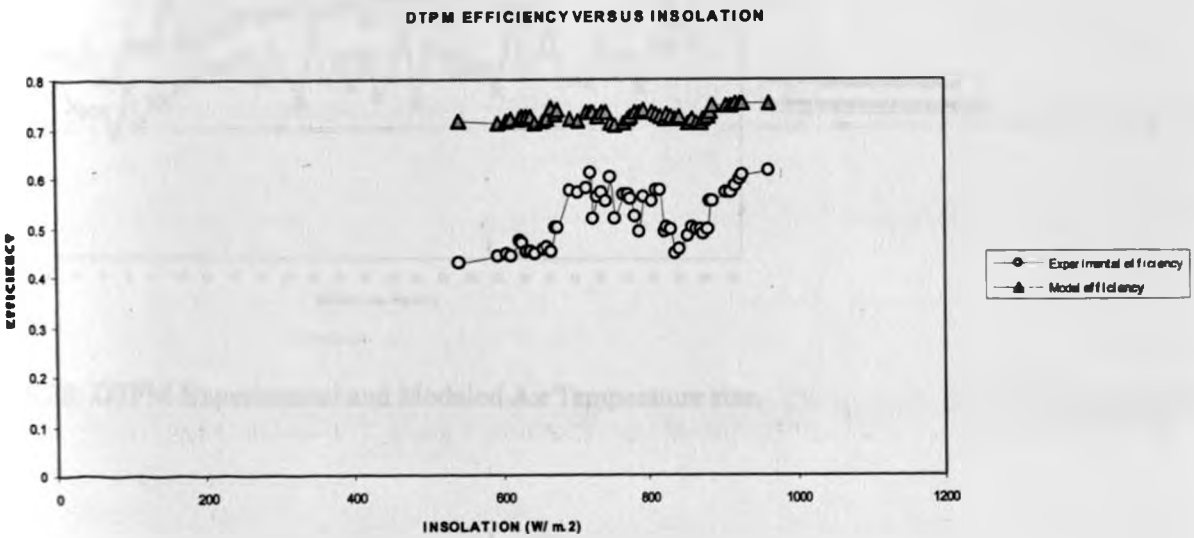

Figure 6.26: DTPM Collector Efficiency versus Solar Insolation. (17/02/2005)

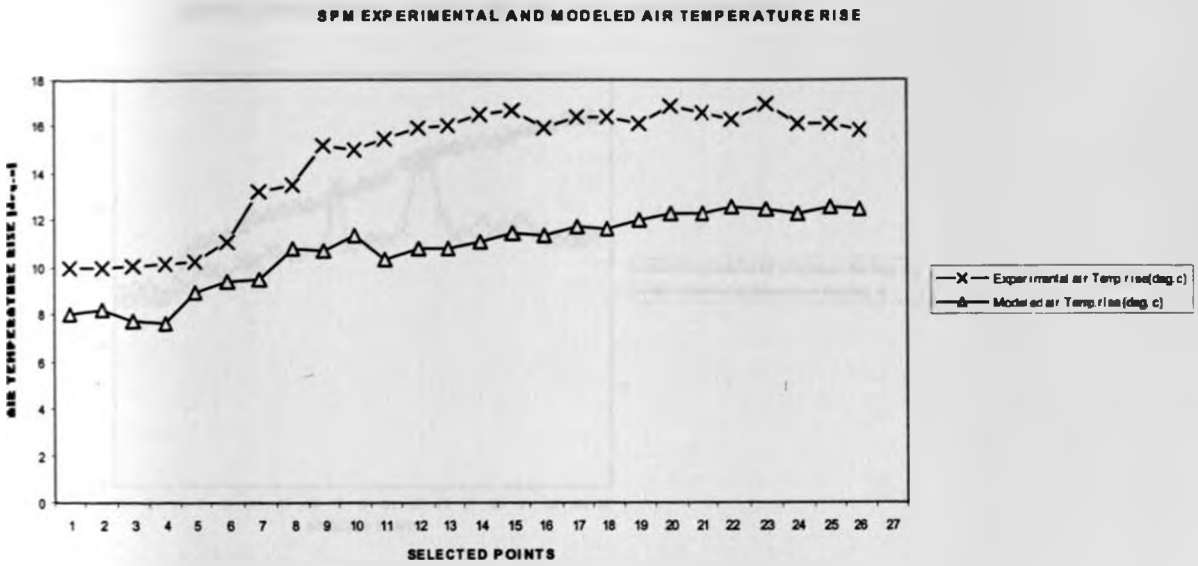

Figure 6.27: SPM Experimental and Modeled Air Temperature Rise.

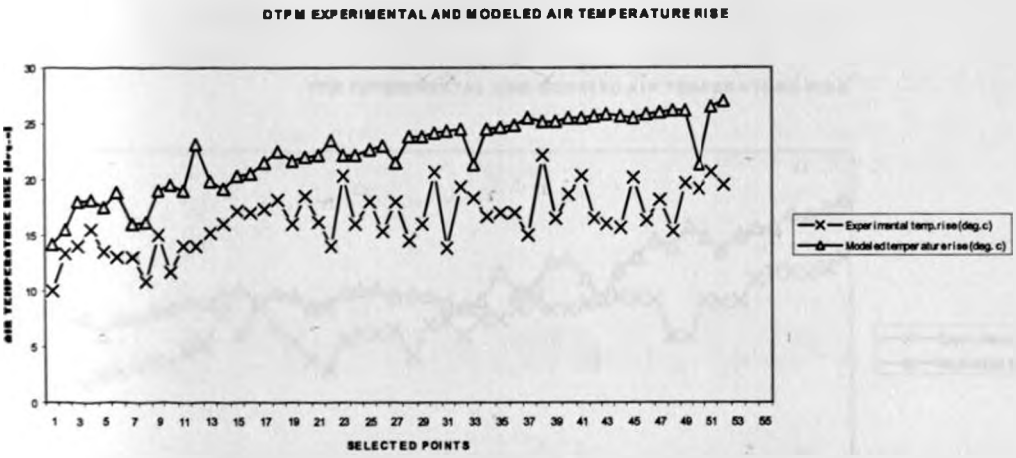

Figure 6.28: DTPM Experimental and Modeled Air Temperature rise.

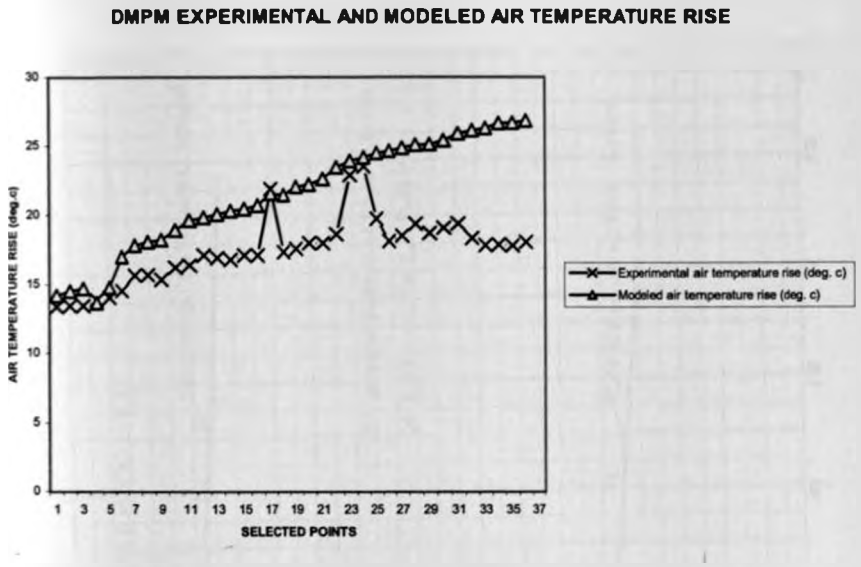

Figure 6.29: DMPM Experimental and Modeled Air Temperature rise.

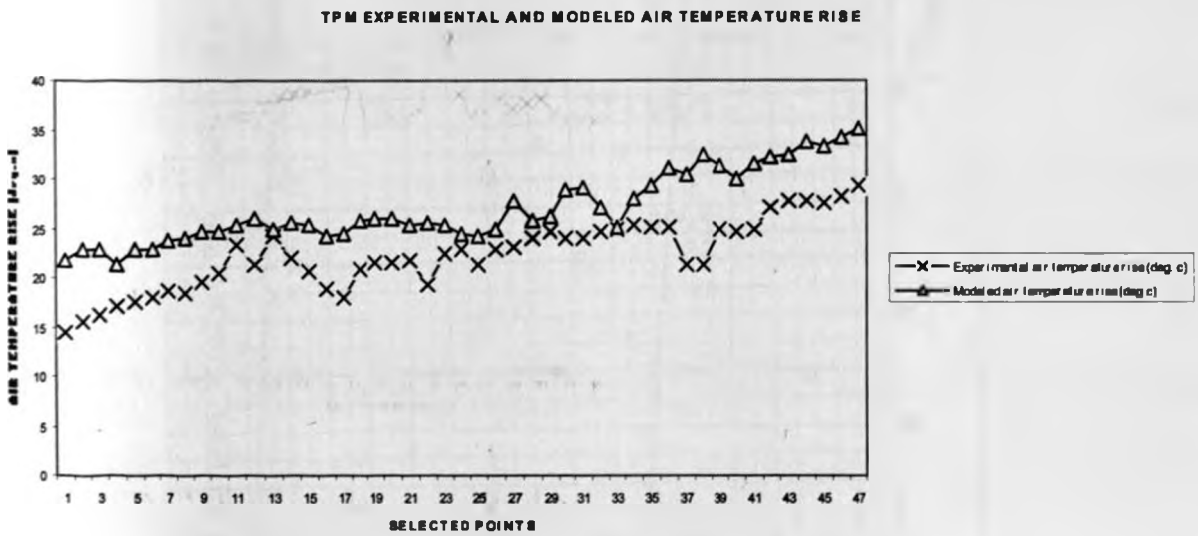

Figure 6.30: TPM Experimental and Modeled Air Temperature rises for selected points.

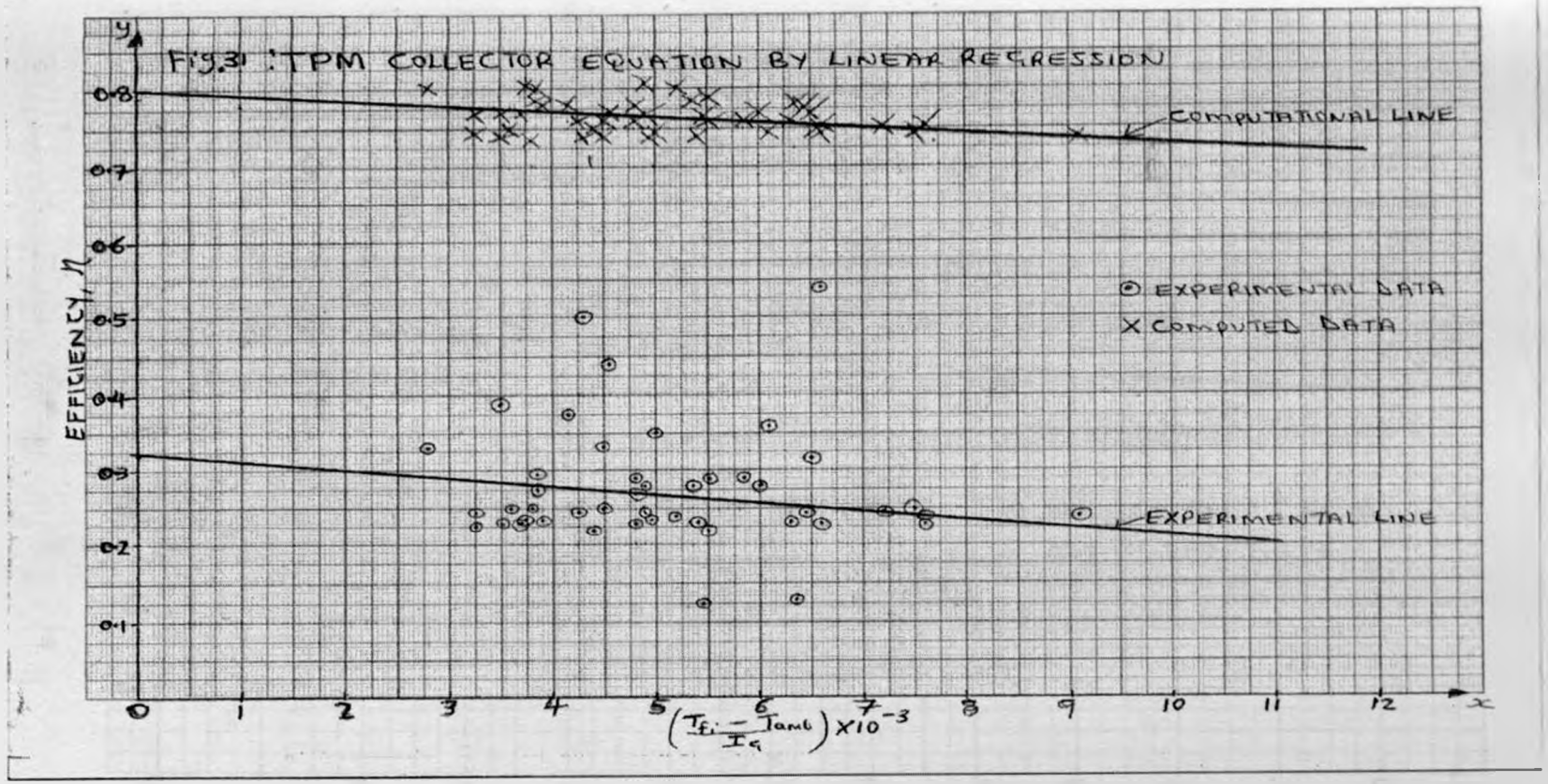
Fig.3: TPM COLLECTOR EQUATION BY LINEAR REGRESSION
y
EFFICIENCY, η
0.8
0.7
0.6
0.5
0.4
0.3
0.2
0.1
0
1
2
3
4
5
6
7
8
9
10
11
12
x
$\left(\frac{T_{fi} - T_{amb}}{I_G}\right) X10^{-3}$
COMPUTATIONAL LINE
EXPERIMENTAL DATA
COMPUTED DATA
EXPERIMENTAL LINE

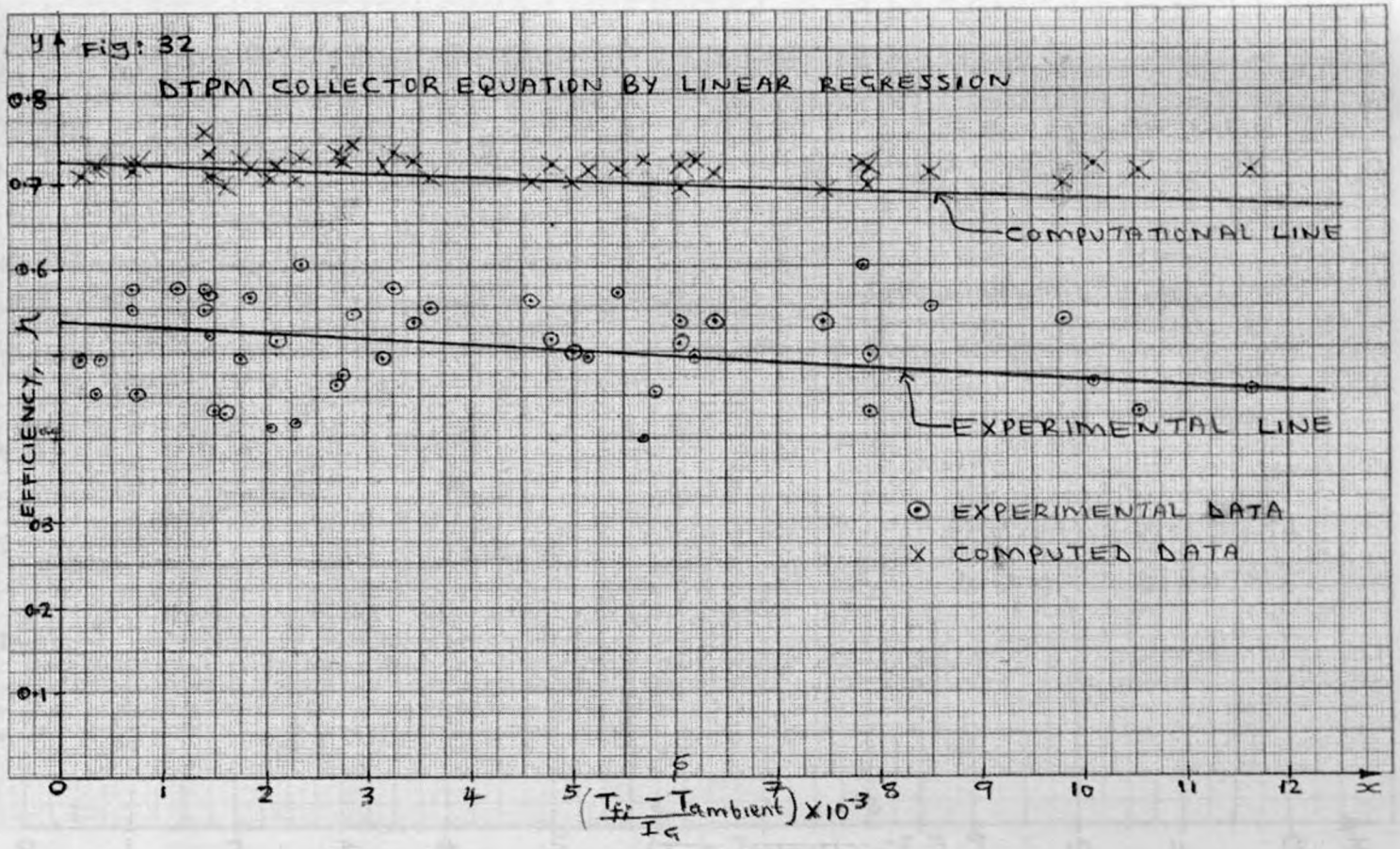
Fig: 32
DTPM COLLECTOR EQUATION BY LINEAR REGRESSION
COMPUTATIONAL LINE
EXPERIMENTAL LINE
EXPERIMENTAL DATA
COMPUTED DATA
EFFICIENCY, η
y
x
0.8
0.7
0.6
0.3
0.2
0.1
0
1
2
3
4
5
6
7
8
9
10
11
12
$\left(\frac{T_{fi} - T_{ambient}}{I_G}\right) \times 10^{-3}$

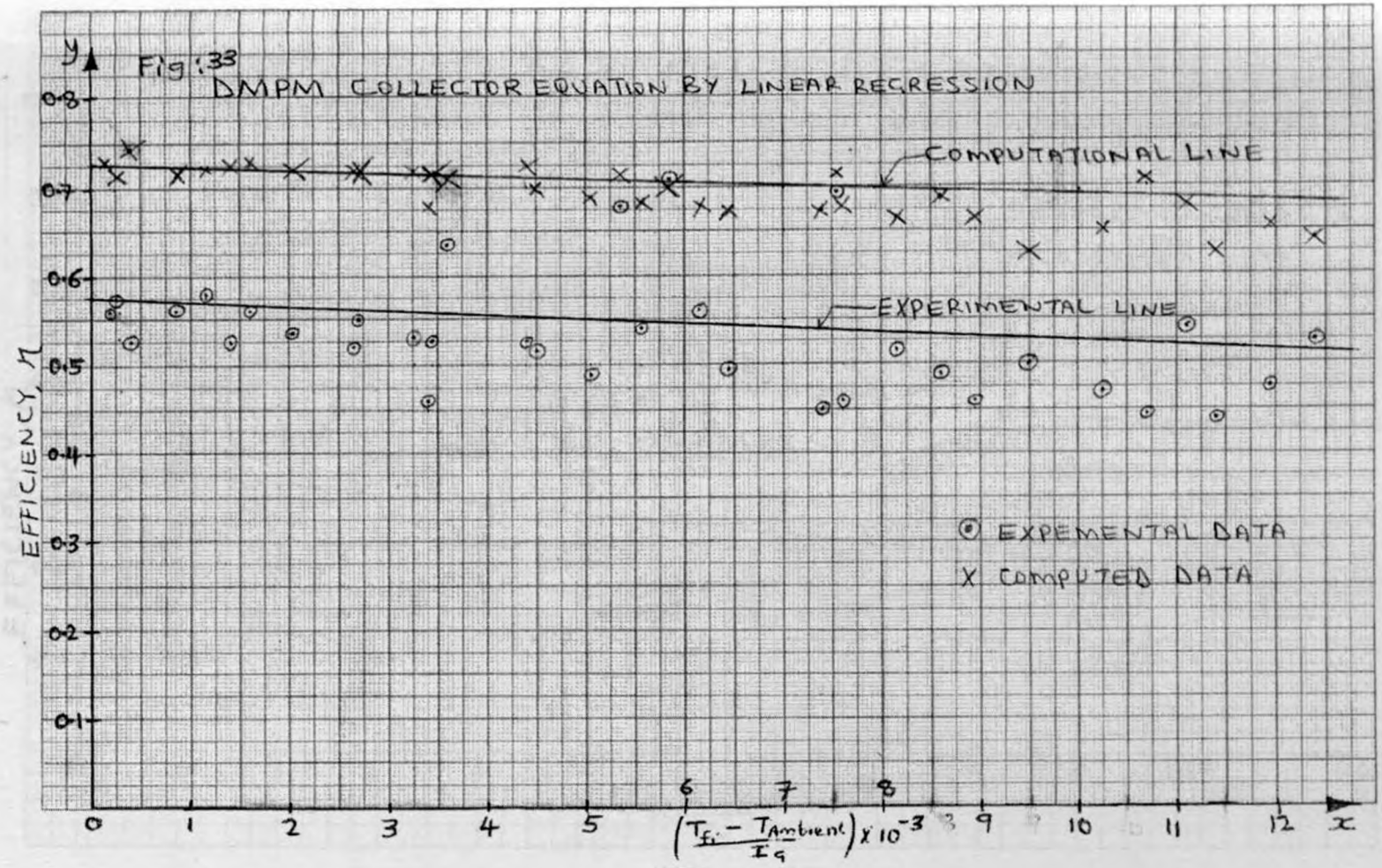
Fig: 33
DMPM COLLECTOR EQUATION BY LINEAR REGRESSION
COMPUTATIONAL LINE
EXPERIMENTAL LINE
EXPEMENTAL DATA
COMPUTED DATA
EFFICIENCY, η
y
x
0.8
0.7
0.6
0.5
0.4
0.3
0.2
0.1
0
1
2
3
4
5
6
7
8
9
10
11
12
$\left(\frac{T_{fi} - T_{Ambient}}{I_G}\right) \times 10^{-3}$

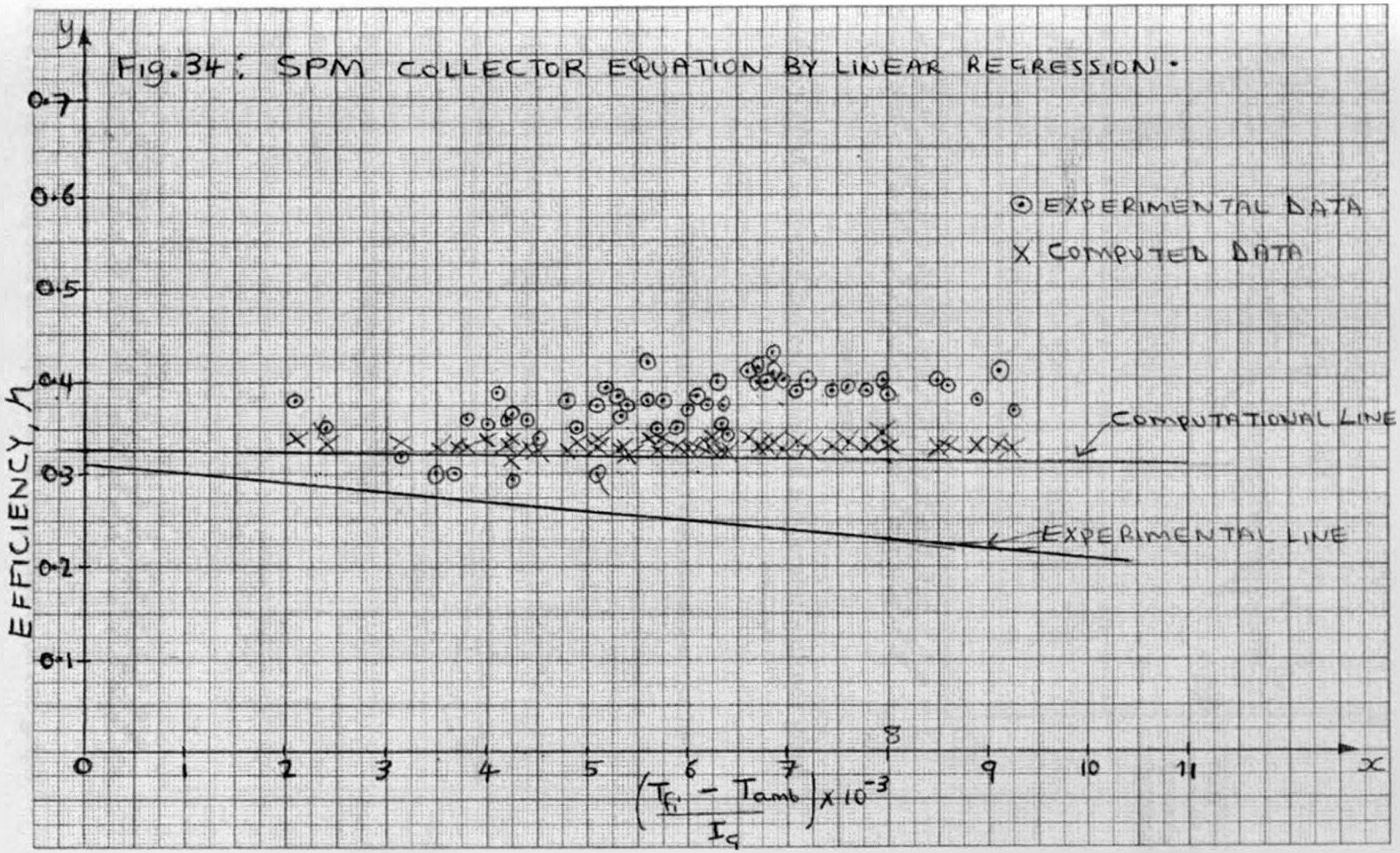
Fig.34: SPM COLLECTOR EQUATION BY LINEAR REGRESSION.
y
0·7
0·6
0·5
0·4
0·3
0·2
0·1
EFFICIENCY, η
⊙ EXPERIMENTAL DATA
X COMPUTED DATA
COMPUTATIONAL LINE
EXPERIMENTAL LINE
0
1
2
3
4
5
6
7
8
9
10
11
x
$\left(\frac{T_{fi} - T_{amb}}{I_G}\right) \times 10^{-3}$

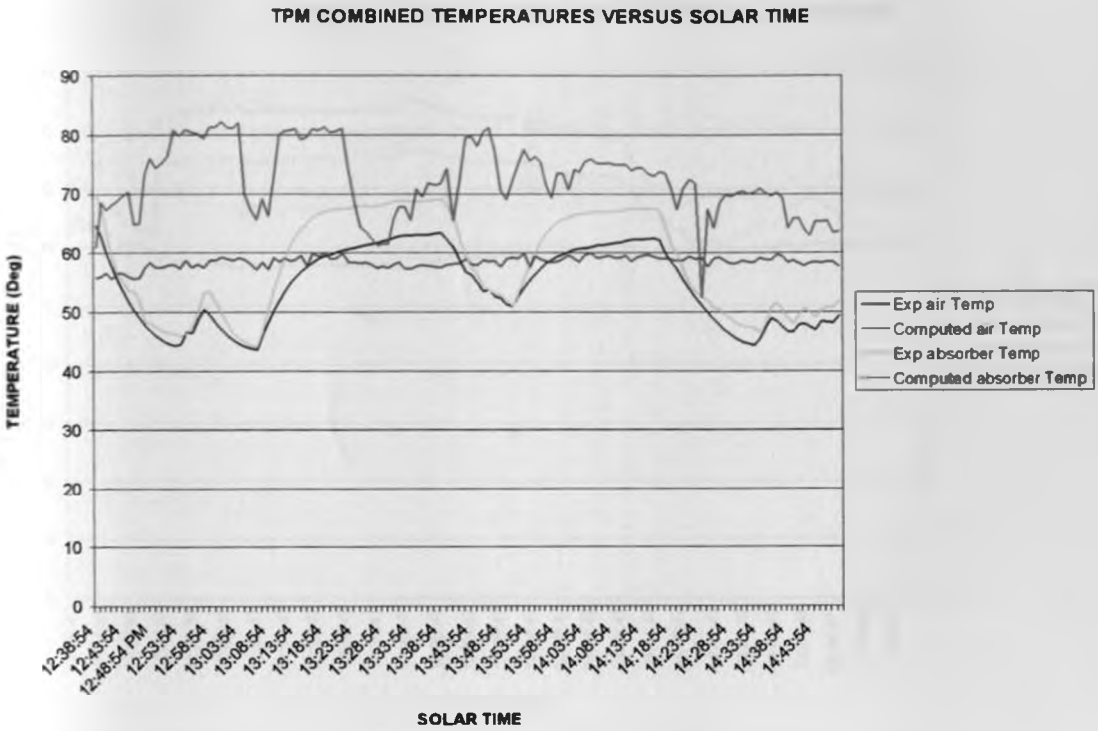

Figure 6.35: TPM computed and experimental temperatures on one graph.

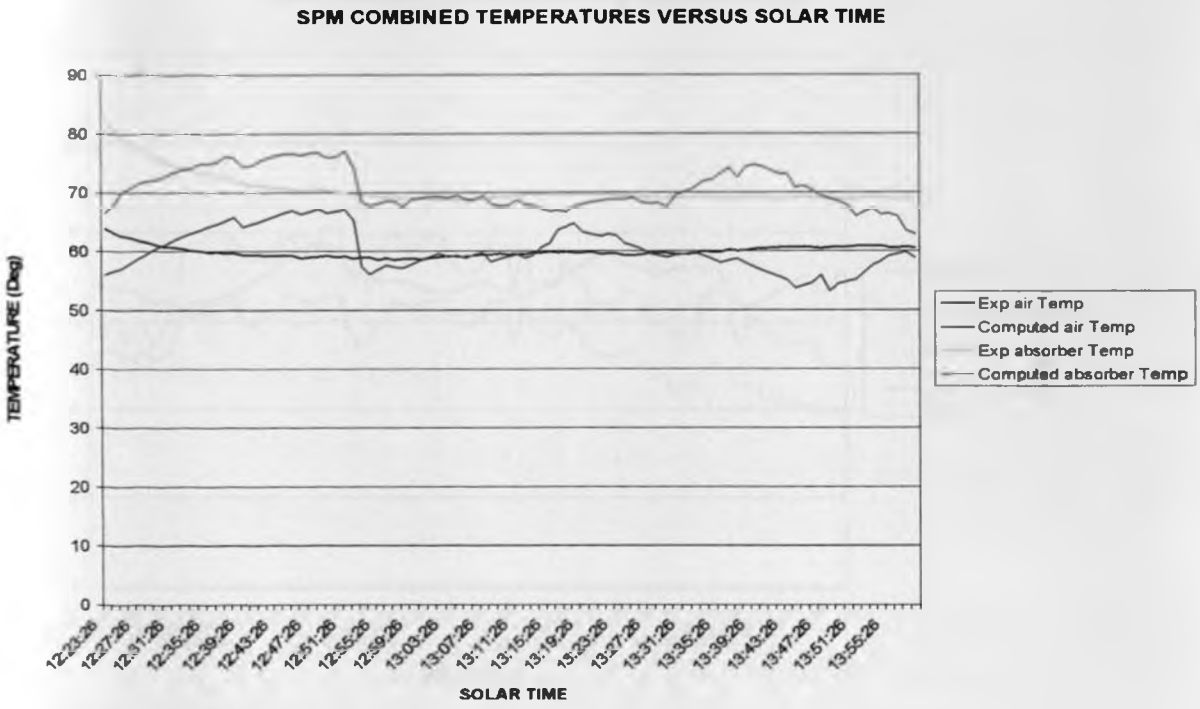

Figure 6.36: SPM computed and experimental temperatures on one graph

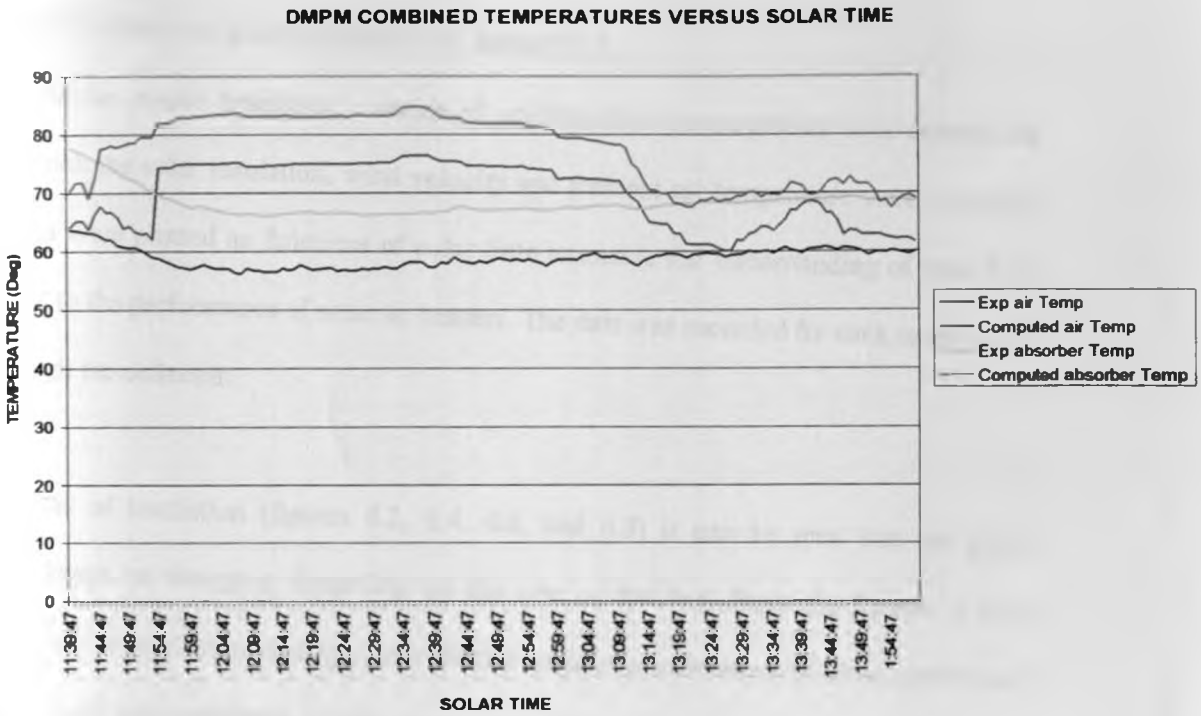

Figure 6.37: DMPM computed and experimental temperatures on one graph.

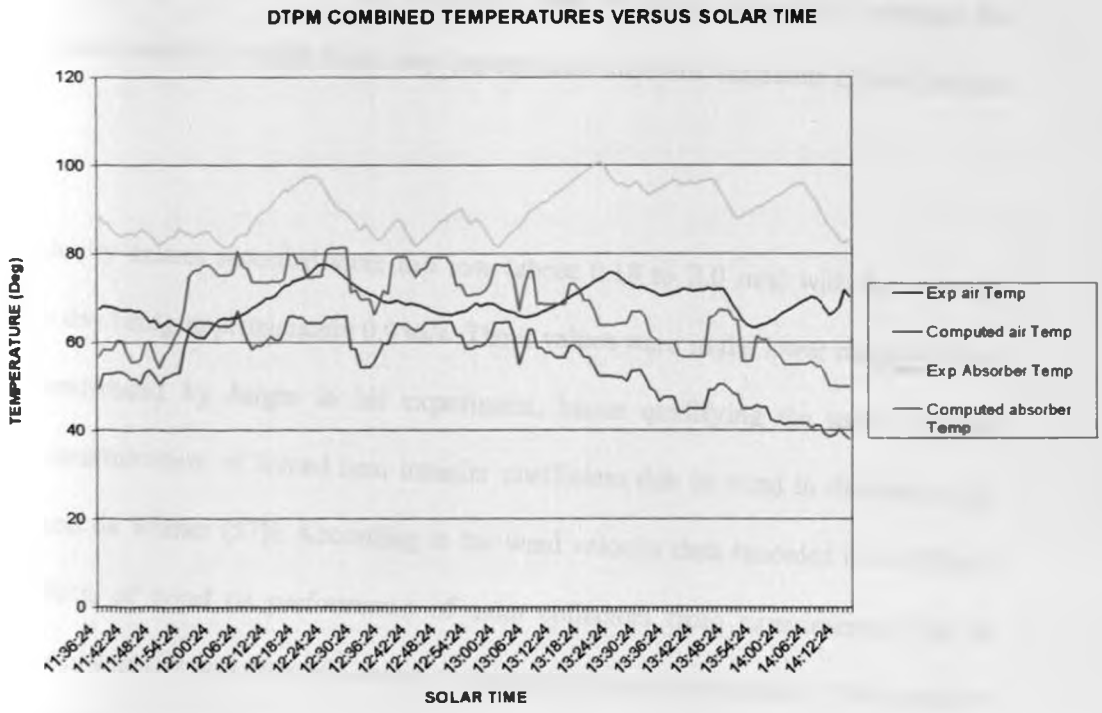

Figure 6.38: DTPM computed and experimental temperatures on one graph

6.9: DISCUSSION OF EXPERIMENTAL RESULTS.

To validate the model developed, a series of experimental measurements were carried out during which the solar insolation, wind velocity and ambient air temperature were recorded. These data were plotted as functions of solar time to enable the understanding of how they are related to the performance of solar air heaters. The data was recorded for each mode of air pass through the collector.

From graphs of insolation (figures 6.2, 6.4, 6.6, and 6.8) it can be seen that the solar insolation keeps on changing depending on the time of the day. From the figures it was observed that the insolation reaching the collector surface is influenced by cloud cover and time of day and, was maximum at solar noon, hence testing solar collectors at hours around solar noon might not be appropriate to give enough information on the expected performance characteristics. With the recorded solar insolation data, a direct comparison between the modes of air pass cannot be made since they experienced different variations of the incident radiation.

The wind velocity values recorded were too low (about 0.18 to 2.0 m/s) with the average value on each day being approximately 0.9 m/s .These values were in the lower range of wind velocity recommended by Jurges in his experiment, hence qualifying the use of Jurges equation for determination of forced heat transfer coefficient due to wind in this study.(As noted by Francis de Winter (57)). According to the wind velocity data recorded it is difficult to tell the effects of wind on performance of solar collectors from experiments. This is because the wind velocity and direction keeps on changing through out the day. This makes it necessary to have computational models for performance prediction, which is a main aim of this study, (figures 6.3, 6.5, 6.7 and 6.9).

From the experiments it was found that the ambient air temperature had a variation of about $\pm 4^0$ C within the day's average value, which was slightly different on each day of experiment. This variation implies an effect on the flowing air inlet temperature hence affecting the solar collector performance.

From the experimental temperature graphs (figures 6.10, 6.11, 6.12, 6.13 and 6.14) which relate temperatures to insolations, it was observed that in all modes of pass, the absorber plate had the highest temperature followed by the flowing air outlet temperature then the back plate. Comparing the individual component temperatures for the different modes of pass in this work, might not be possible because all the experiments were done on different days which mean different weather conditions.

On comparing the solar insolation to the component temperatures, it is clearly evident that the solar insolation has a direct effect on solar collector performance. At times when the solar insolation changed, the recorded component temperatures changed with a lag of about 5 minutes. This lag is attributed to the heat.capacity of the collector materials, and the lag justifies the need for a transient prediction model that is able to respond to a changing weather. At times when the solar insolation increased, the experimental component temperature also rose.

For the single pass mode (SPM) (figure 6.11, the difference between the absorber plate and the exit air temperature was greater compared to the multi-pass modes, this meant a low collector efficiency for the SPM as expected.

On comparing the wind velocity data (figures 6.3, 6.5, 6.7, 6.9 and Appendix 3) with the component temperatures it is evident that the effects of wind velocity in this work can be

neglected with no error due to the low wind velocities encountered during the period of the experiment.

The experimental ambient air temperature data indicated that, all the component temperatures were proportional to the ambient temperatures.

The collector component temperatures were observed to have higher values immediately after starting the experiment (especially on days when the experiment started at late hours of morning) this was because of the heat capacity of collector which is expected to result to high transient effects during the start of operating the solar collectors.

6.10: THEORETICAL COMPARISON BETWEEN THE FOUR MODES.

To obtain the program computed data, the individual collector programs were executed by use of same collector operating parameters (collector area, material properties and air mass flow rate.) The weather input data were the ones obtained experimentally on the days when the experiment for the concerned mode of air flow was carried out.

Appendix 5 presents the theoretically computed temperatures while figures 6.15, 6.16, 6.17 and 6.18 show the variation of the theoretical temperatures with solar time for all the modes of flow, and according to the figures, it depends on the available solar insolation. The absorber plate temperature are highest around solar noon when the insolation values are maximum and then drops gradually as expected from experimental results.

Also it was observed that, all the other temperatures computed followed the trend of the absorber plate temperature which is generally expected since the absorber plate acts as the source of heat for all the other collector components.

The theoretically computed temperatures indicated that the flowing air exit temperature was close to the back plate temperature for all the modes of air pass, but it was noted that for the DMPM and TPM it was closer than for SPM and DTPM, (figures 6.15, 6.16, 6.17 and 6.18). This was attributed to the fact that the air does not have enough time to come in contact with the heated absorber plate, since it comes into contact with it only once and, that is under the absorber plate, (figures 1.1, 1.2, 1.3 and 1.4).

In all theoretical temperatures, the top glass cover temperature was the lowest. On comparing the differences between the absorber plate and the top glass cover temperatures, it was observed that the difference was greatest for the TPM, followed by the DTPM, then the DMPM, with the SPM having the smallest difference. This is attributed to the fact that the flowing air between the glasses in TPM and DTPM cools the glass hence able to minimize heat losses from the collector to the surroundings due to temperature difference. These differences were high at higher solar insulation input values for all the four modes of air pass through the collector.

Also, figures 6.15, 6.16, 6.17 and 6.18 indicate the instantaneous changes of the collector component temperatures with time. Since the input data to the theoretical models were experimentally measured, these figures reveal the transient nature that exists during the operation of the collector due to changing weather conditions. The four modes indicated similar nature of response to changes.

From figures 6.17 and 6.18, it can also be seen that, for the cases of double pass, the exit air temperature is slightly higher for the DMPM where the air flows on the upper surface of the absorber plate than for the DTPM where the air does not flow over the absorber plate.

From figures 6.15, 6.16, 6.17 and 6.18, it is also seen that, there is good agreement between the predications of all the models.

The glass covers temperatures were not affected more by abrupt changes in the input weather data, but took time to respond to the changes. This is attributed to the low heat capacity values of glass.

Figures 6.19, 6.20, 6.21 and 6.22 show a plot of flowing air temperature rise as functions of solar insolation. It was observed that the TPM theoretically had the highest values of air temperature rise for any given value of solar insolation, with the SPM having the lowest value. And the air temperature rise increased with increased insolation values for all the modes of air pass considered.

The DTPM and DMPM values of air temperature rise were almost the same, but the DMPM was slightly superior. These figures indicated changes in the computed air temperature rise for a particular input value of solar insolation, for all the modes of air pass. This is attributed to changes in the other input values (time, ambient temperature and wind velocity).Hence it is clearly evident that the performance of a solar collector is of transient nature.

Since temperature rise is a good factor to use when comparing collectors to use for crop drying, the developed model can be used successfully with no error in selection as it takes into account the transient effects due to change in weather conditions.

When the solar insolations (figures 6.2, 6.4, 6.6, and 6.8) were compared to the computed theoretical temperatures (figures 6.15, 6.16, 6.17, and 6.18) it was observed that they compared in trend. This means the transient collector model developed is able to realize the time lag between the two (as observed by Luti (13)). This suggests that the use of the model developed in this study can be justified for use in prediction of solar collector performance when prolonged nearly constant insolation periods do not prevail during the time of experimental tests.

Figures 6.23, 6.24, 6.25 and 6.26 show the collector efficiency for the four modes of pass as functions of solar insolations. From the figures, it is seen that, this model predicts almost constant values for the collector efficiencies on all models of air pass, although the DMPM model showed a slight increase in collector efficiency with an increase in solar insolation. From the model results, the TPM had the highest efficiency values, followed by the two double pass modes, with SPM having the lowest values. According to the model, the collector efficiency is supposed to be a constant. This was so because the air temperature rise is directly proportional to the solar insolation. On basis of efficiency, the model was able to agree with other prediction relation that, the more the passes in the collector the superior in performance the collector is.

6.11: COMPARISON OF THEORETICAL WITH EXPERIMENTAL RESULTS.

Figures 6.10, 6.11, 6.12, 6.13 and 6.14 shows the experimental temperatures while figures 6.15, 6.16, 6.17 and 6.18 shows the theoretically computed temperature as functions of solar time. Figures 6.35, 6.36, 6.37.and 6.38 show the computed and experimental temperatures for the absorber plate and air. In both cases the absorber plate had the highest temperatures for any given solar insolation value, while the top glass cover had the lowest. Comparing the experimental figures to the theoretical ones, it is seen that there is good agreement between the predictions of the models and the experimental results.

On comparing figures 6.11 and 6.16 for the SPM, it was observed that the initial experimental temperatures are higher than the theoretical by about 14^0 C, but drops soon after starting the experiment to almost the same values. The glass covers in both cases showed almost the same temperatures. The experimental air exit temperature was slightly higher than the theoretical. Also on further comparison, the experimental results had a time lag in responding to changes in weather conditions. Figures 6.20 and table 6.2 indicate that, at high insolation values, the air temperature rise was higher for the experimental case as compared to the theoretical model, but at low values of insolation (below $700w/m^2$) the air temperature rise was the same. On observing figure 6.24 a similar observation was made for the efficiency.

Figures 6.14 and 6.18 compare the experimental and theoretical results for the DTPM mode of air pass through the collector. In this, it is again observed that the initial experimental temperatures are higher than the theoretical by approximately 12^0C.In both cases, the flowing air exit temperatures were in the same range, but table 6.3 and figure 6.22 indicates that the theoretical model gave a higher air temperature rise than the experimental set up at almost all the levels of solar insolation (about 7^0 C higher).Again table 6.2 and figure 6.24 indicate that

for DTPM, the model gave a higher collector efficiency (an average of 0.71) than the experimental set up which gave an average of 0.45.Although the experimental and modeled air exit temperatures were not in good agreement, the collector efficiency confirmed an agreement of the model to the experimental results for DTPM.

Figures 6.12 and 6.17 present the experimental and modeled temperatures for the DMPM. It is seen that the initial experimental temperatures were higher than the theoretical by about 7^0C, but they dropped immediately after proceeding with the experiment. From the figures it can be seen that at higher values of solar insolations, the modeled temperatures were slightly higher, but were also again lower at low values of insolation than the experimental. Table 6.4 and figure 6.21 show that the model gave a higher air temperature rise than the experimental set up (on average 3^0C higher.)But the trend in variation for temperatures due to changes in insolation levels were similar, although figure 6.21 indicates a fall in experimental temperatures at higher insolation levels (above 800 w/m^2) which is attributed to experimental errors and the heat capacity of the collector. Figure 6.25 shows the variation of collector efficiency with solar insolation, it indicates the same trend as observed with the case of temperatures. At all levels of insolation, the theoretical model gave higher collector efficiency than the experimental set up. All the figures discussed above indicate that there was good agreement between the DMPM predictions of the model and the experimental results.

Figures 6.10 and 6.15 present the TPM experimental and theoretical temperatures. Once again it is also noticed that the initial experimental temperatures are higher than the theoretical by about 10^0C, after a short while the theoretical temperatures dominated. The glass cover temperatures were nearly the same in both cases. The theoretical results show a

good respond to changes in insolation than the experimental results. Also at high levels of insolation the theoretical temperatures were higher.

Table 6.5 and figure 6.19 show the air temperature rise for the TPM for both the experimental and theoretical cases. It is evident that in both cases the air temperature rise was nearly the same at all levels of insolation, but there was a lot of scatter due to frequently changing weather conditions during the collection of the data. This indicates that the TPM model is able to respond to transient conditions as it was in good agreement with the experimental results with no great difference. On figure 6.23 which compares the theoretical and experimental collector efficiencies for TPM, it is seen that the theoretical efficiency was higher than the experimental efficiency by about 0.4 (52%).This is attributed to the difficulties experienced in setting up the TPM experiment

Figures 6.27, 6.28, 6.29 and 6.30 represent direct comparison of experimental and theoretical air temperature rises for selected points from the recorded and computed data. Figures 6.28, 6.29 and 6.30 indicated that the model gave slightly higher values for air temperature rise than the experimentally recorded values. The TPM values differed by about 5^0C while the DTPM and DMPM values differed by about 14^0C. All the figures indicated the same trend of the modeled and experimental air temperature values which was a clear indication on the suitability of the developed model for prediction of solar air heater performance on multi-pass modes. Figure 6.27 gave contradicting information to the other figures (6.28, 6.29 and 6.30), since the experimental air temperature rises were higher than the modeled.

A view of all the collector component temperatures shows that the TPM and DMPM air passes responded well to the theoretical model developed with small errors than the DTPM

and SPM air passes. The observation that the initial experimental temperatures were higher than the theoretical is attributed to the effect of heat capacities, the initial guesses made for the input values to the model program and the effectiveness of the stabilization period allowed before the experiment. Since the model was able to adjust after the initial guess, the difference confirms the need of a transient model in order to make predications of the collector performance in situations of changing weather conditions.

The characteristics of the thermal performance of the collector in the four modes of pass were analyzed statistically. This involved comparison of the predicted and experimentally measured performances through the Hottel- Whillier- Bliss equation, standard error and coefficient of correlation. Figures 31 to 34 indicated good thermal performance of the collector by the computational prediction when examined from the Hottel- Whillier- Bliss equation as compared to the experimental data. The triple and double pass modes had the best correlation with the single pass mode having the poorest respond to the correlation.

When subjected to variation statistics, the predicted data had smaller standard deviations (0.018 to 0.021) when compared to the experimental data (0.027 to 0.096). The coefficients of variation for the computational predictions were between 2.4% to 5.6% with the TPM having the lowest while the SPM had the highest. The case was different for the experimental data where the coefficients of variation were between 10.5% and 35.8% with the SPM having the highest value and the TPM the lowest. The great difference between the computational prediction and the experimental results when analyzed statistically was attributed to the experimental difficulties encountered in setting up the experiment and also due to the transient nature of the weather conditions under which the collector operated.

The superiority of the TPM and inferiority of the SPM was once again revealed by the statistical analysis by the fact that the TPM had the lowest values and standard deviations (0.0183) and coefficient of variation (2.4%) while the SPM had the highest.

To be in a poison to obtain the Hottel-Whillier- Bliss equations for the collector, the method of least squares was applied to the thermal efficiencies to give a linear correlation of the data, after which the coefficient of regression was calculated.(The higher the value of the coefficient of regression, the stronger the correlation, with the coefficient lying between -1 and +1.) The coefficient of correlation (0.25- 0.42) for the computational prediction developed in this study indicated how stronger it was when compared to the experimental approach (0.11- 0.21).Once again the TPM had the coefficient of correlation followed by DMPM, DTPM and SPM in that order.

From the foregoing discussions, it is noted that the TPM gave the superior results both experimentally and theoretically in terms of air temperature rise and collector efficiency. The DMPM was ranked second in performance although it gave almost the same results as the DTPM. The SPM had the worst respond to the developed model and also was found to be inferior in terms of collector performance. The superiority of the TPM, DMPM and DTPM were attributed to the long time the air was allowed to be in the collector due to the several passes and also due to the effective cooling of the glass covers. This was reflected in the developed model.

As it can be seen from the results, there were slightly differences between the modeled and experimentally measured values. This could be due to:

I. The choice of the initial input values to the model program which were an approximation. The approximate is required to be close to the expected values in order for the program to converge fast.

II. The heat transfer coefficient correlations used which are approximations to the expected nature of heat transfer in collector.

III. Instrumental and recording errors which could not be completely eliminated.

IV. Experimental difficulties encountered such as leakages, respond time in recording data and accurate position of the collector on a horizontal plane.

V. The heat capacity of the collector may not have been well represented due to all the above noting.

It can be said that, the theoretical model developed in this thesis described the performance of the collector under transient conditions reasonably well.

On the basis of the findings in this study, there is some agreement to the conclusions made by others, in the literature. Kabeel and Mecarik (17) found that increasing the absorber area increased the collector performance. Their model was transient in nature but it considered divided flow in only one direction for triangular and longitudinal fined absorber plates which was different from flat plates. They were able to confirm an air temperature rise of 57.7^0C and an efficiency of 0.657.But their work considered a range of air flow rates (0.005 to 0.05 kg s^{-1}) while in this work the mass flow rate was held constant at 0.0324 kg s^{-1} and a maximum collector efficiency value of 0.831 was attained for the TPM. The TPM has the largest area of contact for the air in the collector hence it gave the best performance.

Korir (4) developed a steady state model for predicting the performance of solar air heaters. In his findings he was able to conclude that the TPM was superior to the other modes of air pass, with the SPM being the inferior in performance. The order in performance was also confirmed by Luti (6) who also considered a quasi-steady- state analysis of the performance multi-pass solar collectors.

Although the present model is based on transient analysis, it is in agreement with the findings of Korir(4) and Luti (6), that the single pass made is inferior in performance when compared to the multi pass modes (DTPM, DMPM and TPM). Since the present model was validated experimentally and the same order of ranking obtained, it shows the approach used in this thesis will add value in predicting the performance of multi- pass solar air heaters operating under changing weather conditions.

Although most of the existing literature is on steady-state, the findings in this thesis do agree with such findings, hence the predication model is in a capacity to give transient predictions of solar collectors.

CHAPTER 7: CONCLUSIONS, LIMITATIONS AND RECOMMENDATIONS.

7.1: CONCLUSIONS.

The objective of this study was to obtain a transient theoretical model that can be able to predict the performance of solar collectors when operating on transient conditions (changing weather conditions). The obtained model can be used to predict the performance of solar collectors operating under transient conditions in the four modes reasonably well.

Developing the model involved taking an energy balance for the collector components then forming differential equations that were solved numerically. A computer program was written in Fortran 90 (appendix 6) in order to facilitate in generating the required data from the model.

The obtained model was validated experimentally and there was good agreement in the results obtained for both cases. To use the model requires an input of weather data, such as insolation, wind velocity, ambient temperature and also the collector parameters (area, mass flow rate, and properties of the materials used in construction).

The introduction of this transient solar thermal collector performance prediction model is expected to bring a benefit in the thermal solar technology world, since it requires a set of input data which can be used repeatedly on a number of collectors if their construction and operating parameters are known. Also the model offers a complete prediction when compared to the present steady- state prediction methods.

The capability of the model to respond to varying weather conditions gives it an added advantage since its results offers a better reflection on the performance of the collector on conditions that might be encountered during real service of the collector

The collector model has the same base and is directly comparable with present steady-state models.

From the theoretical model it was found out that:

I. The triple pass mode is superior to the other modes at all insolation levels
II. The performance of the double pass modes (DTPM and DMPM) were almost the same but the DMPM tended to be better than DTPM in most cases.
III. The single pass mode is the most inferior as compared to the others for all the ranges of insolation levels encountered in this study.
IV. The developed model did not fit well in prediction of solar collector thermal performance for SPM as compared to other modes.
V. Since the wind velocities encountered during the experiments were too low, wind had a negligible effect on the solar collector performance effects in this study.

Since the transient model developed in this Thesis was validated and found to fit well to the experimental data, and also confirmed similar results to other models, it can be used successively to predict the performance of multi-pass solar air heaters which was the aim of this work.

7.2 : LIMITATIONS:

1) The model developed in this thesis requires an initial aproximation of the collector component and flowing air temperatures, which should be close to reality.
2) To use this model, input data of insolation, ambient temperature and wind velocity measured experimentally are required.
3) This model has not compared the effect of changing the collector parameters such as mass flow rate, area and construction on the predicted performance characteristics; these are expected to have optimum design values.
4) This work concentrated on a two glass cover solar air heater operating on single, double and triple pass modes under transient conditions.

7.3: RECOMMENDATIONS FOR FURTHER WORK:

1) The heat capacity of the collector be determined, since there is likely to be a lag between insolation and temperature of the collector or air and these affects the theoretical prediction.
2) A major possible source of deviation of the theoretical predictions were the heat transfer coefficient correlations since the existing ones are outdated hence there is a need for further study on heat transfer coefficients for solar collectors.
3) The Jurges equation for forced convection by wind over the collector surface has an over prediction since even in the absence of wind it presents a coefficient for wind heat transfer, so it needs to be reviewed.
4) The model developed in this thesis used constant values for mass flow rate, collector area and construction parameters. Hence there is a need to investigate the effect of these parameters on the model.

REFERENCES.

1. Kristoferson L.A; and Bokalders V; "Renewable Energy Technologies, their applications in developing countries", *Intermediate Technology Publications, London, Great Britain, 1991.*
2. Persad,P., 'A Generalized analysis for the performance prediction of Flat-plate solar collectors', *A PhD thesis, University of the West Indies, St. Augustine, Trinidad & Tobago, 1981.*
3. Simonson, J.R., 'Computing methods in solar heating design', 1st Edition *chapter 4, page 61-117, The Macmillan press, 1984.*
4. Korir,J.K., 'Theoretical and Experimental Analysis of multi-pass solar air heaters', *A thesis for the degree of Masters of Science in Mechanical Engineering, University of Nairobi, Nairobi, Kenya, 1990.*
5. Arikol,M, and Ozil, E., 'Predicting long term average performance of solar collectors', *Solar energy utilization , page 227, Marmara University, Istanbul, Turkey, 1987.*
6. Luti, F.M., 'A parametric study of the two glass cover solar air heater operating in the single and double pass modes', *AJST Series A vol.7 No. 2, 1988.*
7. Buchberg, H., Catton,I, and Edwards,D.K., 'Natural convection in Enclosed Spaces – A Review of Application to Solar Energy Collection', *Journal of Heat transfer , New York, 1976.*
8. Satcunanathan, S, and Deonarine, S., 'A Two-pass solar air heater', *Solar Energy, Vol.15, page 41-49, Pergamon Press, Great Britain, 1973.*

9. Ezeike,G.O.I., 'Development and Performance of a Triple- pass air collector and Dryer System', *Energy in Agriculture , 5, page 1-20, Elsevier Science Publishers B.V., Amsterdam,Netherlands, 1986.*

10. Wijeysundera,N.E., AH.L.L., and Tjioe,L.E., 'Thermal performance study of Two-pass solar air heaters', *Solar Energy Vol.28 No.5, page 363-370, 1982.*

11. Persad, P., and Satcunanathan,S., 'The thermal performance of the Two-pass, Two-Glass-Cover Solar Air Heater', *Journal of solar Energy Engineering, Vol.105 page 254-258, 1983.*

12. Satcunanathan,S. and Persad,P., 'An experimental Evaluation of Multi-pass solar Air Heaters', *3rd Miami International conference on Alternative Energy Sources , Miami Beach, Florida, 1980.*

13. Luti, F.M., 'Optimization of the Design of multi-pass Solar Air heaters for crop processing', Final project report, *The United Nations Educational Scientific and Cultural Organization, ANSTI Research grant contract No. 250.465.7, 1991.*

14. Maclennan, D., 'Multi-pass Solar Air Heaters', *A report for the degree of B.A.Sc, University of Waterloo, Islington,1980.*

15. Duffie,J.A.and Beckman,W.A., 'Solar Engineering Thermal processes', 2nd Edition. *John Wiley & Sons, Printed in the United States of America, 1980.*

16. Ramjattan, K.B., Design and Testing of Single, Double and Triple pass air heater', *A report for the degree of B.Sc. (Eng), University of the West Indies, St. Augustine,Trinidad & Tobago, 1976.*

17. Kabeel, A.E., and Mecarik, K., 'Computational Modeling and Experimental Analysis for Triangular and Longitudinal Fin-Absorbers of Solar Air Collectors', *Euroson'96, (from Internet).*

18. Amer's, E .H., Nayak,J.K., and Sharma,G,K., "Dynamic testing of solar flat-plate collectors", *A review.* http://wire0.ises.org/wire/doclibs/KoreaConf.nsf/id/AC7894250EE23C3CC12565A0004EA89B/$File/2-651.pdf. *12th march,2004*

19. Munroe, M.M., "Transient tests for flat-plate collector", *Solar World Congress, S.V. Szokoly (eds), vol.2, pp.879-883, 1981.*

20. Souproun, A.V., "Dynamic methods of solar collector testing", *ASME.J. Solar Energy Engineering, 2, 1149-1154, 1992.*

21. Arranovitich, E., "The joint Solar Collector testing programme of the European Community". *In: UK/ ISE, Conference II, Testing of Solar Collectors and Systems, pp. 49-70, 1977.*

22. Perers, B, "Dynamic method for solar collector array testing and evaluation with Standard database and Simulation programs", *Solar Energy, 50, 517-526, 1993.*

23. Hawlader, M.N.A. and Wijeysundera, N.E., "Solar Collector Testing", *Renewable Energy Review Journal 9, 11-28, 1987.*

24. Kamminga, W., "Experiences of a solar collector test method using Fourier transfer functions", *Int. J. Heat & Mass Trans., 28, 1393-1404, 1985.*

25. Saunier, G.Y. and Chungpaibulpatana, S.,"A new inexpensive dynamic method of testing to determine Solar Thermal performance", *Solar World Congress; S.V. Szokolay (eds), vol.2. pp. 910, 1983.*

26. Rogers,B.A., "A method for Collector testing under transient conditions" *,Solar World Forum, Proceeding of the ISES Congress, D.O. Hall and J. Morton (eds), vol.1, pp. 898-902, Brighton ; England, 1981.*

27. Wang, X.A, XU, Y.F and Meng, X.Y., "A filter method for transient testing of collector performance", *Solar Energy.38, 125-134, 1987.*

28. Frid, S.E., "Multi-node models and dynamic testing of Solar collectors", *Solar & Wind Tech.7, 655-661, 1990.*

29. Liu, B.Y.H and Jordan, R.C., "The interrelationship and Characteristic Distribution of Direct, Diffuse and Total Solar Radiation", *Solar Energy 7 (2), 53, 1963.*

30. American Society of Heating, Refrigerating and Air-conditioning Engineers. ASHRAE Standard 93-77: Methods of testing to determine the thermal performance of Solar Collectors. *ASHRAE Inc., New York, USA, 1977.*

31. http// www. Mvs. Ikp.liu.se/staff/karl/phd/node 11,12,13,14 .html.-Kari storck. *The thermodynamic calculation; 1998.*

32. Croft, D.R and Lilley, D.G; "Heat transfer calculations using finite difference equations", *Applied science publishers, London, 1977.*

33. Smith, G.D, "Numerical solution of partial Differential Equations", *Oxford University Press, London. 1965.*

34. Cheremisin off, P, N and Young, R.A: "Pollution Engineering Practice hand book", *Ann Arbor Science, Michigam, 1975.*

35. 1988 ASHRAE HANDBOOK, EQUIPMENT.

36. Robert H.P and Don, W.G; "Perry's Chemical Engineers", *Hand book; 6th ed; McGraw-Hill, 1984.*

37. Air and waste management Association Edited by, Anthony J.buonicore, Wayne T. Davios."Air Pollution Engineering Manual", *Van Nostrand Reinhold, 1992 pg 173-189.*

38. Fox, R.w and Alan, T.McDonald, "Introduction to Fluid Mechanics", *New York, London, 1973.*

39. Ronald K. Mc Laughlin, R. Craig Mc Lean and W.John B," Heating services Design", *Butter worth & co, London, 1981.*

40. Montgomery R.H and Bud nick J, "The solar decision book", *John Wiley $ sons, New York, 1978.*

41. http: // www. Nachhaltgwirts chaften.at / publikationen/ forschungs forum/ 001/teil 2.en.html. 4th May 2004.

42. Yunus A. Cengel, "Heat Transfer": A Practical Approach. Second edition, *McGraw-Hill, New Delhi, 1998.*

43. Kreider J.F and Kreith. F; "Solar heating and cooling ", *Hemisphere publishing corporation, Washington, D.C – 1975.*

44. Gard H.P, Sharma. V.K, Mahajan R.B and Bhargave A.K, "Experimental study of an inexpensive solar Collector Cum Storage system for Agricultural Uses", *Solar Energy Vol. 35, No. 4, pp. 321-331, Pergamon Press, U.S.A, 1985.*

45. Jones W.P; "Air conditioning engineering ", *Edward Arnold publishers, Great Britain, 1967.*

46. Chauliaguet. C, Baratsabal P, and Batellier J.P, "Solar energy in Buildings", *John Wiley & sons, New York, 1977.*

47. Zulovich J.M " Active Solar collectors for farm Buildings", *Agricultural publication GO 1971- Reviewed October 1, 1993, (htt://muextension, Missouri.edu/explore/agguides/agengin/g*1971*.htm)*

48. Module3.2 "Solar air heating",*http://www.Courses.ait.ac.th/*ED06.22*/course 1/lecs/module3/m 32o98.html.5th May 2004.*

49. Baumeister. T; Avallone. E. A; Baumeister 111. T. "Marks' Standard Hand book for Mechanical Engineers", *McGraw-Hill Book company,* New *York.1978.*

50. Kothandaraman, C.P; and Subramanyan, S, "Heat and mass Transfer Data Book, third edition", *Wiley Eastern Limited, New Delhi Bangalore, Bombay, 1975.*

51. Everett, A.A; "Materials", *B.T. Bats ford limited, Great Britain, 1970.*

52. Carrier, W.H; Cherne, R.E; and Grant, W.A; "Modern Air- conditioning, Heating and Ventilating ", *Pitman publishing corporation, U.S.A, 1950.*

53. International Development Research Center, "Solar drying in Africa", *Proceedings of a workshop held in Dakar, Senegal 21-2 4 July 1986, 1987.*

54. Francis de Winter," Heat transfer (loss or Gain) coefficients from bare flat plate solar heat collectors", *3085 carriker lane, Bay D Soquel, California, 2002.*

55. Jansen, T. J; "Solar Engineering technology", *Prentice-Hall Inc; Englewood Cliffs, New Jersey, 1985.*

56. Hodge B.K; "Analysis and Design of Energy Systems", *Prentice- Hall, New Jersey, USA. 1985.*

57. Francis de Winter; "Heat transfer (loss and gain) coefficients from bare flat plate solar heat collectors", *Zomeworks program collections, Mexico, 2002*

58. Holman, J. P; "Heat transfer", 8th Edition, *McGraw-Hill, USA. 1997.*

59. Spirkl, W., Bosanac .M, Brunotte. A, Sizmann. R; "The use of ParameterIdentification for Flat-Plate Collector Testing Under non-Stationary Conditions", *Renewable Energy, Volume 4, Issue 2, March 1994, pages 217- 222.*

SIMPLIFICATION OF DMPM EQUATIONS.

1. TOP GLASS COVER.

$$\rho_g bt_g \frac{dx}{bdx} c_{p_g} \frac{T_t^1 - T_t}{\Delta t} = G_s f_t - h_{ta}(T_t - T_a) - h_{r_{t-a}}(T_t - T_a) + h_{lt}(T_l - T_a) + h_{r_{lt}}(T_l - T_t) - k_g bt_g \frac{dx}{bdx} \frac{T_{t_{x+\Delta x}} - 2T_{t_x} + T_{t_{x-\Delta x}}}{(\Delta x)^2}$$

Or,

$$T_t^1 = T_t + \frac{G_s f_t \Delta t}{\rho_g t_g c_{p_g}} - \frac{h_{ta}\Delta t}{\rho_g t_g c_{p_g}}(T_t - T_a) - \frac{h_{r_{ta}}\Delta t}{\rho_g t_g c_{p_g}}(T_t - T_a) + \frac{h_{lt}\Delta t}{\rho_g t_g c_{p_g}}(T_l - T_t) + \frac{h_{r_{lt}}\Delta t}{\rho_g t_g c_{p_g}}(T_l - T_t) - \frac{k_g \Delta t}{\rho_g c_{p_g}(\Delta x)^2}\left(T_{t_{x+\Delta x}} - 2T_{t_x} + T_{t_{x-\Delta x}}\right)$$

On using;

$$h_{ta} + h_{r_{ta}} = h_a$$

$$h_{lt} + h_{r_{lt}} = h_t$$

$$\frac{1}{\rho_g t_g c_{p_g}} = A$$

$$\frac{k_g}{\rho_g c_{p_g}(\Delta x)^2} = B$$

We get,

$$T_t^1 = T_t + A\Delta t G_s f_t - A\Delta t h_a (T_t - T_a) + A\Delta t h_t (T_l - T_t) - B\Delta t\left(T_{t_{x+\Delta x}} - 2T_{t_x} + T_{t_{x-\Delta x}}\right)$$

Expanding;

$$T_t^1 = T_t + A\Delta t[G_s f_t + h_a T_a + h_t T_l - C_3 T_t] - B\Delta t\left(T_{t_{x+\Delta x}} - 2T_{t_x} + T_{t_{x-\Delta x}}\right) \qquad (1.1)$$

Where,

$$C_3 = h_t + h_a$$

2. FIRST GLASS COVER.

$$\rho_g bt_g c_{p_g} \frac{dx}{bdx} \frac{T_1^1 - T_1}{\Delta t} = G_s f_1 - h_{1t}(T_1 - T_t) - h_{s_{1t}}(T_1 - T_t) - h_{f_{1-1}}(T_1 - T_{fm_1}) + h_{r_{ab-1}}(T_{ab} - T_1) - k_g bt_g \frac{dx}{bdx}\left(\frac{T_{1_{x+\Delta x}} - 2T_{1_x} + T_{1_{x-\Delta x}}}{(\Delta x)^2}\right)$$

Or,

$$T_1^1 = T_1 + \frac{G_s f_1 \Delta t}{\rho_g t_g c_{p_g}} - \frac{h_{1t}\Delta t}{\rho_g t_g c_{p_g}}(T_1 - T_t) - \frac{h_{s_{1t}}\Delta t}{\rho_g t_g c_{p_g}}(T_t - T_t) - \frac{h_{f_{1-1}}\Delta t}{\rho_g t_g c_{p_g}}(T_1 - T_{fm_1}) + \frac{h_{r_{ab-1}}\Delta t}{\rho_g t_g c_{p_g}}(T_{ab} - T_1) - \frac{k_g \Delta t}{\rho_g c_{p_g}(\Delta x)^2}(T_{1_{x+\Delta x}} - 2T_{1_x} + T_{1_{x-\Delta x}})$$

On using the already defined constants (A and B).

$$T_1^1 = T_1 + AG_s f_1 \Delta t + Ah_{r_{ab-1}}\Delta t(T_{ab} - T_1) - Ah_t \Delta t(T_1 - T_t) - Ah_{f_{1-1}}\Delta t(T_1 - T_{fm_1}) - B\Delta t(T_{1_{x+\Delta x}} - 2T_{1_x} + T_{1_{x-\Delta x}})$$

Where, $h_{1t} + h_{s_{1t}} = h_t$

Hence,

$$T_1^1 = T_1 + A\Delta t[G_s f_1 + h_{r_{ab-1}} T_{ab} + h_t T_t + h_{f_{1-1}} T_{fm_1} - D_2 T_1] - B\Delta t(T_{1_{x+\Delta x}} - 2T_{1_x} + T_{1_{x-\Delta x}}) \quad (1.2)$$

Where, $D_2 = h_{r_{ab-1}} + h_{f_{1-1}} + h_t$.

3. FLOWING FLUID IN THE FIRST FLOW CHANNEL.

$$\rho_{f_1} bt_{f_1} c_{p_f} \frac{dx}{bdx} \frac{T_{f_1}^1 - T_{f_1}}{\Delta t} = h_{f_{1-1}}(T_1 - T_{fm_1}) + h_{f_{1-ab}}(T_{ab} - T_{fm_1}) - \frac{m}{bdx} c_{pf} \frac{\partial T_{f_1}}{\partial x} dx$$

Rewriting,

$$T_{f_1}^1 = T_{f_1} + \frac{h_{f_{1-1}}\Delta t}{\rho_{f_1} t_{f_1} c_{p_f}}(T_1 - T_{fm_1}) + \frac{h_{f_{1-ab}}\Delta t}{\rho_{f_1} t_{f_1} c_{p_f}}(T_{ab} - T_{fm_1}) - \frac{m\Delta t}{\rho_{f_1} t_{f_1} b} \frac{T_{f_{1_{x+\Delta x}}} - T_{f_{1_x}}}{\Delta x}$$

On using,

$$\frac{1}{\rho_{f_1} t_{f_1} c_{p_{f_1}}} = H_3$$

$$\frac{\dot{m}}{\rho_{f_1} t_{f_1} b\Delta x} = J_3$$

$$T'_{f_1} = T_{f_1} + H_3 h_{f_{1-1}} \Delta t\left(T_1 - T_{fm_1}\right) + H_3 h_{f_{1-ab}} \Delta t\left(T_{ab} - T_{fm_1}\right) - J_3 \Delta t\left(T_{f_{1_{x+\Delta x}}} - T_{f_{1_x}}\right)$$

Or,

$$T'_{f_1} = T_{f_1} + H_3 \Delta t\left(h_{f_{1-1}} T_1 + h_{f_{1-ab}} T_{ab} - K_3 T_{fm_1}\right) - J_3 \Delta t\left(T_{f_{1_{x+\Delta x}}} - T_{f_{1_x}}\right) \qquad (1.3)$$

Where,

$$h_{f_{1-1}} + h_{f_{1-ab}} = K_3$$

4. ABSORBER PLATE.

$$\rho_{ab} b t_{ab} c_{p_{ab}} \frac{dx}{bdx} \frac{T'_{ab} - T_{ab}}{\Delta t} = G_s f_{ab} - h_{f_{1-ab}}\left(T_{ab} - T_{fm_1}\right) - h_{f_{2-ab}}\left(T_{ab} - T_{fm_2}\right) - h_{r_{ab-bp}}\left(T_{ab} - T_{bp}\right)$$
$$- h_{r_{ab-1}}\left(T_{ab} - T_1\right) - k_{ab} b t_{ab} \frac{dx}{bdx}\left(\frac{T_{ab_{x+\Delta x}} - 2T_{ab_x} + T_{ab_{x-\Delta x}}}{(\Delta x)^2}\right)$$

Or,

$$T'_{ab} = T_{ab} + \frac{G_s f_{ab} \Delta t}{\rho_{ab} t_{ab} c_{p_{ab}}} - \frac{h_{f_{1-ab}} \Delta t}{\rho_{ab} t_{ab} c_{p_{ab}}}\left(T_{ab} - T_{fm_1}\right) - \frac{h_{f_{2-ab}} \Delta t}{\rho_{ab} t_{ab} c_{p_{ab}}}\left(T_{ab} - T_{fm_2}\right) - \frac{h_{r_{ab-1}} \Delta t}{\rho_{ab} t_{ab} c_{p_{ab}}}\left(T_{ab} - T_1\right)$$
$$- \frac{h_{r_{ab-bp}} \Delta t}{\rho_{ab} t_{ab} c_{p_{ab}}}\left(T_{ab} - T_{bp}\right) - \frac{k_{ab} \Delta t}{\rho_{ab} c_{p_{ab}} (\Delta x)^2}\left(T_{ab_{x+\Delta x}} - 2T_{ab_x} + T_{ab_{x-\Delta x}}\right)$$

On using;

$$\frac{1}{\rho_{ab} t_{ab} c_{p_{ab}}} = E$$

$$\frac{k_{ab}}{\rho_{ab} c_{p_{ab}} (\Delta x)^2} = F$$

$$h_{f_{ab-bp}} = h_{ab}$$

$$h_{f_{2-ab}} = h_{f_2}$$

$$T'_{ab} = T_{ab} + EG_3 f_{ab}\Delta t - Eh_{f_{1-ab}}\Delta t(T_{ab} - T_{fm_1}) - Eh_{f_2}\Delta t(T_{ab} - T_{fm_2}) - Eh_{c_{ab-1}}\Delta t(T_{ab} - T_1)$$
$$- Eh_{ab}\Delta t(T_{ab} - T_{bp}) - F\Delta t\left(T_{ab_{x+\Delta x}} - 2T_{ab_x} + T_{ab_{x-\Delta x}}\right)$$

Or,

$$T'_{ab} = T_{ab} + E\Delta t[G_3 f_{ab} + h_{f_{1-ab}} T_{fm_1} + h_{f_2} T_{fm_2} + h_{c_{ab-1}} T_1 + h_{ab} T_{bp} - G_3 T_{ab}]$$
$$- F\Delta t\left(T_{ab_{x+\Delta x}} - 2T_{ab_x} + T_{ab_{x-\Delta x}}\right) \qquad (1.4)$$

Where,

$$G_3 = h_{f_{1-ab}} + h_{f_2} + h_{ab}$$

5. FLOWING FLUID IN THE SECOND FLOW CHANNEL.

$$\rho_{f_2} t_{f_2} bc_{p_f} \frac{dx}{bdx} \frac{T'_{f_2} - T_{f_2}}{\Delta t} = h_{f_{2-ab}}(T_{ab} - T_{fm_2}) + h_{f_{2-bp}}(T_{bp} - T_{fm_2}) - \dot{m} c_{p_f} \frac{dx}{bdx} \frac{T_{f_{2_{x+\Delta x}}} - T_{f_{2_x}}}{\Delta x}$$

Rewritten as,

$$T'_{f_2} = T_{f_2} + \frac{h_{f_{2-ab}}\Delta t}{\rho_{f_2} t_{f_2} c_{p_f}}(T_{ab} - T_{fm_2}) + \frac{h_{f_{2-bp}}\Delta t}{\rho_{f_2} t_{f_2} c_{p_f}}(T_{bp} - T_{fm_2}) - \frac{\dot{m}\Delta t}{\rho_{f_2} t_{f_2} b\Delta x}(T_{f_{2_{x+\Delta x}}} - T_{f_{2_x}})$$

Letting;

$$\frac{1}{\rho_{f_2} t_{f_2} c_{p_{f_2}}} = H_4$$

$$\frac{\dot{m}}{\rho_{f_2} t_{f_2} b\Delta x} = J_4$$

$$T'_{f_2} = T_{f_2} + H_4 h_{f_2} \Delta t(T_{ab} - T_{fm_2}) + H_4 h_{f_b} \Delta t(T_{bp} - T_{fm_2}) - J_4 \Delta t(T_{f_{2_{x+\Delta x}}} - T_{f_{2_x}})$$

Where, $h_{f_2} = h_{f_{2\text{-}ab}}$ and $h_{f_b} = h_{f_{2\text{-}bp}}$.

On factoring common terms, we get;

$$T'_{f_2} = T_{f_2} + H_4 \Delta t[h_{f_2} T_{ab} + h_{f_b} T_{bp} - K_4 T_{fm_2}] - J_4 \Delta t(T_{f_{2_{x+\Delta x}}} - T_{f_{2_x}}) \qquad (1.5)$$

Where,

$$K_4 = h_{f_2} + h_{f_b}.$$

6. BACK PLATE.

$$\rho_{bp} b t_{bp} c_{p_{bp}} \frac{dx}{bdx} \frac{T'_{bp} - T_{bp}}{\Delta t} = h_{f_{ab\text{-}bp}}(T_{ab} - T_{bp}) - h_{f_{2\text{-}bp}}(T_{bp} - T_{fm_2}) - U_L(T_{bp} - T_{ins}) - k_{bp} b t_{bp} \frac{dx}{bdx} \frac{T_{bp_{x+\Delta x}} - 2T_{bp_x} + T_{bp_{x-\Delta x}}}{(\Delta x)^2}$$

Or,

$$T'_{bp} = T_{bp} + \frac{h_{ab}\Delta t}{\rho_{bp} t_{bp} c_{p_{bp}}}(T_{ab} - T_{bp}) - \frac{h_{f_b}\Delta t}{\rho_{bp} t_{bp} c_{p_{bp}}}(T_{bp} - T_{fm_2}) - \frac{U_L \Delta t}{\rho_{bp} t_{bp} c_{p_{bp}}}(T_{bp} - T_{ins}) - \frac{k_{bp}\Delta t}{\rho_{bp} c_{p_{bp}} (\Delta x)^2}(T_{bp_{x+\Delta x}} - 2T_{bp_x} + T_{bp_{x-\Delta x}})$$

Where, $h_{ab} = h_{f_{ab\text{-}bp}}$ and $h_{f_b} = h_{f_{2\text{-}bp}}$

On using,

$$\frac{1}{\rho_{bp} t_{bp} c_{p_{bp}}} = L$$

$$\frac{k_{bp}}{\rho_{bp} c_{p_{bp}} (\Delta x)^2} = M$$

$$T'_{bp} = T_{bp} + Lh_{ab}\Delta t(T_{ab} - T_{bp}) - Lh_{f_b}\Delta t(T_{bp} - T_{fm_2}) - LU_L \Delta t(T_{bp} - T_{ins}) - M\Delta t(T_{ab_{x+\Delta x}} - 2T_{bp_x} + T_{bp_{x-\Delta x}})$$

Expanding,

$$T_{bp}^{1} = T_{bp} + L\Delta t(h_{ab}T_{ab} + h_{f_b}T_{fm_2} - N_2T_{bp}) - LU_L\Delta t(T_{bp} - T_{ins}) - M\Delta t(T_{ab_{x+\Delta x}} - 2T_{bp_x} + T_{bp_{x-\Delta x}}) \quad (1.6)$$

Where, $N_2 = h_{ab} + h_{f_b}$

7. INSULATION.

$$\rho_{ins}bt_{ins}c_{p_{ins}}\frac{dx}{bdx}\frac{T_{ins}^{1} - T_{ins}}{\Delta t} = U_L\left(T_{bp} - T_{ins}\right) - h_{ins\text{-}a}(T_{ins} - T_a) - h_{r_{ins\text{-}e}}(T_{ins} - T_a) - k_{ins}bt_{ins}\frac{dx}{bdx}\left(\frac{T_{ins_{x+\Delta x}} - 2T_{ins_x} + T_{ins}}{(\Delta x)^2}\right)$$

Rewriting,

$$T_{ins}^{1} = T_{ins} + \frac{U_L\Delta t}{\rho_{ins}t_{ins}c_{p_{ins}}}(T_{bp} - T_{ins}) - \frac{h_{ins}\Delta t}{\rho_{ins}t_{ins}c_{p_{ins}}}(T_{ins} - T_a) - \frac{k_{ins}\Delta t}{\rho_{ins}c_{p_{ins}}(\Delta x)^2}\left(T_{ins_{x+\Delta x}} - 2T_{ins_x} + T_{ins_{x-\Delta x}}\right)$$

Where, $h_{ins} = h_{ins\text{-}e} + h_{r_{ins\text{-}e}}$

On using,

$$\frac{1}{\rho_{ins}t_{ins}c_{p_{ins}}} = P \text{ and } \frac{k_{ins}}{\rho_{ins}c_{p_{ins}}(\Delta x)^2} = Q, \text{ the equation reduces to;}$$

$$T_{ins}^{1} = T_{ins} + PU_L\Delta t(T_{bp} - T_{ins}) - Ph_{ins}\Delta t(T_{ins} - T_a) - Q\Delta t\left(T_{ins_{x+\Delta x}} - 2T_{ins_x} + T_{ins_{x-\Delta x}}\right) \quad (1.7)$$

Equations (1.1to 1.7) were used to predict the future temperatures of the collector components and the flowing fluid.

APPENDIX 2

SIMPLIFICATION OF TPM EQUATIONS

1. TOP GLASS COVER.

$$\rho_t t_t b \frac{dx}{bdx} c_{p_g} \frac{dT_t}{dt} = G_s f_t + h_{r_{t-l}}(T_l - T_t) - h_{r_{t-a}}(T_t - T_a) - h_{t-a}(T_t - T_a)$$
$$- h_{f_{t-f}}(T_l - T_{fm_l}) - k_g t_g b \frac{dx}{bdx} \frac{T_{t_{x+\Delta x}} - 2T_{t_x} + T_{t_{x-\Delta x}}}{(\Delta x)^2}$$

Or,

$$T_t^1 = T_t + \frac{G_s f_t \Delta t}{\rho_g t_g c_{p_g}} + \frac{h_{r_{t-l}} \Delta t}{\rho_g t_g c_{p_g}}(T_l - T_t) - \frac{h_{r_{t-a}} \Delta t}{\rho_g t_g c_{p_g}}(T_t - T_a) - \frac{h_{t-a} \Delta t}{\rho_g t_g c_{p_g}}(T_t - T_a)$$
$$- \frac{h_{f_{t-f}} \Delta t}{\rho_g t_g c_{p_g}}(T_l - T_{fm_l}) - \frac{k_g \Delta t}{\rho_g c_{p_g} (\Delta x)^2}(T_{t_{x+\Delta x}} - 2T_{t_x} + T_{t_{x-\Delta x}})$$

On using,

$$\frac{1}{\rho_g t_g c_{p_g}} = A$$

$$\frac{k_g}{\rho_g c_{p_g} (\Delta x)^2} = B$$

$$h_{t-a} + h_{r_{t-a}} = h_a$$

$$T_t^1 = T_t + A\Delta t G_s f_t + A\Delta t h_{r_{t-l}}(T_l - T_t) - A\Delta t h_a (T_t - T_a) - A\Delta t h_{f_{t-f}}(T_l - T_{fm_l})$$
$$- B\Delta t(T_{t_{x+\Delta x}} - 2T_{t_x} + T_{t_{x-\Delta x}})$$

Or,

$$T_t^1 = T_t + A\Delta t[G_s f_t + h_{r_{t-l}} T_l + h_a T_a + h_{f_{t-f}} T_{fm_l} - C_4 T_t]$$
$$- B\Delta t(T_{t_{x+\Delta x}} - 2T_{t_x} + T_{t_{x-\Delta x}}) \qquad (2.1)$$

Where, $C_4 = h_{r_{t-l}} + h_a + h_{f_{t-f}}$

2. FLOWING FLUID IN THE FIRST FLOW CHANNEL.

$$\rho_{f_1} bt_{f_1} \frac{dx}{bdx} c_{p_f} \frac{T_{f_1}^1 - T_{f_1}}{\Delta t} = h_{f_{1-4}}(T_t - T_{fm_1}) + h_{f_{1-1}}(T_1 - T_{fm_1}) \dot{m} c_{p_f} \frac{dx}{bdx}\left(\frac{T_{f_{1_{x+\Delta x}}} - T_{f_{1_x}}}{\Delta x}\right)$$

Or,

$$T_{f_1}^1 = T_{f_1} + \frac{h_{f_{1-4}} \Delta t}{\rho_{f_1} t_{f_1} c_{p_{f_1}}}(T_t - T_{fm_1}) + \frac{h_{f_{1-1}} \Delta t}{\rho_{f_1} t_{f_1} c_{p_{f_1}}}(T_1 - T_{fm_1}) - \frac{\dot{m} \Delta t}{\rho_{f_1} t_{f_1} b \Delta x}\left(T_{f_{1_{x+\Delta x}}} - T_{f_{1_x}}\right)$$

On using,

$$\frac{1}{\rho_{f_1} t_{f_1} c_{p_f}} = H_4$$

$$\frac{\dot{m}}{\rho_{f_1} t_{f_1} b \Delta x} = J_4$$

$$T_{f_1}^1 = T_{f_1} + H_4 \Delta t h_{f_{1-4}}(T_t - T_{fm_1}) + H_4 \Delta t h_{f_{1-1}}(T_1 - T_{fm_1}) - J_4 \Delta t\left(T_{f_{1_{x+\Delta x}}} - T_{f_{1_x}}\right)$$

Or,

$$T_{f_1}^1 = T_{f_1} + H_4 \Delta t[h_{f_{1-4}} T_t + h_{f_{1-1}} T_1 - K_4 T_{fm_1}] - J_4 \Delta t\left(T_{f_{1_{x+\Delta x}}} - T_{f_{1_x}}\right) \quad (2.2)$$

Where,

$$K_4 = h_{f_{1-4}} + h_{f_{1-1}}$$

3. FIRST GLASS COVER.

$$\rho_g t_g b \frac{dx}{bdx} c_{p_g} \frac{T_t^1 - T_t}{\Delta t} = G_s f_1 + h_{r_{ab-1}}(T_{ab} - T_1) - h_{f_{1-1}}(T_1 - T_{fm_1}) - h_{f_{2-1}}(T_1 - T_{fm_2})$$
$$- h_{f_{1-4}}(T_1 - T_t) - k_g t_g b \frac{dx}{bdx} \frac{\left(T_{1_{x+\Delta x}} - 2T_{1_x} + T_{1_{x-\Delta x}}\right)}{(\Delta x)^2}$$

On using the constants A and B as defined earlier,

$$T_t^1 = T_t + A\Delta t G_s f_1 + A\Delta t h_{r_{ab-1}}(T_{ab} - T_1) - A\Delta t h_{f_{1-1}}(T_1 - T_{fm_1}) - A\Delta t h_{f_{2-1}}(T_1 - T_{fm_2})$$
$$- A\Delta t h_{r_{t-1}}(T_1 - T_t) - B\Delta t\left(T_{1_{x+\Delta x}} - 2T_{1_x} + T_{1_{x-\Delta x}}\right)$$

Or,

$$T_t^1 = T_t + A\Delta t[G_s f_1 + h_{r_{ab-1}} T_{ab} + h_{f_{1-1}} T_{fm_1} + h_{f_{2-1}} T_{fm_2} + h_{r_{t-1}} T_t - D_4 T_1]$$
$$- B\Delta t\left(T_{1_{x+\Delta x}} - 2T_{1_x} + T_{1_{x-\Delta x}}\right) \qquad (2.3)$$

Where,

$$D_4 = h_{r_{ab-1}} + h_{f_{1-1}} + h_{f_{2-1}} + h_{r_{t-1}}$$

4. FLOWING FLUID IN THE SECOND FLOW CHANNEL.

$$\rho_{f_2} t_{f_2} b \frac{dx}{bdx} c_{p_f} \frac{T_{f_2}^1 - T_{f_2}}{\Delta t} = h_{f_{2-1}}\left(T_1 - T_{fm_2}\right) + h_{f_{2-ab}}\left(T_{ab} - T_{fm_2}\right) - \dot{m} c_{p_f} \frac{dx}{bdx} \frac{T_{f_{2_{x+\Delta x}}} - T_{f_{2_x}}}{\Delta x}$$

Rearranging we get,

$$T_{f_2}^1 = T_{f_2} + \frac{h_{f_{2-1}} \Delta t}{\rho_{f_2} t_{f_2} c_{p_f}}\left(T_1 - T_{fm_2}\right) + \frac{h_{f_{2-ab}} \Delta t}{\rho_{f_2} t_{f_2} c_{p_f}}\left(T_{ab} - T_{fm_2}\right) - \frac{\dot{m} \Delta t}{\rho_{f_2} t_{f_2} b \Delta x}\left(T_{f_{2_{x+\Delta x}}} - T_{f_{2_x}}\right)$$

Letting;

$$\frac{1}{\rho_{f_2} t_{f_2} c_{p_f}} = H_5$$

$$\frac{\dot{m}}{\rho_{f_2} t_{f_2} b \Delta x} = J_5$$

We get,

$$T_{f_2}^1 = T_{f_2} + H_5 h_{f_{2-1}} \Delta t\left(T_1 - T_{fm_2}\right) + H_5 h_{f_{2-ab}} \Delta t\left(T_{ab} - T_{fm_2}\right) - J_5 \Delta t\left(T_{f_{2_{x+\Delta x}}} - T_{f_{2_x}}\right)$$

Or,

$$T_{f_2}^1 = T_{f_2} + H_5 \Delta t[h_{f_{2-1}} T_1 + h_{f_{2-ab}} T_{ab} - K_5 T_{fm_2}] - J_5 \Delta t\left(T_{f_{2_{x+\Delta x}}} - T_{f_{2_x}}\right) \qquad (2.4)$$

Where, $K_5 = h_{f_{2-1}} + h_{f_{2-ab}}$

5. ABSORBER PLATE.

$$\rho_{ab} t_{ab} b \frac{dx}{bdx} c_{p_{ab}} \frac{T'_{ab} - T_{ab}}{\Delta t} = G_s f_{ab} - h_{f_{2\text{-}ab}}(T_{ab} - T_{fm_2}) - h_{f_{3\text{-}ab}}(T_{ab} - T_{fm_3}) - h_{r_{1\text{-}ab}}(T_{ab} - T_1)$$
$$- h_{r_{bp\text{-}ab}}(T_{ab} - T_{bp}) - k_{ab} t_{ab} b \frac{dx}{bdx} \frac{(T_{ab_{x+\Delta x}} - 2T_{ab_x} + T_{ab_{x-\Delta x}})}{(\Delta x)^2}$$

On rearranging;

$$T'_{ab} = T_{ab} + \frac{G_s f_{ab} \Delta t}{\rho_{ab} t_{ab} c_{p_{ab}}} - \frac{h_{f_{2\text{-}ab}} \Delta t}{\rho_{ab} t_{ab} c_{p_{ab}}}(T_{ab} - T_{fm_2}) - \frac{h_{f_{3\text{-}ab}} \Delta t}{\rho_{ab} t_{ab} c_{p_{ab}}}(T_{ab} - T_{fm_3}) - \frac{h_{r_{1\text{-}ab}} \Delta t}{\rho_{ab} t_{ab} c_{p_{ab}}}(T_{ab} - T_1)$$
$$- \frac{h_{r_{bp\text{-}ab}} \Delta t}{\rho_{ab} t_{ab} c_{p_{ab}}}(T_{ab} - T_{bp}) - \frac{k_{ab} \Delta t}{\rho_{ab} c_{p_{ab}} (\Delta x)^2}(T_{ab_{x+\Delta x}} - 2T_{ab_x} + T_{ab_{x-\Delta x}})$$

On using the earlier definitions of E and F we have,

$$T'_{ab} = T_{ab} + E\Delta t G_s f_{ab} - E\Delta t h_{f_{2\text{-}ab}}(T_{ab} - T_{fm_2}) - E\Delta t h_{f_{3\text{-}ab}}(T_{ab} - T_{fm_3}) - E\Delta t h_{r_{1\text{-}ab}}(T_{ab} - T_1)$$
$$- E\Delta t h_{r_{bp\text{-}ab}}(T_{ab} - T_{bp}) - F\Delta t(T_{ab_{x+\Delta x}} - 2T_{ab_x} + T_{ab_{x-\Delta x}})$$

Or,

$$T'_{ab} = T_{ab} + E\Delta t[G_s f_{ab} + h_{f_{2\text{-}ab}} T_{fm_2} + h_{f_{3\text{-}ab}} T_{fm_3} + h_{r_{ab\text{-}1}} T_1 + h_{r_{bp\text{-}ab}} T_{bp} - G_4 T_{ab}]$$
$$- F\Delta t\left(T_{ab_{x+\Delta x}} - 2T_{ab_x} + T_{ab_{x-\Delta x}}\right) \qquad (2.5)$$

where,

$$G_4 = h_{f_{2\text{-}ab}} + h_{f_{3\text{-}ab}} + h_{r_{ab\text{-}1}} + h_{r_{bp\text{-}ab}}$$

6. FLOWING FLUID IN THE THIRD FLOW CHANNEL.

$$\rho_{f_3} t_{f_3} b \frac{dx}{bdx} c_{p_{f_3}} \frac{T'_{f_3} - T_{f_3}}{\Delta t} = h_{f_{3\text{-}ab}}(T_{ab} - T_{fm_3}) + h_{f_{3\text{-}bp}}(T_{bp} - T_{fm_3}) - \dot{m} c_{p_{f_3}} \frac{dx}{bdx} \frac{T_{f_{3_{x+\Delta x}}} - T_{f_{3_x}}}{\Delta x}$$

Or,

$$T_{f_3}^1 = T_{f_3} + \frac{h_{f_{3\text{-}ab}}\Delta t}{\rho_{f_3} t_{f_3} c_{p_f}}(T_{ab} - T_{fm_3}) + \frac{h_{f_{3\text{-}bp}}\Delta t}{\rho_{f_3} t_{f_3} c_{p_f}}(T_{bp} - T_{fm_3}) - \frac{m\Delta t}{\rho_{f_3} t_{f_3} b\Delta x}(T_{f_{3_{x+\Delta x}}} - T_{f_{3_x}})$$

On using;

$$\frac{1}{\rho_{f_3} t_{f_3} c_{p_f}} = H_6$$

$$\frac{m}{\rho_{f_3} t_{f_3} b\Delta x} = J_6$$

$$T_{f_3}^1 = T_{f_3} + H_6 h_{f_{3\text{-}ab}}\Delta t(T_{ab} - T_{fm_3}) + H_6 h_{f_{3\text{-}bp}}\Delta t(T_{bp} - T_{fm_3}) - J_6\Delta t(T_{f_{3_{x+\Delta x}}} - T_{f_{3_x}})$$

Or in simpler form,

$$T_{f_3}^1 = T_{f_3} + H_6\Delta t[h_{f_{3\text{-}ab}} T_{ab} + h_{f_{3\text{-}bp}} T_{bp} - K_6 T_{fm_3}] - J_6\Delta t(T_{f_{3_{x+\Delta x}}} - T_{f_{3_x}}) \qquad (4.6)$$

Where,

$$K_6 = h_{f_{3\text{-}ab}} + h_{f_{3\text{-}bp}}$$

7. BACK PLATE.

$$\rho_{bp} t_{bp} b\frac{dx}{bdx} c_{p_{bp}} \frac{T_{bp}^1 - T_{bp}}{\Delta t} = h_{_{bp\text{-}ab}}(T_{ab} - T_{bp}) - h_{f_{3\text{-}bp}}(T_{bp} - T_{fm_3}) - U_L(T_{bp} - T_{ins}) - k_{bp} t_{bp} b\frac{dx}{bdx}\frac{(T_{bp_{x+\Delta x}} - T_{bp_x} + T_{bp_{x-\Delta x}})}{(\Delta x)^2}$$

Or,

$$T_{bp}^1 = T_{bp} + \frac{h_{_{bp\text{-}ab}}\Delta t}{\rho_{bp} t_{bp} c_{p_{bp}}}(T_{ab} - T_{bp}) - \frac{h_{f_{3\text{-}bp}}\Delta t}{\rho_{bp} t_{bp} c_{p_{bp}}}(T_{bp} - T_{fm_3}) - \frac{U_L\Delta t}{\rho_{bp} t_{bp} c_{p_{bp}}}(T_{bp} - T_{ins}) - \frac{k_{bp}\Delta t}{\rho_{bp} c_{p_{bp}}(\Delta x)^2}(T_{bp_{x+\Delta x}} - 2T_{bp_x} + T_{bp_{x-\Delta x}})$$

On using,

$$\frac{1}{\rho_{bp} t_{bp} c_{p_{bp}}} = L$$

$$\frac{k_{bp}}{\rho_{bp} c_{p_{bp}} (\Delta x)^2} = M$$

$$T^1_{bp} = T_{bp} + Lh_{f_{bp-ab}} \Delta t(T_{ab} - T_{bp}) - Lh_{f_{3-bp}} \Delta t(T_{bp} - T_{fm_3}) - LU_L \Delta t(T_{bp} - T_{ins}) - M\Delta t(T_{bp_{x+\Delta x}} - 2T_{bp_x} + T_{bp_{x-\Delta x}})$$

$$T^1_{bp} = T_{bp} + L\Delta t[h_{f_{bp-ab}} T_{ab} + h_{f_{3-bp}} T_{fm_3} - N_3 T_{bp}] - LU_L \Delta t(T_{bp} - T_{ins}) - M\Delta t(T_{bp_{x+\Delta x}} - 2T_{bp_x} + T_{bp_{x-\Delta x}}) \quad (2.7)$$

Where, $N_3 = h_{f_{bp-ab}} + h_{f_{3-bp}}$

8. INSULATION.

$$\rho_{ins} t_{ins} b \frac{dx}{bdx} c_{p_{ins}} \frac{T^1_{ins} - T_{ins}}{\Delta t} = U_L(T_{bp} - T_{ins}) - h_{ins-a}(T_{ins} - T_a) - h_{r_{ins-a}}(T_{ins} - T_a) - k_{ins} t_{ins} b \frac{dx}{bdx} \frac{(T_{ins_{x+\Delta x}} - 2T_{ins_x} + T_{ins_{x-\Delta x}})}{(\Delta x)^2}$$

Or,

$$T^1_{ins} = T_{ins} + \frac{U_L \Delta t}{\rho_{ins} t_{ins} c_{p_{ins}}}(T_{bp} - T_{ins}) - \frac{h_{ins} \Delta t}{\rho_{ins} t_{ins} c_{p_{ins}}}(T_{ins} - T_a) - \frac{k_{ins} \Delta t}{\rho_{ins} c_{p_{ins}} (\Delta x)_2}(T_{ins_{x+\Delta x}} - 2T_{ins_x} + T_{ins_{x-\Delta x}})$$

On using,

$$\frac{1}{\rho_{ins} t_{ins} c_{p_{ins}}} = P$$

$$\frac{k_{ins}}{\rho_{ins} c_{p_{ins}} (\Delta x)^2} = Q$$

$$T^{t}_{ins} = T_{ins} + PU_L\Delta t(T_{bp} - T_{ins}) - Ph_{ins}\Delta t(T_{ins} - T_a) - Q\Delta t\left(T_{ins_{x+\Delta x}} - 2T_{ins_x} + T_{ins_{x-\Delta x}}\right) \quad (2.8)$$

Equations (2.1 to 2.8) were used to predict the future temperatures of the collector components and the flowing air.

APPENDIX 3

SOLAR INSOLATIONS AND WIND VELOCITIES

Table 3.1: DTPM Solar Insolations and Wind Velocities.(17/02/2005, day of the year: 48)

TIME	SOLAR INSOLATION (W/m^2)	WIND VELOCITY (m/s)	AMBIENT TEMPERATURE (^0C)
11:20:14	644.4	0.525	28.00
11:22:14	738.9	0.558	27.78
11:24:14	711.1	0.500	29.90
11:26:14	716.7	1.125	30.26
11:28:14	772.2	0.975	31.73
11:30:14	744.4	0.525	29.01
11:32:14	666.7	0.600	28.82
11:34:14	627.8	0.833	29.72
11:36:14	861.1	0.517	29.95
11:38:14	694.4	0.658	28.35
11:40:14	761.1	0.317	30.12
11:42:14	827.8	0.458	30.02
11:44:14	677.8	1.133	28.42
11:46:14	616.7	0.808	28.72
11:48:14	772.2	0.625	31.68
11:50:14	816.7	0.542	30.96
11:52:14	855.6	0.758	31.87
11:54:14	866.7	0.575	31.96
11:56:14	922.2	1.200	30.57
11:58:14	866.7	1.442	30.73

12:00:14	933.3	1.217	30.71
12:02:14	927.8	1.225	30.53
12:04:14	922.2	1.267	29.90
12:06:14	905.6	0.917	29.45
12:08:14	861.1	0.600	28.82
12:10:14	844.4	0.383	31.68
12:12:14	886.1	0.817	31.56
12:14:14	886.1	1.283	29.14
12:16:14	916.7	1.583	29.18
12:18:14	911.1	0.775	27.96
12:20:14	861.1	0.425	31.85
12:22:14	833.3	0.708	31.20
12:24:14	811.1	0.675	27.37
12:26:14	811.1	0.525	27.10
12:28:14	833.3	0.350	31.08
12:30:14	833.3	0.867	29.97
12:32:14	855.6	0.633	29.72
12:34:14	872.2	0.450	31.10
12:36:14	827.8	0.408	27.29
12:38:14	877.8	0.600	31.54
12:40:14	905.6	0.300	28.20
12:42:14	872.2	0.908	28.13
12:44:14	827.8	0.533	30.40
12:46:14	827.8	0.733	32.26
12:48:14	816.7	1.583	31.39
12:50:14	838.9	1.492	32.10
12:52:14	872.2	0.742	31.06
12:54:14	861.1	1.258	32.60
12:56:14	911.1	0.850	31.98
12:58:14	883.3	0.550	32.14

13:00:14	877.8	1.100	32.67
13:02:14	888.9	1.358	31.91
13:04:14	883.3	0.867	32.25
13:06:14	794.4	1.042	30.26
13:08:14	733.3	1.108	32.07
13:10:14	744.4	0.967	32.00
13:12:14	788.9	0.817	32.02
13:14:14	738.9	0.492	31.75
13:16:14	672.2	0.492	32.50
13:18:14	783.3	0.308	32.36
13:20:14	805.6	0.508	31.31
13:22:14	738.9	0.658	31.49
13:24:14	872.2	1.208	31.83
13:26:14	911.1	1.300	32.93
13:28:14	877.8	1.092	32.60
13:30:14	872.2	1.092	30.26
13:32:14	794.4	0.700	29.75
13:34:14	772.2	0.716	32.07
13:36:14	855.6	0.875	31.67
13:38:14	844.4	0.983	32.00
13:40:14	888.9	1.125	31.34
13:42:14	844.4	1.308	31.69
13:44:14	838.9	0.700	32.89
13:46:14	827.8	0.833	31.28
13:48:14	805.6	0.583	32.14
13:50:14	755.6	0.333	32.69
13:52:14	794.4	0.546	30.45
13:54:14	744.4	0.450	30.07
13:56:14	777.8	0.416	31.25
13:58:14	794.4	0.475	31.13

14:00:14	788.9	0.525	31.32
14:02:14	816.7	0.775	31.87
14:04:14	827.8	0.850	31.53
14:06:14	855.6	0.825	30.22
14:08:14	916.7	0.778	30.81
14:10:14	894.4	0.583	30.24
14:12:14	822.2	1.200	32.28
14:14:14	766.7	0.625	30.91
14:16:14	722.2	0.708	30.80
14:18:14	816.7	0.708	31.00
14:20:14	838.9	0.400	32.26
14:22:14	822.2	0.425	30.21
14:24:14	722.2	0.842	30.74
14:26:14	755.6	0.525	29.63
14:28:14	722.2	0.592	29.60
14:30:14	750.0	0.433	29.48
14:32:14	738.9	0.433	30.49
14:34:14	744.4	0.683	30.20
14:36:14	766.7	0.867	30.38
14:38:14	816.7	0.716	30.51
14:40:14	794.4	1.100	31.66
14:42:14	750.0	1.283	30.26
14:44:14	727.8	0.567	31.32
14:46:14	727.8	0.733	32.39
14:48:14	716.7	1.083	32.49
14:50:14	672.2	0.533	31.87
14:52:14	705.6	0.95	31.73
14:54:14	694.4	1.592	31.30
14:56:14	716.7	0.933	30.21
14:58:14	716.7	0.867	28.99

15:00:14	705.6	0.758	32.69
15:02:14	744.4	0.758	30.95
15:04:14	794.4	1.175	30.31
15:06:14	772.2	0.558	32.57
15:08:14	777.8	1.283	29.79
15:10:14	722.2	0.867	29.85
15:12:14	700.0	0.867	29.90
15:14:14	694.4	0.733	30.16
15:16:14	616.7	0.958	29.80
15:18:14	611.1	0.825	30.96
15:20:14	633.3	1.167	29.33
15:22:14	666.7	0.858	30.08
15:24:14	605.6	0.817	29.60
15:26:14	605.6	1.417	30.43
15:28:14	650.0	0.725	30.63
15:30:14	644.4	0.725	30.81
15:32:14	650.0	0.658	29.79
15:34:14	638.9	0.533	30.43
15:36:14	733.3	0.567	28.39
15:38:14	738.9	0.567	27.71
15:40:14	750.0	0.567	27.50
15:42:14	716.7	0.667	31.63
15:44:14	694.4	0.667	30.53
15:46:14	672.2	0.608	29.06
15:48:14	672.2	0.567	29.31
15:50:14	622.2	0.867	29.14
15:52:14	627.8	0.500	30.12
15:54:14	694.4	0.408	28.79
15:56:14	733.3	0.583	28.86
15:58:14	655.6	0.417	30.62

16:00:14	683.3	0.417	30.48
16:02:14	622.2	0.642	29.75
16:04:14	611.1	0.967	29.58
16:06:14	594.4	0.525	31.34
16:08:14	588.9	0.483	30.25
16:10:14	616.7	0.367	29.24
16:12:14	627.8	0.367	31.85
16:14:14	638.9	0.400	32.16
16:16:14	650.0	0.217	32.33
16:18:14	633.3	0.600	30.43
16:20:14	572.2	0.625	30.24
16:22:14	616.7	0.617	28.91
16:24:14	594.4	0.708	28.79
16:26:14	572.2	1.267	31.92
16:28:14	555.6	0.850	31.95
16:30:14	527.8	0.450	32.16
16:32:14	544.4	0.325	31.13
16:34:14	533.3	0.767	30.96
16:36:14	611.1	0.467	31.49
16:38:14	594.4	0.933	30.86
16:40:14	594.4	1.275	31.10
16:42:14	594.4	0.925	30.91
16:44:14	527.8	0.875	28.40
16:46:14	511.1	0.675	31.39
16:48:14	505.6	0.683	31.01

Table 3.2: DMPM Solar Insolations and Wind Velocities.(03/02/2005, day of the year: 34)

SOLAR TIME	SOLAR INSOLATION (W/m.2)	WIND VELOCITY (m/s)	AMBIENT TEMPERATURE (0.C)
11:30:47	783.3	1.150	30.14
11:32:47	805.6	0.600	29.85
11:34:47	805.6	0.575	26.19
11:36:47	783.3	0.425	28.79
11:38:47	800.0	0.250	25.74
11:40:47	816.7	0.650	26.80
11:42:47	811.1	0.483	28.00
11:44:47	744.4	0.633	28.23
11:46:47	794.4	0.425	29.16
11:48:47	827.8	0.417	29.97
11:50:47	833.3	0.983	27.56
11:52:47	844.4	0.875	29.06
11:54:47	816.7	0.425	29.68
11:56:47	838.9	0.575	28.89
11:58:47	844.4	0.575	29.26
12:00:47	838.9	0.583	30.02
12:02:47	855.6	0.625	29.21
12:04:47	855.6	0.725	28.45
12:06:47	850.0	0.667	27.69
12:08:47	866.7	0.408	29.31
12:10:47	855.6	0.375	28.72
12:12:47	866.7	0.533	28.69
12:14:47	877.8	0.633	29.68
12:16:47	866.7	0.350	30.48

12:18:47	872.2	0.675	27.93
12:20:47	883.3	0.633	26.70
12:22:47	883.3	0.517	29.38
12:24:47	883.3	0.875	28.57
12:26:47	888.9	1.025	29.18
12:28:47	883.3	0.617	30.86
12:30:47	888.9	0.492	29.14
12:32:47	894.4	0.725	26.46
12:34:47	883.3	1.089	27.71
12:36:47	872.2	1.088	27.24
12:38:47	883.3	0.558	26.36
12:40:47	888.9	0.533	28.50
12:42:47	883.3	0.417	27.00
12:44:47	883.3	0.350	28.15
12:46:47	888.9	0.383	26.70
12:48:47	888.9	0.333	26.90
12:50:47	883.3	0.317	26.95
12:52:47	866.7	0.300	28.00
12:54:47	872.2	0.517	27.56
12:56:47	877.8	0.408	27.54
12:58:47	877.8	0.667	27.19
13:00:47	866.7	0.583	29.21
13:02:47	877.8	0.408	29.65
13:04:47	877.8	0.558	28.47
13:06:47	872.2	1.233	29.21
13:08:47	872.2	1.133	28.62
13:10:47	866.7	0.717	30.96
13:12:47	888.9	1.308	30.53
13:14:47	877.8	0.867	28.15
13:16:47	866.7	0.600	30.28

13:18:47	872.2	0.358	28.89
13:20:47	872.2	0.425	28.15
13:22:47	877.8	0.350	28.79
13:24:47	877.8	0.500	30.50
13:26:47	883.3	0.325	28.94
13:28:47	894.4	0.750	30.26
13:30:47	894.4	0.700	29.70
13:32:47	894.4	0.383	31.13
13:34:47	883.3	0.617	28.57
13:36:47	872.2	0.317	29.53
13:38:47	855.6	0.842	29.72
13:40:47	838.9	0.450	29.77
13:42:47	838.9	0.416	30.16
13:44:47	844.4	0.604	29.23
13:46:47	838.9	0.604	30.14
13:48:47	833.3	0.425	28.74
13:50:47	833.3	0.425	30.93
13:52:47	833.3	0.808	30.96
13:54:47	833.3	1.142	30.31
13:56:47	844.4	0.833	30.81
13:58:47	850.0	0.808	31.44
14:00:47	850.0	0.717	28.45
14:02:47	850.0	0.533	30.48
14:04:47	850.0	0.225	31.54
14:06:47	850.0	0.292	31.03
14:08:47	827.8	0.792	31.20
14:10:47	833.3	0.875	29.53
14:12:47	838.9	0.333	28.82
14:14:47	827.8	0.525	30.74
14:16:47	827.8	1.183	32.21

14:18:47	827.8	0.917	29.97
14:20:47	822.2	0.342	32.28
14:22:47	827.8	0.308	32.45
14:24:47	827.8	0.842	30.26
14:26:47	822.2	0.842	29.63
14:28:47	816.7	0.353	30.36
14:30:47	816.7	0.353	30.89
14:32:47	811.1	0.250	30.89
14:34:47	805.6	0.725	32.69
14:36:47	805.6	0.275	30.48
14:38:47	811.1	0.500	32.67
14:40:47	805.6	0.583	29.63
14:42:47	783.3	0.600	31.18
14:44:47	777.8	0.633	31.32
14:46:47	772.2	0.850	30.86
14:48:47	772.2	0.917	29.60
14:50:47	777.8	0.850	29.58
14:52:47	766.7	0.508	29.50
14:54:47	777.8	0.975	29.70
14:56:47	766.7	1.083	29.48
14:58:47	766.7	0.833	29.80
15:00:47	738.9	0.692	29.60
15:02:47	755.6	0.650	30.72
15:04:47	755.6	1.183	32.07
15:06:47	755.6	0.833	29.50
15:08:47	738.9	0.692	31.54
15:10:47	733.3	0.583	30.09
15:12:47	727.8	0.683	31.15
15:14:47	733.3	0.742	30.50
15:16:47	722.2	0.750	28.79

15:18:47	727.8	0.417	29.48
15:20:47	716.7	0.267	31.75
15:22:47	722.2	0.575	30.84
15:24:47	711.1	0.908	28.79
15:26:47	705.6	0.475	30.48
15:28:47	683.3	0.550	28.55
15:30:47	688.9	0.392	31.51
15:32:47	672.2	0.842	30.33
15:34:47	672.2	0.853	28.96
15:36:47	672.2	0.450	30.86
15:38:47	666.7	0.450	31.13
15:40:47	666.7	0.975	30.43
15:42:47	672.2	0.842	30.36
15:44:47	666.7	0.692	30.84
15:46:47	661.1	0.533	29.36
15:48:47	661.1	0.408	32.04
15:50:47	638.9	0.417	31.03
15:52:47	627.8	1.092	31.10
15:54:47	611.1	0.483	30.16
15:56:47	616.7	0.258	30.67
15:58:47	616.7	0.242	29.63
16:00:47	611.1	0.508	29.87
16:02:47	605.6	0.500	31.56
16:04:47	600.0	0.442	30.62
16:06:47	600.0	0.417	29.04
16:08:47	594.4	0.733	30.84
16:10:47	600.0	1.167	30.74
16:12:47	577.8	0.667	30.14
16:14:47	600.0	0.856	30.40
16:16:47	572.2	1.092	30.31

APPENDIX 4

EXPERIMENTAL TEMPERATURES

Table 4.1: SPM Experimental Temperatures (20/1/2005)

Label	COLDJNCT	TEMP3	TEMP6	TGC7	FGC8	ABP9	BBP10	INS11	AMBT
Unit	deg C	deg C	deg C	deg C	deg C	deg C	deg C	deg C	deg C
Minimum value	33.49	40.84	55.76	39.31	48.16	66.48	53.84	39.78	26.78
Maximum value	37.63	45.72	63.84	46.08	58.08	82.08	66.00	43.73	34.91
12:23:26	33.49	45.72	63.84	45.76	55.60	82.08	66.00	41.08	28.62
12:24:26	33.56	45.52	63.12	45.84	55.60	80.64	65.36	40.69	27.88
12:25:26	33.60	44.72	62.56	45.68	55.44	79.36	64.80	40.29	27.81
12:26:26	33.70	44.16	62.32	44.88	55.60	78.32	64.56	40.27	26.78
12:27:26	33.75	43.44	61.84	45.04	55.6	77.52	63.92	39.78	27.59
12:28:26	33.86	43.8	61.52	45.04	55.68	76.72	62.96	39.98	28.35
12:29:26	33.99	43.88	61.12	44.40	56.64	76.00	62.64	40.75	29.45
12:30:26	34.11	43.72	60.72	45.52	56.72	75.20	63.12	40.69	28.23
12:31:26	34.19	43.48	60.64	44.96	56.72	74.56	63.04	40.58	28.32
12:32:26	34.19	43.08	60.4	44.64	56.64	74.08	62.80	40.38	28.03
12:33:26	34.29	42.92	60.08	43.92	56.00	73.68	62.56	40.73	27.19
12:34:26	34.38	42.52	60.00	42.72	55.92	73.28	62.08	40.67	30.43
12:35:26	34.42	42.28	59.76	43.28	55.76	72.96	62.08	40.73	29.70
12:36:26	34.38	42.28	59.84	43.68	55.92	72.72	61.92	40.61	30.38
12:37:26	34.39	42.28	59.60	43.36	55.84	72.32	61.84	40.63	30.07
12:38:26	34.42	41.80	59.60	41.36	55.84	72.00	61.12	40.88	32.48
12:39:26	34.59	42.48	59.36	43.92	55.84	71.52	60.48	41.12	32.43
12:40:26	34.74	42.72	59.36	45.36	56.08	71.20	60.96	41.08	29.75
12:41:26	34.81	42.64	59.28	44.72	56.16	71.04	61.20	40.94	29.75
12:42:26	34.79	42.64	59.20	44.16	56.08	70.88	61.2	40.88	29.87

12:43:26	34.67	42.64	59.20	42.48	56.00	70.80	61.28	40.71	29.50
12:44:26	34.65	42.32	59.20	42.80	55.92	70.64	60.96	40.69	29.70
12:45:26	34.73	42.24	59.20	43.12	55.84	70.48	60.96	40.94	30.53
12:46:26	34.69	41.84	58.80	40.60	55.84	70.32	60.64	40.50	29.77
12:47:26	34.82	42.00	58.96	41.20	55.68	70.32	60.96	40.61	28.84
12:48:26	34.87	42.08	59.04	39.85	55.92	70.40	61.44	40.81	28.89
12:49:26	34.83	43.84	59.20	39.75	55.92	70.40	61.52	40.94	30.91
12:50:26	34.72	43.52	58.96	39.75	56.00	70.08	61.20	41.17	30.31
12:51:26	34.74	43.28	59.12	39.46	56.08	69.92	60.96	41.35	30.50
12:52:26	34.87	43.04	58.72	40.43	55.92	69.68	60.72	41.25	29.72
12:53:26	34.92	42.20	58.96	40.46	56.16	69.60	61.04	41.21	29.58
12:54:26	35.05	42.56	58.88	40.96	55.92	69.44	60.08	41.56	32.65
12:55:26	35.21	42.32	58.48	42.40	55.84	69.20	60.84	41.79	30.81
12:56:26	35.34	42.88	58.80	42.96	55.84	69.12	60.24	41.54	30.81
12:57:26	35.40	42.88	58.48	42.56	55.84	69.04	60.24	41.39	29.31
12:58:26	35.31	42.96	58.64	41.28	55.92	69.12	60.48	41.17	30.31
12:59:26	35.24	42.90	58.72	41.76	55.76	69.04	60.08	41.56	30.91
13:00:26	35.24	42.88	58.56	41.20	55.92	68.88	60.08	41.29	30.24
13:01:26	35.35	42.96	58.80	42.24	56.16	68.80	60.92	41.64	32.09
13:02:26	35.43	43.28	58.96	42.24	56.40	68.72	60.40	41.77	31.51
13:03:26	35.51	43.36	59.12	42.88	56.48	68.72	60.72	41.68	30.19
13:04:26	35.56	43.28	59.04	42.00	56.64	68.64	60.64	41.47	29.92
13:05:26	35.71	43.12	59.04	42.08	56.64	68.80	60.24	41.62	32.79
13:06:26	35.86	43.20	59.20	43.36	56.96	68.80	60.40	41.93	31.73
13:07:26	35.99	43.44	59.36	43.68	56.64	68.80	60.72	41.79	31.18
13:08:26	36.00	43.60	59.36	42.80	56.72	69.04	60.96	41.85	31.66
13:09:26	36.04	43.36	59.52	43.44	56.48	69.12	61.20	41.97	31.37
13:10:26	36.14	43.20	59.36	42.16	56.48	69.20	60.88	41.48	29.95
13:11:26	36.25	43.20	59.44	40.96	56.16	69.36	61.04	41.54	31.63
13:12:26	36.33	43.60	59.44	42.72	56.24	69.60	60.96	41.95	32.67

13:13:26	36.35	43.76	59.68	43.20	56.64	69.68	60.88	42.32	31.13
13:14:26	36.36	43.60	59.68	42.64	56.48	69.60	60.80	42.45	30.72
13:15:26	36.41	43.76	59.84	42.40	56.72	69.60	61.12	42.22	31.06
13:16:26	36.37	43.68	59.68	42.72	56.72	69.52	61.28	41.83	31.03
13:17:26	36.26	43.60	59.84	42.24	56.40	69.60	61.20	41.45	29.82
13:18:26	36.18	43.52	59.68	40.96	56.32	69.60	61.20	41.56	30.96
13:19:26	36.10	43.36	59.68	40.96	56.32	69.68	61.12	41.54	30.36
13:20:26	35.99	43.12	59.76	40.29	56.08	69.68	61.28	41.72	29.38
13:21:26	35.99	43.64	59.44	39.31	56.08	69.68	60.80	41.60	31.10
13:22:26	36.06	42.64	59.52	41.92	56.08	69.60	60.72	42.14	32.00
13:23:26	36.20	42.48	59.52	41.68	56.08	69.44	60.48	42.37	30.98
13:24:26	36.35	42.32	59.20	42.88	56.40	69.28	60.16	42.28	30.69
13:25:26	36.55	42.40	59.20	42.80	56.40	69.28	60.48	42.06	30.60
13:26:26	36.66	43.72	59.36	44.00	56.56	69.20	60.80	42.61	30.53
13:27:26	36.66	43.72	59.60	42.48	56.56	69.12	60.80	42.49	31.56
13:28:26	36.63	43.96	59.60	42.16	56.64	69.04	60.96	42.34	30.98
13:29:26	36.66	43.72	59.6	42.32	56.40	69.04	60.48	42.43	31.78
13:30:26	36.77	43.40	59.44	43.44	56.32	69.04	60.00	42.51	33.18
13:31:26	36.84	43.56	59.44	43.68	56.32	69.04	60.08	42.59	31.80
13:32:26	36.87	42.10	59.52	43.52	56.56	69.12	60.48	42.68	31.30
13:33:26	36.94	44.20	59.92	44.08	56.96	69.12	60.80	42.66	30.55
13:34:26	36.97	43.88	59.76	42.24	56.88	69.04	60.56	42.66	32.86
13:35:26	37.06	44.04	59.76	44.40	57.20	68.96	60.88	42.94	32.26
13:36:26	36.91	44.60	60.16	44.56	57.44	68.96	61.28	42.88	32.40
13:37:26	36.89	44.60	60.00	44.08	57.52	69.04	61.04	42.95	33.01
13:38:26	36.93	44.52	60.08	44.56	57.68	69.04	60.88	43.15	32.91
13:39:26	37.02	44.76	60.32	44.08	57.44	69.12	61.04	43.21	33.20
13:40:26	37.07	44.60	60.40	43.84	57.52	69.04	61.12	43.24	31.75
13:41:26	37.11	44.44	60.48	43.36	57.68	68.96	61.28	43.21	32.31
13:42:26	37.22	44.60	60.56	43.12	57.44	68.88	61.68	42.47	30.31

13:43:26	37.23	44.28	60.56	41.36	57.36	68.96	61.52	42.34	32.72
13:44:26	37.19	44.52	60.64	43.28	57.20	69.04	62.00	42.57	30.53
13:45:26	37.14	44.20	60.64	40.92	57.20	69.28	61.76	42.88	32.04
13:46:26	37.15	43.80	60.56	42.64	57.04	69.04	61.20	43.13	33.59
13:47:26	37.30	43.96	60.40	44.00	57.36	68.96	61.12	43.52	33.06
13:48:26	37.35	44.12	60.56	45.12	57.76	68.96	60.96	43.44	33.46
13:49:26	37.42	43.44	60.56	45.60	57.68	68.88	61.20	43.63	32.81
13:50:26	37.46	43.60	60.64	44.32	57.76	68.88	61.60	43.11	33.03
13:51:26	37.49	44.00	60.80	44.96	58.08	69.04	61.24	42.68	29.60
13:52:26	37.55	44.60	60.80	45.52	57.68	69.04	61.92	42.55	32.53
13:53:26	37.58	44.84	60.80	45.36	57.68	69.12	62.24	42.80	31.54
13:54:26	37.39	44.28	60.88	43.44	57.20	69.04	62.76	43.01	33.46
13:55:26	37.46	43.80	60.56	43.60	56.96	69.04	63.12	43.28	32.81
13:56:26	37.50	43.96	60.48	44.16	57.04	68.80	61.36	43.26	32.62
13:57:26	37.50	44.12	60.64	44.64	57.28	68.88	62.76	42.82	30.50
13:58:26	37.37	44.20	60.48	43.44	56.96	68.96	62.60	42.34	32.12
13:59:26	37.25	43.88	60.64	42.96	56.88	68.96	62.36	42.59	33.03
14:00:26	37.25	43.88	60.56	44.56	56.64	68.96	64.20	42.72	31.97
14:01:26	37.24	43.64	60.16	43.92	56.72	68.88	62.96	42.74	32.69
14:02:26	37.29	43.48	60.32	45.68	56.56	68.88	62.88	42.57	31.51
14:03:26	37.33	43.48	60.08	44.80	56.40	68.88	63.20	42.32	31.46
14:04:26	37.26	43.24	60.08	42.40	56.32	68.88	62.80	42.37	31.90
14:05:26	37.22	43.40	60.08	44.96	56.24	68.88	62.80	42.63	30.43
14:06:26	37.19	43.24	60.00	44.64	56.16	68.96	62.80	42.59	31.80
14:07:26	37.20	44.16	60.00	44.08	56.16	68.80	62.80	43.09	32.09
14:08:26	37.24	44.40	60.24	45.28	56.40	68.88	62.48	43.40	33.34
14:09:26	37.27	44.08	60.08	44.00	56.48	68.88	62.32	43.26	32.19
14:10:26	37.37	44.16	60.08	45.52	56.56	68.88	62.16	43.34	33.08
14:11:26	37.48	45.08	60.08	45.60	56.24	69.04	62.40	42.88	31.10
14:12:26	37.52	45.92	59.92	44.80	56.16	69.04	62.16	42.66	31.92

14:13:26	37.56	45.16	60.00	45.76	56.32	69.12	62.32	43.11	31.90
14:14:26	37.50	44.84	59.92	44.64	56.56	69.04	63.08	43.11	33.54
14:15:26	37.47	45.00	60.00	43.04	56.16	69.04	63.40	42.86	31.51
14:16:26	37.46	44.76	60.00	44.00	55.92	69.04	62.76	43.13	33.71
14:19:26	37.49	45.00	60.00	45.92	56.32	69.12	62.84	43.28	32.93
14:20:26	37.60	45.48	60.32	45.52	56.64	69.36	63.16	43.73	32.84
14:21:26	37.56	45.32	60.32	45.28	56.64	69.28	63.24	43.23	31.44
14:22:26	37.49	44.92	60.08	43.68	56.40	69.28	63.08	42.86	32.28
14:23:26	37.52	44.68	60.24	45.52	56.24	69.28	63.08	43.01	32.45
14:24:26	37.54	44.60	60.08	43.76	55.84	69.36	63.08	42.61	32.31
14:25:26	37.60	44.68	60.24	44.72	56.08	69.44	63.32	42.70	32.81
14:26:26	37.63	44.44	60.16	44.16	55.76	69.44	63.00	42.72	31.95
14:27:26	37.54	44.60	60.24	44.88	55.76	69.44	67.40	42.57	32.74
14:28:26	37.43	44.76	60.00	44.72	55.84	69.52	63.56	42.41	31.49
14:29:26	37.35	44.36	59.92	43.20	55.52	69.52	63.16	42.30	32.00
14:30:26	37.23	44.20	59.68	43.68	55.28	69.52	63.00	42.37	32.21
14:31:26	37.19	44.20	59.92	44.56	55.20	69.60	63.08	42.35	32.12
14:32:26	37.03	44.68	59.68	44.08	55.60	69.76	63.76	42.82	33.66
14:33:26	36.94	44.60	59.68	44.72	55.52	69.84	63.76	43.07	32.91
14:34:26	36.96	44.36	59.68	44.56	55.36	69.84	63.60	42.97	33.92
14:35:26	36.95	44.20	59.52	43.68	55.52	69.68	63.28	42.90	34.21
14:36:26	36.88	44.12	59.44	44.88	55.60	69.68	63.44	42.95	32.55
14:37:26	36.80	43.96	59.60	44.48	55.44	69.52	63.44	43.05	32.57
14:38:26	36.75	43.96	59.36	45.92	55.44	69.52	62.68	42.51	31.83
14:39:26	36.67	43.88	59.28	44.16	55.12	69.68	62.36	42.03	33.22
14:40:26	36.65	43.80	59.12	45.76	55.12	69.68	62.80	42.28	33.27
14:41:26	36.59	43.48	59.20	46.08	54.88	69.68	62.72	42.51	33.44
14:42:26	36.44	43.48	59.04	45.12	54.88	69.68	62.80	42.30	32.45
14:43:26	36.29	43.40	58.80	44.16	54.56	69.52	63.64	41.95	31.25
14:44:26	36.13	43.32	58.72	43.44	54.48	69.44	63.64	41.97	31.85

14:45:26	36.06	43.08	58.64	42.80	54.24	69.44	63.56	41.76	30.72
14:46:26	35.98	42.52	58.32	43.84	53.92	69.36	63.08	41.76	32.02
14:47:26	35.90	42.60	58.40	43.12	53.60	69.36	62.92	41.68	32.65
14:48:26	35.84	43.40	58.64	43.28	54.16	69.52	62.24	42.35	32.04
14:49:26	35.80	42.92	58.56	43.20	54.00	69.36	61.68	42.24	32.33
14:50:26	35.79	42.60	58.48	43.84	54.08	69.28	60.96	42.51	33.73
14:51:26	35.62	43.08	58.32	44.80	54.64	69.28	61.28	42.43	32.67
14:52:26	35.61	43.16	58.48	44.64	54.48	69.20	61.36	42.55	32.91
14:53:26	35.47	43.32	58.16	44.16	54.16	69.28	61.20	42.64	32.02
14:54:26	35.46	42.92	58.16	44.32	54.00	69.20	61.04	42.70	33.97
14:55:26	35.51	42.44	58.08	45.52	53.84	69.04	60.80	42.57	33.37
14:56:26	35.49	42.44	57.84	44.64	53.92	68.96	59.72	42.64	33.27
14:57:26	35.48	42.20	57.68	44.40	53.84	68.88	59.48	42.43	31.73
14:58:26	35.32	42.44	57.68	43.60	53.60	68.88	59.04	41.76	31.30
14:59:26	35.22	42.12	56.68	43.44	53.44	68.88	56.96	41.62	33.20
15:00:26	35.21	41.80	55.36	43.60	53.20	68.80	56.56	41.68	33.10
15:01:26	35.24	41.96	55.44	44.00	53.20	68.88	56.80	41.60	33.03
15:02:26	35.29	41.56	55.36	43.36	53.12	68.96	56.48	41.39	30.84
15:03:26	35.33	41.40	55.12	44.80	53.04	68.88	56.24	41.43	33.06
15:04:26	35.27	41.64	55.12	44.72	52.88	68.88	56.72	41.62	30.93
15:05:26	35.10	41.56	55.04	42.88	52.96	68.80	56.64	41.60	31.30
15:06:26	35.05	41.40	54.96	43.84	51.04	68.72	56.32	41.68	32.50
15:07:26	34.93	41.24	54.88	43.12	50.88	68.64	55.84	41.72	33.71
15:08:26	34.94	41.64	54.88	45.76	51.12	68.64	55.92	42.08	33.44
15:09:26	34.87	41.80	54.96	45.60	51.36	68.72	56.16	42.20	32.45
15:10:26	34.84	41.64	54.96	45.36	51.28	68.72	56.00	42.08	33.66
15:11:26	34.87	41.88	55.12	45.60	51.60	68.80	56.08	42.26	33.20
15:12:26	34.79	41.64	55.04	44.40	51.44	68.72	55.68	41.87	32.69
15:13:26	34.80	41.72	54.88	44.56	51.44	68.64	55.92	41.83	32.09
15:14:26	34.73	41.80	53.96	44.56	51.28	68.64	55.84	41.77	33.32

15:15:26	34.65	41.72	54.04	43.60	51.96	68.64	55.92	41.37	33.18
15:16:26	34.62	41.40	53.96	43.84	51.96	68.56	55.52	41.85	32.98
15:17:26	34.67	41.88	53.96	45.68	51.96	68.56	55.44	42.57	33.10
15:18:26	34.70	42.28	53.12	44.16	50.20	68.56	55.52	42.92	34.91
15:19:26	34.66	42.04	53.12	44.96	50.20	68.48	55.52	42.84	33.13
15:20:26	34.46	42.20	53.04	44.16	50.04	68.40	55.68	42.03	32.24
15:21:26	34.38	41.88	53.04	42.40	49.72	68.32	55.36	42.08	33.59
15:22:26	34.36	41.72	52.80	44.00	49.56	68.16	55.12	42.45	33.87
15:23:26	34.31	41.72	52.80	43.60	49.48	68.08	55.20	42.51	32.62
15:24:26	34.21	41.32	52.64	43.28	49.40	67.92	54.80	42.51	34.12
15:25:26	34.20	41.56	52.64	44.40	49.32	67.84	54.88	42.92	33.73
15:26:26	34.14	41.64	52.64	44.72	49.48	67.68	55.04	42.68	32.12
15:27:26	34.10	41.64	51.88	43.76	49.56	67.68	55.28	42.55	32.04
15:28:26	34.13	41.40	51.72	43.84	49.56	67.60	54.88	42.59	34.00
15:29:26	34.17	41.32	51.80	44.56	49.64	67.60	54.72	42.74	34.84
15:30:26	34.19	41.32	51.64	44.56	49.72	67.60	54.88	42.82	33.32
15:31:26	34.14	41.40	51.56	43.84	49.72	67.44	54.96	42.68	31.90
15:32:26	34.08	41.40	51.48	44.40	49.64	67.28	54.96	42.66	32.21
15:33:26	33.98	41.16	51.32	44.08	49.48	67.20	54.64	42.82	33.22
15:34:26	33.92	41.16	51.24	43.04	49.32	67.20	54.72	42.61	31.20
15:35:26	33.93	41.08	51.24	42.48	49.32	67.20	54.80	42.84	32.57
15:36:26	33.85	40.92	51.16	43.52	49.08	67.04	54.64	42.94	32.89
15:37:26	33.80	41.08	51.16	44.96	49.32	66.96	54.64	42.99	32.55
15:38:26	33.74	41.08	51.07	44.24	49.24	66.96	54.48	42.99	33.61
15:39:26	33.70	40.84	51.08	43.84	49.08	66.72	54.16	42.97	33.22
15:40:26	33.66	40.92	51.08	43.84	48.4	66.72	54.08	43.07	33.92
15:41:26	33.62	41.16	51.16	43.84	48.56	66.72	54.16	43.17	33.13
15:42:26	33.60	41.00	51.03	44.08	48.32	66.56	54.08	42.99	32.53
15:43:26	33.54	40.84	50.84	42.72	48.32	66.48	53.92	42.72	34.04
15:44:26	33.58	41.00	50.76	45.21	48.16	66.48	53.84	43.38	34.45

Table 4.2 TPM Experimental Temperatures. (29/10/2004)

SOLAR TIME	TEMP1 deg C	TEMP4 deg C	TEMP5 deg C	TEMP2 deg C	TEMP3 deg C	TEMP6 deg C	TGC7 Deg C	FGC8 deg C	ABP9 deg C	BBP10 deg C	AMBT deg C
Min value	35.85	36.56	36.37	36.7	38.23	40.53	39	35.9	39.1	39.24	24.5
Max value	43.84	46.72	46.08	51.68	50.48	64.64	42.1	57.5	70	59.28	29.7
12:38:54	41.28	42.24	43.04	51.68	50.24	64.64	36.8	57.5	70	58.32	25.9
12:39:54	40.75	41.12	41.52	51.68	48.32	62.72	37.8	55.8	67.4	56.4	25.6
12:40:54	39.41	39.82	40.19	50.08	48.16	59.84	36.9	54.6	63.4	53.76	25.6
12:41:54	38.6	39.58	39.65	48.24	48.72	57.76	37.8	52.6	59.6	52	25
12:42:54	37.91	38.99	38.92	46.56	47.44	55.44	37.3	51	56.2	50.24	24.7
12:43:54	37.42	38.55	38.45	45.04	46.4	53.52	37.4	49.2	55.1	48.56	25.1
12:44:54	37.13	38.16	38.01	43.76	44.6	51.76	38.1	47.4	53.6	47.12	24.7
12:45:54	36.83	37.94	37.72	42.64	42.94	50.24	38.3	45.8	53.4	46.08	24.5
12:46:54	36.64	37.59	37.45	41.68	42.34	48.96	38.6	44.3	51.7	45.12	24.6
12:47:54	36.32	37.18	37.05	40.83	40.58	47.76	39	43	48.2	44.08	25
12:48:54	36.17	36.86	36.83	40.07	40.06	46.8	38.7	41.8	48.2	43.36	25.1
12:49:54	36.05	36.59	36.56	39.46	39.77	45.92	38.7	40.9	47.4	42.72	25.1
12:50:54	35.93	36.59	36.37	39	38.52	45.2	38.6	40.1	46.9	42.08	24.9
12:51:54	35.93	36.61	36.51	38.6	38.38	44.64	38.7	39.4	46.5	41.84	25.4
12:52:54	35.93	36.83	36.69	38.33	38.45	44.32	38.8	39.7	46.4	41.76	25.3
12:53:54	35.85	37.15	37.1	38.19	38.33	44.48	39.5	40.9	45.9	41.92	25.9
12:54:54	36.2	38.92	38.33	38.58	39.36	46.56	39.4	41	46.4	43.92	26.6
12:55:54	36.83	38.13	37.99	39.38	40	46.48	38.3	40.9	47.4	43.76	24.9
12:56:54	37.1	39.92	39.38	40.13	40.94	48.8	38	40.9	50.1	46	25.6
12:57:54	38.13	40.29	39.6	41.28	42.24	50.48	37.5	41.4	53.4	47.2	25.9
12:58:54	38.38	38.6	38.57	41.84	41.76	49.36	37.7	41	53.4	46.16	26.2
12:59:54	37.91	37.94	38.16	41.44	40.96	48	38.9	40.5	51.4	45.04	25.9
13:00:54	37.45	37.45	37.74	40.75	40.31	46.88	38.2	41	49.5	44	25.5
13:01:54	37.08	37.18	37.37	39.98	39.77	45.92	38.6	41	47.8	43.36	25.3
13:02:54	36.81	36.96	37.23	39.36	39.28	45.2	38.7	40.7	46.4	42.56	25.5

13:03:54	36.69	36.88	37	38.96	39.24	44.56	38.5	40.2	45.5	42.08	25
13:04:54	36.51	36.91	37	38.6	38.94	44.16	38.3	40.6	44.8	41.84	25.5
13:05:54	36.44	36.76	36.88	38.39	38.77	43.84	38.1	41.2	44.3	41.6	25.1
13:06:54	36.17	36.93	37.13	38.16	38.52	43.6	37.5	41.6	44	41.6	24.9
13:07:54	36.49	38.97	38.7	38.58	39.68	46.24	38.2	42.5	46.6	43.84	26.8
13:08:54	37.47	39.87	39.48	39.78	41.12	48.4	37.5	42.9	50.6	46	27.4
13:09:54	38.33	40.75	40.36	41.12	42.16	50.32	37.6	43.4	53.8	47.52	27.6
13:10:54	39.14	41.6	41.04	42.48	43.68	52	38.1	43.4	56.8	49.2	26.6
13:11:54	39.55	42.08	41.6	43.68	44.56	53.44	38.4	43.6	59.2	50.48	26.8
13:12:54	40.02	42.64	42.16	44.72	45.44	54.8	39.2	39.8	61.1	51.76	26.7
13:13:54	40.34	43.2	42.56	45.6	46	55.84	40.4	41	62.7	52.64	26.8
13:14:54	40.72	43.52	42.96	46.32	46.64	56.88	40	42.2	64	53.6	26.3
13:15:54	40.94	43.6	43.12	46.96	46.88	57.68	40.1	43.1	65	54.16	27.1
13:16:54	41.04	43.84	43.12	47.44	47.52	58.4	39.7	44	66	54.56	27.1
13:17:54	41.12	43.92	43.44	48.08	47.44	59.04	40.1	45	66.6	55.12	27.3
13:18:54	41.28	43.92	43.36	48.32	47.92	59.44	40.3	45.7	67	55.44	26.6
13:19:54	41.28	44.08	43.6	48.72	47.92	59.68	40.3	46.2	67.3	55.68	26.6
13:20:54	41.52	44.48	43.92	48.88	47.92	60.08	40.7	46.7	67.4	56	27.1
13:21:54	41.6	44.48	43.84	49.2	48.16	60.4	40.6	47.1	67.5	56.4	28
13:22:54	41.68	44.56	44	49.28	48.32	60.64	40.5	47.5	67.6	56.64	27.1
13:23:54	41.68	44.72	43.92	49.52	48.72	60.88	40.3	47.8	67.8	56.48	26.8
13:24:54	41.76	44.72	44	49.68	48.8	61.12	41.1	48	67.9	56.88	26.6
13:25:54	41.76	44.96	44.32	49.92	48.8	61.36	41.4	48.2	68	56.96	27.3
13:26:54	41.92	45.28	44.64	50	48.64	61.52	41	48.3	67.8	57.28	29
13:27:54	42.16	45.6	44.56	50.16	49.12	61.68	39.6	48.6	68	57.12	26.7
13:28:54	42.24	45.76	44.72	50.56	49.44	62	40.1	48.9	68.2	57.68	27
13:29:54	42.16	45.68	44.64	50.48	49.44	62.16	39.6	49	68.3	57.84	27.9
13:30:54	42.4	46.24	44.96	50.96	50.16	62.56	40.2	49.3	68.7	58.4	27.1
13:31:54	42.24	46.48	45.2	51.04	49.92	62.8	39.7	49.4	68.8	58.72	28
13:32:54	42.48	46.48	45.44	51.12	49.68	62.96	39.8	49.4	68.8	58.8	28.2

13:33:54	42.56	46.24	45.28	51.28	49.68	62.96	40.2	49.5	68.6	58.64	28.5
13:34:54	42.72	46.24	45.36	51.2	49.76	63.04	40	49.6	68.6	58.96	28
13:35:54	42.64	46.16	45.2	51.28	49.84	63.04	40.4	49.7	68.7	58.72	28.2
13:36:54	42.64	46	45.2	51.12	50	63.04	40.3	49.8	68.8	58.64	27.3
13:37:54	42.8	46.24	45.36	51.36	50.16	63.28	40.4	49.9	69	59.28	28
13:38:54	42.72	46.4	45.52	51.52	50.08	63.44	40.7	50	69	59.2	29.1
13:39:54	43.04	44.96	44.48	51.44	49.68	62.24	40.7	50.8	68.1	57.76	28.4
13:40:54	42.8	44.08	43.6	50.72	49.12	60.96	40.5	51.1	66.1	56.32	27.6
13:41:54	41.84	42.88	42.64	49.76	47.76	58.72	41.1	51.4	62.7	54.24	27.5
13:42:54	40.96	42.32	42.08	48.56	46.4	56.8	40.3	50.9	59.4	52.72	27.1
13:43:54	40.46	42.8	42.32	47.36	45.76	56.24	39.7	49.2	57.6	52.48	27.4
13:44:54	40.53	41.68	41.44	46.64	45.2	54.88	39.4	48.4	56.2	51.12	27.1
13:45:54	40	41.36	41.04	45.92	44.56	53.44	39.6	47.8	54.1	49.76	26.5
13:46:54	39.9	42.24	41.6	45.2	44.48	53.84	39.8	46	53.8	50.4	27.5
13:47:54	39.63	41.44	41.44	44.88	43.76	52.64	39.5	45.6	53	49.6	27.7
13:48:54	40	40.96	40.8	44.56	44.16	52.32	39.7	45	52.9	48.96	26.7
13:49:54	39.58	40.7	40.55	44.24	43.76	51.28	40	44.8	51.8	48.16	26.5
13:50:54	38.84	41.28	41.2	43.76	43.04	50.96	39.2	44.1	51	48.32	27.3
13:51:54	39.41	42.72	42.32	43.68	43.76	52.72	39.4	42.5	53	50.08	28.4
13:52:54	40.21	43.12	42.72	44.32	44.8	54.16	39.1	42	55.7	51.44	28.3
13:53:54	40.96	43.68	43.28	45.28	45.92	55.36	39.1	42.2	58.2	52.72	27.7
13:54:54	41.36	44	43.6	46.08	46.64	56.4	39.6	43	60.2	53.52	28.1
13:55:54	41.76	44.56	44	46.88	47.6	57.36	40.5	43.8	62	54.48	28.3
13:56:54	41.92	44.64	44.24	47.6	47.92	58.24	40.4	44.9	63.3	55.28	28.5
13:57:54	42.24	44.8	44.48	48	48.32	58.8	40.8	45.7	64.2	55.44	27.9
13:58:54	42.32	44.88	44.56	48.48	48.8	59.36	41.3	46.5	65.1	55.84	27.9
13:59:54	42.4	44.96	44.56	48.8	48.96	59.76	41.3	47.2	65.7	56.32	28
14:00:54	42.48	45.2	44.8	49.12	48.88	60.16	41.1	47.8	66	56.64	27.7
14:01:54	42.64	45.12	44.72	49.36	49.52	60.56	41.4	48.3	66.5	56.8	28.8
14:02:54	42.48	45.12	44.72	49.36	49.2	60.72	40.7	48.6	66.6	56.8	29

14:03:54	42.32	45.2	44.72	49.6	49.44	60.8	40.6	48.9	66.7	57.2	27
14:04:54	42.16	45.04	44.64	49.6	49.52	60.96	40.7	49.1	66.8	57.12	28.4
14:05:54	42.24	45.2	44.88	49.76	49.28	61.28	40.2	49.4	67	57.2	29.1
14:06:54	42.4	45.52	45.2	49.92	49.2	61.36	39.5	49.4	66.9	57.44	29.1
14:07:54	42.56	45.76	45.36	50	49.52	61.52	39.7	49.5	67	57.92	28.6
14:08:54	42.8	46.08	45.44	50.16	49.92	61.68	39.9	49.7	67.1	57.76	28.3
14:09:54	42.8	46.16	45.68	50.16	49.68	61.76	39.8	49.6	67	58	29.2
14:10:54	42.96	46.72	45.84	50.32	50.08	62.08	39.9	49.8	67.4	58.16	29.2
14:11:54	43.2	46.64	46	50.56	50.24	62.24	40.4	49.8	67.4	58.56	28.3
14:12:54	43.28	46.48	45.92	50.72	50.32	62.32	40.2	50.2	67.5	58.56	28.1
14:13:54	43.28	46.32	45.84	50.64	50.24	62.32	40.4	50.2	67.5	58.72	28.3
14:14:54	43.28	46.48	45.92	50.8	50.24	62.4	40.8	50.3	67.5	58.72	29
14:15:54	43.36	46.48	46.08	50.8	50.24	62.48	40.9	50.3	67.4	59.04	29.1
14:16:54	43.84	45.76	45.28	50.64	50.48	62.16	40.4	50.5	67.2	58.24	28.4
14:17:54	43.28	43.92	43.84	50.48	49.2	59.92	40.3	51.4	64.6	56	27.7
14:18:54	41.76	44.24	44.08	49.52	48	58.48	40.3	51	61.6	55.04	27
14:19:54	41.76	42.56	42.56	48.56	47.2	57.2	39.5	50.3	59.8	53.44	27.7
14:20:54	41.04	41.92	42	47.68	46.08	55.44	39.4	49.7	57.2	51.84	27.3
14:21:54	40.46	41.28	41.36	46.56	44.96	53.84	39.6	48.7	54.6	50.48	27.5
14:22:54	39.9	40.68	40.82	45.44	44	52.4	39.1	47.6	53.5	49.2	27.3
14:23:54	39.41	40.26	40.41	44.48	43.12	51.12	39.1	46.3	52.6	47.92	27.7
14:24:54	39.11	39.87	40	43.52	42.56	49.84	38.8	45.3	52	47.04	27.1
14:25:54	38.72	39.24	39.46	42.8	42.08	48.72	38.5	44.2	50.7	46	27.3
14:26:54	38.38	38.89	39.24	42	41.28	47.76	38.2	43.4	50.4	45.12	27.5
14:27:54	38.18	38.55	38.92	41.28	41.04	46.8	38.6	42.5	49.5	44.32	26.8
14:28:54	37.89	38.18	38.6	40.74	40.72	46.08	38.4	41.8	48.8	43.76	26.6
14:29:54	37.64	38.01	38.4	40.2	40.19	45.36	38.3	41	48	43.12	27.1
14:30:54	37.59	37.96	38.28	39.84	40.24	44.88	37.9	40.5	47.6	42.72	26.5
14:31:54	37.54	37.86	38.18	39.59	40.29	44.64	38.3	40.2	47.5	42.64	26.8
14:32:54	37.13	37.86	38.38	41.23	41.73	44.32	38.7	41.7	47.3	42.56	27.2

14:33:54	36.98	39.33	39.63	41.96	42.19	45.44	38.4	41.7	46.6	43.76	27.3
14:34:54	37.99	40.21	40.43	41.36	41.52	47.36	37.8	41	47.8	45.6	27.8
14:35:54	39.19	40.41	40.51	42.3	43.04	48.96	38.2	41.1	50.9	46.72	27.7
14:36:54	39.38	39.33	39.73	42.28	42.96	48.4	38.2	40.8	51.5	46.16	27.4
14:37:54	38.87	38.6	39.19	42.36	42.4	47.44	38.3	40.9	50.3	45.2	26.6
14:38:54	38.25	38.11	38.77	40.96	41.52	46.64	39.2	41.3	48.8	44.4	26.4
14:39:54	37.47	39.01	39.6	40.36	41.12	46.64	39.4	41	48.1	44.72	26.6
14:40:54	37.81	39.82	40.38	41.15	41.76	47.84	39.4	40.2	49.4	46	27.1
14:41:54	38.82	38.82	39.38	41.72	42.56	48	38.1	40.3	50.6	45.68	27.1
14:42:54	38.35	38.45	39.11	41.89	41.92	47.52	38.1	40.9	50	45.2	27.5
14:43:54	37.59	38.67	39.53	40.7	41.28	46.96	38.9	41.2	49	44.88	27.2
14:44:54	37.89	39.8	40.29	41.34	41.92	48.4	38.8	40.4	50.3	46.16	28.2
14:45:54	38.08	39.38	40.09	41.81	42	48.32	38.1	40.8	50.8	46.08	28.1
14:46:54	38.21	39.31	40	41.04	42.08	48.16	38.1	41.1	50.8	45.92	27.5
14:47:54	38.92	39.77	40.26	41.04	42.88	49.36	38.4	40.7	52	46.96	27.9
14:48:54	39.01	38.92	39.53	41.44	42.56	48.4	39	41.6	51.4	46.08	27.2
14:49:54	38.67	38.65	39.21	41.36	42.32	47.76	39	42.1	50.3	45.36	26.8
14:50:54	38.3	38.35	38.99	40.96	41.68	47.2	39.1	41.9	49.2	44.8	27.2
14:51:54	38.23	38.43	38.99	40.68	41.36	46.64	39.2	41.7	48.2	44.48	27.3
14:52:54	38.08	38.5	39.04	40.2	40.85	46.32	39	41	47.4	44.32	27.5
14:53:54	37.72	39.24	39.82	39.98	40.85	46.4	38.4	40.8	47.3	44.48	27.4
14:54:54	38.25	40.53	40.96	39.92	41.76	48	38.7	40.8	49.1	46.24	27.9
14:55:54	39.04	40.96	41.44	42.64	43.2	49.44	39.2	40.8	51.6	47.28	28.5
14:56:54	39.43	41.44	42.08	43.44	43.92	50.72	40	41.3	53.8	48.48	29.7
14:57:54	39.95	41.92	42.48	44.24	44.8	51.84	39.5	42	55.7	49.6	29.2
14:58:54	40.29	42.24	42.8	45.04	45.76	52.88	39.6	42.9	57.4	50.4	27.3
14:59:54	40.58	42.64	43.2	45.76	46.08	53.84	40	43	58.6	51.28	29.3
15:00:54	40.7	42.64	43.36	46.4	46.56	54.56	40.1	43.8	59.7	52	28
15:01:54	40.8	42.88	43.52	46.88	46.88	55.2	40.2	44.6	60.5	52.4	27.2
15:02:54	40.9	42.64	43.44	46.28	47.28	55.68	41	45.2	61.1	52.8	28.3

15:03:54	40.7	42.72	43.44	46.52	47.04	55.84	41.2	45.8	61.3	53.04	28
15:04:54	40.72	43.12	43.76	46.68	47.12	56.24	40.9	46.1	61.4	53.28	27.4
15:05:54	40.82	43.36	44	46	47.52	56.72	40.2	46.4	61.9	53.44	27.8
15:06:54	40.96	43.28	43.92	46.24	48	57.12	39.7	46.8	62.4	54.16	28.1
15:07:54	40.6	43.04	43.68	46.4	47.92	57.36	39.6	47	62.6	53.68	27.9
15:08:54	41.36	41.84	42.48	46.96	47.76	56.88	40.1	47.8	62.3	53.12	28.5
15:09:54	40.8	41.28	41.84	46.72	46.24	55.12	40.1	48.3	59.8	51.68	26.9
15:10:54	40.09	40.94	41.52	45.84	45.12	53.84	39.2	48	57.3	50.56	27.8
15:11:54	39.28	41.36	42.08	44.8	44.72	53.68	39.6	46.9	56	50.4	28.2
15:12:54	39.55	41.04	41.76	44.56	44.4	53.12	39.2	46.4	55.4	50	28.6
15:13:54	39.41	42.08	42.72	44.24	44.96	53.52	39.6	45.8	55.6	50.48	28.5
15:14:54	40.17	41.92	42.64	44.48	45.52	53.84	40.2	45.4	56.3	50.8	28.8
15:15:54	40.04	42.4	43.2	44.64	45.84	54.32	40.9	45.3	56.8	51.28	28.3
15:16:54	40.24	42.8	43.6	44.8	46.48	54.8	40.5	45.4	57.8	51.68	28.5
15:17:54	40.63	42.96	43.92	45.12	46.64	55.28	41.9	45.8	58.6	52.24	29.2
15:18:54	40.92	43.12	44.16	45.52	47.2	55.68	41.5	46.2	59.2	52.48	28.5
15:19:54	40.96	42.88	43.92	45.76	47.76	55.92	42.1	46.6	59.8	52.64	26.8
15:20:54	40.9	42.72	43.84	46.08	47.6	56.08	41.9	47	60.1	52.8	27.9
15:21:54	40.77	42.88	44	46.16	47.36	56.08	41.1	47.3	60	52.72	28.7
15:22:54	41.04	43.04	44.16	46.24	47.76	56.24	41.8	47.5	60.1	52.64	27.7
15:23:54	41.04	43.12	44.24	46.32	47.76	56.32	40.6	47.6	60	52.96	28.2
15:24:54	41.12	43.2	44.32	46.32	47.68	56.32	40.7	47.7	59.8	52.96	28.3
15:25:54	41.76	42	42.8	46.48	46.88	54.8	41	48	58.3	51.6	27.9
15:26:54	41.2	41.52	42.24	45.92	45.76	53.2	40.2	48	55.7	50.24	27.6
15:27:54	40.07	42.32	43.28	44.88	45.76	53.44	40.1	47	55	50.48	27.7
15:28:54	39.97	42.72	43.52	44.48	46.16	53.92	40.1	46.2	55.6	50.8	27.8
15:29:54	40.29	42.48	43.44	44.56	46.56	54.32	39.7	45.9	56.4	51.2	27.8
15:30:54	40.53	42.8	43.76	44.88	46.88	54.72	39.3	45.9	57	51.76	28.6
15:31:54	41.44	41.68	42.48	45.2	46.8	54.16	38.8	46.1	57	51.28	28.3
15:32:54	40.12	41.6	42.64	45.12	45.76	53.04	38.8	46.8	55.2	50.24	27.2

15:33:54	39.82	41.84	42.96	45.32	45.76	53.52	38.9	45.9	55.2	50.56	28.9
15:34:54	40	42	43.2	45.4	46.08	53.84	39.5	45.5	55.7	50.96	28.6
15:35:54	40.26	42.24	43.52	45.4	46.4	54.24	39.4	45.5	56.3	51.28	28.2
15:36:54	40.65	42.32	43.6	46.64	46.96	54.56	40.1	45.7	57	51.76	27.8
15:37:54	40.46	42.16	43.52	46.8	47.2	54.8	39.7	45.9	57.4	51.68	27.7
15:38:54	40.38	42.08	43.6	46.96	47.12	54.96	38.6	46.1	57.8	52	29
15:39:54	40.24	42	43.44	47.28	47.44	55.12	41.1	46.5	58.2	51.92	28.9
14:40:54	40.29	42.08	43.6	47.36	47.28	55.36	41	46.8	58.5	51.92	28.6
15:41:54	40.31	41.92	43.6	47.36	47.28	55.44	40.8	47	58.6	51.76	29.2
15:42:54	40.43	42.4	43.84	47.44	47.44	55.6	41.5	47	58.7	52.16	28.5
15:43:54	40.65	42.64	44.16	47.6	47.6	55.76	40.5	47.2	58.9	52.48	28.4
15:44:54	40.75	42.56	44.24	46.6	47.44	55.76	41.2	47.3	58.8	52.48	29
15:45:54	40.72	42.4	44	46.68	47.76	55.84	41.5	47.4	59	52.24	28.6
15:46:54	40.68	42.4	43.92	46.68	47.76	56	40	47.6	59.1	52.4	28.4
15:47:54	40.58	42.16	43.84	46.6	47.44	55.84	40.2	47.6	59	52.32	28.8
15:48:54	40.72	42.32	44	46.6	47.44	55.84	40.3	47.5	59	52.4	28.6
15:49:54	40.9	42.56	44.16	46.76	47.68	55.92	40.1	47.7	59	52.4	28.4
15:50:54	41.04	42.48	44.08	46.84	48.16	56.08	39.5	47.8	59.2	52.64	28.8
15:51:54	40.87	42.24	43.92	46.92	48.00	56.08	40.3	47.8	59.2	52.4	28.4
15:52:54	40.51	42	43.76	47.84	47.84	56.08	40.3	47.8	59.2	52.48	28
15:53:54	40.53	42.08	43.84	47.84	47.76	56.16	40.3	47.8	59.2	52.56	28.8
15:54:54	40.6	42.16	44	47.76	47.44	56.16	39.5	47.8	59	52.48	28.6
15:55:54	40.82	42.32	44.08	47.68	47.6	56.08	39.1	47.8	58.9	52.32	27.8
15:56:54	41.04	42.48	44.16	47.68	47.6	56.00	38.5	47.8	58.7	52.40	28.5
15:57:54	41.28	42.64	44.4	47.68	47.68	56.00	37.5	47.7	58.6	52.56	28.5
15:58:54	41.12	42.64	44.24	47.76	47.92	55.92	40.6	47.8	58.5	52.32	28.4
15:59:54	41.28	42.64	44.32	47.68	47.84	55.92	40.3	47.8	58.4	52.48	28.8
16:00:54	41.44	42.96	44.48	47.76	48	55.84	39.9	47.7	58.3	52.4	28.7
16:01:54	41.68	43.12	44.64	47.84	48.24	55.92	39.4	47.8	58.3	52.56	28
16:02:54	41.84	43.04	44.64	47.84	48.56	56.08	39.9	47.8	58.4	52.48	28.2

16:03:54	41.6	42.8	44.4	47.84	48.4	56.08	40	47.8	58.4	52.56	27.6
16:04:54	41.6	42.72	44.4	47.76	48.24	56.08	40.4	47.8	58.4	52.48	28.3
16:05:54	41.6	42.64	44.4	47.76	48.16	56.00	40.2	47.8	58.4	52.48	28.3
16:06:54	41.68	42.88	44.48	47.76	48.24	56.00	40.6	47.8	58.3	52.56	28.5
16:07:54	41.76	42.8	44.48	47.84	48.16	55.84	39.8	47.8	58.1	52.48	28.3
16:08:54	41.92	42.8	44.32	47.68	48.00	55.68	39.9	47.8	57.8	52.4	28.4
16:09:54	42.08	42.56	43.76	47.68	47.52	54.8	40.1	47.8	56.8	51.76	28.2
16:10:54	41.84	42.16	43.12	46.44	47.04	53.84	40	47.8	55.4	50.72	27.6
16:11:54	41.36	42.4	43.68	46.04	46.96	53.84	39.8	47.3	54.9	50.64	28
16:12:54	41.28	42.4	43.84	45.64	46.88	53.84	39.7	46.8	54.8	50.8	27.9
16:13:54	41.28	42.16	43.68	45.56	46.96	53.92	40.1	46.5	54.9	50.72	28.00
16:14:97	41.28	42.08	43.76	45.4	46.88	53.92	39.9	46.3	55.00	50.8	28.2
16:15:54	41.44	42.08	43.68	45.4	46.8	53.84	39.6	46.2	55.1	50.56	28.7
16:16:54	41.52	42.16	43.84	45.4	46.8	53.84	39.2	46.2	55	50.8	28.2
16:17:54	41.6	42.16	43.76	45.4	46.96	53.84	39.2	46.2	55.2	50.72	28.2
16:18:54	41.6	42.08	43.76	45.4	47.2	53.84	39.5	46.2	55.4	50.8	28.4
16:19:54	41.6	42	43.68	45.4	47.04	53.84	39.3	46.2	55.3	50.64	28.4
16:20:54	41.92	41.76	43.04	45.48	47.36	53.68	39.6	46.2	55.4	50.64	27.2
16:21:54	41.52	40.94	41.76	45.56	46	52.16	39.2	46.4	54	49.28	27
16:22:54	40.43	40.68	41.68	44.92	44.56	50.88	39.1	46.3	51.8	48.08	27.5
16:23:54	40.55	40.29	41.04	43.2	44.16	50.24	39.1	45.3	50.6	47.6	28.4
16:24:54	39.82	40.51	42	43.48	43.84	50.08	39.2	44.8	49.8	47.36	28.4
16:25:54	40.29	40.63	42.24	44.16	44.4	50.32	39.3	44.1	50.2	47.6	28.6
16:26:54	40.55	40.55	42.24	44.16	44.96	50.64	38.4	43.9	50.9	47.84	27.9
16:27:54	40.63	40.48	42.24	45.24	45.12	50.72	38.8	43.9	51.4	48.00	27.9
16:28:54	40.58	40.24	42.08	45.4	45.12	50.8	39.2	44	51.6	47.92	28.2
16:29:54	40.46	40.26	42.16	45.32	45.04	50.88	39.9	44	51.8	48	27.4
16:30:54	40.53	40.29	42.16	45.48	45.28	51.04	39.4	44.2	52.2	48.16	27.4
16:31:54	40.51	40.24	42.16	45.56	45.12	51.12	39.4	44.2	52.3	48.16	27.6
16:32:54	40.58	40.34	42.32	45.56	45.2	51.12	39.4	44.3	52.6	48.24	27.7

16:33:54	40.65	40.34	42.4	45.64	45.2	51.2	39.4	44.3	52.7	48.48	28
16:34:54	40.82	40.51	42.56	45.64	45.2	51.28	39.3	44.4	52.7	48.4	28.4
16:35:54	41.04	40.68	42.72	45.72	45.44	51.36	39.7	44.5	52.9	48.64	27.7
16:36:54	41.2	40.8	42.8	45.88	45.6	51.52	39.9	44.6	53	48.72	27.5
16:37:54	41.36	40.85	42.88	45.88	45.76	51.68	40.1	44.7	53.2	49.04	27.6
16:38:54	41.36	40.68	42.72	45.96	45.76	51.76	39.9	44.8	53.2	48.88	28.7
16:39:54	41.12	40.38	42.48	45.96	45.6	51.68	40.1	44.9	53.2	48.8	28.4
16:40:54	41.2	40.68	42.72	46.04	45.6	51.68	39.8	45	53.2	48.8	27.7
16:41:54	41.36	40.75	42.8	45.96	45.52	51.68	39.3	45	53.1	48.88	28.1
16:42:54	41.52	40.8	42.88	45.04	45.68	51.6	39.3	45	53	48.8	28.2
16:43:54	41.52	40.58	42.72	44.96	45.68	51.52	40.1	45	52.8	48.56	28.1
16:44:54	41.36	40.43	42.56	44.96	45.76	51.44	40	45	52.7	48.56	27.2
16:45:54	41.28	40.29	42.4	44.96	45.76	51.36	39.3	45.1	52.7	48.4	29
16:46:54	41.12	40.43	42.56	44.88	45.52	51.28	39.9	45.2	52.5	48.4	29
16:47:54	41.2	40.63	42.72	44.72	45.12	51.04	39.6	45	52	48.24	28.7
16:48:54	41.36	40.53	41.6	43.8	44.72	50.16	39.2	44.8	51.2	47.84	28.3
16:49:54	40.8	40.12	41.04	43.48	43.84	49.04	39	44.6	49.8	46.72	27.7
16:50:54	40.51	40	41.6	43.92	43.68	48.88	38.6	44.1	48.9	46.4	28.1
16:51:54	40.87	40.14	41.92	43.68	44.16	49.04	38.4	43.8	49	46.64	28.1
16:52:54	40.87	39.97	41.68	43.52	44.32	48.96	38.9	43.5	49	46.64	27.2
16:53:54	40.96	39.87	41.04	43.52	44.16	48.64	38.6	43.1	48.8	46.32	27.6
16:54:54	40.55	39.82	41.52	43.28	43.68	48.4	39.5	43.3	48.4	46.16	27.9
16:55:54	40.7	39.6	40.53	43.28	43.52	47.76	39.7	42.9	48	45.76	27.1
16:56:54	39.75	39.21	40.53	42.04	42.64	46.96	40	43	48	44.96	27.5
16:57:54	39.92	39.16	40.92	42.58	42.8	46.04	40	42.5	47.6	44.96	27.6
16:58:54	40.17	39.24	40.96	42.37	43.12	46.2	39.2	42.2	47.7	44.96	27.5
16:59:54	40.14	39.01	40.8	42.26	42.88	46.96	39.2	42.1	47.6	44.72	27.8
17:00:54	40.26	39.06	40.77	42.2	43.12	46.88	39.7	42	47.7	44.8	27.1
17:01:54	40.17	39.04	40.85	42.11	42.88	46.88	39.4	42	47.6	44.72	27.6
17:02:54	40.29	39.16	40.94	42.03	42.96	46.8	39.1	41.9	47.6	44.72	27.4

17:03:54	40.36	39.14	40.96	42.05	43.04	46.88	38.2	41.8	47.7	44.72	27.8
17:04:54	40.21	39.06	40.29	42.18	42.48	46.24	38.4	41.8	47.4	44.48	27.4
17:05:54	40.07	39.01	40.63	41.86	42.32	46.08	38.2	41.8	46.8	44.16	27.8
17:06:54	40.21	38.97	40.7	41.67	42.56	46.08	38.4	41.6	46.8	44.08	27.2
17:07:54	40.34	39.04	40.51	41.65	42.64	46.08	38.8	41.4	46.8	44.16	27.1
17:08:54	40.29	39.04	40.53	41.63	42.48	45.92	38.4	41.4	46.6	44	27.4
17:09:54	39.9	38.67	39.43	41.65	42	45.12	38.2	41.3	46.1	43.36	26.7
17:10:54	39.09	38.16	38.77	41.34	41.12	44.16	38.4	41.1	45	42.48	26.7
17:11:54	38.52	37.74	38.3	39.88	40.46	43.36	38	40.7	44.9	41.76	26.5
17:12:54	38.01	37.32	37.89	39.31	39.75	42.64	38.2	40.1	44.8	41.04	26.4
17:13:54	37.76	37.18	37.64	38.87	39.28	42	37.6	39.6	44	40.55	26.4
17:14:54	37.47	36.93	37.37	38.47	38.89	41.44	38.1	39	43.3	40.04	26.4
17:15:54	37.2	36.64	37.08	38.04	38.48	40.94	38.4	39.5	42.6	39.6	26.1
17:16:54	37.03	36.56	36.96	38.7	38.23	40.53	37.5	39	42.1	39.24	26

APPENDIX 5

THEORETICALLY COMPUTED TEMPERATURES

Table 5.1: DTPM Computed Temperatures (17/02/2005, day of the year: 48)

Atmospheric pressure: 84052.08 Pa

SOLAR TIME	Tt1 (Deg.C)	Tf11 (Deg.C)	T11 (Deg.C)	Tab1 (Deg.C)	Tf21 (Deg.C)	Tbp1 (Deg.C)	AINTf (Deg.C)	CEF
11:18	34.02	34.73	35.47	56.67	49.57	46.84	30.58	0.711
11:20	33.9	34.73	35.51	56.67	49.61	46.83	30.63	0.718
11:22	35.85	35.71	36.64	58.22	52.75	50.77	29.93	0.746
11:24	36.1	35.78	37.65	58.22	52.79	50.91	31.36	0.722
11:26	36.15	35.82	38.66	58.24	52.85	50.96	31.33	0.759
11:28	39.21	40.23	42.31	60.23	53.14	52.61	29.63	0.736
11:30	39.07	41.25	42.3	60.24	53.18	52.6	30.06	0.751
11:32	36.29	41.05	43.74	57.37	52.57	50.98	32.86	0.721
11:34	35.28	38.3	41.25	55.43	51.61	50.93	32.65	0.691
11:36	35.43	38.28	41.25	55.43	51.61	50.94	30.14	0.71
11:38	35.14	38.25	41.31	55.91	50.56	49.58	31.6	0.709
11:40	39.74	45.15	50.63	59.71	52.95	51.74	30.63	0.73
11:42	41.26	47.61	50.04	60	53.66	52.98	32.63	0.719
11:44	34.77	40.22	45.6	56.36	52.15	51.17	33.05	0.739
11:46	34.07	36.72	39.3	54.03	50.42	48.92	33.26	0.709
11:48	40.28	46.16	45.11	56.8	51.79	49.34	30.25	0.73
11:50	41.35	46.19	46.09	58.34	52.29	49.68	30.89	0.723
11:52	42.41	47.93	47.51	60.85	52.92	51.68	31.78	0.711
11:54	43.65	48.47	49.37	63.08	52.99	52.62	32.62	0.709
11:56	41.2	48.98	49.83	67.43	58.78	52.93	34.43	0.692
11:58	40.92	53.92	56.72	74.79	62.73	60.36	36.29	0.711

12:00	41.48	54.65	57.91	76.13	64.25	62.19	37.69	0.69
12:02	41.45	54.67	57.91	76.22	64.34	62.26	38.86	0.692
12:04	41.32	54.68	57.86	77.28	64.34	62.25	38.96	0.693
12:06	41.37	54.62	57.81	77.3	64.41	62.31	38.23	0.7
12:08	42.05	54.91	57.77	76.26	64.1	62.41	35.63	0.717
12:10	45.15	56.56	58.05	75.05	63.62	62.72	35.41	0.724
12:12	44.88	56.58	58.02	75.05	63.58	62.55	34.76	0.705
12:14	43.92	56.5	57.98	75.09	63.52	62.19	35	0.713
12:16	40.17	54.3	57.91	75.5	63.92	60.91	34.72	0.693
12:18	41.66	56.18	60.77	80.43	66.94	65.29	37.86	0.683
12:20	46.06	58.58	60.97	77.16	63.35	65.08	37.81	0.719
12:22	43.12	54.86	56.54	76.57	60.32	60.35	36.35	0.726
12:24	39.08	50.32	51.48	73.57	58.31	55.5	31.83	0.731
12:26	39.16	50.3	51.38	73.53	59.27	55.5	31.77	0.73
12:28	39.78	50.28	51.3	73.53	59.24	55.71	31.42	0.72
12:30	39.88	50.45	51.24	73.53	60.3	55.67	31.39	0.723
12:32	40.09	50.52	51.2	73.57	61.31	55.7	31.14	0.712
12:34	40.91	50.78	51.26	73.69	60.4	55.95	30.95	0.707
12:36	40.81	50.97	51.22	73.68	60.48	55.88	31.63	0.726
12:38	41.6	51.26	51.41	74.25	62.55	55.78	31	0.705
12:40	43.2	54.93	56.73	79.85	65.79	60.52	32.71	0.698
12:42	42.67	54.95	56.67	79.87	65.84	60.37	33.21	0.711
12:44	43.08	54.48	55.84	77.86	65.55	59.74	32.69	0.728
12:46	43.19	54.47	55.74	77.82	65.51	59.73	32.63	0.727
12:48	39.76	51.17	52.51	74.67	64.3	55.4	29.71	0.729
12:50	39.75	51.15	52.43	74.67	64.26	55.41	29.35	0.719
12:52	40.61	51.29	52.39	74.77	64.29	55.56	28.84	0.707
12:54	40.82	51.43	52.35	74.8	64.34	55.59	29.02	0.711
12:56	43.66	55.58	57.57	80.81	65.65	60.27	33.46	0.696
12:58	44.03	55.64	57.51	81.26	65.66	59.95	33.94	0.706

13:00	43.88	55.72	57.47	81.29	65.74	60	33.97	0.711
13:02	43.18	55.55	57.51	81.35	65.82	60.02	33.95	0.705
13:04	43.3	55.42	57.48	81.36	65.85	60.19	34.05	0.707
13:06	39.78	50.1	50.36	71.2	58.41	54.04	29.23	0.708
13:08	39.71	47.17	48.57	71.66	58.39	52.44	33.98	0.724
13:10	39.77	47.15	48.52	69.63	54.34	52.42	30.55	0.719
13:14	39.92	47.15	48.51	69.68	54.31	52.43	30.28	0.73
13:14	38.11	47.19	48.46	69.64	54.28	52.48	32.31	0.722
13:16	40.26	44.78	45.23	66.14	55.51	50.11	32.48	0.731
13:18	42.67	48.74	50.88	68.56	57.47	53.73	33.51	0.734
13:20	41.54	48.86	52.24	71.58	59.82	53.78	35.92	0.726
13:22	40.9	48.45	51.91	70.93	59.59	54.34	35.28	0.716
13:24	41.12	51.61	58.1	78.65	62.22	55.35	37.71	0.705
13:26	42.83	52.84	60.92	79.26	64.22	58.04	39.79	0.695
13:28	42.89	52.86	60.87	79.27	64.02	58.12	39.54	0.709
13:30	42.59	52.87	60.81	79.27	64.08	58.2	39.92	0.711
13:32	40.71	50.92	55.05	76.53	63.12	58.24	38.59	0.724
13:34	42.09	51	54.85	74.65	62.5	57.48	39.89	0.721
13:36	41.81	51.41	55.07	76.32	62.93	56.53	40.39	0.71
13:38	41.76	51.41	55.09	76.69	64.36	56.68	40.1	0.715
13:40	41.42	52.59	57.83	79.18	64.43	59.1	39.71	0.7
13:42	41.36	52.61	57.77	79.17	64.39	59.04	39.9	0.719
13:44	41.79	52.58	57.72	79.15	64.43	59.05	43.75	0.721
13:46	41.84	52.69	57.66	79.12	64.45	59.02	42.31	0.727
13:48	43.64	53.61	57.76	77.23	64.52	58.97	42.83	0.734
13:50	44.06	51.98	53.82	72.86	61.58	58.96	39.53	0.728
13:52	43.69	51.95	53.77	72.88	61.43	59	39.52	0.732
13:54	40.7	48.57	50.36	70.53	58.38	56.95	36.39	0.712
13:56	40.87	48.54	50.31	70.54	58.46	56.89	36.19	0.714
13:58	41.14	48.63	51.29	70.84	58.97	58.72	35.01	0.73

14:00	41.19	48.68	51.26	70.87	59.01	58.78	35.11	0.733
14:02	41.29	49.03	51.85	71.67	59.69	59.34	35.38	0.72
14:04	41.05	49.4	52.8	73.28	60.99	60.35	36.48	0.716
14:06	40.69	50.34	55.06	77.34	64.34	63.04	40	0.708
14:08	40.78	50.36	55.02	77.33	64.39	63.12	39.91	0.725
14:10	40.88	50.38	54.96	77.29	64.43	63.2	40.27	0.736
14:12	40.92	50.41	54.94	77.3	64.46	63.24	39.93	0.722
14:14	41.32	50.01	53.63	73.85	61.2	61.48	38.59	0.712
14:16	39.55	46.4	48.17	67	54.94	53.53	32.4	0.72
14:18	40.78	48.52	51.34	72	58.03	56.68	33.77	0.718
14:20	44.12	52.44	55.84	75.93	62.68	61.1	37.96	0.713
14:22	43.88	52.46	55.82	75.96	62.72	61.04	38.23	0.721
14:24	39.05	45.93	47.74	68.56	58.66	57.05	37.98	0.69
14:26	39.1	45.91	47.71	68.57	58.61	57.02	36.47	0.707
14:28	39.07	45.9	47.65	68.53	57.59	56.97	35.9	0.725
14:30	39.14	45.88	47.62	68.53	57.55	56.96	35.5	0.71
14:32	39.3	45.88	47.59	68.5	56.54	56	34.63	0.716
14:34	39.28	45.92	47.56	68.49	56.53	55.95	34.54	0.713
14:36	39.22	45.92	47.56	68.51	56.51	55.89	34.24	0.701
14:38	40.34	48.01	50.75	73.02	59.1	56.81	34.96	0.715
14:40	40.29	48.03	50.74	73.04	59.15	56.83	35.32	0.725
14:42	38.18	46.49	49.7	71.85	58.23	55.94	36.14	0.711
14:44	40.73	47.39	49.01	69.36	56.57	55.09	34.86	0.72
14:46	40.78	47.38	48.97	69.31	56.53	55.07	34.82	0.72
14:48	39.89	46.23	47.5	67.08	54.51	53.22	33.04	0.723
14:50	39.69	43.94	44.13	63.79	52.37	52.16	32.75	0.707
14:52	39.51	43.92	44.12	63.8	52.33	52.05	31.26	0.721
14:54	39	43.85	44.1	63.78	52.28	51.88	31.78	0.713
14:56	38.77	43.66	44.09	63.8	52.2	51.76	31.04	0.713
14:58	38.17	43.34	44.03	64.12	52.05	51.22	30.92	0.712

15:00	38.47	43.19	44.01	64.13	52.02	51.35	31	0.719
15:02	38.55	43.25	44.01	64.24	51.08	51.41	31.48	0.734
15:04	38.13	44.77	46.48	66.8	53.5	53.76	30.03	0.714
15:06	38.66	44.79	46.48	66.81	53.54	54	30.03	0.725
15:08	38.41	44.97	46.49	66.84	53.64	53.94	30.39	0.723
15:10	38.21	44.65	46.04	65.45	51.83	52.48	30.35	0.718
15:12	37.69	43.2	44.65	61.6	49.53	49.68	28.83	0.714
15:14	38.1	43.16	44.19	60.67	48.81	48.17	28.54	0.722
15:16	34.99	36.91	37.77	59.66	46.62	46.6	28.35	0.715
15:18	35.32	36.93	38.7	59.78	47.55	48.51	29.35	0.719
15:20	35.13	36.98	38.7	59.77	47.54	48.43	32.04	0.705
15:22	35.22	36.94	38.74	59.8	47.51	48.44	29.31	0.695
15:24	34.78	36.05	37.26	56.9	44.26	45.67	26.29	0.716
15:26	34.64	35.92	37.12	56.64	44.03	45.47	26.09	0.715
15:28	34.86	35.9	37.15	56.66	44.99	45.49	25.49	0.724
15:30	35.06	35.97	37.17	56.66	44.98	45.5	25.54	0.728
15:32	35.13	36.06	37.2	56.66	44.98	45.47	25.48	0.724
15:34	35.29	36.12	37.22	56.65	44.98	45.49	25.86	0.722
15:36	36.61	39.89	43.23	65.41	49.07	51.14	27.23	0.719
15:38	36.46	39.9	43.35	65.83	49.19	51.01	27.38	0.715
15:40	36.39	40.32	43.33	67.14	50.45	52.18	28.41	0.71
15:42	36.83	40.34	44.34	67.14	50.49	52.4	28.92	0.727
15:44	37.03	40.5	44.34	67.09	49.58	52.51	29.28	0.706
15:46	37.04	40.44	43.79	65.17	48.38	51.72	28.58	0.701
15:48	37.25	40.45	43.65	64.81	48.09	51.52	28.33	0.71
15:50	34.9	36.24	37.52	55.65	44.91	44.61	26.32	0.721
15:52	35.33	36.29	37.49	55.56	45.05	44.67	26.2	0.725
15:54	35.46	36.36	37.55	55.61	45.03	44.62	25.43	0.718
15:56	37.18	39.62	42.13	61.39	45.66	48.29	25.32	0.702
15:58	38.48	40.23	41.99	60.45	45.23	48.72	25.81	0.715

16:00	38.51	40.23	42.03	60.43	45.3	48.69	24.77	0.718
16:02	36.16	36.87	37.52	58.59	42.48	44.38	24.98	0.718
16:04	34.92	36.23	37.48	57.84	42.02	44.19	25.18	0.705
16:06	36.92	36.98	38	56.62	41.93	43.2	25.51	0.707
16:08	36	36	37.94	54.89	41.4	43.65	25.05	0.711
16:10	35.96	35.98	37.96	54.86	41.75	43.57	25.73	0.67
16:12	36.24	35.97	37.99	54.85	41.7	43.62	26.61	0.696
16:14	36.52	36.06	38.04	54.84	41.7	43.66	25.49	0.725
16:16	36.84	36.2	38.11	54.85	41.71	43.7	25.41	0.716
16:18	36.75	36.43	38.2	55.01	41.72	43.47	25.69	0.724
16:20	35.22	35.98	37.67	55.51	40.48	42.94	24.56	0.714
16:22	35.13	35.95	37.71	54.5	41.24	42.83	25.77	0.722
16:24	34.99	35.93	37.73	54.46	41.05	42.74	25.55	0.712
16:26	35.76	36.02	37.26	52.87	39.18	42.14	24.28	0.713
16:28	36.01	36.55	38.04	50.13	38.51	41.19	24.29	0.709
16:30	36.08	36.48	37.81	49.98	38.91	40.22	25.26	0.716
16:32	36.04	36.46	37.83	49.94	40.22	40.13	26.12	0.714
16:34	34.83	35.51	37.1	49.87	38.99	40.12	25.28	0.711
16:36	35.09	35.48	37.17	49.9	38.06	40.1	25.48	0.694

Table 5.2: TPM Program Computed Temperatures (29/10/2004, day of the year: 303)

Atmospheric Pressure: 83918.7 Pascals.

SOLAR TIME	Tt1 (Deg C)	Tf11 (Deg C)	T11 (Deg C)	Tf21 (Deg C)	Tab1 (Deg C)	Tf31 (Deg C)	Tbp1 (Deg C)	Efficiency
12:38	27	34.02	40.77	39.85	60.11	49	47.91	0.837
12:40	29.6	31.55	41.97	40.71	81.7	55.66	57.8	0.812
12:42	29.57	30.6	40.91	39.14	75.82	53.02	55.12	0.812
12:44	29.41	29.66	40.71	38.9	80.15	53.87	56.21	0.786
12:46	29.68	29.69	40.66	38.88	79.8	53.85	56.33	0.778
12:48	30.02	29.71	40.84	39.16	81.92	54.57	57.16	0.763
12:50	30.02	29.43	41.34	39.46	85.64	55.87	59.08	0.77
12:52	27.74	29.02	38.58	37.89	68.77	49.63	55.19	0.8
12:54	27.74	28.89	38.48	36.77	68.64	49.5	51.04	0.792
12:56	30.95	29.8	42.08	40.43	90.56	58	61.81	0.742
12:58	32.28	30.75	44.49	42.19	96.46	61.07	65.6	0.745
13:00	31.55	30.76	44.67	42.07	95.08	60.77	65.65	0.779
13:02	31.68	30.8	44.98	42.2	96.66	61.3	66.11	0.766
13:04	32.33	31.02	45.6	42.89	99.25	62.47	67.58	0.76
12:06	33.67	31.29	48.35	44.95	101.5	67.78	75.13	0.757
13:08	33.49	31.12	48.55	44.79	101.12	67.68	75.37	0.775
13:10	33.99	31.69	48.72	45.24	100.82	67.92	75.33	0.764
13:12	32.78	31.38	49.12	45.19	102.1	68.22	75.85	0.769
13:14	33.36	31.49	49.21	45.14	100.81	67.91	75.59	0.776
13:16	33.06	31.27	49.12	44.85	99.92	67.44	75.1	0.783
13:18	33.98	31.77	49.43	45.47	101.6	68.22	75.49	0.758
13:20	34.08	32.02	49.52	45.7	101.77	68.45	75.68	0.76
13:22	34.51	32.41	49.95	46.19	102.8	69.1	76.29	0.756
13:24	34.41	32.46	50.11	46.15	101.86	68.92	76.33	0.772
13:26	32.87	32.31	48.93	44.97	103.98	65.64	71.85	0.786
13:28	34.32	32.5	50.13	46.29	105.86	69.17	76.31	0.758

13:30	30.43	31.88	43.86	41.15	81.07	56.01	58.53	0.806
13:32	29.86	31.48	41.32	39.47	72.45	52.3	53.69	0.798
13:34	29.13	30.78	39.88	38.32	68.95	50.46	51.53	0.805
13:36	30.57	31.09	40.44	39.44	75.78	52.98	54.21	0.742
13:38	29.33	30.63	39.69	38.38	70.65	50.98	52.3	0.794
13:40	32.35	31.46	42.26	41.06	84.96	56.8	59.18	0.735
13:42	34.18	31.72	47.67	44.83	88.54	66.75	73.35	0.754
13:44	34.25	32.13	48.1	45.25	98.88	67.17	73.72	0.752
13:46	34.36	32.15	48.98	45.59	100.55	67.96	74.89	0.76
13:48	33.73	32.23	49.31	45.74	101.03	68.24	75.26	0.76
13:50	33.89	32.63	49.59	46.02	100.26	68.29	75.18	0.764
13:52	33.85	31.98	49.61	45.5	100.18	67.93	75.2	0.782
13:54	34.97	32.72	49.73	45.93	98.8	67.78	74.37	0.763
13:56	34.94	32.82	49.84	46.06	99.19	67.91	74.41	0.763
13:58	34.65	33.2	49.94	46.39	99.39	68.17	74.42	0.756
14:00	34.66	32.88	49.96	46.16	99.38	68.04	74.49	0.77
14:02	34.66	32.75	49.99	46.06	99.48	68	74.57	0.765
14:04	34.98	33.09	50.05	46.32	99.32	68.17	74.56	0.763
14:06	32.42	32.42	46.84	43.36	82.75	61.1	65.34	0.801
14:08	31.02	31.94	42.77	40.49	76.43	54.18	55.99	0.8
14:10	29.47	31.5	39.13	37.93	61.85	48.22	48.29	0.788
14:12	29.36	31.35	37.87	37.2	58.15	46.64	46.24	0.758
14:14	28.94	31.05	36.94	36.52	55.34	45.38	44.74	0.754
14:16	28.29	30.6	38.08	35.77	52.9	44.18	43.37	0.754
14:18	28.37	30.53	36	35.69	52.81	44.08	43.26	0.731
14:20	28.38	30.35	35.87	35.56	53.06	43.99	43.09	0.71
14:22	29.95	30.62	37.64	37.52	65.8	48.75	48.75	0.715
14:24	30.76	30.98	39.06	38.63	71.3	51.12	51.78	0.727
14:26	28.94	30.59	39.78	38.84	74.7	52.25	53.53	0.756
14:28	28.96	30.39	38.95	37.75	67.76	49.7	50.67	0.779

14:30	30.76	30.62	41.34	40.02	72.68	55.39	57.73	0.745
14:32	39.61	30.75	39.73	38.3	69.13	50.5	51.58	0.772
14:34	31.99	31.32	42.08	40.73	73.25	56.07	58.28	0.737
14:36	31.95	30.98	42.13	40.91	73.24	56.21	58.37	0.748
14:38	29.4	30.92	39.93	38.41	68.39	50.39	51.38	0.794
14:40	29.48	30.96	38.33	37.34	61.57	47.69	47.79	0.764
14:42	29.85	31.71	38.35	37.73	64.67	48.64	48.55	0.727
14:44	33.23	32.55	44.15	42.4	92.4	59.98	63.5	0.735
14:46	34.94	33.01	47.7	44.89	93.72	65.21	70.3	0.736
14:48	35.12	32.23	48.44	45.45	94.53	65.9	71.08	0.743
14:50	33.96	32.25	48.74	44.96	95.26	65.88	71.85	0.769
14:52	33.93	32.2	49.72	45.63	99.51	67.65	74.26	0.754
14:54	34.22	32.14	50.44	46	102.16	68.77	75.97	0.755
14:56	31.72	31.47	48.99	44.52	91.8	64.68	70.49	0.776
14:58	30.47	31.75	44.71	41.34	84.48	57.16	60.3	0.797
15:00	31.52	32.07	42.48	40.17	75.3	53.61	55.24	0.769
15:02	32.9	32.2	43.39	41.51	83.53	56.73	58.76	0.738
15:04	33.86	32.78	45.46	43.02	92.96	60.64	64.2	0.746
15:06	35.48	31.91	47.22	44.34	98.29	63.18	67.32	0.738
15:08	34.41	32.4	47.41	43.77	98.96	63.08	68.02	0.771
15:10	34.67	32.33	47.44	43.88	96.59	62.55	67.15	0.76
15:12	33.15	32.09	47.31	43.66	95.31	62.03	66.51	0.77
15:14	32.33	31.77	45.13	41.89	84.6	57.58	60.53	0.781
15:16	31.07	31.77	41.88	39.63	71.39	52.12	53.27	0.78
15:18	33.01	32.01	44.59	42.17	89.69	59.05	62.22	0.744
15:20	33.24	32.39	44.87	42.3	88.76	59.01	62.32	0.754
15:22	32.72	32.32	43.74	41.25	78.87	55.4	57.27	0.755
15:24	33.76	32.05	45.56	42.86	90.79	59.87	63.04	0.743
15:26	33.74	32.48	45.6	42.67	90.78	59.78	63.11	0.753
15:28	33.4	32.89	46.33	43.33	92.82	60.81	64.18	0.731

15:30	34.12	32.68	46.79	43.79	93.49	61.34	64.68	0.73
15:32	33.86	32.66	46.94	43.67	93.71	61.37	64.97	0.744
15:34	33.79	32.79	47	43.67	93.62	61.38	65.06	0.747
15:36	33.95	32.66	47.15	43.74	93.28	61.38	65.08	0.746
15:38	33.91	32.6	47.18	43.64	93.28	61.31	65.08	0.747
15:40	33.92	32.75	47.2	43.6	93.26	61.28	65.08	0.747
15:42	33.35	32.34	47.33	43.66	92.62	61.15	64.85	0.745
15:44	33.05	32.46	47.33	43.29	92.25	60.82	64.72	0.758
15:46	33.39	32.68	47.33	43.33	91.79	60.7	64.43	0.746
15:48	33.79	32.39	47.34	43.41	91.02	60.51	64.01	0.742
15:50	33.67	32.07	47.24	43.08	90.29	60.09	63.68	0.754
15:52	33.38	32.24	47.14	42.78	89.94	59.78	63.44	0.755
15:54	33.45	32.33	47.13	42.89	89.97	59.83	63.38	0.735
15:56	33.29	32.25	47.1	42.91	89.39	59.68	63.06	0.739
15:58	32.78	32.04	45.76	41.81	82.31	56.84	59.32	0.747
16:00	31.5	31.98	43.76	40.44	74.41	53.57	55.02	0.748
16:02	32.44	32.34	44.51	41.31	81.39	55.99	57.78	0.713
16:04	33.47	32.29	45.17	42.21	85.74	57.89	60.17	0.722
16:06	33.15	32.34	45.58	42.07	84.39	57.57	60.16	0.726
16:08	33.3	31.6	45.68	42.1	84.24	57.54	60.07	0.721
16:10	31.8	31.8	43.71	40.06	74.19	53.25	54.84	0.53
16:12	31.22	32.09	39.98	37.9	58.89	47.38	46.97	0.699
16:14	33.18	32	42.11	39.92	71.65	52.16	52.51	0.675
16:16	33.64	31.71	44	40.89	78.49	54.84	56.22	0.694
16:18	32.99	31.66	44.27	40.77	78.92	54.92	56.56	0.7
16:20	33.7	31.85	44.81	40.97	80.26	55.44	57.25	0.693
16:22	33.59	31.81	44.85	41.11	80.29	55.56	57.3	0.685
16:24	33.64	31.73	45.02	41.09	80.03	55.54	57.43	0.697
16:26	33.02	32.11	44.81	41.51	84.19	56.96	59.3	0.739
16:28	33.55	32.17	45.75	41.54	81.08	56.55	58.45	0.685

16:30	33.83	32.15	46.02	41.45	79.72	55.8	57.79	0.691
16:32	33.47	32.6	46.09	41.33	78.72	55.42	57.29	0.691
16:34	33.9	32.67	46.18	41.55	77.59	55.22	56.67	0.672
16:36	31.58	32.07	46.09	41.39	75.88	54.64	55.93	0.679
16:38	32.12	31.96	42.17	38.7	61.59	48.72	48.57	0.694
16:40	32.46	31.69	42.33	39.07	65.3	49.81	49.51	0.637
16:42	31.17	31.31	42.82	39.08	66.79	50.24	50.22	0.642
16:44	30.96	31.31	41.72	38.13	62.2	48.46	48.5	0.668
16:46	32.37	31.46	40.22	37.28	56.73	46.34	45.79	0.64
16:48	32.15	31.46	41.58	38.38	63.66	48.83	48.37	0.603
16:50	32.42	31.56	41.91	38.5	64.19	49.08	48.78	0.605
16:52	31.86	31.55	42.06	38.6	64.34	49.21	48.92	0.597
16:54	32.07	31.23	41.22	37.79	58.35	47.15	46.7	0.618
16:56	32.28	31.41	41.44	37.8	60.43	47.56	46.93	0.597

COMPUTER PROGRAM

6.1: Program Flow Chart for Solving the temperature equations.

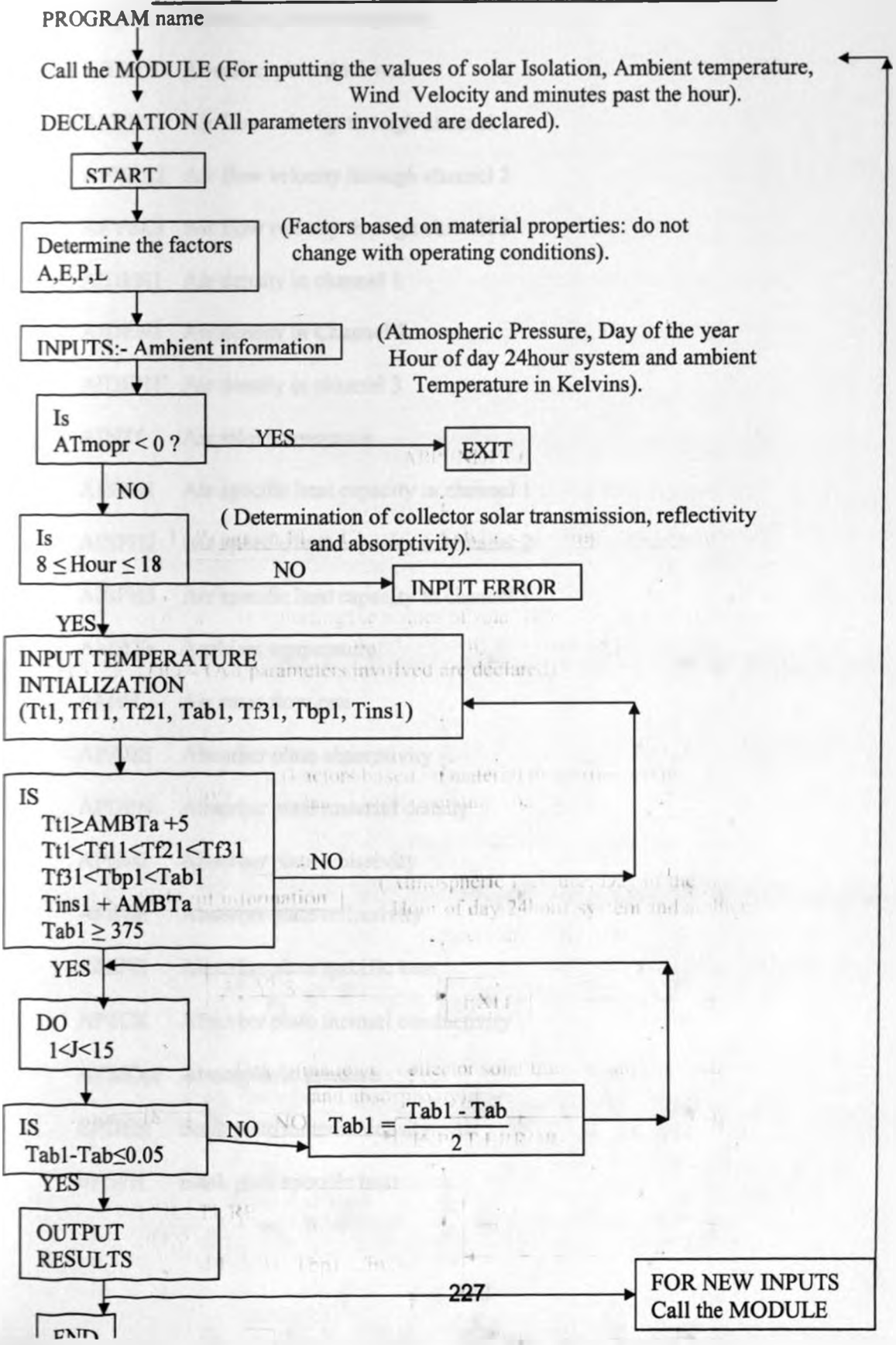

6.2 NOMENCLATURE FOR COMPUTER PROGRAM

ABpab	Absorber plate absorptivity
ABTHI	Absorber plate thickness
AFVEL1	Air flow velocity through channel 1
AFVEL2	Air flow velocity through channel 2
AFVEL3	Air flow velocity through channel 3
AIDEN1	Air density in channel 1
AIDEN2	Air density in Channel 2
AIDEN3	Air density in channel 3
AINTf	Air inlet temperature
AISPH1	Air specific heat capacity in channel 1
AISPH2	Air specific heat capacity in channel 2
AISPH3	Air specific heat capacity in channel 3
AMBTa	Ambient temperature
AMFR	Air mass flow rate
APABS	Absorber plate absorptivity
APDEN	Absorber plate material density
APEMI	Absorber plate emissivity
APREF	Absorber plate reflectivity
APSPH	Absorber plate specific heat
APTCK	Absorber plate thermal conductivity
ATMOpr	Atmospheric pressure
BPDEN	Back plate material density
BPSPH	Back plate specific heat

BPTCK	Back plat material thermal conductivity
BPTHI	Back plate thickness
CLENG	Collector length
CWIDTH	Collector width
Declin	Declination angle
DISINT	Distance interval
Emiabb	Emissivity for air gap between absorber and back plates
Emiab1	Emissivity of air gap between absorber plate and first glass cover
EXCO	Extinction coefficient
FAGH1	First air gap height
FChtc1	Forced convection Nusselt number in first flow channel
FChtc2	Forced convection Nusselt number in second flow channel
FChtc3	Forced convection Nusselt number in third flow channel
F1gab	First glass cover absorption fraction
GASCR	Gas constant
GDEN	Glass density
GEMI	Glass emissivity
GPalre	Glass parallel reflectivity
Gperef	Glass perpendicular reflectivity
GRVACC	Gravitational acceleration
GSPH	Glass specific heat capacity
GTabre	Glass transmittance with both absorption and reflection
GTCK	Glass thermal conductivity
GTHI	Glass thicknesss
GTnoa	Glass transmittance when not absorbing

GTwoa	Glass transmittance with only aborptivity
Hangle	Hour angle
Hour	Local time hour
HTCtf1	Forced convection heat transfer coefficient for first flow channel
HTCtf2	Forced convection heat transfer coefficient for second flow channel
HTCtf3	Forced convection heat transfer coefficient for third flow channel
Hydrad1	Hydraulic diameter for first flow channel
Hydrad2	Hydraulic diameter for second flow channel
Hydrad3	Hydraulic diameter for third flow channel
INang	Incident angle in degrees
INMDEN	Insulation material density
INMSPH	Insulation material specific heat
INS	Insulation
INSem	Insulation emissivity
INShtc	Insulation heat transfer coefficient
INMTCK	Insulation material thermal conductivity
INMTHI	Insulation material thickness
J, K	Integers to determine number of iterations
Lat	Latitude
LE	Less than
PI	Phi
Prand1	Prandtl number in first flow channel
Prand2	Prandtl number in second flow channel
Prand3	Prandtl number in third flow channel
REang	Refractive angle in degrees

Renno1	Reynolds number in first flow channel
Renno2	Reynolds number in second flow channel
Renno3	Reynolds number in third flow channel
RHabbp	Radiation heat transfer coefficient between absorber and back plates
RHBab1	Radiation heat transfer coefficient between absorber plate and first glass cover
Rhina	Radiation heat transfer coefficient between insulation and ambient
RIA	Refractive index of air
RIG	Refractive index of glass
SAGHI	Second air gap height
SIN	Sine
STBCON	Stefan-Boltzmann constant
Tab1	Temperature of the absorber plate
TAGHI	Third air gap height
Tbp1	Temperature of the back plate
Tf11	Temperature of air in the first flow channel
Tf21	Temperature of air in the second flow channel
Tf31	Temperature of air in the third flow channel
TILAN	Tilt angle
TIMINT	Time interval
Tins1	Temperature of insulation
TOPgap	Top glass cover absorption fraction
TPMC	Trple pass mode colector
Tt1	Temperature of top cover
Yn	Day of the year

6.3: COMPUTER PROGRAM FOR THE TRIPLE PASS MODE

```
PROGRAM TPMC
        (!TPMC:Triple pass mode flat plate collector predicts the performance of the
        collector under transient conditions.
        !A list of all variable types and parameters that will be used .
        !Also includes those calculated constants that will not change as the program
        runs).
USE INS     (A Module for inputing the values of solar Insolation, Ambient temperatures,
        Wind velocity, Minutes past the hour)
INTEGER::J,K
REAL::Yn,Hour,DLH,Dsn,RES
REAL:: A,E,C4,L,P,G4,H4,K4,H5,K5,H6,N3,D4,Ub
REAL:: AMBTa,AINTf,AMHChw,SKYTEM,AMRhtc,RHftc,Glref,INang,REang,CEF
REAL::GTnoa,GPeref,GPalre,GTwoa,GTabre,TOPgab,F1rgab,ABpab,RHBab1,HTCtf1,FCh
      tc1,FChtc2
REAL::Renno1,Renno2,Renno3,HTCtf3,HTCtf2,Hydrad1,Hydrad2,FChtc3
REAL::Hydrad3,INShtc,Declin,Hangle,ATMopr,Rhina,Ha,Hab
REAL::Tt1,Tf11,T11,Tab1,Tf21,Tfm1,Tfm2,Tfm3
REAL::Tbp1,Tf31,Tins1
REAL::AIDEN1,AIDEN2,AIDEN3,AISPH1,AISPH2,AISPH3,ADVIS1,ADVIS2,
      ADVIS3,Prand1,Prand2,Prand3,Cp

!Declare Parameters
REAL,PARAMETER::GDEN=2500.0,GSPH=670.0,GTCK=1.04,APDEN=7850.0,
      APSPH=465.0,APTCK=53.6,BPDEN=7850.0,BPSPH=465.5
REAL,PARAMETER::BPTCK=53.6,INMDEN=50.0,TIMINT=100.0,DISINT=0.0078,
      GTHI=0.003,ABTHI=0.0016
REAL,PARAMETER::BPTHI=0.0012,INMSPH=670.0,INMTCK=0.03,CLENG=1.50,
      CWIDTH=0.90,FAGHI=0.02,SAGHI=0.03,TAGHI=0.025
REAL,PARAMETER::STBCON=5.669E8,RIA=1.0,RIG=1.526,EXCO=4.0,
      GEMI=0.012,TILAN=0.0,GRVACC=9.81
REAL,PARAMETER::APEMI=0.94,APREF=0.06,APABS=0.94,GASCR=287.0,
      Lat=0.023,INMTHI=0.01,INSem=0.012
REAL,PARAMETER::Emiab1=83.4,Emiabb=4.41,AFVEL1=1.5,AFVEL2=1.0,
      AFVEL3=1.2,PI=3.14159,AMFR=0.0324

        A=1/(GDEN*GSPH*GTHI)
        E=1/(APDEN*APSPH*ABTHI)
        P=1/(INMDEN*INMTHI*INMSPH)
        L=1/(BPDEN*BPTHI*BPSPH)
WRITE(6,*)'A, E, P'
WRITE(6,*)A,E,P

      DO    380 K=1,1
!Please enter atmospheric pressure, N/m2, Day of the year (count), Hour of day in 24 hour
system, and ambient Temperature, K.
WRITE (6,*) 'Enter ATMOPr,Yn,Hour,AMBTa in this order.'
READ (5,*)ATMOPr,Yn,Hour, AMBTa
```

```
IF (ATMOPr.LE.0) Exit

'Now the Innerloop that inputs data and does preliminary calculations.
        DO 370 I=1,5
    AINTf = T(I)
        AMBTa = T(I)
'For determination of collector components transmission and absorption, enter hours
between 8 and 18.
    Declin=(23.45*SIN(360*((284+Yn)/365)))*PI/180
        IF(Hour.GE.8.AND.Hour.LE.18)THEN
        Hangle=(((Hour-12)*60+U(I))*15/60)*PI/180
        ELSE
                Hangle = 0
        ENDIF
'Morning hours will give a negative value for Hangle.

WRITE(6,*)'Now calculating the angle of incidence,angles should be in radians'
    DLH=COS(Declin)*COS(Lat)*COS(Hangle)
        Dsn=SIN(Declin)*SIN(Lat)
        INang=ACOS(DLH+Dsn)
WRITE(6,*)'INang'
WRITE(6,*)INang
WRITE(6,*)'Refractive angle is,REang'
      RES=SIN(INang)*(RIA/RIG)
        REang=ASIN(RES)
WRITE(6,*)REang
        GPeref=(SIN(REang-INang))**2/(SIN(REang+INang))**2
        GPalre=(TAN(REang-INang))**2/(TAN(REang+INang))**2
WRITE(6,*)'Glass reflactance is,Glref'
      Glref=0.5*(GPeref+GPalre)
WRITE(6,*)Glref

WRITE(6,*)'Glass transmitancewith reflection only,GTnoa'
    GTnoa=0.5*((1-GPeref)/(1+GPeref)+(1-GPalre)/(1+GPalre))
WRITE(6,*)GTnoa
WRITE(6,*)'Glass transmitance with only absorption,GTwoa'
      GTwoa=EXP(-EXCO*GTHI/COS(REang))
WRITE(6,*)GTwoa
WRITE(6,*)'Glass transmissivity with both absorption and reflection,GTabre'
      GTabre=GTnoa*GTwoa
WRITE(6,*)GTabre
WRITE(6,*)'Top glass cover absorption fraction,TOPgab'
      TOPgab=(1-Glref-GTabre)*(1+Glref*GTabre)
WRITE(6,*)TOPgab
WRITE(6,*)'First glass cover absorption fraction,F1rgab'
              F1rgab=(1-Glref-GTabre)*(GTabre+GTabre*Glref**2)
WRITE(6,*)F1rgab
WRITE(6,*)'Absorber plate absorption fraction,ABpab'
              ABpab=(GTabre**2)*APABS*(1+Glref**2+Glref*APREF)
WRITE(6,*)ABpab
```

```
WRITE(6,*)'Calculation of heat transfer coefficient by wind,AMHChw'

              AMHChw=5.7+3.8*V(I)
WRITE(6,*)AMHChw
WRITE(6,*)'Sky temperature,K,SKYTEM'
             SKYTEM=0.0552*(T(I)**1.5)
WRITE(6,*)SKYTEM
  !Have to initialise the temperatures.(Should be according to a pre-experiment data)

         Tt1=
         Tf11=
         T11=
         Tf21=
         Tab1=
         Tf31=
         Tbp1=
         Tins1=
        DO 150 J = 1,15
                Tfm1 = (AINTf+Tf11)*0.5
                Tfm2 = (Tf21+Tf11)*0.5
               Tfm3 = (Tf31+Tf21)*0.5
              AIDEN1 = ATMOPr/(GASCR*Tfm1)
              AIDEN2 = ATMOPr/(GASCR*Tfm2)
              AIDEN3 = ATMOPr/(GASCR*Tfm3)
       AISPH1 = 970.174 + 6.788E-2*Tfm1 + 1.657E-4*(Tfm1**2)- 6.787E-8*(Tfm1**3)
       AISPH2 = 970.174 + 6.788E-2*Tfm2 + 1.657E-4*(Tfm2**2)- 6.787E-8*(Tfm2**3)
       AISPH3 = 970.174 + 6.788E-2*Tfm3 + 1.657E-4*(Tfm3**2)- 6.787E-8*(Tfm3**3)
       AThco1 = 7.2E-5*Tfm1 +4.64E-3
       AThco2 = 7.2E-5*Tfm2 +4.64E-3
      AThco3 = 7.2E-5*Tfm3 +4.64E-3
       ADVIS1 = 4.4E-8*Tfm1 + 4.64E-6
      ADVIS2 = 4.4E-8*Tfm2 + 4.64E-6
       ADVIS3 = 4.4E-8*Tfm3 + 4.64E-6
       Cp = (AISPH1 + AISPH2 + AISPH3)/3
       Prand1 = (AISPH1*ADVIS1)/AThco1
      Prand2 = (AISPH2*ADVIS2)/AThco2
       Prand3 = (AISPH3*ADVIS3)/AThco3
       H4 = 1/(AIDEN1*AISPH1*TAGHI)
       H5 = 1/(AIDEN2*AISPH2*SAGHI)
       H6 = 1/(AIDEN3*AISPH3*FAGHI)
WRITE(6,*)'Cp,Prand1,Prand2,Prand3'
WRITE(6,*)Cp,Prand1,Prand2,Prand3
WRITE(6,*)'Top glass to ambient radiation heat transfer coefficient, AMRhtc'
       AMRhtc=STBCON*GEMI*(Tt1**4-SKYTEM**4)/(Tt1-T(I))
WRITE(6,*)AMRhtc
WRITE(6,*)'Radiation heat transfer coefficient between first and top glass,RHftc'
         RHftc=STBCON*(T11**2+Tt1**2)*(T11+Tt1)/((2/GEMI)-1)
         Ha=AMHChw+AMRhtc
WRITE(6,*)RHftc,Ha
WRITE(6,*)'Forced convection heat transfer for the first flow channel,HTCtf1'
```

```
      Hydrad1=4*CWIDTH*TAGHI/(2*(CWIDTH+TAGHI))

      Renno3=AFVEL3*Hydrad1*AIDEN1/ADVIS1
      FChtc1=0.0158*(Renno3**(4/5))
      HTCtf1=FChtc1*AThco1/Hydrad1
WRITE(6,*)'Renno3,  HTCtf1'
WRITE(6,*)Renno3,HTCtf1
WRITE(6,*)'Forced convection heat transfer coefficient between top glass and fluid is
          equalto & that between the first glass and the flowing fluid'

            C4=Ha+HTCtf1+RHftc
           K4=HTCtf1*2
WRITE(6,*)'C4 , K4'
WRITE(6,*)C4,K4
WRITE(6,*)'Insulation heat transfer coefficient, INShtc'
            Rhina=STBCON*INSem*(Tins1**4-SKYTEM**4)/(Tins1-T(I))
            INShtc=INMTCK/INMTHI  + BPTHI/BPTCK + 1/(Rhina+AMHChw)
            Ub = 1/INShtc
            Hins=Rhina+AMHChw
WRITE(6,*)'INShtc , Rhina , Hins,Ub'
WRITE(6,*)INShtc,Rhina,Hins,Ub
WRITE(6,*)'Radiation heat transfer coefficient between absorber first glass plates,RHBab1'
             RHBab1=STBCON*(Tab1**2+T11**2)*(Tab1+T11)/Emiab1
WRITE(6,*)RHBab1
WRITE(6,*)'Forced convection heat transfer coefficient for the second flow channel,HTCtf2'

            Hydrad2=4*CWIDTH*SAGHI/(2*(CWIDTH+SAGHI))
            Renno2=AFVEL2*Hydrad2*AIDEN2/ADVIS2
            FChtc2=0.0158*(Renno2**(4/5))
            HTCtf2=FChtc2*AThco2/Hydrad2
WRITE(6,*)'Renno2 , HTCtf2'
WRITE(6,*)Renno2,HTCtf2
WRITE(6,*)'Forced convection heat transfer coefficient between absorber and fluid is equal
          to& that between first glass and flowing fluid'

            D4=RHBab1+HTCtf1+HTCtf2+RHftc
           K5=2*HTCtf2
WRITE(6,*)'D4 , K5'
WRITE(6,*)D4,K5
WRITE(6,*)'Forced convection heat transfer coefficient for the third flow channel, HTCtf3'

            Hydrad3=4*CWIDTH*FAGHI/(2*(CWIDTH+FAGHI))

      Renno1=AFVEL1*Hydrad3/ADVIS3
      FChtc3=0.0158*(Renno1**(4/5))
      HTCtf3=FChtc3*AThco3/Hydrad3
WRITE(6,*)'Renno1 , HTCtf3'
WRITE(6,*)Renno1,HTCtf3
WRITE(6,*)'Radiation heat transfer coefficient between absorber and back plates,Hab'
```

```
            Hab=STBCON*(Tab1**2+Tbp1**2)*(Tab1+Tbp1)/Emiabb

        G4=HTCtf2+HTCtf3+Hab+RHBab1
        N3=Hab+HTCtf3
WRITE(6,*)'Hab , G4 , N3'
WRITE(6,*)Hab , G4 , N3

!Calculation of the component temperatures and the collector efficiency.

      Tt1=Tt1+A*TIMINT*(S(I)*TOPgab+Ha*T(I)+HTCtf1*Tf11+RHftc*T11-C4*Tt1)
      Tf11=Tf11+H4*TIMINT*(HTCtf1*Tt1+HTCtf1*T11-K4*Tf11)
      T11=T11+A*TIMINT*(S(I)*F1rgab+RHBab1*Tab1+HTCtf1*Tf11+HTCtf2*Tf21+
          RHftc*Tt1-D4*T11)
      Tf21=Tf21+H5*TIMINT*(HTCtf2*T11+HTCtf2*Tab1-K5*Tf21)
      Tab1=Tab1+E*TIMINT*(S(I)*ABpab+HTCtf2*Tf21+HTCtf3*Tf31+RHBab1*T11+
          Hab*Tbp1-G4*Tab1)

IF (Tab1 – Tab.GE. 0.05) THEN

        Tf31=Tf31+H6*TIMINT*(HTCtf3*Tab1+HTCtf3*Tbp1-K5*Tf31)
        Tbp1=Tbp1+L*TIMINT*Hab*(Tab1-Tbp1)- L*TIMINT*HTCtf3*(Tbp1-Tf31)-
            L*Ub*TIMINT*(Tbp1-T(I))
ELSE
    WTITE* 'No convergence'
          Tab1 = (Tab1+Tab)/2
END IF
       CEF=AMFR*Cp*(Tf31-AINTf)/(CLENG*CWIDTH*S(I))
  150 CONTINUE
WRITE (6,'(15F7.2)')S(I),V(I),T(I),Tt1,Tf11,T11,Tf21,Tab1,Tf31,Tbp1,Tins1,CEF

  370 CONTINUE
  380 CONTINUE
END PROGRAM TPMCmo
```

```
MODULE INS
INTEGER::I

REAL:: S(5)= (/654.8,764.5,948.7,961.2,734.9/)

REAL:: T(5)= (/297.3,298.01,298.94,298.50,298.45/)

REAL:: V(5)= (/0.958,1.458,0.208,0.233,0.633/)

INTEGER:: U(5)= (/0,2,4,6,8/)

END MODULE INS
```

APPENDIX 7
A CD copy of the computer program.